ansa Bridged metallocene chemistry of niobium

by

Nigel J. Bailey

A thesis submitted in part fulfilment of the requirements for the degree of Doctor of Philosophy at the University of Oxford

St John's College

Oxford

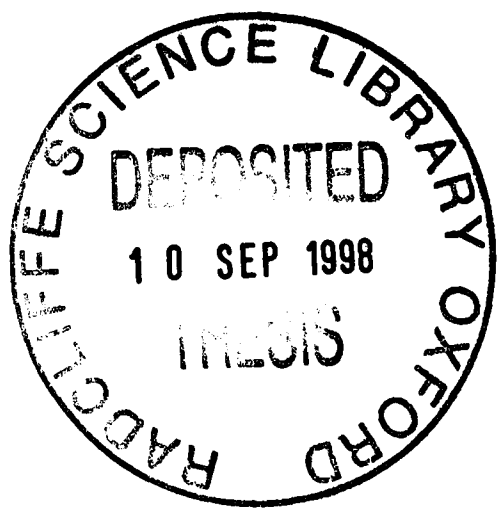

April 1998

The work described in this thesis was carried out in the Inorganic Chemistry Laboratory, Oxford, from September 1994 to December 1997 under the supervision of Professor M. L. H. Green F. R. S. All the work is my own unless stated to the contrary and has not been submitted previously for any other degree at this, or any other, university.

Abstract

ansa Bridged metallocene chemistry of niobium

Nigel J. Bailey

St John's College

Trinity Term 1998

Submitted for D. Phil.

This thesis is concerned with the synthesis and characterisation of new *ansa* bridged *bis*-η-cyclopentadienyl derivatives of niobium.

Chapter 1 provides an introduction to the area of early transition metal bent metallocene derivatives and charts the development of *ansa* bridged metallocenes.

Chapter 2 presents the synthesis and characterisation of some new *ansa* niobocene derivatives prepared from niobium(IV) chloride. The compounds [Nb(η-C_5H_4-CMe_2-η-C_5H_4)(η^2-BH_4)],* [Nb(η-C_5H_4-CMe_2-η-C_5H_4)(PMe_3)H],* [Nb(η-C_5H_4-CMe_2-η-C_5H_4)(PPh_3)H], [Nb(η-C_5H_4-CMe_2-η-C_5H_4)$(SPh)_2$] and [Nb(η-C_5H_4-CMe_2-η-C_5H_4)$(CH_2Ph)_2$]* are described. An asterisk indicates that the X-ray crystal structure was determined.

Chapter 3 describes the synthesis and characterisation of some *ansa* niobocene derivatives containing ancillary imido ligands. The compounds [Nb(η-C_5H_4-CMe_2-η-C_5H_4)($NSiMe_3$)Cl],* [Nb(η-C_5H_4-CMe_2-η-C_5H_4)(NBu^t)X] (X = Cl,* Br,* I,* Me), [Nb(η-C_5H_4-CMe_2-η-C_5H_4)(NHBu^t)Cl][BF_4] and [Nb(η-C_5H_4-CMe_2-η-C_5H_4)(O)Cl]* are described. An asterisk indicates that the X-ray crystal structure was determined. Photoelectron spectra were recorded for [Nb(η-C_5H_4-CMe_2-η-C_5H_4)(NBu^t)X] (X = Cl, Me) and compared to a geometry optimisation calculation obtained using density functional theory. In these formally twenty electron compounds the HOMO has negligible metal contribution and the eighteen electron rule is not violated.

Chapter 4 describes the results of a preliminary investigation into *ansa* niobium(III) *bis*-η-cyclopentadienyl derivatives containing phosphorus donor ligands. The compound [Nb(η-C_5H_4-CMe_2-η-C_5H_4)(PMe_3)Cl] is characterised spectroscopically. The synthesis and full characterisation details of the compound [Nb(η-C_5H_4-CMe_2-η-C_5H_4){$P(OMe)_3$}Cl] are given, including the X-ray crystal structure.

Chapter 5 provides the experimental details for the preceding Chapters and **Chapter 6** contains the characterising data for the new compounds described in this thesis.

Full details of the X-ray crystallographic structure determinations are given in **Appendices A - I.**

Acknowledgements

First of all, I would like to thank my supervisor, Professor M. L. H. Green F. R. S., for giving me the opportunity to work in group and for all his ideas and enthusiasm during my time of study in the ICL.

Most people in the Green group have helped me in some way or another at some time. I would like to thank particularly Jane Galsworthy for very helpful discussions, for giving up her time to proof-read this manuscript and for being difficult to find in Prague. I would also like to thank Andreas Danopoulos who was a great help during the 'twilight months.' Before the arrival of Jane and Andreas I was kept in my place by Richard Douthwaite, Nils Metzler and Jess Cook. Since the departure of Joanne Souter, who introduced me to the delights of working with *ansa* bridges, I had been battling with the *'aggro effect'* on my own until I was joined by Adam Stephens and Steve Conway, whom I thank for having the good grace to find it about as difficult as I have.

Thanks to Mike Leech and Linda Doerrer for the crystallography, Tessa Dijkstra for recording the photoelectron spectra and Andrew Graham (partner in chime) for help with the now departed mass spec machine and for always having a little bit of dry 40-60. Also, I am very grateful to the analysis staff, glassblowers and all the other staff in the ICL. Thanks to Sean McGrady for turning my d_5-ethyl iodide into diethylzinc, which never made it onto the pages of this thesis.

I owe a big thank you to Jenny Green for her help with the assignment of the photoelectron spectroscopy and for letting me reproduce some figures for the introduction.

Another thank you to Malcolm, for providing funds when the EPSRC money ran out. I am also pleased to have had the challenge of teaching inorganic chemistry at St Hilda's (and the cash). Many thanks to Victor Christou, firstly for teaching me the basic techniques of Schlenk lines back in my Part II days, and secondly for giving me the OPSYS job during writing up and not minding that I have taken two months longer than I said I would.

Thanks to Caroline for lending me her computer and letting me put the task bar on the right. Thanks to Karen, Chris, Alex, Mark and Tuan, the Christou Kids, for keeping me up until four in the morning too often. Thanks to Nic and Sparrow for their constant distracting influence and for never tiring of drinking the same beer in the same pubs with the same people.

Finally, I must acknowledge my parents, for everything they did to get me this far.

Contents

Appendices

List of figures

List of tables

List of abbreviations

General abbreviations

a_{iso}	hyperfine splitting parameter (EPR spectroscopy)
Ar	aryl group
b. p.	boiling point
Bu^t	*tertiary*-butyl
Cp	cyclopentadienyl
Cp_{cent}	cyclopentadienyl ring centroid
DFT	density functional theory
DME	1,2-dimethoxyethane
DMSO	dimethylsulphoxide
EI	electron impact (mass spectrometry)
EPR	electron paramagnetic resonance
Et	ethyl
FAB	fast atom bombardment (mass spectrometry)
g_{iso}	isotropic g value (EPR spectroscopy)
HOMO	highest occupied molecular orbital
hν	irradiation
IE	ionisation energy
IR	infra-red
L	two electron donor ligand
LUMO	lowest unoccupied molecular orbital
M	metal atom
M^+	molecular ion
MAO	methylaluminoxane
Me	methyl
MO	molecular orbital
m/z	atomic mass units per unit charge
NMR	nuclear magnetic resonance
Ph	phenyl
Pr^i	*iso*-propyl

py	pyridine
R	alkyl or aryl group
RT	room temperature
THF	tetrahydrofuran
X	generic ligand

NMR spectroscopic abbreviations

br	broad
δ	chemical shift
d	doublet
fwhh	full width at half height
$\{^1H\}$	proton decoupled
$^nJ_{AB}$	n bond coupling constant between A and B
m	multiplet
ppm	parts per million
q	quartet
s	singlet
t	triplet

IR spectroscopic abbreviations

br	broad
m	medium intensity
s	strong intensity
vs	very strong intensity
w	weak intensity
vw	very weak intensity

Chapter 1

Introduction

1.0 General introduction

This thesis is concerned with the synthesis, structure and reactivity of new organometallic compounds of niobium containing *ansa* bridged ligands. The first part of this chapter provides an introduction to the area of early transition metal metallocene chemistry, covering briefly the history of metallocenes and the nature of bonding in bent metallocene derivatives. The second part of this chapter describes the development of *ansa* metallocenes and reviews the areas of this chemistry most pertinent to the new results described in this thesis.

Two publications have arisen from this work.[1, 2]

1.1 Metallocenes

In 1952 the pentahapto mode of bonding of the η^5-C_5H_5 cyclopentadienyl ring in ferrocene was discovered.[3, 4] Since then, the chemistry of this ligand has dominated the growth of organotransition metal chemistry, especially in the area of early transition metal complexes. Compounds containing two η^5-C_5H_5 rings bonded to a transition metal are known as metallocenes. In such molecules, the cyclopentadienyl ligand, with few exceptions, performs the role of an essentially inert spectator ligand. However, the steric and electronic requirements of the cyclopentadienyl ligand may be readily tuned by facile substitution of the hydrogens on the ring with other hydrocarbon groups. Thus, the use of this ligand offers a convenient method of controlling the stereoelectronic properties of the metal centre.

The cyclopentadienyl ligand is ubiquitous in early organotransition metal chemistry as witnessed by the abundance of cyclopentadienyl derivatives of the group 3, 4, 5 and 6 elements in the literature.[5]

As early as 1957, $[Ti(\eta\text{-}C_5H_5)_2Cl_2]$, in conjunction with diethylaluminium chloride, was used for homogeneous Ziegler-Natta catalysis as demonstrated by Breslow.[6] This was the earliest example of a homogeneous Ziegler-Natta catalyst, although its activity could not compete with that of the classic heterogeneous Ziegler-Natta catalyst systems at that time.

In the 1980's there was a dramatic resurgence of interest in early transition metal metallocene chemistry prompted by Kaminsky[7] who discovered that zirconocenes in conjunction with the co-catalyst methylaluminoxane (MAO) are excellent homogenous Ziegler-Natta catalysts, giving polymers with high molecular weights and low monodispersity and, consequently, advantageous physical properties.

1.2 The nature of bonding in bent metallocenes

The early history of bent metallocene chemistry provides fascinating insight into the development of the molecular orbital theory of metallocenes. It was shown by Wilkinson[8] that the basicity of $[Re(\eta\text{-}C_5H_5)_2H]$ is comparable in strength to that of ammonia and that it undergoes reversible protonation. Fischer demonstrated that the same is true of $[Mo(\eta\text{-}C_5H_5)_2H_2]$ and $[W(\eta\text{-}C_5H_5)_2H_2]$.[9] These were the first well established examples of organometallic bases. A typical reaction is shown in **Figure 1.1**.

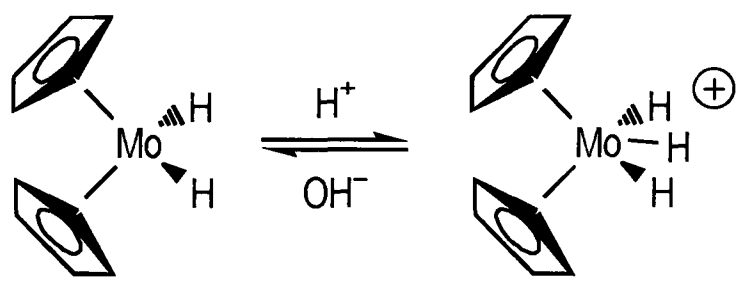

Figure 1.1 Reversible protonation of $[Mo(\eta\text{-}C_5H_5)_2H_2]$

The nature of the frontier orbitals used to bind the additional hydride ligands was a topic of considerable interest. At the time the geometry of these substituted metallocenes was still uncertain. For instance, it had even been suggested that $[Re(\eta\text{-}C_5H_5)_2H_2]^+$ has a structure with collinear ring axes and the hydride ligands lying at the cyclopentadienyl ring centroids.[10] In one of the first forays into the NMR spectroscopy of organometallic compounds the spectra of the cations $[Mo(\eta\text{-}C_5H_5)_2H_3]^+$ and $[W(\eta\text{-}C_5H_5)_2H_3]^+$ and the neutral molecule $[Ta(\eta\text{-}C_5H_5)_2H_3]$ were determined.[11] In each of these spectra the signals assigned to the metal hydrides exhibit A_2B type patterns, indicating low symmetry and lending support to the angular structure, which was later confirmed by X-ray crystallography.[12]

Subsequently, Ballhausen and Dahl provided a molecular orbital description of the bonding in bent metallocenes.[13] They proposed that there are three metal based orbitals not involved in bonding with the η-cyclopentadienyl rings, and that these orbitals are symmetrically disposed in the *yz* plane of the metallocene unit. Under their scheme the lone pair of a metallocene dihydride was expected to be located in the inter-ligand wedge defined by the H–M–H fragment (**Figure 1.2a**).

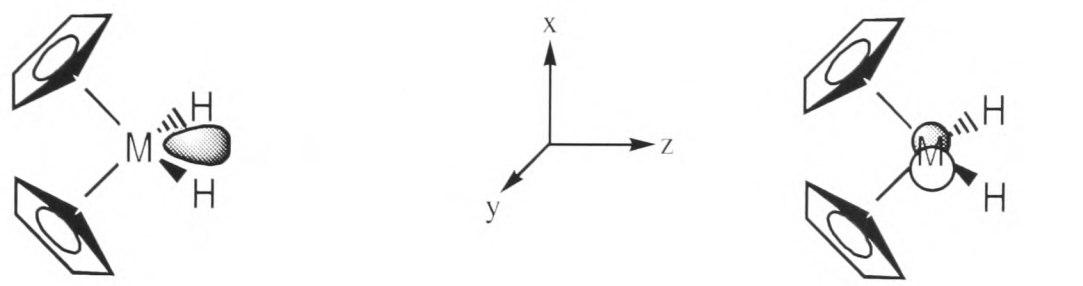

(a) Ballhausen and Dahl model

(b) Alcock model

Figure 1.2 Models for the frontier orbitals in bent metallocenes

However, a surprising result was obtained from the reaction between $[Re(\eta\text{-}C_5H_5)_2H]$ and *n*-butyllithium followed by methyl iodide, which produces the ring-substituted compound $[Re(\eta^5\text{-}C_5H_5)(\eta^4\text{-}C_5H_5Me)Me_2]$ as shown in **Figure 1.3**.[14] The molecular structure of this compound was determined by Alcock[15] and shows that the angle between the two methyl groups is too small to accommodate a pair of electrons.

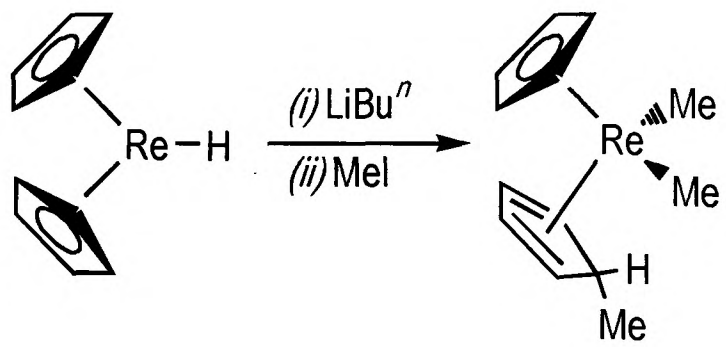

Figure 1.3 Synthesis of $[Re(\eta^5\text{-}C_5H_5)(\eta^4\text{-}C_5H_5Me)Me_2]$

Alcock proposed an alternative bonding scheme for the three frontier orbitals using the same atomic orbitals as in Ballhausen and Dahl's model and thus preserving their description of the metal-ring bonding. This modified description places the lone pair in an orbital lying in the same plane as the X–M–X fragment but oriented at 90° to the position suggested by Ballhausen and Dahl (**Figure 1.2b**).

Alcock's theory was supported by subsequent developments. The molecular structures of $[M(\eta\text{-}C_5H_5)_2Cl_2]$ (M = Zr, Nb, Mo) were determined and show that as the electron population of the metal increases from d^0 to d^1 to d^2 the Cl–M–Cl angle becomes smaller rather than larger.[16] On this basis it is clearly indicated that the additional d electrons are occupying the orbital suggested by Alcock. Various $[M(\eta\text{-}C_5H_5)_2X_2]$ compounds were studied and the X–M–X angles determined experimentally for d^0 compounds are in the range 94-97°; for d^1 compounds, 85-88° and for d^2 compounds, 76-82°.

More elaborate descriptions of the molecular orbitals in these compounds have been provided by Lauher and Hoffmann using extended Hückel type calculations.[17] The generally accepted three frontier orbitals of the $[M(\eta\text{-}C_5H_5)_2]$ fragment are depicted in **Figure 1.4**, which shows the MO scheme for a d^0 *bis*-η-cyclopentadienyl compound of the $[M(\eta\text{-}C_5H_5)_2X_2]$ type, where X is a σ-donor ligand. The numbering system is that used by Lauher and Hoffmann, and does not include the metal-ring bonding orbitals at lower energy. This axis system and orbital numbering scheme will be used throughout this thesis.

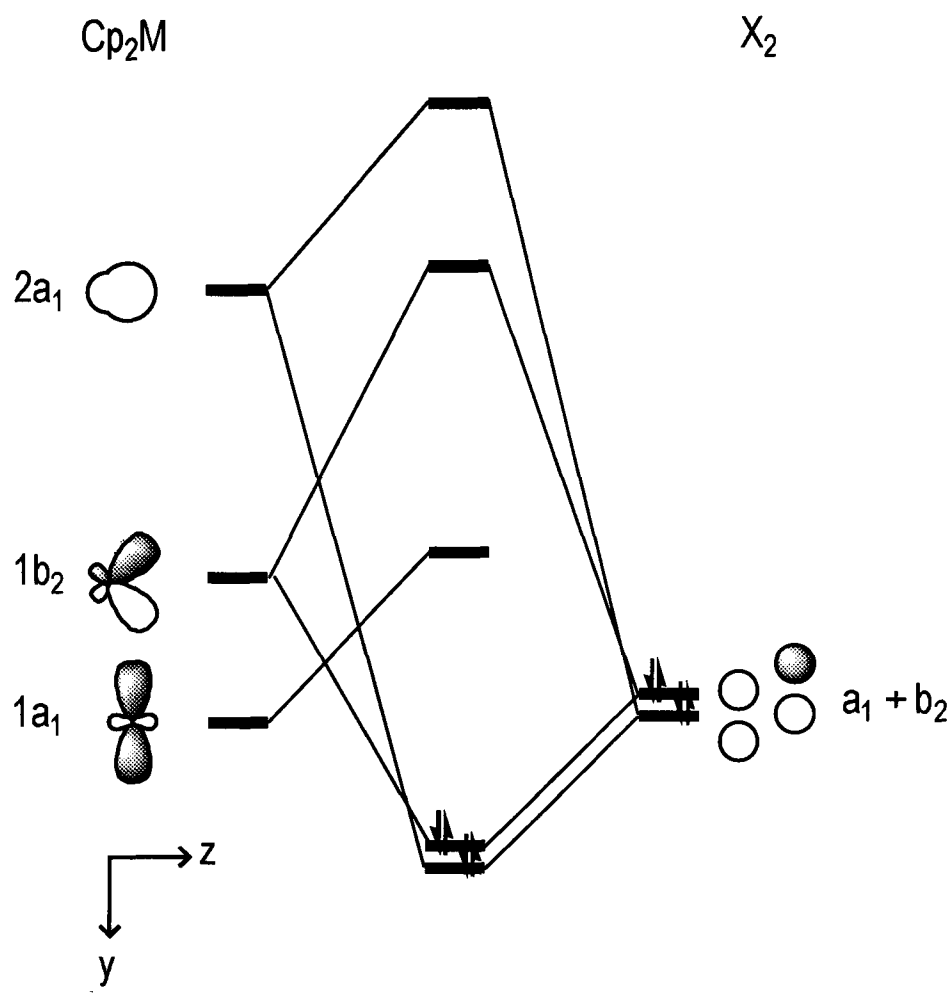

Figure 1.4 MO scheme for d^0 $[M(\eta^5\text{-}C_5H_5)_2X_2]$

Lauher and Hoffmann performed a calculation on the model compound $[Ti(\eta\text{-}C_5H_5)_2H_2]$. The variation in the total energy of the molecule and in the energy of the $1a_1$ orbital as a function of the X–M–X angle was examined. The X–M–X angle was predicted to be 110° for a d^0 compound, 85° for a d^1 compound and 78° for a d^2 compound, a trend in agreement with the experiments of Green *et al.*

Modern computer technology has allowed the molecular orbital theory of bent metallocenes to be developed with greater sophistication. Three dimensional representations of the three frontier orbitals of $[M(\eta\text{-}C_5H_5)_2]$ calculated using Density Functional Theory (DFT) are reproduced in **Figure 1.5.**[18]

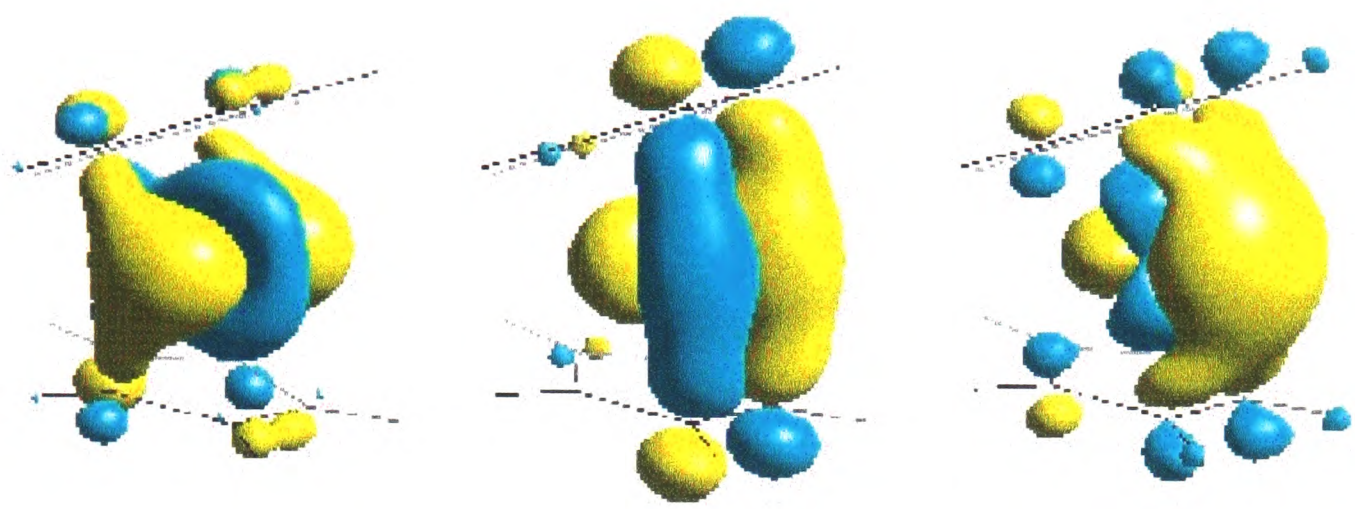

$1a_1$ $1b_2$ $2a_1$

Figure 1.5 The frontier orbitals of a bent metallocene unit, generated by the Cerius^2 package, Molecular Simulations Inc.

With the aid of DFT, energy minimisation calculations have been carried out for ferrocene and the hypothetical triplet zirconocene as a function of the angle between the ring planes.[18] The energy of the $2a_1$ orbital in particular is found to rise sharply with increased bending from D_{5h} symmetry. Thus, as illustrated in **Figure 1.6**, the total energy of ferrocene rises by about 3 eV on bending from 0 to 40°, whereas the total energy of the hypothetical zirconocene, in which the $2a_1$ orbital is unoccupied, remains virtually unchanged over the same range. These results present a good case for d orbital occupancy exerting a strong influence over the angle between the rings.

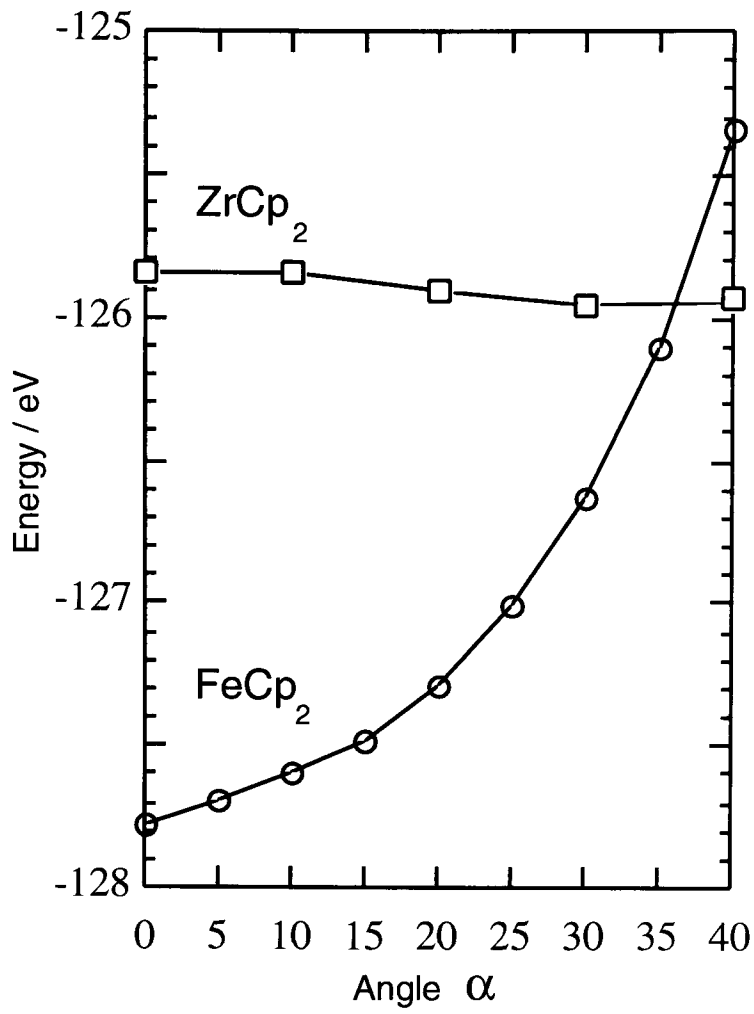

Figure 1.6 Total energy of ferrocene and triplet zirconocene as a function of the angle between the cyclopentadienyl ring planes, α

The three frontier orbitals shown in **Figure 1.5** are the orbitals which give group 4 metallocene derivatives the ability to carry out Ziegler-Natta polymerisation reactions. The widely accepted mechanism for olefin polymerisation was originally proposed by Cossee[19, 20] and **Figure 1.7** shows the key migratory insertion step. The carbons of the coordinated ethene and the terminal carbon of the growing polymer chain lie in a plane which also contains the metal centre. Migration of the polymer chain to the coordinated ethene gives rise to chain growth. It is possible that the intermediate is stabilised by *agostic* bonding[21] using the empty $1a_1$ orbital.

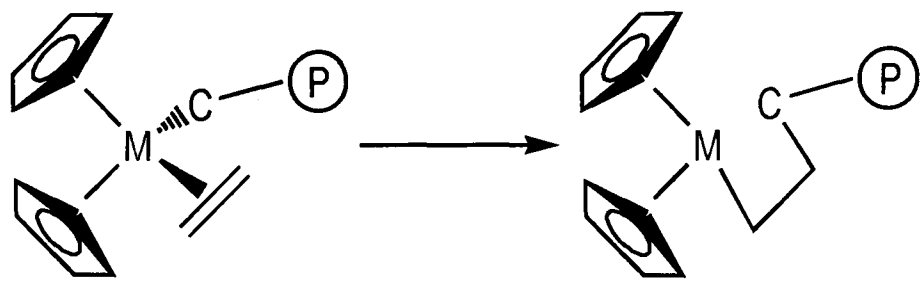

Figure 1.7 Migratory insertion step in olefin polymerisation. The growing polymer chain is denoted by the encircled P.

It is reasonable to expect that any modifications to the relative energies or dispositions of the frontier orbitals will be highly relevant to our understanding of the activity and specificity of Ziegler-Natta catalysis.

1.3 The development of *ansa* bridged metallocenes of the early transition metals

A particular feature of the early development of homogeneous Ziegler-Natta catalyst systems was the study, by Brintzinger and Kaminsky, of compounds where there is a linkage between the two cyclopentadienyl rings. Brintzinger adopted the prefix *ansa* for these compounds. This term had been first mentioned in a chemical context in 1942 by Lüttringhaus,[22] who used it to describe bridged aromatic compounds, introducing it with the footnote:

> *ansa* (Lat.) = der Henkel.

When Brintzinger[23] reintroduced the term in 1979 in what was to be the first of a series of related papers he offered the translation:

> *ansa*- (latin = bent handle, attached at both ends).

Since then the term *ansa* has enjoyed widespread use to describe *bis*-η-cyclopentadienyl compounds containing an interannular bridge. It has also been

employed for metallocene analogues such as bridged η-cyclopentadienyl imido compounds[24-27] and bridged *bis*imido compounds.[28]

The first ever bridged metallocene reported, before the term *ansa* had been adopted, was 1,1'-α-ketotrimethylene ferrocene.[29] The first series of bridged metallocenes of a transition metal triad was the trimethylene bridged metallocene dichlorides of the group 4 metals.[30]

A simple representation of an *ansa* metallocene is shown in **Figure 1.8**. The bridging functionality E may be varied from a single atom bridge (for example E = CMe_2, $SiMe_2$) to a two-membered bridge (for example E = CH_2CH_2 or CR_2CR_2) and so on. Various examples of bridging units are tabulated in a recent study by Corey.[31]

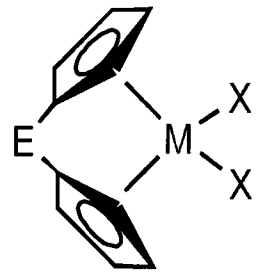

Figure 1.8 A generalised *ansa bis*-η-cyclopentadienyl compound

In 1984 Ewen reported that the *ansa* metallocene ethylene*bis*(1-indenyl)titanium dichloride catalyses propene polymerisation giving mixtures of isotactic and atactic polypropene.[32] Hitherto only atactic polypropene had been obtainable. Shortly afterwards, Kaminsky and Brintzinger demonstrated that the chiral *ansa* metallocene ethylene*bis*(4,5,6,7-tetrahydro-1-indenyl)zirconium dichloride (**Figure 1.9**) in conjunction with MAO catalyses the polymerisation of propene with remarkable activity and gives polymer with an isotacticity previously unobtainable.[33]

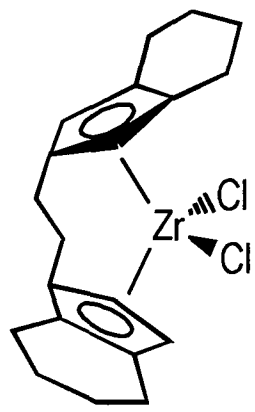

Figure 1.9 Ethylene*bis*(4,5,6,7-tetrahydro-1-indenyl)zirconium dichloride

In these systems the function of the *ansa* bridge is to generate a rigid system in which the orientation of the indenyl groups is fixed such that propene polymerisation occurs isospecifically.

In view of these results, there was very considerable interest at the outset of this thesis in the understanding and development of the *ansa* metallocenes of the early transition metals.

1.4 Structural features of *ansa* metallocenes

Some structural parameters for an *ansa* metallocene unit which will be used in this thesis are defined in **Figure 1.10**. For *ansa* compounds containing a single bridging atom **E** we may define the angle α as the C_{ipso}–**E**–C_{ipso} bond angle. The angle between the rings is usually reported in one of two ways. The angle subtended by the two vectors normal to the planes of the cyclopentadienyl rings, the bending angle, is denoted β. More frequently the angle subtended by the two ring centroid to metal vectors, γ, is quoted.

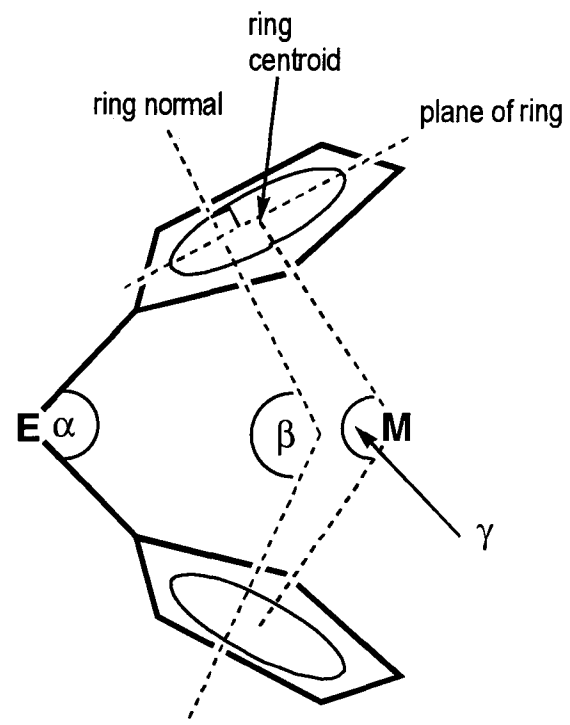

Figure 1.10 Structural parameters for an *ansa* metallocene unit.

A recent study compares the crystal structures of the *ansa* metallocenes [M(η-C_5H_4-CMe_2-η-C_5H_4)Cl_2] (M = Ti, Zr and Hf) with their unbridged analogues.[31] Some data are reproduced in **Table 1.1**. The M–Cl bond distances and the average M–C distances vary little between the *ansa* compounds and their parent metallocenes. Of note, however, is that a bridging silicon atom reduces γ by about 0-4° and a bridging carbon atom causes a reduction in γ of typically 10° or more. A bridging unit of two carbon atoms produces a similar change in γ as a single silicon atom.[31, 34]

The molecular strain caused by the increased bending angle in *ansa* metallocenes is also manifest in the metal-carbon distances, which are longer to the ring carbons opposite the *ipso* carbon than to the *ipso* carbon itself. Thus, in *ansa* compounds the rings are prised off the metal and the opposite face is more accessible to incoming substrates. This could be a distinct advantage in the co-polymerisation of ethene with longer chain alkenes.

Compound	γ / °	M–Cl / Å	average M–Cp / Å
[Ti(η-C_5H_5)$_2$$Cl_2$]	131.0	2.364(1)	2.059
[Ti(η-C_5H_4-$SiMe_2$-η-C_5H_4)Cl_2]	128.7	2.356(1)	2.075
[Ti(η-C_5H_4-CMe_2-η-C_5H_4)Cl_2]	121.5	2.340(10)	2.056
[Zr(η-C_5H_5)$_2$$Cl_2$]	129.3	2.447(1)	2.203
[Zr(η-C_5H_4-$SiMe_2$-η-C_5H_4)Cl_2]	125.4	2.435(1)	2.197
[Zr(η-C_5H_4-CMe_2-η-C_5H_4)Cl_2]	116.6	2.432(6)	2.192
[Hf(η-C_5H_5)$_2$$Cl_2$]	127.1	2.423(2)	2.18
[Hf(η-C_5H_4-$SiMe_2$-η-C_5H_4)Cl_2]	126.8	2.424(2)	2.191
[Hf(η-C_5H_4-CMe_2-η-C_5H_4)Cl_2]	117.1	2.409(5)	2.174

Table 1.1 Structural parameters for metallocene dichlorides

In a recent DFT study, Woo, Fan and Ziegler modelled ethylene insertion into [Zr(η-C_5H_5)$_2$Me]$^+$ and [Zr(η-C_5H_4-SiH_2-η-C_5H_4)Me]$^+$ and indeed predicted that the *ansa* bridge opens up the coordination site by pulling back the cyclopentadienyl rings. Consequently, the electron deficiency of the metal centre is predicted to increase, since the cyclopentadienyl ring orbitals cannot interact optimally with the metal d orbitals. The effect on the energetics of ethylene insertion is small, however. The presence of the *ansa* bridge does not alter the activation barrier to any significant degree and it only increases the reaction enthalpy by 14 kJ mol^{-1}.[35]

1.5 A study of *ansa* metallocenes of the group 6 transition metals

Recently, a systematic attempt to compare the chemistry of *ansa* metallocene derivatives of molybdenum and tungsten with the chemistry of their non *ansa* analogues has been described.[36] The metallocene derivatives of molybdenum and tungsten were chosen because there is a considerable body of prior work on the non *ansa* metallocenes of these elements.[5] Major differences in reactivity were found between *ansa* and non *ansa* tungstenocene dihydride complexes. These findings, which are specific examples of what may be termed a more general '*ansa effect,*' are discussed below.

Photolysis of unbridged $[W(\eta\text{-}C_5H_5)_2H_2]$ produces the sixteen electron intermediate tungstenocene, $[W(\eta\text{-}C_5H_5)_2]$, with concomitant formation of H_2.[37, 38] Tungstenocene is sufficiently reactive to insert into C–H bonds, thus the photolysis reaction in benzene gives the phenyl hydride complex $[W(\eta\text{-}C_5H_5)_2(Ph)H]$. However, the corresponding singly bridged *ansa* complex is inert under the same conditions (**Figure 1.11**).

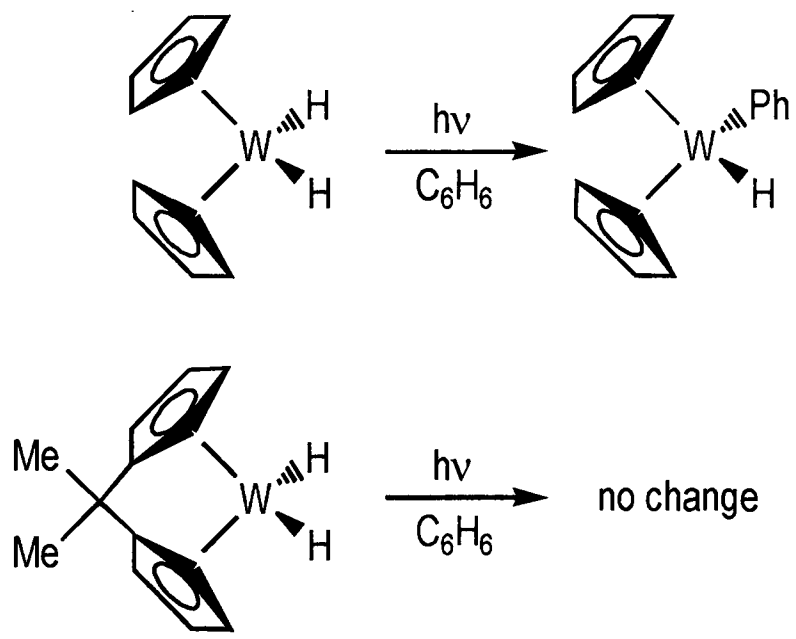

Figure 1.11 Reactivity of *ansa* and non *ansa* bridged tungstenocene dihydrides

Similarly $[W(\eta\text{-}C_5H_5)_2(Me)H]$[39] eliminates methane at 60 °C whereas the bridged compound $[W(\eta\text{-}C_5H_4\text{-}CMe_2\text{-}\eta\text{-}C_5H_4)(Me)H]$ is stable at 110 °C. This is particularly interesting since, for both compounds, studies on isotopically labelled species show the occurrence of intramolecular hydrogen exchange between the methyl group and the metal hydride.[40, 41]

It has been proposed that these differences between *ansa* and non *ansa* compounds may be accounted for by the inability of the *ansa* systems to attain the energetically favourable parallel ring structure in the sixteen electron intermediate (**Figure 1.12**).[36]

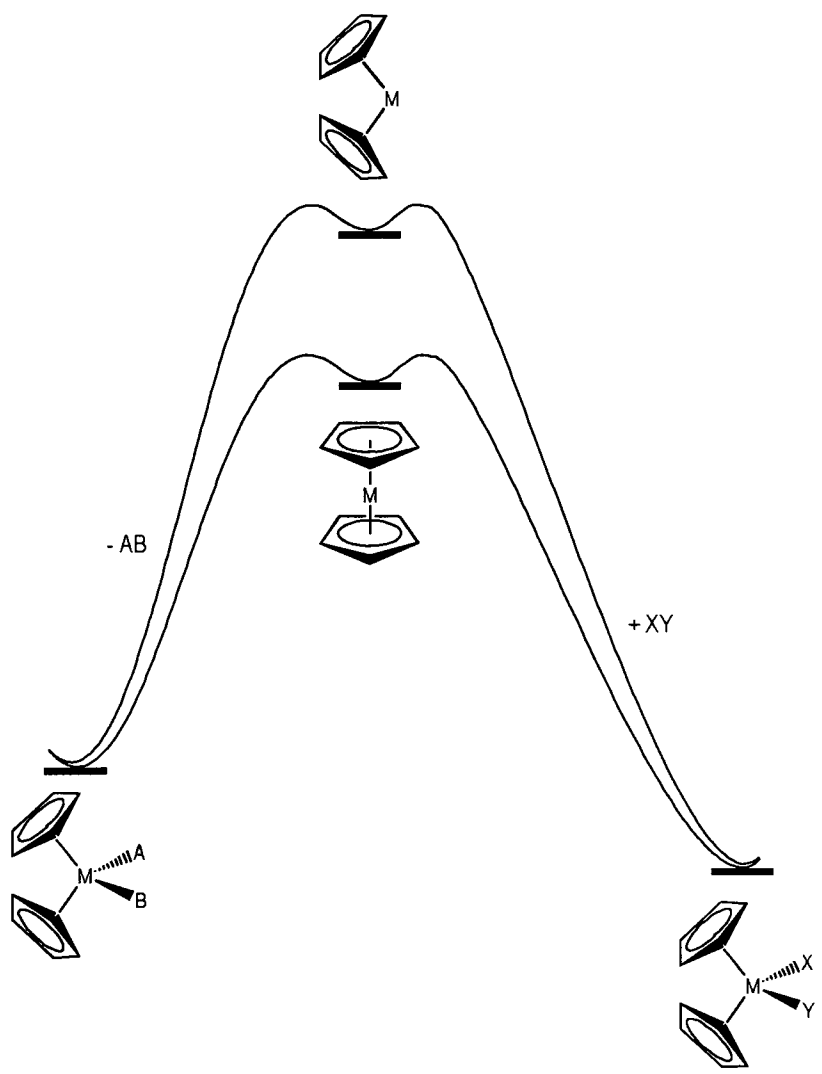

Figure 1.12 Proposed energetics for reactions proceeding *via* reductive elimination from *ansa* and non *ansa* metallocenes

This idea was first put forward by Smith and Brintzinger.[42] They reported different reactivities for ethylene bridged and unbridged titanocene dichlorides, despite their molecular structures being very similar,[23] and considered the reactions to be blocked by the unavailability of [Ti(η-C_5H_4-C_2H_4-η-C_5H_4)] as an intermediate.

A recent theoretical study by Green and Jardine[43] addresses this concept more rigorously with reference to the contrast between [W(η-C_5H_5)$_2$(Me)H] and [W(η-C_5H_4-CH_2-η-C_5H_4)(Me)H]. Both molecules pass through an η^2-CH_4 structure at the mid-point of the intramolecular exchange process and the transition states for the exchange are calculated using Density Functional Theory to be at very similar energies. Methane loss was modelled by using the W–C distance as the reaction coordinate and performing geometry optimisations at several points, with the constraint of overall C_{2v} symmetry. Total energies were calculated for both the singlet electronic configuration and the triplet electronic configuration expected for the resulting tungstenocene and are reproduced in **Figure 1.13**.

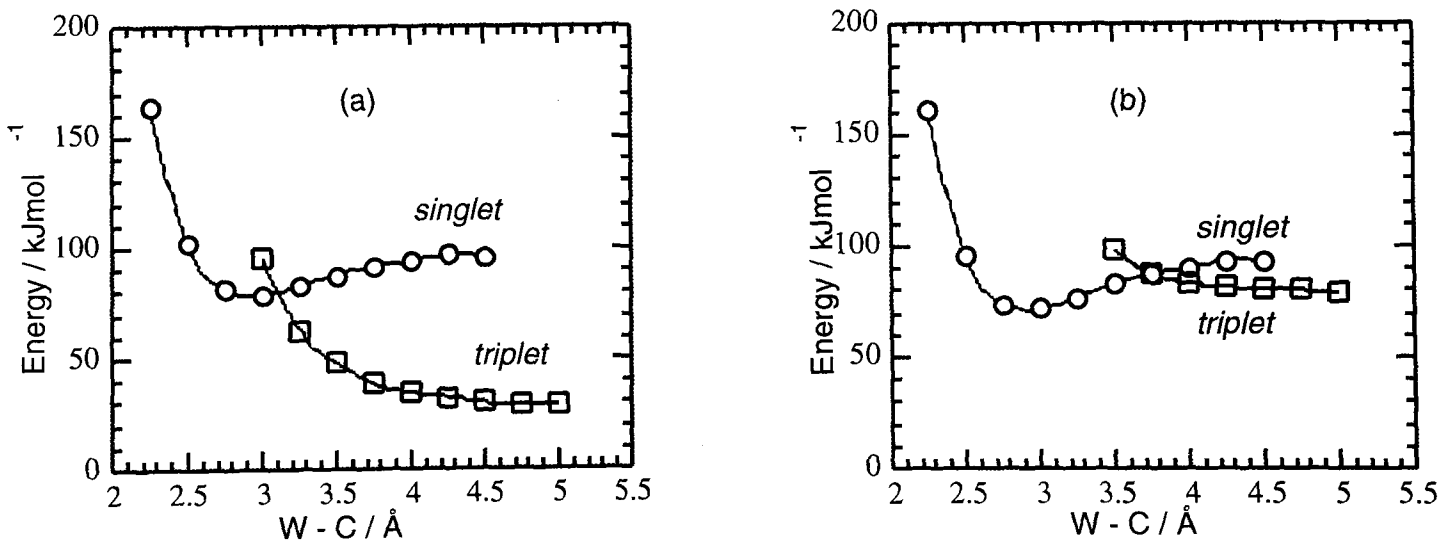

Figure 1.13 Energies of triplet and singlet C_{2v} methane complexes **(a)** [W(η-C_5H_5)$_2$(η^2-CH_4)] and **(b)** [W(η-C_5H_4-CH_2-η-C_5H_4)(η^2-CH_4)] at varying W–C distance. Energies are with respect to the corresponding methyl hydride.

The results show that for the singlet electronic configuration the difference between the reaction profiles for the *ansa* and the non *ansa* compounds is slight. However, on cross-over to the triplet states a marked change in behaviour is predicted. The unbridged triplet state is stabilised considerably with increasing W–C distance. This is associated with relaxation to the parallel ring structure. The *ansa* bridged compound gains little energy on forming the triplet state since the rings are constrained. These results are depicted in an energy scheme diagram in **Figure 1.14**.

The difference in the methane elimination reactions is, therefore, attributable to the low energy of the tungstenocene product accessible in the absence of an *ansa* bridge.

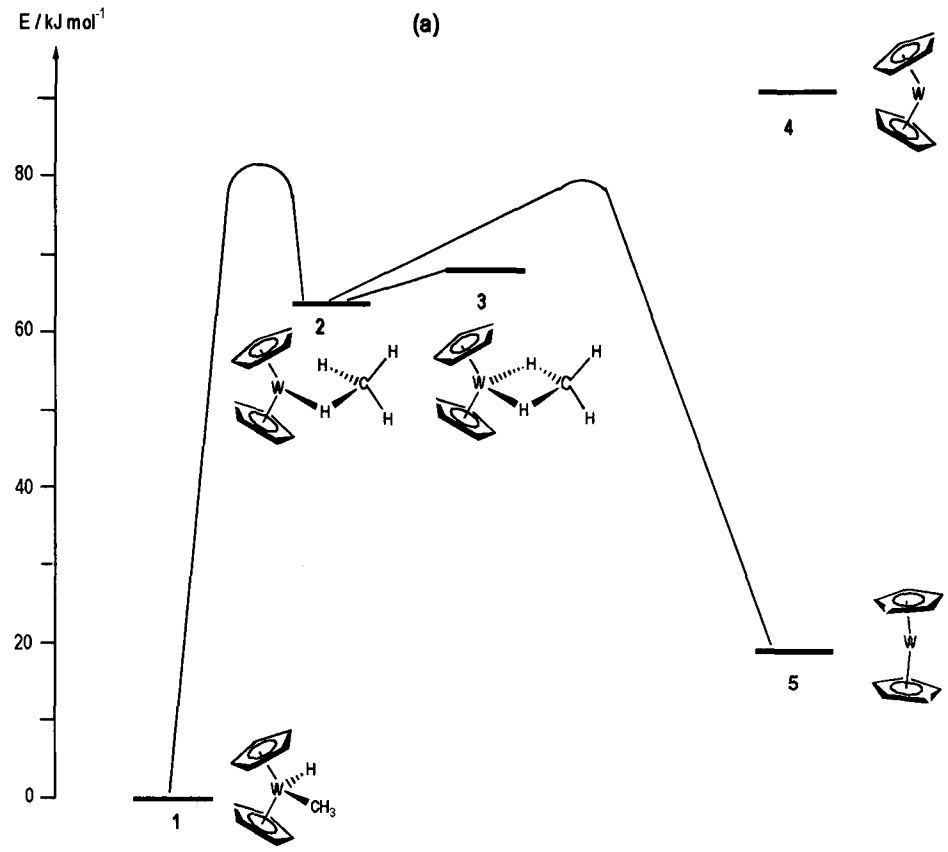

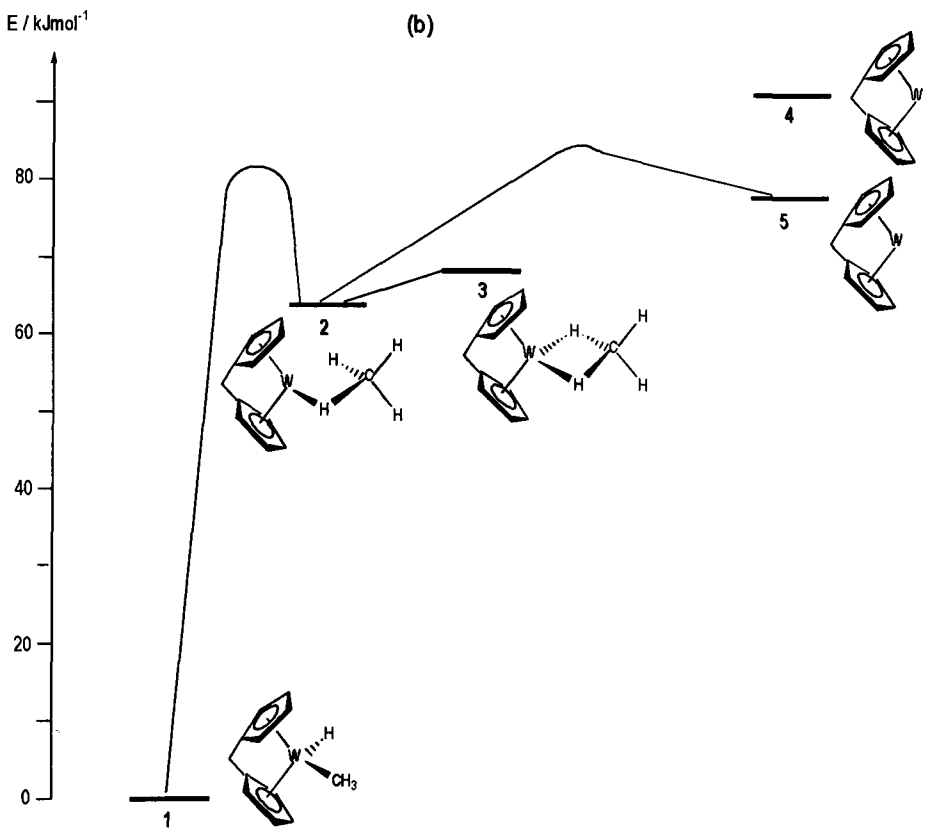

Legend 1 Methyl hydride complex, **2** η^1 σ-complex, **3** η^2 σ-complex, **4** singlet tungstenocene, **5** triplet tungstenocene

Figure 1.14 Energy scheme for methane elimination from **(a)** $[W(\eta\text{-}C_5H_5)_2(Me)H]$ and **(b)** $[W(\eta\text{-}C_5H_4\text{-}CH_2\text{-}\eta\text{-}C_5H_4)(Me)H]$

1.6 General principles of synthesis of *ansa* metallocenes

ansa Metallocenes are most commonly synthesised by treatment of the appropriate metal chloride with a main group element salt of the *ansa bis*cyclopentadienide system. The main group element of choice is usually lithium although other group 1 metal salts and Grignard reagents are also commonly used. A typical reaction is illustrated in **Figure 1.15**. For the group 4 transition metals this is a straightforward, high yield reaction.[44]

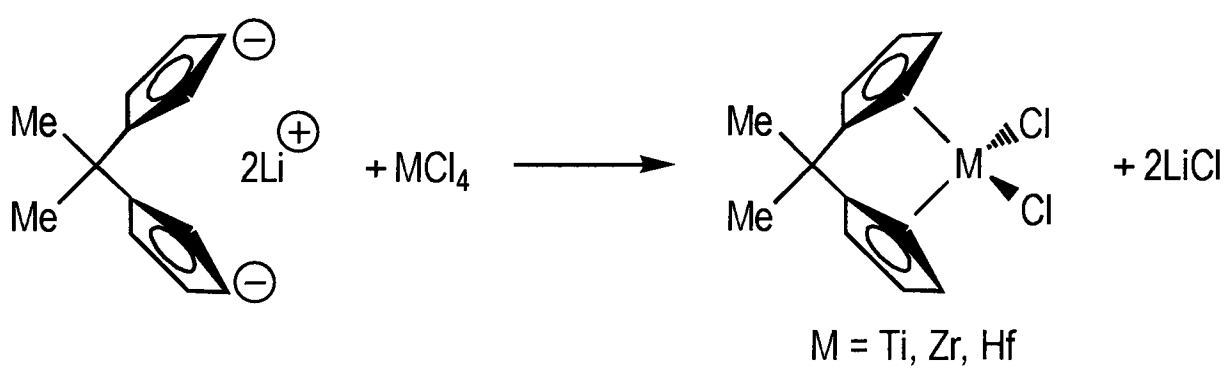

Figure 1.15 Synthesis of a group 4 *ansa bis*-η-cyclopentadienyl compound

However, for group 6 elements considerable difficulty is experienced and poor yields of the desired compounds are common. Although the general principles remain the same, the choice of solvent, temperature of addition, choice of main group element and indeed choice of starting transition metal halide are all crucial. The introduction of molecular strain derived from the *ansa* ligand may be partly responsible for the low yields obtained. A further complication is the formation of unidentified material presumed to be oligomeric. This material has not yet been characterised but can be a dominant product.

One successful synthesis of the group 6 *ansa* metallocene [W(η-C_5H_4-CMe_2-η-C_5H_4)Cl_2], in modest yield (35 %), was achieved by adding a large volume of diethyl

ether to a mixture of the solids [Li(C_5H_4-CMe_2-C_5H_4)Li] and [WCl_4(DME)]. This procedure is analogous to that used by Persson and Andersson[45] for the synthesis of [W(η-C_5H_5)$_2Cl_2$], which gives the crude product as a brown solid, insoluble in diethyl ether, which is then purified by Soxhlet extraction. It is not clear why this particular approach is successful.

Once formed the group 6 *ansa* metallocene halides appear to be quite robust, can be handled with relative ease and, to a substantial extent, can be derivatised in a manner analogous to their non *ansa* counterparts. A scheme showing a range of *ansa* metallocene derivatives of tungsten is shown in **Figure 1.16**.[46]

It is also possible to employ neutral *ansa* ligands in the preparation of *ansa* metallocene derivatives. The amine elimination reaction between group 4 metal *tetrakis*amides and neutral *ansa* ligands under fairly rigorous conditions has been successful for the group 4 metals.[47-49] An example is illustrated in **Figure 1.17**.[47]

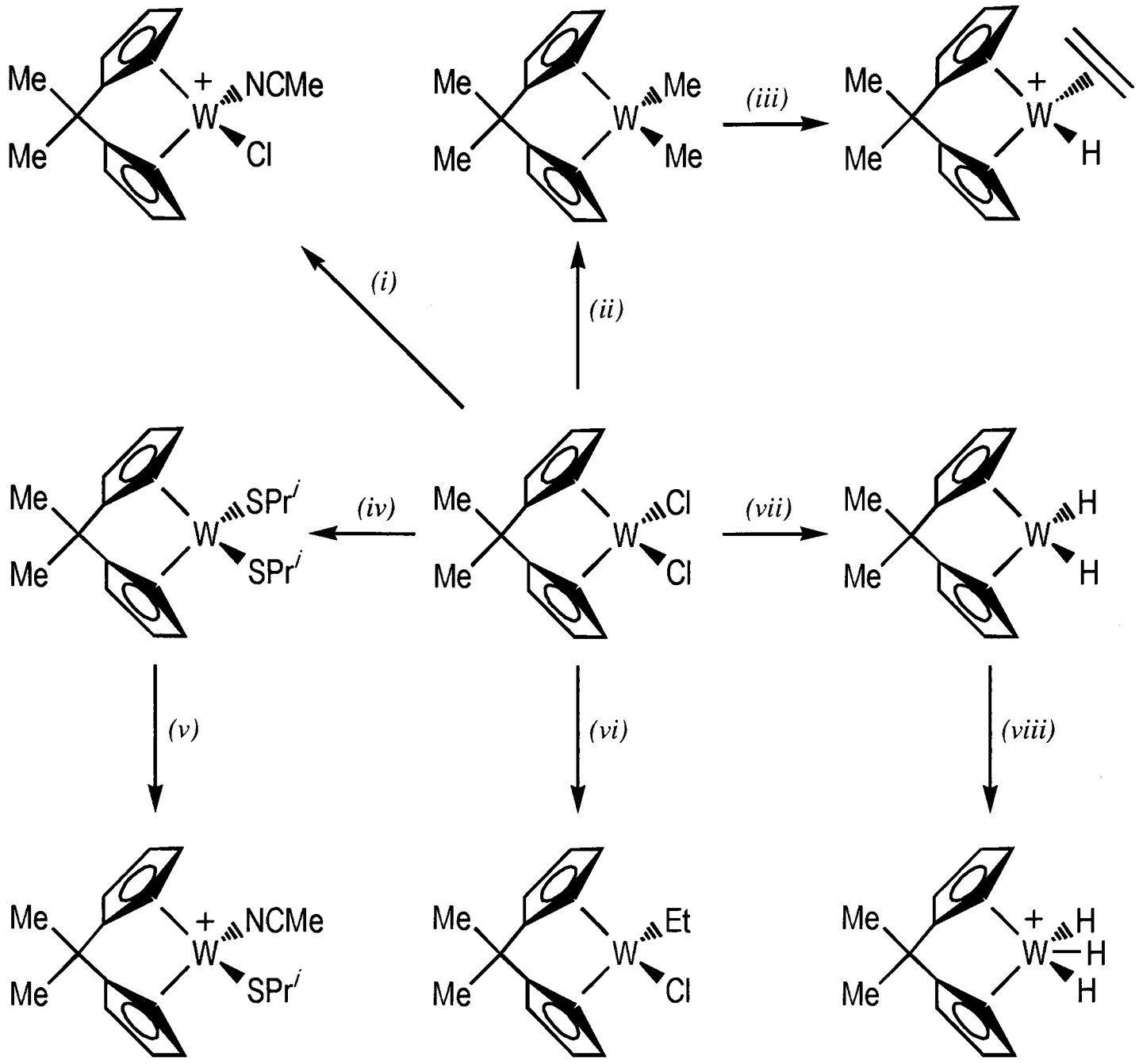

Reagents: *(i)* $TlPF_6$ in CH_3CN; *(ii)* $ZnMe_2$ in $PhCH_3$;
(iii) $[Ph_3C][B(C_6F_5)_4]$; *(iv)* $NaSPr^i$ in EtOH; *(v)* $NOBF_4$, CH_3CN;
(vi) $(EtAlCl_2)_2$ in $PhCH_3$; *(vii)* $LiBEt_3H$ in THF; *(viii)* HCl, NH_4PF_6

Figure 1.16 Some *ansa* metallocene derivatives of tungsten.

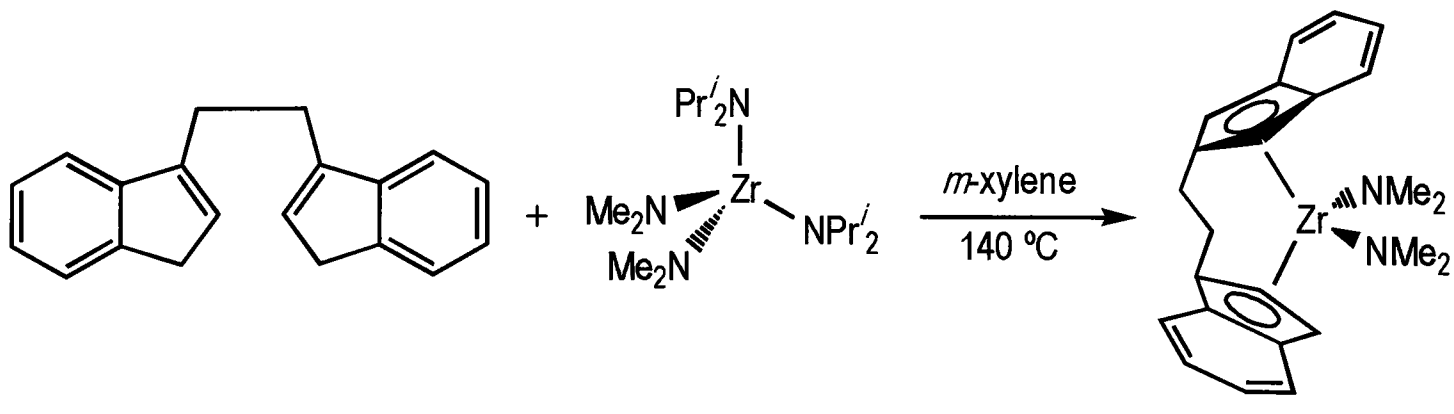

Figure 1.17 Preparation of an *ansa* complex by amine elimination

1.7 A brief survey of *ansa* metallocenes of the early transition metals

By virtue of the fact that the *ansa bis*-η-cyclopentadienyl system contributes ten electrons to the metal centre the derivatives which obey the eighteen electron rule are effectively limited to the early transition metals. *ansa* Bridged ferrocenes (ferrocenophanes) are included in this class but there is no possibility for further functionalisation with the neutral molecules. At the outset of the work described in this thesis the known chemistry of *ansa* metallocenes of group 4 metals was extensive,[44] group 5 was largely unexplored, a number of *ansa* metallocenes of group 6 metals were known[36, 46, 50-52] and there were no examples of group 7 *ansa* metallocenes. Very recently, in this laboratory, the group 7 *ansa* metallocene, [Re(η-C_5H_4-CMe_2-η-C_5H_4)Cl], was prepared for the first time.[53]

The small number of *ansa bis*-η-cyclopentadienyl compounds of group 5 known at the outset of this work are listed in **Table 1.2**. Those which have been reported during the course of this work are listed in **Table 1.3**.

Compound	Reference
[V(η-C_5H_4-C_2Me_4-η-C_5H_4)Cl_2]	54
[V(η-C_5H_4-C_2Me_4-η-C_5H_4)Cl]	
[V(η-C_5H_4-C_2Me_4-η-C_5H_4)L_2][X]	
L = $CNBu^t$, X = Cl; L = CO, X = BPh_4	
[V{η-C_5H_3-$(C_2H_4)_2$-η-C_5H_3}Cl_2]	55

Table 1.2 Group 5 *ansa bis*-η-cyclopentadienyl compounds known at the outset of this work

Compound	Reference
[Nb(η-C_5H_4-$SiMe_2$-η-C_5H_4)Cl_2]	56
[Nb(η-C_5H_4-$SiMe_2$-η-C_5H_4)(RCCR)Cl] R = Me, Ph	
[M(η-C_5H_4-CMe_2-η-C_5H_4)(NBu^t)X]	2
M = V, X = Cl; M = Ta, X = Cl, Me	
[M(η-C_5H_4-CMe_2-η-C_5H_4)(NAr)Cl]	57
[M(η-C_5H_4-CMe_2-η-C_5H_4)(NAr)$NHMe_2$][BPh_4]	
M = Nb, Ta; Ar = 2,6-$Pr^i_2C_6H_4$	
[V(η-$C_5H_2Me_2$-C_6H_4-C_6H_4-η-$C_5H_2Me_2$)Cl_2]	58
[V(η-$C_5H_2Me_2$-C_6H_4-C_6H_4-η-$C_5H_2Me_2$)($CNBu^t$)$_2$][Cl]	

Table 1.3 Group 5 *ansa bis*-η-cyclopentadienyl compounds reported during the course of this work

A small number of group 5 compounds containing an *ansa bis*cyclopentadienyl ligand in the η^5:η^1 coordination mode are also known,[57, 59] along with a number of *ansa* bridged η-cyclopentadienyl imido derivatives.[24-27] A dimeric *bis*-η-cyclopentadienyl niobium system containing the {$SiMe_2OSiMe_2$} bridging unit has also been reported.[60]

It was decided to search for further examples of the *ansa effect* amongst the under-developed class of *ansa* group 5 metallocene derivatives in order to improve our understanding of the stereoelectronic consequences of the *ansa* bridge.

There is a rich chemistry of unbridged niobocene derivatives to be found in the literature[61] and there is a long history of niobocene chemistry in this group. Also, at the start of this work, no examples of *ansa bis*-η-cyclopentadienyl niobium compounds had yet been published. Therefore, the *ansa* chemistry of niobium was the logical starting point for this investigation.

References for Chapter 1

1. N. J. Bailey, M. L. H. Green, M. A. Leech, J. F. Saunders and H. M. Tidswell, *J. Organomet. Chem.*, 1997, **538**, 111.

2. N. J. Bailey, J. A. Cooper, H. Gailus, M. L. H. Green, J. T. James and M. A. Leech, *J. Chem. Soc., Dalton Trans.*, 1997, 3579.

3. G. Wilkinson, M. Rosenblum, M. C. Whiting and R. B. Woodward, *J. Am. Chem. Soc.*, 1952, **74**, 2125.

4. E. O. Fischer and W. Pfab, *Z. Naturforsch.*, 1952, **7b**, 377.

5. see for example G. Wilkinson, F. G. A. Stone and E. W. Abel, *Comprehensive Organometallic Chemistry,* Pergamon Press, Oxford, 1982.

6. D. S. Breslow and N. R. Newburg, *J. Am. Chem. Soc.*, 1957, **79**, 5072.

7. see for example H. Sinn and W. Kaminsky, *Adv. Organomet. Chem.*, 1980, **18**, 99.

8. M. L. H. Green, L. Pratt and G. Wilkinson, *J. Chem. Soc.*, 1958, 3916.

9. E. O. Fischer and Y. Hristidu, *Z. Naturforsch.*, 1960, **15b**, 135.

10. A. D. Liehr, *Naturwissenschaft,* 1957, **44**, 61.

11. M. L. H. Green, J. A. McCleverty, L. Pratt and G. Wilkinson, *J. Chem. Soc.*, 1961, 4854.

12. M. Gerloch and R. Mason, *J. Chem. Soc.*, 1965, 296.

13. C. J. Ballhausen and J. P. Dahl, *Acta. Chem. Scand.*, 1961, **15**, 1333.

14. R. L. Cooper, M. L. H. Green and J. T. Moelwyn-Hughes, *J. Organomet. Chem.*, 1965, **3**, 261.

15. N. W. Alcock, *J. Chem. Soc. (A)*, 1967, 2001.

16. J. C. Green, M. L. H. Green and C. K. Prout, *J. Chem. Soc., Chem. Commun.*, 1972, 421.

17. J. W. Lauher and R. Hoffmann, *J. Am. Chem. Soc.*, 1976, **98**, 1729.

18. J. C. Green, *Chem. Soc. Rev.*, 1998, in press.

19. P. Cossee, *Tetrahedron Lett.*, 1960, **17**, 12.

20. P. Cossee, *J. Catal.*, 1964, **3**, 80.

21. M. Brookhart and M. L. H. Green, *J. Organomet. Chem.*, 1983, **250**, 395.

22. A. Lüttringhaus and H. Gralheer, *Annalen der Chemie*, 1942, **550**, 67.

23. J. A. Smith, J. von Seyerl, G. Huttner and H. H. Brintzinger, *J. Organomet. Chem.*, 1979, **173**, 175.

24. D. M. Antonelli, M. L. H. Green and P. Mountford, *J. Organomet. Chem.*, 1992, **438**, C4.

25. W. A. Herrmann and W. Baratta, *J. Organomet. Chem.*, 1996, **506**, 357.

26. D. M. Antonelli, P. T. Gomes, M. L. H. Green, A. M. Martins and P. Mountford, *J. Chem. Soc., Dalton Trans.*, 1997, 2435.

27. P. T. Gomes, M. L. H. Green, A. M. Martins and P. Mountford, *J. Organomet. Chem.*, 1997, **541**, 121.

28. V. C. Gibson, C. Redshaw, W. Clegg, M. R. J. Elsegood, U. Siemeling and T. Türk, *J. Chem. Soc., Dalton Trans.*, 1996, 4513.

29. K. L. Rhinehart and R. J. Curby, *J. Am. Chem. Soc.*, 1957, **79**, 3290.

30. M. Hillman and A. J. Weiss, *J. Organomet. Chem.*, 1972, **42**, 123.

31. R. M. Shaltout, J. Y. Corey and N. P. Rath, *J. Organomet. Chem.*, 1995, **503**, 205.

32. J. A. Ewen, *J. Am. Chem. Soc.*, 1984, **106**, 6355.

33. W. Kaminsky, K. Külper, H. H. Brintzinger and F. R. W. P. Wild, *Angew. Chem. Int. Ed. Engl.*, 1985, **24**, 507.

34. S. L. J. Conway, T. Dijkstra, L. H. Doerrer, J. C. Green, M. L. H. Green and A. H. H. Stephens, *J. Chem. Soc., Dalton Trans.*, 1998, in press.

35. T. K. Woo, L. Fan and T. Ziegler, *Organometallics*, 1994, **13**, 2252.

36. L. Labella, A. Chernega and M. L. H. Green, *J. Chem. Soc., Dalton Trans.*, 1995, 395.

37. M. L. H. Green, *Pure Appl. Chem*, 1978, **50**, 27.

38. P. Grebenik, A. J. Downs, M. L. H. Green and R. N. Perutz, *J. Chem. Soc., Chem. Commun.*, 1979, 742.

39. N. J. Cooper, M. L. H. Green and R. Mahtab, *J. Chem. Soc., Dalton Trans.*, 1979, 1557.

40. R. M. Bullock, C. E. L. Headford, K. M. Hennessy, S. E. Kegley and J. R. Norton, *J. Am. Chem. Soc.*, 1989, **111**, 3897.

41. A. Chernega, J. Cook, M. L. H. Green, L. Labella, S. J. Simpson, J. Souter and A. H. H. Stephens, *J. Chem. Soc., Dalton Trans.*, 1997, 3225.

42. J. A. Smith and H. H. Brintzinger, *J. Organomet. Chem.*, 1981, **218**, 159.

43. J. C. Green and C. N. Jardine, *J. Chem. Soc., Dalton Trans.*, 1998, 1057.

44. see for example R. L. Halterman, *Chem. Rev.*, 1992, **92**, 965.

45. C. Persson and C. Andersson, *Organometallics*, 1993, **12**, 2370.

46. J. Souter, *D. Phil. Thesis*, University of Oxford, 1996.

47. G. M. Diamond, R. F. Jordan and J. L. Petersen, *Organometallics*, 1996, **15**, 4030.

48. J. N. Christopher, G. M. Diamond, R. F. Jordan and J. L. Petersen, *Organometallics*, 1996, **15**, 4038.

49. G. M. Diamond, R. F. Jordan and J. L. Petersen, *Organometallics*, 1996, **15**, 4045.

50. H. G. Alt, S. J. Palackal and R. D. Rogers, *J. Organomet. Chem.*, 1990, **388**, 105.

51. H. G. Alt, J. S. Han and R. D. Rogers, *J. Organomet. Chem.*, 1993, **445**, 115.

52. T. Mise, M. Maeda, T. Nakajima, K. Kobayashi, I. Shimizu, Y. Yamamoto and Y. Wakatsuki, *J. Organomet. Chem.*, 1994, **473**, 155.

53. M. L. H. Green and A. H. H. Stephens, 1998, unpublished results.

54. B. Dorer, J. Diebold, O. Weyand and H. H. Brintzinger, *J. Organomet. Chem.*, 1992, **427**, 245.

55. B. Dorer, M.-H. Prosenc, U. Rief and H. H. Brintzinger, *Organometallics,* 1994, **13**, 3868.

56. A. Antiñolo, M. Martinez-Ripoll, Y. Mugnier, A. Otero, S. Prashar and A. M. Rodriguez, *Organometallics,* 1996, **15**, 3241.

57. W. A. Herrmann, W. Baratta and E. Herdtweck, *J. Organomet. Chem.,* 1997, **541**, 445.

58. M. E. Huttenloch, B. Dorer, U. Rief, M.-H. Prosenc, K. Schmidt and H. H. Brintzinger, *J. Organomet. Chem.,* 1997, **541**, 219.

59. A. N. Chernega, M. L. H. Green and A. G. Suárez, *Can. J. Chem.,* 1995, **73**, 1157.

60. D. A. Lemenovskii, V. P. Fedin, A. V. Aleksandrov, Yu. L. Slovohotov and Yu. T. Struchkov, *J. Organomet. Chem.,* 1980, **201**, 257.

61. J. A. Labinger, in *Comprehensive Organometallic Chemistry* (G. Wilkinson, F. G. A. Stone and E. W. Abel, eds.), Pergamon Press, Oxford, 1982.

Chapter 2

Synthesis of *ansa* complexes from niobium(IV) chloride

2.1 Introduction to Chapter 2

This chapter describes new *ansa* metallocene complexes prepared from the niobium(IV) complex [$NbCl_4$.2THF].

As was stated in the introductory chapter, the aim of this thesis was to prepare *ansa* bridged group 5 compounds in order to examine structure and reactivity relationships between *ansa* and non *ansa* analogues. Many known *bis*cyclopentadienyl niobium compounds have been prepared from the niobium(IV) compound [$Nb(\eta\text{-}C_5H_5)_2Cl_2$]. An *ansa* analogue of [$Nb(\eta\text{-}C_5H_5)_2Cl_2$] was therefore the obvious choice for a starting point into this chemistry. A ligand system containing a single carbon atom bridging unit was chosen since this is known to produce marked structural differences. It was hoped that this strategy would lead to the discovery of further examples of the *ansa effect.*

The compounds [$Nb(\eta\text{-}C_5H_4\text{-}CMe_2\text{-}\eta\text{-}C_5H_4)X_2$] ($X_2$ = Cl_2, η^2-BH_4 and {SPh}$_2$) were first prepared and partly characterised by H. M. Tidswell of this laboratory.[1] The initial aim was to improve synthetic routes to these compounds and obtain complete characterising data.

2.2 Preparation of [$Nb(\eta\text{-}C_5H_4\text{-}CMe_2\text{-}\eta\text{-}C_5H_4)Cl_2$] (1)

The unbridged niobocene dichloride, [$Nb(\eta\text{-}C_5H_5)_2Cl_2$], has been known for many years. Various procedures for its synthesis have been reported. For example, the action of NaCp on $NbCl_5$ followed treatment with HCl in diethyl ether and sublimation of the final product gives 41 % yield of [$Nb(\eta\text{-}C_5H_5)_2Cl_2$] on a 5 g scale.[2]

In a later report, treatment of $NbCl_5$ with TlCp followed by extraction with concentrated HCl in air gives a red orange solution which, after reduction with $SnCl_2$, gives large brown crystals of $[Nb(\eta\text{-}C_5H_5)_2Cl_2]$ in 40 % yield.[3] A modification of the latter method, involving oxidation by liquid bromine during the extraction stage, gives a 75 % yield of $[Nb(\eta\text{-}C_5H_5)_2Cl_2]$ on a 40 g scale in a one-day procedure.[4, 5] It is clear from the success of these procedures that the unbridged *bis*cyclopentadienyl niobium system is very robust.

However, it was suspected that the desired strained *ansa* metallocene $[Nb(\eta\text{-}C_5H_4\text{-}CMe_2\text{-}\eta\text{-}C_5H_4)Cl_2]$ would not survive the vigorous reaction conditions described above. Therefore preliminary investigations focused on the metathesis reaction between $[NbCl_4.2THF]$, in which the metal centre already has a d^1 electronic configuration, and the dianion of an *ansa* ligand.

2.2.1 Preparation of $[NbCl_4.2THF]$

$[NbCl_4.2THF]$ is conveniently prepared by reduction of $NbCl_5$ with aluminium powder in acetonitrile followed by addition of THF according to the method of Manzer.[6] The yellow powder is indefinitely stable at room temperature under an inert atmosphere. It has a low solubility in common organic solvents, being insoluble in THF and only sparingly soluble in dichloromethane.

2.2.2 Preparation of [K(C_5H_4-CMe_2-C_5H_4)K]

The neutral ligand [C_5H_5-CMe_2-C_5H_5] is prepared from the reaction between 6,6-dimethylfulvene and cyclopentadiene monomer in the presence of sodium hydroxide, according to the method published by Nifant'ev (**Figure 2.1**).[7] The resulting orange oil is purified by vacuum distillation. Subsequent treatment with potassium hydride in THF gives [K(C_5H_4-CMe_2-C_5H_4)K] as a pyrophoric cream-coloured powder.

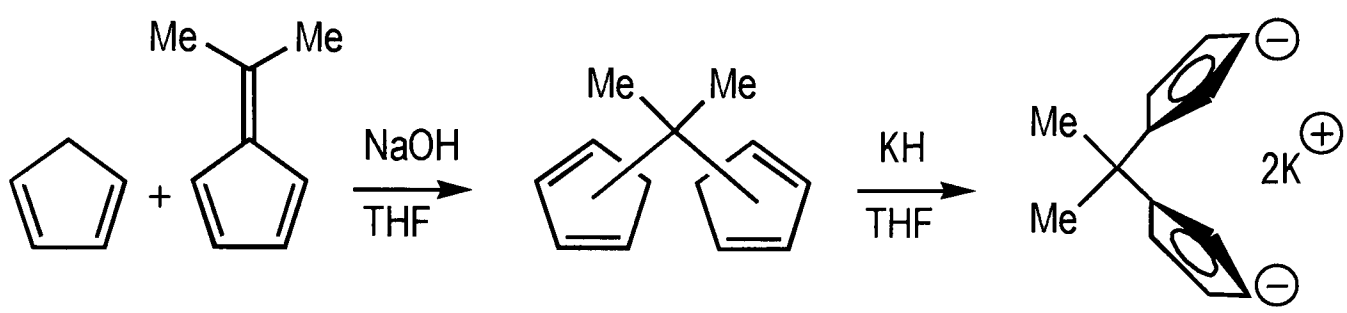

Figure 2.1 Preparation of [K(C_5H_4-CMe_2-C_5H_4)K]

2.2.3 Preparation of [Nb(η-C_5H_4-CMe_2-η-C_5H_4)Cl_2] (1)

First attempts at the preparation of [Nb(η-C_5H_4-CMe_2-η-C_5H_4)Cl_2] centred on the reaction between the lithium reagent, [Li(C_5H_4-CMe_2-C_5H_4)Li], and [$NbCl_4$.2THF].[1] This reaction was difficult to reproduce and the yields were poor. Substitution of lithium by potassium gave better and more reproducible yields. Otero and co-workers, who independently published the synthesis of the analogous silicon-bridged complex, [Nb(η-C_5H_4-$SiMe_2$-η-C_5H_4)Cl_2],[8] during the course of this work, also mentioned a lack of success when using the lithium reagent and their procedure employed [Tl(C_5H_4-$SiMe_2$-C_5H_4)Tl].

The reaction between equimolar amounts of $[K(C_5H_4\text{-}CMe_2\text{-}C_5H_4)K]$ and $[NbCl_4.2THF]$ in THF at room temperature produces a purple-brown solution from which, after removal of the solvent and Soxhlet extraction into dichloromethane, purple crystals of $[Nb(\eta\text{-}C_5H_4\text{-}CMe_2\text{-}\eta\text{-}C_5H_4)Cl_2]$ (**1**) are isolated (**Figure 2.2**). Elemental analysis data for a sample of these crystals confirms the expected empirical formula. A further quantity of crude product is obtained by removal the volatiles from the mother liquor of the Soxhlet extraction. The yield obtained for compound **1** is *ca.* 55% which is comparable to that reported for $[Nb(\eta\text{-}C_5H_4\text{-}SiMe_2\text{-}\eta\text{-}C_5H_4)Cl_2]$.[8]

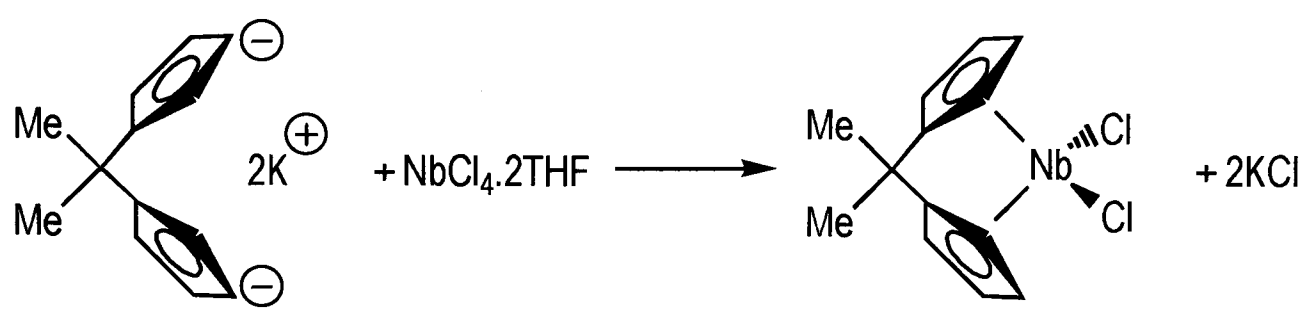

Figure 2.2 Preparation of $[Nb(\eta\text{-}C_5H_4\text{-}CMe_2\text{-}\eta\text{-}C_5H_4)Cl_2]$ (**1**)

The compound **1** slowly decomposes in air and is only slightly soluble in dichloromethane and tetrahydrofuran and is insoluble in toluene. The reaction appears to be heterogeneous and, in addition to the desired product, gives an amount of insoluble material which is presumed to be oligomeric in nature. Compound **1** sublimes at 180 °C under a reduced pressure of 10^{-3} mmHg but involatile decomposition products are also formed and thus sublimation is not an efficient method for purification of the bulk material.

The EPR spectrum of compound **1** shows ten lines, as expected for an unpaired electron mainly located at the ^{93}Nb ($I = {}^9/_2$) nucleus, with a value of $g_{iso} = 1.992$ and a hyperfine splitting $|a_{iso}| = 90.5$ G, analogous to data reported for unbridged niobocene

dichloride.[9] For comparison, the EPR spectrum reported for [Nb(η-C_5H_4-$SiMe_2$-η-C_5H_4)Cl_2] gives a value of g_{iso} = 2.0034 and $|a_{iso}|$ = 100.0 G.

The Electron Impact ionisation mass spectrum shows a peak due to the parent ion. The IR spectrum of compound **1** contains two bands in the region expected for Nb–Cl stretching vibrations. These are assigned by analogy to the spectrum of [$NbMe_3Cl_2$].[10] In [$NbMe_3Cl_2$] the antisymmetric Nb–Cl stretching band occurs at 377 cm^{-1} in the IR spectrum and the symmetric stretching band at 328 cm^{-1} in the Raman spectrum. Therefore, bands at 352 cm^{-1} and 338 cm^{-1} in the spectrum of compound **1** are tentatively assigned as the antisymmetric and symmetric Nb–Cl stretching modes respectively. IR frequencies in the same region for unbridged [Nb(η-C_5H_5)$_2Cl_2$], reported without assignment,[5] are 308 (m), 290 (s) and 268 (s) cm^{-1}.

Various attempts were made to grow single crystals of **1** for X-ray crystallography. However, its solubility is very low and powders precipitated from the most concentrated solutions which could be made in all the commonly used solvents. Both slow cooling from room temperature to temperatures down to –80 °C, and cooling of boiling solutions down to room temperature were tried. A few less commonly used solvents were employed, including chlorobenzene and *tertiary*-butyl alcohol, in both of which **1** is insoluble even at the boiling point, and 1,2-dichloroethane, in which **1** is very sparingly soluble.

2.3 Preparation of [Nb(η-C_5H_4-CMe_2-η-C_5H_4)(η^2-BH_4)] (2)

Treatment of the compound **1** with lithium borohydride in 1,2-dimethoxyethane at room temperature, according to the equation below,[5] gives green, air sensitive crystals of the borohydride compound [Nb(η-C_5H_4-CMe_2-η-C_5H_4)(η^2-BH_4)] (**2**) in moderate yield.

$$2\ [Nb(\eta\text{-}C_5H_4\text{-}CMe_2\text{-}\eta\text{-}C_5H_4)Cl_2] + 4\ LiBH_4 \rightarrow$$
$$4\ LiCl + 2\ [Nb(\eta\text{-}C_5H_4\text{-}CMe_2\text{-}\eta\text{-}C_5H_4)(\eta^2\text{-}BH_4)] + H_2 + B_2H_6$$

The IR spectrum of compound **2** contains two bands in the terminal B–H region, at 2461 cm^{-1} and 2419 cm^{-1}, consistent with an η^2 bidentate binding mode for the borohydride ligand.[11, 12] These values agree closely with those obtained for the terminal B–H stretching modes of [Nb(η-C_5H_5)$_2$(η^2-BH_4)],[11] 2460 and 2423 cm^{-1}, and of [Nb(η-C_5Me_5)$_2$(η^2-BH_4)],[13] 2452 and 2428 cm^{-1}.

The ^{1}H NMR (C_6D_6) spectrum of compound **2** (**Figure 2.3**) shows two multiplet resonances for the eight C_5H_4 hydrogens and a singlet assigned to the bridging methyl groups, as expected for a molecule with C_{2v} symmetry.

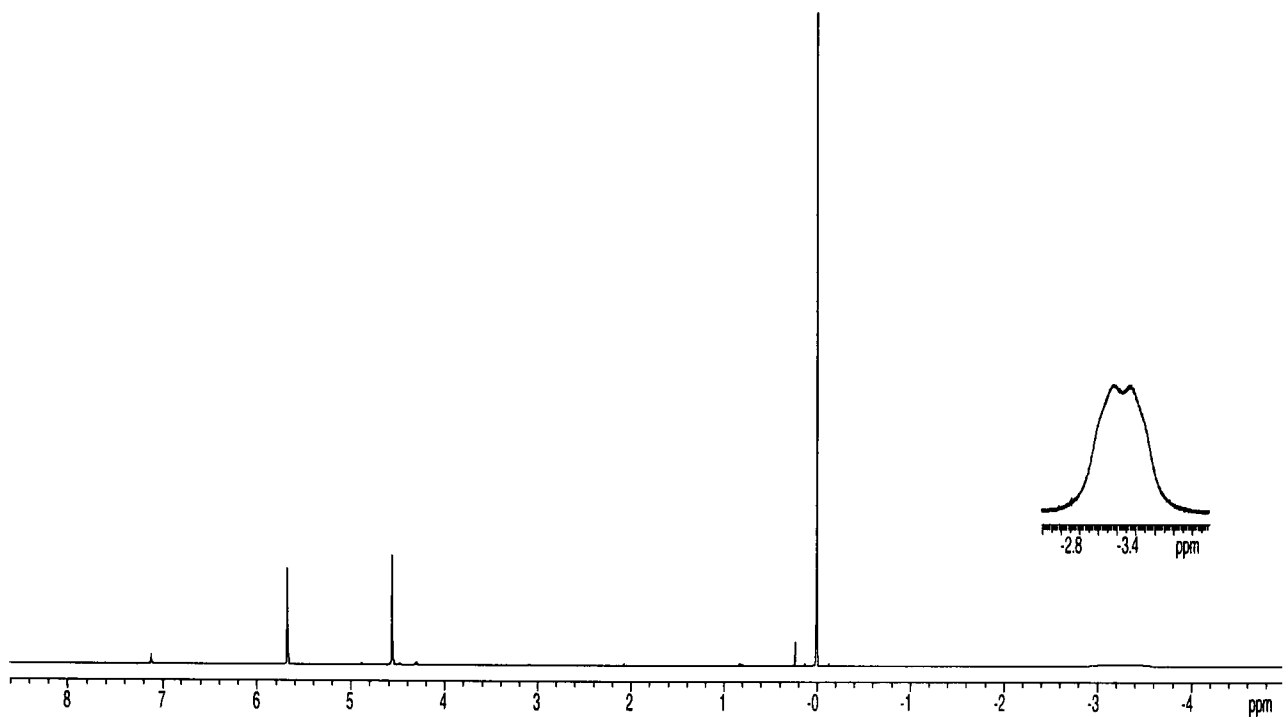

Figure 2.3 ^{1}H NMR (C_6D_6) spectrum of [Nb(η-C_5H_4-CMe_2-η-C_5H_4)(η^2-BH_4)] (**2**)

One very broad resonance (fwhh = 300 Hz) centred at δ –3.2 ppm (J = 85 Hz) is observed for the BH_4 group indicating that the terminal-bridging hydrogen exchange process is rapid on the 500 MHz NMR timescale. The fluxionality is too facile to allow decoalescence to be obtained; no change in this ^{1}H NMR spectroscopic resonance was observed on cooling a d_8-toluene solution to –90 °C. Equivalence of terminal and bridging hydrogens in ^{1}H NMR spectra at ambient temperatures is a common feature for transition metal tetrahydroborate complexes.[12] An exception is found in the unbridged analogue, [Nb(η-C_5H_5)$_2$(η^2-BH_4)], which is at the slow exchange limit at room temperature. The ^{1}H NMR spectrum of [Nb(η-C_5H_5)$_2$(η^2-BH_4)] at room temperature[13] shows separate resonances for the terminal and bridging hydrogens, at δ 5.2 and –18.2 ppm respectively. Coalescence to an average chemical shift of *ca.* –7 ppm begins at 346 K. An activation energy of 61.1 kJ mol^{-1} was calculated for the exchange process. High energy barriers are also found for the

terminal-bridging hydrogen exchange processes in $[Nb(\eta\text{-}C_5Me_5)_2(\eta^2\text{-}BH_4)]$,[13] 68.6 kJ mol^{-1}, and $[Ta(\eta\text{-}C_5Me_5)(\eta\text{-}C_5H_5)(\eta^2\text{-}BH_4)]$,[14] 68.7 kJ mol^{-1}. The terminal-bridging hydrogen exchange processes in the latter compound have been studied by two-dimensional exchange NMR spectroscopy.[14] It was found that there is no direct exchange between the two terminal hydrogens. This was interpreted in terms of an associative mechanism proceeding *via* a $\{Ta(\eta^3\text{-}BH_4)\}$ intermediate accompanied by an $\eta^5 \leftrightarrow \eta^3$ shift of one of the C_5 rings. The rate constants for exchange between either of the distinct terminal hydrogens and the bridging hydrogens in this mixed ring compound were found to be identical within the limits of experimental error. A possible explanation given by the authors for this observation is that the rate-limiting step is coordination of the terminal hydrogens to the metal centre. An associative mechanism for BH_4 scrambling has also been postulated for $[Hf(\eta\text{-}C_5H_4Me)_2(\eta^2\text{-}BH_4)]$ on the basis of structural evidence.[15] As mentioned in **Section 1.4**, calculations predict that the presence of a single atom *ansa* bridge generates a more electron deficient metal centre.[16] Thus, assuming that the associative mechanism is correct, a possible explanation for the observation of rapid bridging-terminal hydrogen exchange in $[Nb(\eta\text{-}C_5H_4\text{-}CMe_2\text{-}\eta\text{-}C_5H_4)(\eta^2\text{-}BH_4)]$ (**2**), and not in $[Nb(\eta\text{-}C_5H_5)_2(\eta^2\text{-}BH_4)]$, is that increased electron deficiency at the niobium centre in the *ansa* compound lowers the energy barrier towards association of a terminal hydrogen and formation of a $\{Nb(\eta^3\text{-}BH_4)\}$ intermediate.

The proton-decoupled ^{13}C NMR (C_6D_6) spectrum of compound **2** contains three singlets in the cyclopentadienyl region, a singlet at δ 32.2 ppm assigned to the bridging quaternary carbon and a singlet at δ 20.9 ppm assigned to the bridging

methyl groups. The ^{1}H coupled ^{11}B NMR (C_6D_6) spectrum is shown in **Figure 2.4**. A binomial quintet centred at δ 23.1 ppm (J = 90 Hz) is observed, as expected for a fluxional BH_4 group.

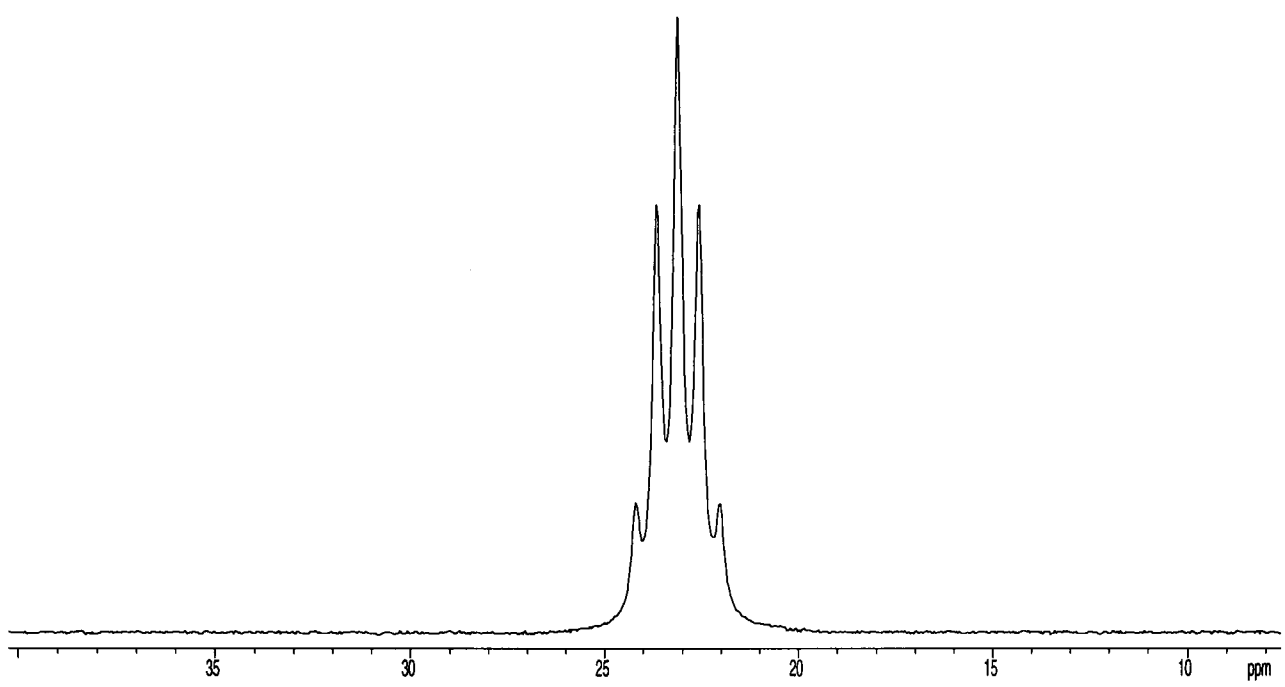

Figure 2.4 ^{11}B NMR (C_6D_6) spectrum of [Nb(η-C_5H_4-CMe_2-η-C_5H_4)(η^2-BH_4)] (**2**)

The Fast Atom Bombardment mass spectrum (NOBA matrix) of compound **2** contains a peak at *m/z* = 280 (base peak) with an envelope in agreement with the correct isotope pattern calculated for M+2. Elemental analysis data were fully consistent with the proposed empirical formula.

Single crystals of compound **2** suitable for an X-ray structure analysis were grown by cooling a solution in petroleum ether (b. p. 100-120 °C) to –80 °C. The crystal structure was determined and the molecular structure is shown, with atomic numbering scheme, in **Figure 2.5**. Selected bond distances and angles are given in **Table 2.1**. Full details of the crystal structure determination are given in **Appendix A**. The compound crystallises in the monoclinic space group *C* 2/*c* and the asymmetric

unit comprises half of the molecule. The remainder of the molecule is generated by the operation (–x, y, ½–z).

All hydrogen atoms were located in difference Fourier maps and their positions were refined. Therefore, the data confidently confirm the assignment of η^2 binding between the borohydride ligand and the metal centre. Inspection of the distances between the niobium atom and the carbon atoms of the cyclopentadienyl rings is informative. The shortest of these is to the *ipso* carbon, Nb(1)–C(4) = 2.26 Å, the carbon atoms adjacent to the *ipso* carbon are at a greater separation from the niobium atom, Nb(1)–C(5) = 2.31 Å, Nb(1)–C(8) = 2.30 Å, and the two carbons opposite the *ipso* carbon are furthest away, Nb(1)–C(6) = 2.42 Å, Nb(1)–C(7) = 2.42 Å. If the metal atom were to be positioned on the vector normal to the plane of the ring and passing through the ring centroid all the niobium-carbon distances would be equal. We may conclude that the *ansa* bridge is pulling the rings away from the metal and opening up the coordination site on the opposite face. This is a general feature of single atom bridged *ansa* compounds.

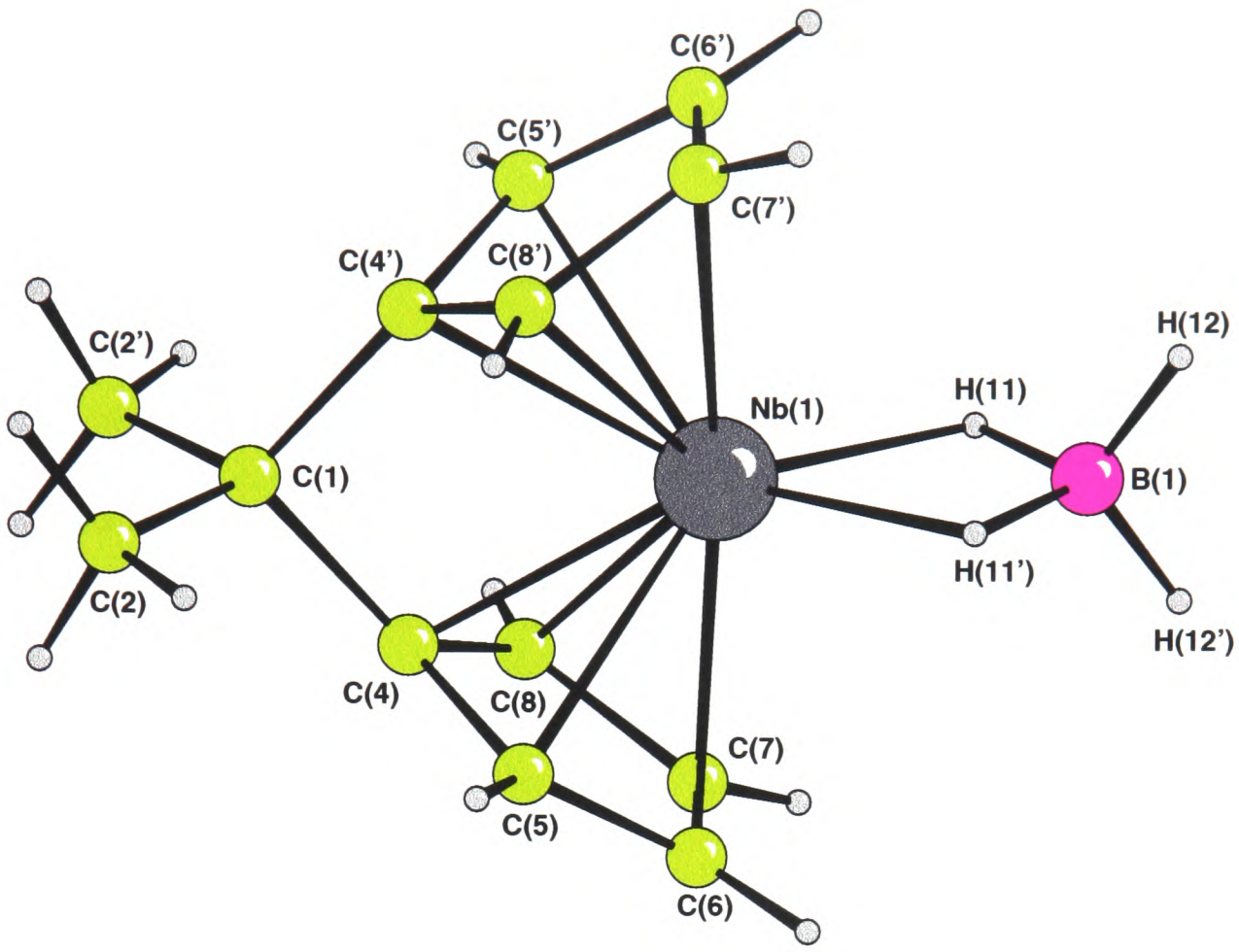

Figure 2.5 The molecular structure of [Nb(η-C_5H_4-CMe_2-η-C_5H_4)(η^2-BH_4)] (**2**). Atoms labelled with a prime are generated by the symmetry operation (–x, y, ½–z). Hydrogen atom labels on the *ansa* ligand are omitted for clarity

Bond	Length / Å	Bond	Angle / °
Nb(1)–C(4)	2.262(4)	C(2)–C(1)–C(2′)	108.5(6)
Nb(1)–C(5)	2.308(5)	C(4)–C(1)–C(4′)	96.9(5)
Nb(1)–C(6)	2.419(5)	H(11)–Nb(1)–H(11′)	64.0(42)
Nb(1)–C(7)	2.418(5)	H(11)–B(1)–H(11′)	110.4(67)
Nb(1)–C(8)	2.302(5)	Bending angle, β	114.1
Nb(1)–H(11)	1.94(7)	Cp_{cent}–Nb(1)–Cp_{cent}, γ	125.0
B(1)–H(11)	1.25(7)	Cp_{cent}–C(4)–C(1)	163.9
B(1)–H(12)	1.07(6)		
Nb(1)–Cp_{cent}	2.01		

Table 2.1 Selected interatomic distances and angles for [Nb(η-C_5H_4-CMe_2-η-C_5H_4)(η^2-BH_4)] (**2**)

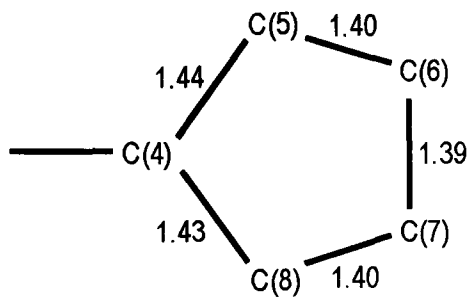

Figure 2.6 Carbon-carbon distances (Å) for the cyclopentadienyl ring of **2**

Figure 2.6 shows the carbon-carbon bond distances around the cyclopentadienyl ring in compound **2**. The bond length between the two carbons opposite the *ipso* carbon is shortened relative to the other carbon-carbon bond lengths. It has been suggested that this is due to a small π-bonding contribution from an η^3-allyl or η^2-olefin resonance structure.[17]

The X-ray crystal structure of the unbridged analogue, $[Nb(\eta\text{-}C_5H_5)_2(\eta^2\text{-}BH_4)]$, has been published,[18] although the quality of the structure determination was low (R = 12.8 %) and a meaningful comparison with that of compound **2** cannot be made. However, it is worth commenting that the angle γ subtended by the two ring centroid to niobium vectors in *ansa* bridged compound **2** is 125° compared to 130° reported for unbridged $[Nb(\eta\text{-}C_5H_5)_2(\eta^2\text{-}BH_4)]$.

2.4 Preparation of [Nb(η-C_5H_4-CMe_2-η-C_5H_4)(PMe_3)H] (3) and [Nb(η-C_5H_4-CMe_2-η-C_5H_4)(PPh_3)H] (4)

The reactions between compound **2** and two equivalents of a tertiary phosphine, PR_3 (R = Me, Ph), at room temperature in light petroleum give the phosphine-hydride complexes [Nb(η-C_5H_4-CMe_2-η-C_5H_4)(PR_3)H] (R = Me **3**, R = Ph **4**) according to the equation below.[5]

$$[Nb(\eta\text{-}C_5H_4\text{-}CMe_2\text{-}\eta\text{-}C_5H_4)(\eta^2\text{-}BH_4)] + 2\ PR_3 \rightarrow [Nb(\eta\text{-}C_5H_4\text{-}CMe_2\text{-}\eta\text{-}C_5H_4)(PR_3)H] + H_3B\text{–}PR_3$$

These complexes were isolated as red crystals in *ca.* 40 % yield. The ^{1}H NMR (C_6D_6) spectra for compounds **3** and **4** are consistent with their formulation as phosphine hydrides. The ^{1}H NMR (C_6D_6) spectrum of **3** is given in **Figure 2.7** and shows peaks due to the *ansa* ligand, a doublet centred at δ 0.82 ppm ($^2J_{PH}$ = 7 Hz) assigned to the coordinated trimethylphosphine ligand and a well resolved doublet centred at δ –5.03 ppm ($^2J_{PH}$ = 39 Hz) assigned to the Nb–H resonance. Similarly, the Nb–H resonance in the ^{1}H NMR (C_6D_6) spectrum of **4** is a doublet at δ –4.11 ppm ($^2J_{PH}$ = 34 Hz). The hydride resonance in the unbridged analogue of **4** appears at δ –6.65 ppm ($^2J_{PH}$ = 27 Hz).[4]

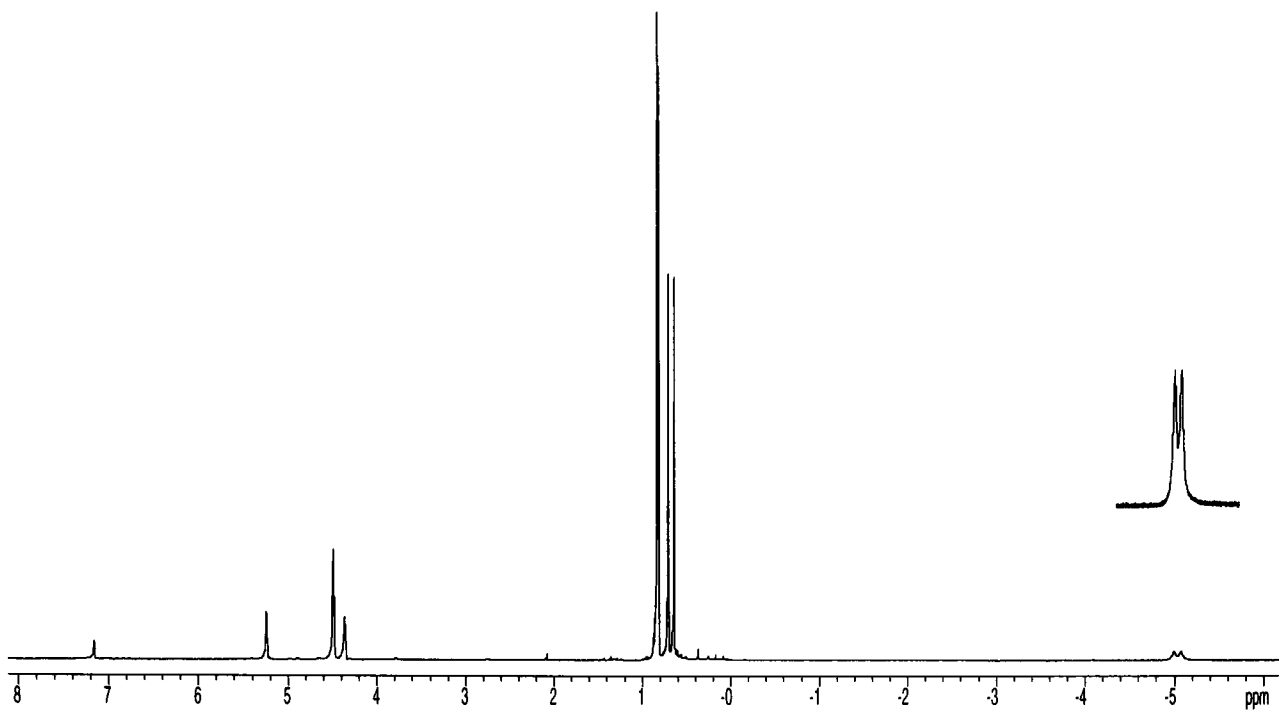

Figure 2.7 ^{1}H NMR (C_6D_6) spectrum of [Nb(η-C_5H_4-CMe_2-η-C_5H_4)(PMe_3)H] (**3**)

The ^{31}P NMR (C_7D_8) spectra each show a broad singlet at room temperature which sharpens considerably on cooling, as expected for a phosphorus nucleus coupling to quadrupolar niobium. However, coupling to the hydride resonance is not resolved at accessible temperatures.

The $^{13}C\{^{1}H\}$ NMR (C_6D_6) spectrum of compound **3** contains five singlets for the cyclopentadienyl rings in the range δ 97.1 - δ 61.6 ppm. Of these resonances, the one at highest field has markedly lower intensity than the others and is assigned to the *ipso* carbon. A doublet ($^{1}J_{PC}$) is expected for the coordinated PMe_3 and two singlets are expected for the bridging methyl groups. The $^{13}C\{^{1}H\}$ spectrum contains four such peaks but they are closely spaced and their intensities do not permit an unambiguous assignment to be made. However, inspection of the cross peaks in a ^{13}C–^{1}H correlation spectrum obtained by the heteronuclear single quantum coherence technique allowed assignment of a doublet centred at δ 23.1 ppm ($^{1}J_{PC}$ = 20 Hz) to

the PMe_3 ligand and two singlets at δ 22.8 ppm and δ 22.4 ppm to the bridging methyl groups. The remaining resonance at δ 33.2 ppm is assigned to the bridgehead quaternary carbon atom by analogy to the $^{13}C\{^1H\}$ NMR spectrum of compound **2**. The $^{13}C\{^1H\}$ NMR (C_6D_6) spectrum of compound **4** is entirely consistent with that of compound **3** and was assigned accordingly.

The IR spectra of **3** and **4** are complex and it is not possible to assign unambiguously the Nb–H stretching frequencies. Despite repeated attempts by both the Electron Impact and Fast Atom Bombardment techniques, meaningful mass spectra could not be obtained. Elemental analysis data are consistent with the proposed empirical formulae.

Single crystals of compound **3** were obtained by the slow cooling of a solution in pentane to –80 °C. The X-ray crystal structure was determined and the molecular structure is shown, with atomic numbering scheme, in **Figure 2.8**. Selected bond distances and angles are given in **Table 2.2**. Full crystallographic details are given in **Appendix B**.

The geometry of the *ansa* ligand in **3** is similar to that observed in **2**; the distance from the ring centroids to the niobium atom and the angles β and γ are very similar. Inspection of the Nb–C distances in compound **3** shows that the rings are prised away from the metal in an unsymmetrical fashion. The ring atoms C(7) and C(12), on the same side of the molecule as the trimethylphosphine ligand, are furthest from the metal.

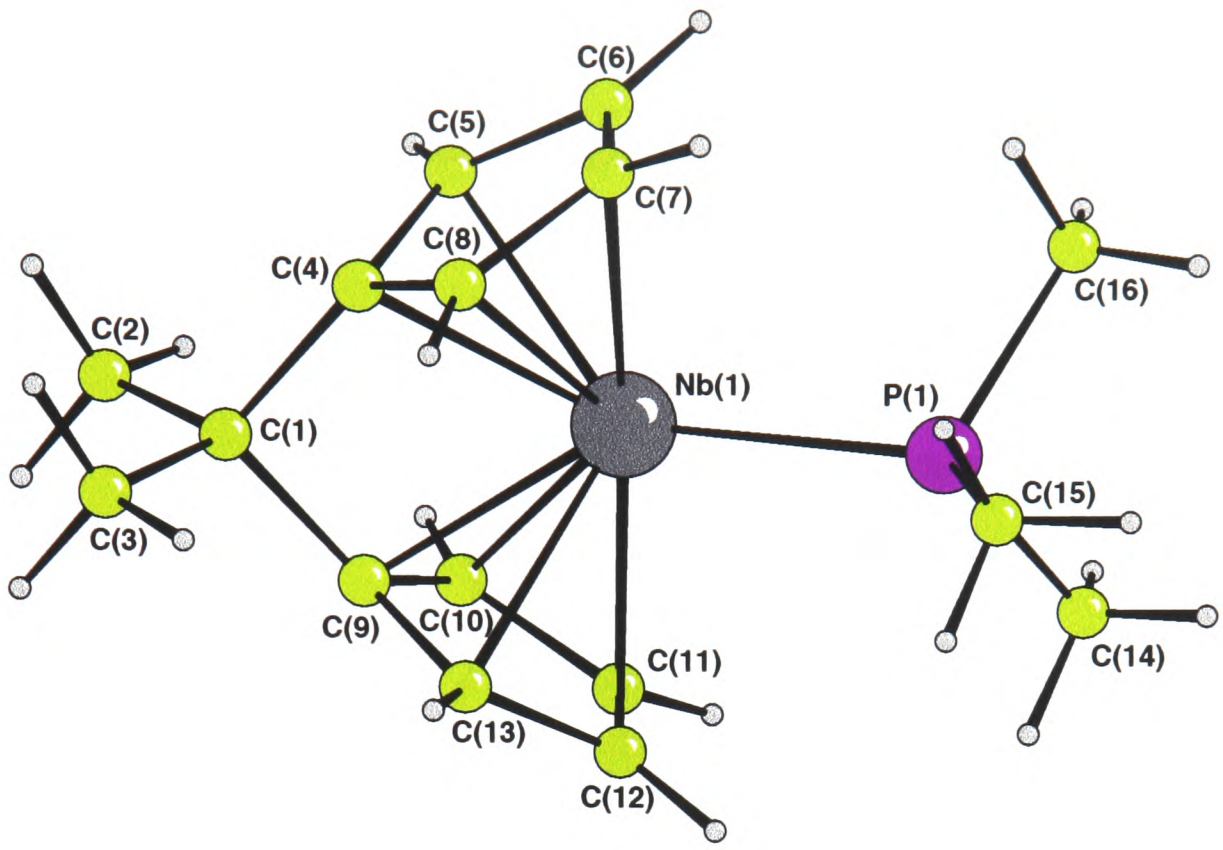

Figure 2.8 The molecular structure of [Nb(η-C_5H_4-CMe_2-η-C_5H_4)(PMe_3)H] (**3**). Hydrogen atom labels are omitted for clarity

Bond	Length / Å	Bond	Angle / °
Nb(1)–P(1)	2.553(2)	C(2)–C(1)–C(3)	109.4(8)
Nb(1)–C(4)	2.273(7)	C(4)–C(1)–C(9)	98.5(6)
Nb(1)–C(5)	2.294(6)	C(1)–Nb(1)–P(1)	156
Nb(1)–C(6)	2.382(7)	Bending angle, β	117.3
Nb(1)–C(7)	2.437(8)	Cp_{cent}–Nb(1)–Cp_{cent}, γ	126.1
Nb(1)–C(8)	2.347(6)	Cp_{cent}–C(4)–C(1)	162.0
Nb(1)–C(9)	2.272(9)	Cp_{cent}–C(9)–C(1)	161.8
Nb(1)–C(10)	2.295(8)		
Nb(1)–C(11)	2.388(8)		
Nb(1)–C(12)	2.434(7)		
Nb(1)–C(13)	2.366(9)		
Nb(1)–Cp_{cent}	2.01, 2.01		

Table 2.2 Selected interatomic distances and angles for [Nb(η-C_5H_4-CMe_2-η-C_5H_4)(PMe_3)H] (**3**)

The dominance of the niobium atom in the electron density map precluded direct location of the hydride ligand but its presence may be inferred from the non-linear phosphorus-niobium-bridging carbon angle, P(1)–Nb(1)–C(1) = 156°, as illustrated in **Figure 2.9**.

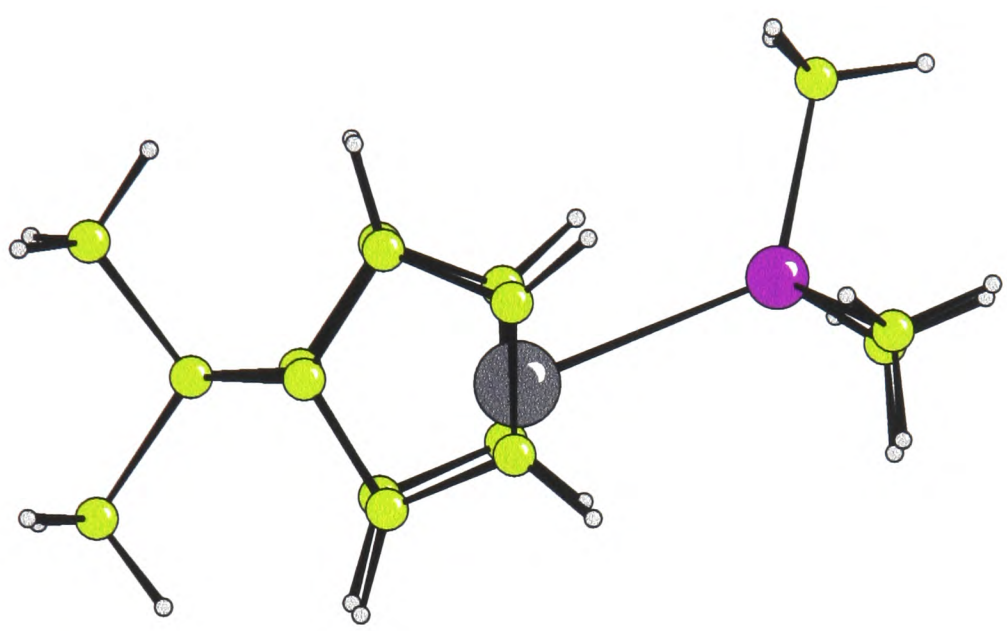

Figure 2.9 The molecular structure of **3** showing the bent geometry caused by the presence of the hydride ligand. As shown, the C(9)-C(13) cyclopentadienyl ring is uppermost

2.5 Preparation of [Nb(η-C_5H_4-CMe_2-η-C_5H_4)(SPh)$_2$] (5)

When compound **1** is treated with two equivalents of NaSPh in THF at reflux for 16 h the corresponding dithiolate, [Nb(η-C_5H_4-CMe_2-η-C_5H_4)(SPh)$_2$] (**5**), is eventually obtained as purple-black crystals (**Figure 2.10**). These crystals slowly decompose if exposed to air. The EPR spectrum of compound **5** shows ten lines, a value of g_{iso} = 1.978, comparable to that for the unbridged analogue,[3] and a hyperfine splitting $|a_{iso}|$ = 115 G. Electron Impact ionisation mass spectrometry showed only peaks due to

decomposition products, the base peak being m/z = 218, corresponding to $[(SPh)_2]^+$. The IR spectrum shows bands due to the Nb–S stretches at 484 cm^{-1} (antisymmetric) and 385 cm^{-1} (symmetric). Analytical data were consistent with the proposed empirical formula.

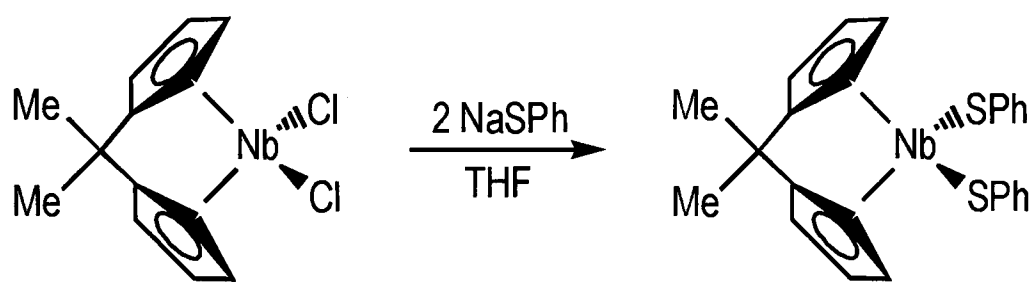

Figure 2.10 Preparation of $[Nb(\eta\text{-}C_5H_4\text{-}CMe_2\text{-}\eta\text{-}C_5H_4)(SPh)_2]$ (**5**)

The crystal structure of the unbridged analogue has been reported.[19] Unfortunately, attempts to grow single crystals of **5** for comparison were unsuccessful.

The preparation of unbridged $[Nb(\eta\text{-}C_5H_5)_2(SPh)_2]$ is reported as a rapid reaction which proceeds in high yield.[3] However, *ansa* bridged **5** was produced only in low yield after prolonged heating of the reaction mixture and its chemistry was not pursued.

2.6 Preparation of $[Nb(\eta\text{-}C_5H_4\text{-}CMe_2\text{-}\eta\text{-}C_5H_4)(CH_2Ph)_2]$ (6)

Alkylation of **1** with two equivalents of $PhCH_2MgBr$ in diethyl ether at room temperature affords the compound $[Nb(\eta\text{-}C_5H_4\text{-}CMe_2\text{-}\eta\text{-}C_5H_4)(CH_2Ph)_2]$ (**6**) as dark red blocks (**Figure 2.11**). The Fast Atom Bombardment mass spectrum of **6** contained peaks corresponding to the molecular ion and to fragmentation products arising from the loss of phenyl or benzyl groups. The parent metallocene $[Nb(\eta\text{-}C_5H_4\text{-}CMe_2\text{-}\eta\text{-}$

$C_5H_4)^+$] was also observed. Analytical data were in accordance with the proposed empirical formula.

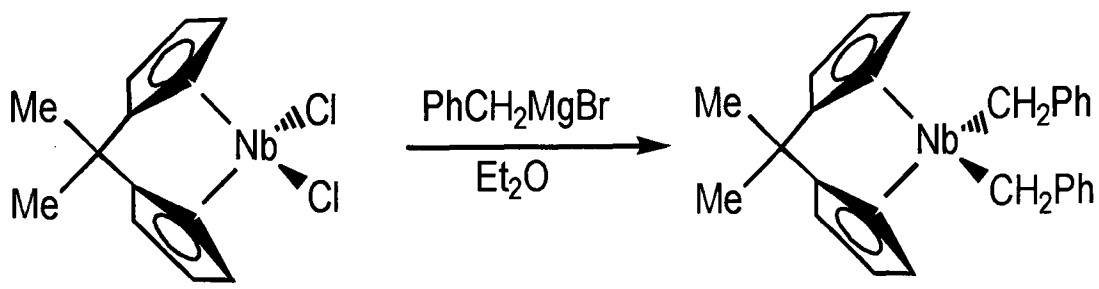

Figure 2.11 Preparation of [Nb(η-C_5H_4-CMe_2-η-C_5H_4)(CH_2Ph)$_2$] (**6**)

The crystals were suitable for X-ray diffraction studies and the crystal structure was solved in the triclinic space group P –1. The molecular structure, along with atom labelling scheme, is shown in **Figure 2.12**. Selected bond distances and angles are given in **Table 2.3**. Full details of the structure determination appear in **Appendix C**.

The structural parameters for **6** reveal similar features to those discussed earlier in this chapter. The metal lies closer to the *ipso* carbon than the carbons on the opposite side of the ring and the C–C bond opposite the *ipso* carbon is shorter than the other ring bonds. The angle between the two benzyl groups, C(14)–Nb(1)–C(21), is 83.0° which is in the range expected for a d^1 metal, where the highest occupied molecular orbital (HOMO) is $1a_1$ (see **Section 1.2**). For example the Cl–Nb–Cl angle in [Nb(η-$C_5H_5)_2Cl_2$] is 85.6°.[20]

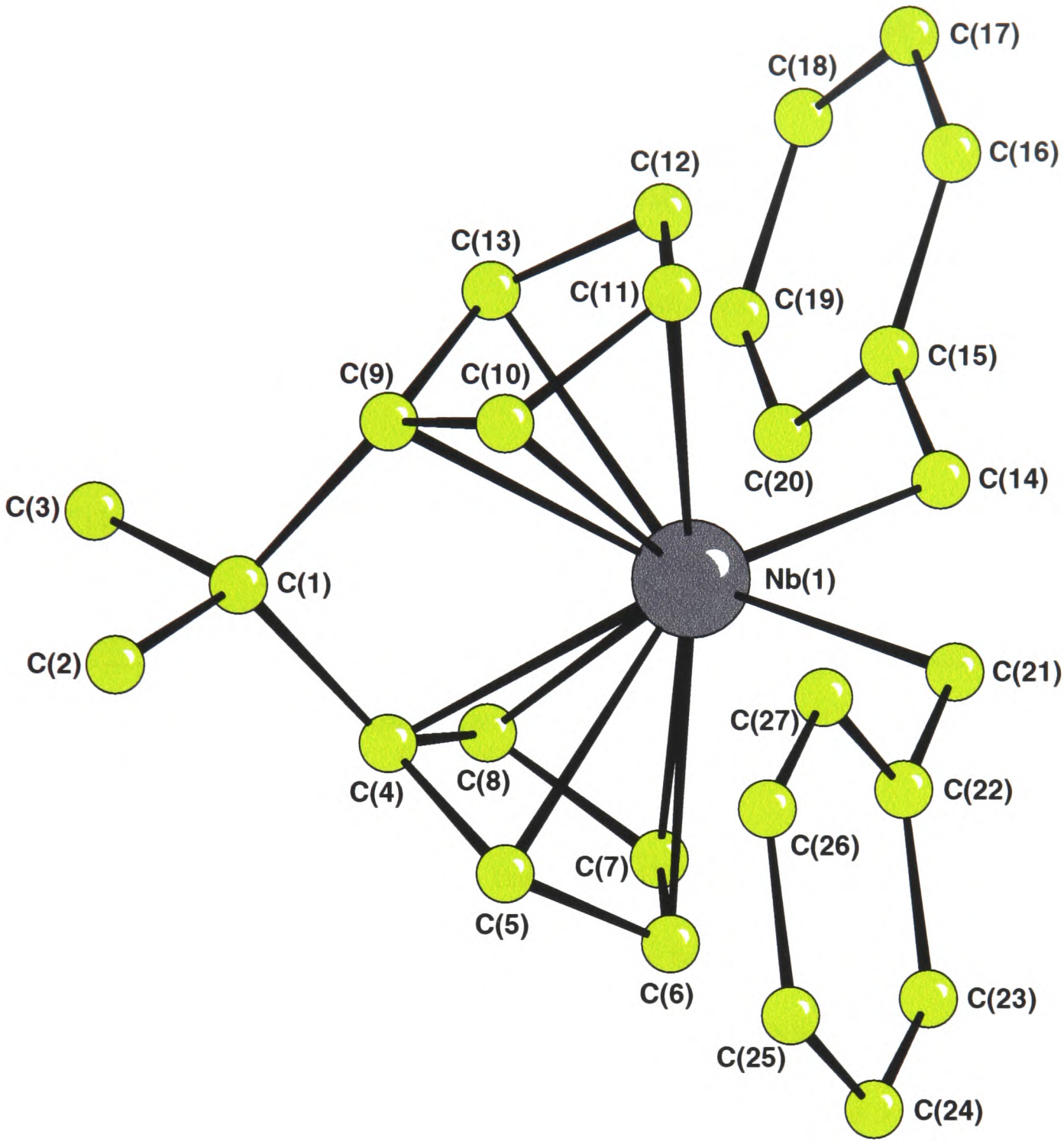

Figure 2.12 The molecular structure of $[Nb(\eta\text{-}C_5H_4\text{-}CMe_2\text{-}\eta\text{-}C_5H_4)(CH_2Ph)_2]$ (**6**). Hydrogen atoms are omitted for clarity

Bond	Length / Å	Bond	Angle / °
Nb(1)–C(4)	2.325(1)	C(2)–C(1)–C(3)	109.5(1)
Nb(1)–C(5)	2.361(2)	C(4)–C(1)–C(9)	98.8(1)
Nb(1)–C(6)	2.451(1)	C(14)–Nb(1)–C(21)	83.04(5)
Nb(1)–C(7)	2.461(1)	Bending angle, β	114.5
Nb(1)–C(8)	2.367(1)	Cp_{cent}–Nb(1)–Cp_{cent}, γ	123.1
Nb(1)–C(9)	2.322(1)	Cp_{cent}–C(4)–C(1)	163.0
Nb(1)–C(10)	2.368(1)	Cp_{cent}–C(9)–C(1)	163.1
Nb(1)–C(11)	2.457(1)		
Nb(1)–C(12)	2.443(1)		
Nb(1)–C(13)	2.354(1)		
Nb(1)–C(14)	2.277(1)		
Nb(1)–C(21)	2.284(1)		
Nb(1)–Cp_{cent}	2.07, 2.06		

Table 2.3 Selected interatomic distances and angles for [Nb(η-C_5H_4-CMe_2-η-C_5H_4)(CH_2Ph)$_2$] (**6**)

The crystal structure of the analogous compound [Nb(η-C_5H_5)$_2$(CH_2Ph)$_2$] has been reported.[21] As expected there is a marked difference between the bending angle β in compound **6**, 114.5°, and that reported for unbridged [Nb(η-C_5H_5)$_2$(CH_2Ph)$_2$], 133.1°. Apart from this there are no striking differences between the two structures. In **6** the average Nb–C_{benzyl} bond is 2.28 Å whereas in [Nb(η-C_5H_5)$_2$(CH_2Ph)$_2$] it is 2.30 Å, the average Nb–C_{ring} distance is 2.39 Å whereas in [Nb(η-C_5H_5)$_2$(CH_2Ph)$_2$] it is 2.41 Å and the C_{benzyl}–Nb–C_{benzyl} angle is 83.0° whereas in [Nb(η-C_5H_5)$_2$(CH_2Ph)$_2$] it is 79.0°. The benzyl groups adopt the *exo* configuration, as is illustrated in **Figure 2.13**, and there is no evidence for coordination higher than η^1. The separations between the niobium and the *ipso* carbons of the phenyl rings are Nb(1)–C(15) = 3.27 Å and Nb(1)–C(22) = 3.23 Å, too distant for any interaction.

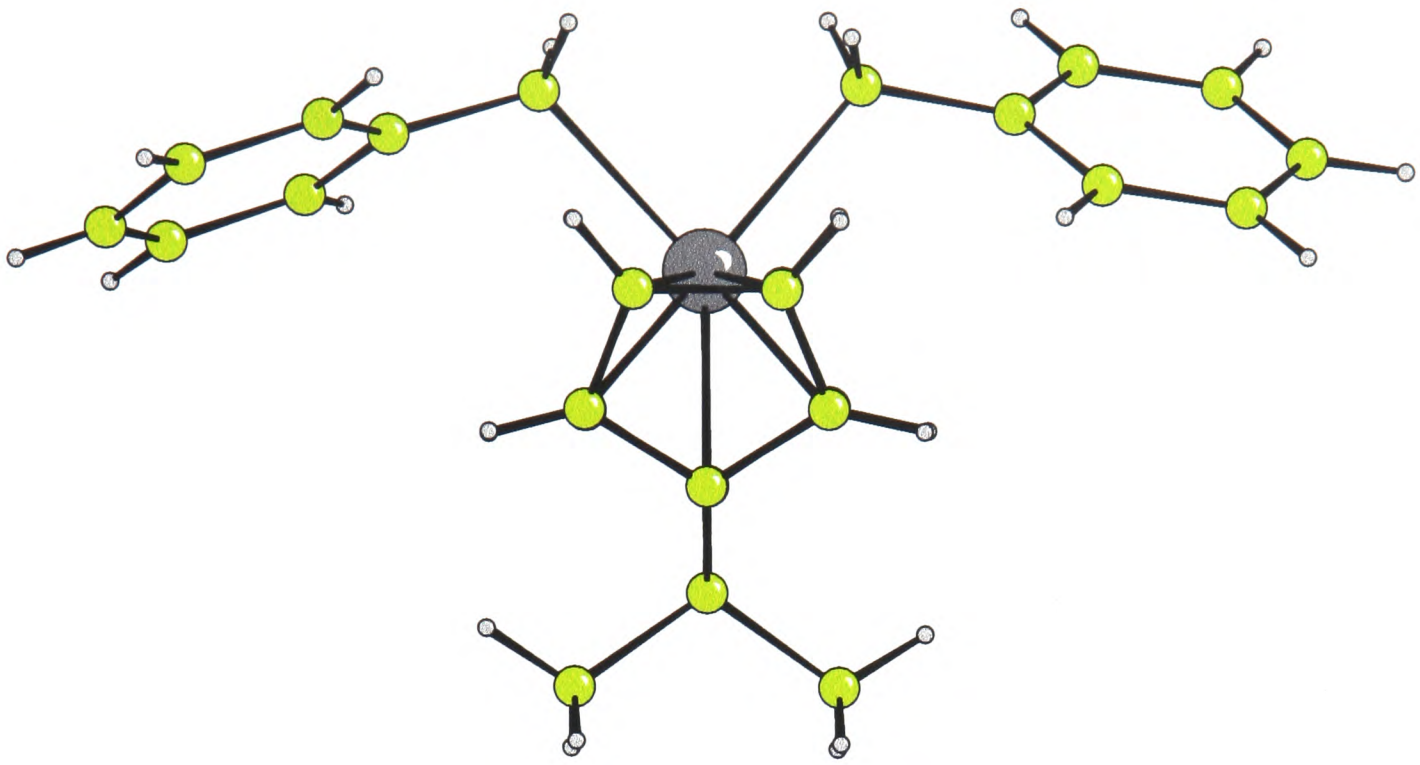

Figure 2.13 Alternative view of the molecular structure of [Nb(η-C_5H_4-CMe_2-η-C_5H_4)(CH_2Ph)$_2$] (**6**) showing the *exo* configuration of the benzyl groups

2.7 Attempt to prepare [Nb(η-C_5H_4-CMe_2-η-C_5H_4)Me_2]

Treatment of compound **1** with two equivalents of methyl magnesium bromide gives an orange crystalline solid. The Electron Impact ionisation mass spectrum of this substance shows a peak corresponding to *m/z* for the cation [Nb(η-C_5H_4-CMe_2-η-C_5H_4)Me_2]$^+$. The EPR spectrum displays ten lines (g_{iso} = 2.0205, $|a_{iso}|$ = 73 G). However, the solid is extremely air sensitive and satisfactory elemental analysis data could not be obtained. The use of alternative methylating reagents (MeLi and Me_2Zn) yielded intractable mixtures of products.

2.8 Attempts to prepare [Nb(η-C_5H_4-CMe_2-η-C_5H_4)H_3]

A number of attempts were made to synthesise the trihydride compound, [Nb(η-C_5H_4-CMe_2-η-C_5H_4)H_3]. This compound is envisaged to have potential as a starting material for the facile preparation of niobium(III) complexes since the reductive elimination of hydrogen from the unbridged analogue [Nb(η-C_5H_5)$_2H_3$] in the presence of a donor ligand L leads to compounds of the type [Nb(η-C_5H_5)$_2$(L)H]. For example, the alkyne hydride complex [Nb(η-C_5H_5)$_2$(η^2-MeCCMe)H] is formed when [Nb(η-C_5H_5)$_2H_3$] is heated in the presence of dimethylacetylene.[22] The *ansa* bridged trihydride is also of interest in the light of the recent observation that the ^{1}H NMR spectrum of [W(η-C_5H_4-CMe_2-η-C_5H_4)H_A(H_B)$_2$][PF_6] at –70 °C shows a coupling constant of 16 000 Hz between H_A and H_B. This is the largest two bond coupling yet reported.[23]

The unbridged trihydride, [Nb(η-C_5H_5)$_2H_3$], has been prepared by various methods. The original synthesis by Tebbe and Parshall involves heating a mixture of $NbCl_5$, NaCp and $NaBH_4$ under 800 atm pressure of hydrogen in toluene.[24] Labinger and Schwartz then published a milder procedure in which a toluene suspension of [Nb(η-C_5H_5)$_2Cl_2$] is treated with [$NaAlH_2(OCH_2CH_2OMe)_2$] ("Red-Al") at atmospheric pressure. After hydrolysis with aqueous NaOH the trihydride is isolated.[22] $LiAlH_4$ has also been used as the source of hydride.[25] Bercaw and co-workers reported the synthesis of [Nb(η-C_5Me_5)$_2H_3$] under 1 atm H_2 by abstraction of a borane equivalent from [Nb(η-C_5Me_5)$_2$(η^2-BH_4)] as the pyridine adduct, with concomitant oxidative addition of hydrogen.[13]

Treatment of compound **1** with $[NaAlH_2(OCH_2CH_2OMe)_2]$, $LiEt_3BH$ or $LiAlH_4$ gave mixtures of products from which no pure compound could be isolated. In the case of reaction with $[NaAlH_2(OCH_2CH_2OMe)_2]$ the ^1H NMR spectrum of the crude reaction mixture contained a broad (fwhh = 30 Hz) weak resonance centred at δ –12.95 ppm, suggesting that a niobium hydride species had formed. If the *ansa* bridged trihydride had indeed been formed it did not survive the aqueous work-up procedure. Attempts employing a stoichiometric amount of hydride transfer reagent without subsequent hydrolysis were also unsuccessful, giving negligible yields of the trihydride.

Bercaw's procedure was also attempted. A solution of compound **2** in toluene was treated with pyridine under an atmosphere of H_2. This gave only an intractable brown oil. An adaptation of the same procedure, using triethylamine in the place of pyridine, has been successfully implemented to prepare unbridged $[Nb(\eta\text{-}C_5H_5)_2H_3]$.[26] A solution of **2** in light petroleum was saturated with H_2 and Et_3N added dropwise. In the case of the unbridged compound an off-white precipitate of the trihydride is formed at this point. However, removal of the volatiles from the mixture gave a residue which was shown by ^1H NMR spectroscopy to contain only the starting material. It is not understood why *ansa* bridged **2** is inert under these conditions.

2.9 Attempts to prepare $[Nb(\eta\text{-}C_5H_4\text{-}CMe_2\text{-}\eta\text{-}C_5H_4)(\eta^2\text{-}CH_2{=}CHCH_3)H]$

Considerable effort was invested in the search for a synthesis of the propene hydride complex $[Nb(\eta\text{-}C_5H_4\text{-}CMe_2\text{-}\eta\text{-}C_5H_4)(\eta^2\text{-}CH_2{=}CHCH_3)H]$. A series of papers describes NMR spectroscopic studies of the exchange processes observed in $[Nb(\eta\text{-}C_5H_5)_2(\eta^2\text{-}CH_2{=}CHCH_3)H]$.[27-30] This molecule exists as both *endo* and *exo* isomers.

In the *exo* isomer the metal hydride is observed to exchange with the vinylic CH_2 hydrogens and with the *exo* methyl group at similar rates, both of which are *ca.* 2 orders of magnitude faster than exchange of the inequivalent C_5 rings. Insertion of the alkene into the Nb–H bond gives a 16 electron isopropyl intermediate, in which rotation about the M–C bond effects exchange of the C_5 rings. It has been proposed that a symmetrical agostic interaction between the isopropyl methyl groups and the niobium atom is responsible for the energy barrier to this rotation. Measurement of rate constants for the exchange processes in the *ansa* complex, where the rings are expected to be held back from the coordination site, would give us further insight into the mechanism of the exchange process.

The literature procedure for the preparation of $[Nb(\eta\text{-}C_5H_5)_2(\eta^2\text{-}CH_2{=}CHCH_3)H]$ is a straightforward reaction between $[Nb(\eta\text{-}C_5H_5)_2Cl_2]$ and two equivalents of Pr^iMgCl in diethyl ether, believed to proceed *via* β-hydride abstraction from the monoalkyl species.[31] Attempts to apply this reaction to the *ansa* bridged system **1** were unsuccessful, resulting in insoluble decomposition products. Addition was carried out in diethyl ether, THF or pentane at various temperatures and the reaction time was also varied. In each case the ^1H NMR spectrum of the pentane soluble fraction from the reaction mixture indicated that the desired propene hydride complex had not been formed.

2.10 General comments

A study of *ansa* compounds of the group 6 transition metals carried out in this laboratory[32] suggests that these *ansa* derivatives are more robust than their non-

bridged counterparts. The extension of this study to the group 5 metals, as detailed in this chapter, demonstrates that this is not a general phenomenon.

The *ansa* niobium compound **1** is difficult to prepare in high purity, has a low solubility in common organic solvents and it is more sensitive to air and moisture than its unbridged analogue. The effort spent on the exploration of its chemistry was not well rewarded. Compound **1** is less conducive to ligand substitution reactions than its non *ansa* counterpart and several successful transformations of $[Nb(\eta\text{-}C_5H_5)_2Cl_2]$ are not applicable to **1**.

Generally, where experiments failed it was not because the *ansa* compounds were inert under the reaction conditions but because pathways leading to decomposition seemed to prevail. These observations are suggestive of destabilisation of the metal-ring bonding interaction, presumably a result of the strain imposed by the single atom bridge.

2.11 Summary

The new chemistry described in this chapter is summarised in **Figure 2.14**.

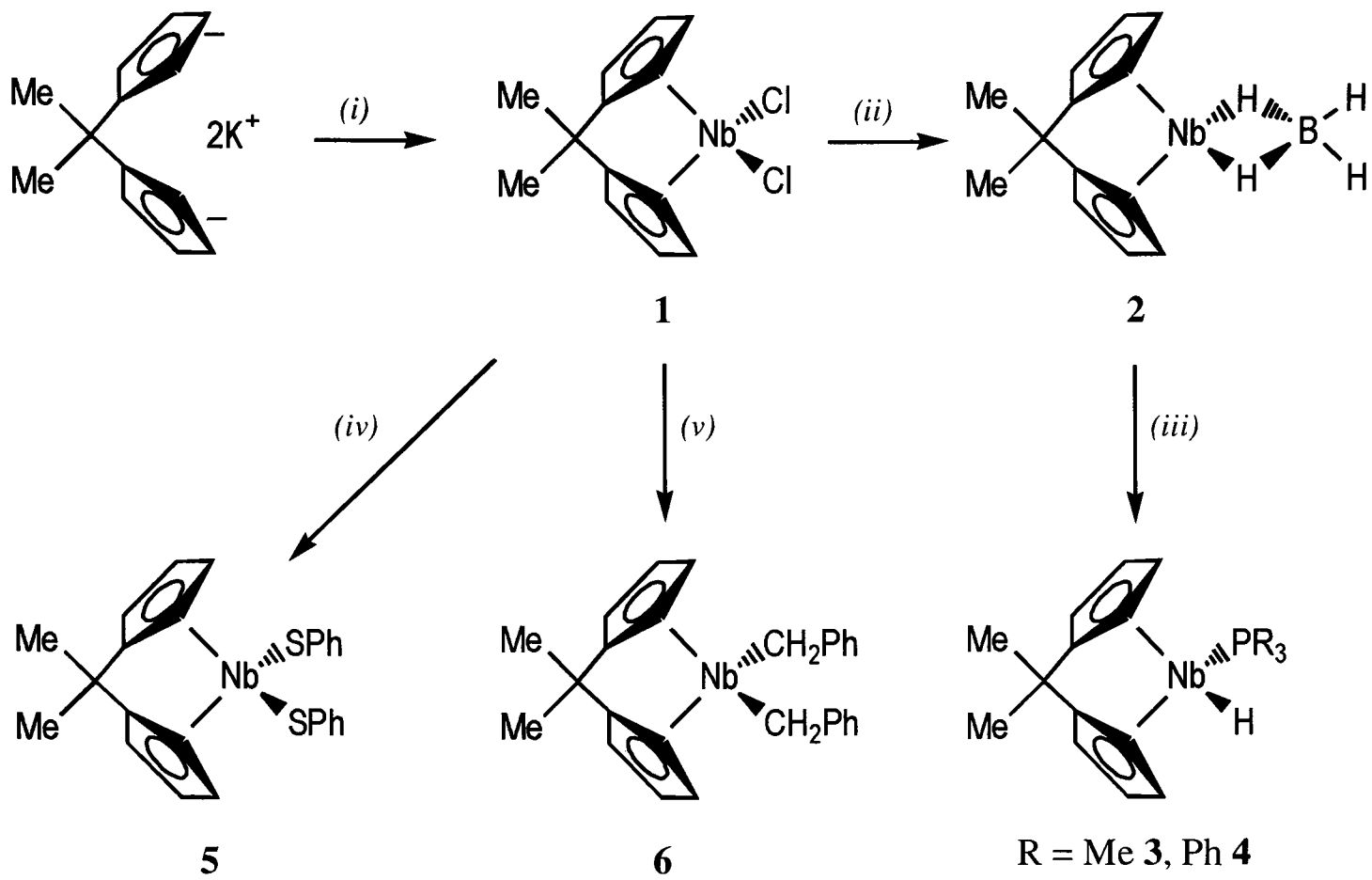

Reagents: *(i)* $[NbCl_4.2THF]$ in THF
(ii) $LiBH_4$ in DME
(iii) PR_3 (R = Me, Ph) in light petroleum
(iv) NaSPh in THF
(v) $PhCH_2MgBr$ in Et_2O

Figure 2.14 Summary of reactions presented in **Chapter 2**

References for Chapter 2

1. H. M. Tidswell, *Part II Thesis,* University of Oxford, 1995.

2. F. W. Siegert and H. J. de Liefde Meijer, *J. Organomet. Chem.,* 1970, **23**, 177.

3. W. E. Douglas and M. L. H. Green, *J. Chem. Soc., Dalton Trans.,* 1972, 1796.

4. C. R. Lucas and M. L. H. Green, *J. Chem. Soc., Chem. Commun.,* 1972, 1005.

5. C. R. Lucas, in *Inorganic Syntheses* (F. Basolo, ed.), Vol. 16, p. 107, McGraw-Hill, NY, 1976.

6. L. E. Manzer, *Inorg. Chem.,* 1977, **16**, 525.

7. I. E. Nifant'ev, P. V. Ivchenko and M. V. Borzov, *J. Chem. Research (S),* 1992, 162.

8. A. Antiñolo, M. Martinez-Ripoll, Y. Mugnier, A. Otero, S. Prashar and A. M. Rodriguez, *Organometallics,* 1996, **15**, 3241.

9. I. H. Elson and J. K. Kochi, *J. Am. Chem. Soc.,* 1975, **97**, 1262.

10. G. S. McGrady, 1995, personal communication.

11. T. J. Marks and W. J. Kennelly, *J. Am. Chem. Soc.,* 1975, **97**, 1439.

12. T. J. Marks and J. R. Kolb, *Chem. Rev.,* 1977, **77**, 263.

13. R. A. Bell, S. A. Cohen, N. M. Doherty, R. S. Threlkel and J. E. Bercaw, *Organometallics,* 1986, **5**, 972.

14. M. L. H. Green and L.-L. Wong, *J. Chem. Soc., Dalton Trans.,* 1989, 2133.

15. P. L. Johnson, S. A. Cohen, T. J. Marks and J. M. Williams, *J. Am. Chem. Soc.*, 1978, **100**, 2709.

16. T. K. Woo, L. Fan and T. Ziegler, *Organometallics*, 1994, **13**, 2252.

17. C. S. Bajgur, W. R. Tikkanen and J. L. Petersen, *Inorg. Chem.*, 1985, **24**, 2539.

18. N. I. Kurillova, A. I. Gusev and Y. T. Struchkov, *Zh. Strukt. Khim.*, 1974, **15**, 718.

19. M. Y. Darensbourg, C. J. Bischoff, S. A. Houliston, M. Pala and J. Reibenspies, *J. Am. Chem. Soc.*, 1990, **112**, 6905.

20. J. C. Green, M. L. H. Green and C. K. Prout, *J. Chem. Soc., Chem. Commun.*, 1972, 421.

21. P. B. Hitchcock, M. F. Lappert and C. R. C. Milne, *J. Chem. Soc., Dalton Trans.*, 1981, 180.

22. J. A. Labinger and J. Schwartz, *J. Am. Chem. Soc.*, 1975, **97**, 1596.

23. A. Chernega, J. Cook, M. L. H. Green, L. Labella, S. J. Simpson, J. Souter and A. H. H. Stephens, *J. Chem. Soc., Dalton Trans.*, 1997, 3225.

24. F. N. Tebbe and G. W. Parshall, *J. Am. Chem. Soc.*, 1971, **93**, 3793.

25. J. A. Labinger and K. S. Wong, *J. Organomet. Chem.*, 1979, **170**, 373.

26. G. Nikonov, 1997, personal communication.

27. B. J. Burger, B. D. Santarsiero, M. S. Trimmer and J. E. Bercaw, *J. Am. Chem. Soc.*, 1988, **110**, 3134.

28. J. E. Bercaw, B. J. Burger, M. L. H. Green, B. D. Santarsiero, A. Sella, M. S. Trimmer and L.-L. Wong, *J. Chem. Soc., Chem. Commun.*, 1989, 734.

29. M. L. H. Green, A. Sella and L.-L. Wong, *Organometallics*, 1992, **11**, 2650.

30. M. L. H. Green, L.-L. Wong and A. Sella, *Organometallics*, 1992, **11**, 2660.

31. A. H. Klazinga and J. H. Teuben, *J. Organomet. Chem.*, 1980, **194**, 309.

32. J. Souter, *D. Phil. Thesis*, University of Oxford, 1996.

Chapter 3

ansa Niobium(V) imido complexes

3.1 Introduction to Chapter 3

It was reported in the previous chapter that the procedure for the preparation and purification of [Nb(η-C_5H_4-CMe_2-η-C_5H_4)Cl_2] **1** is laborious and that the compound has low solubility in commonly used organic solvents. Many of the attempts to derivatise **1** by substitution of the chloride ligands were unsuccessful. It was decided to look for alternative entry points into *ansa bis*cyclopentadienyl niobium chemistry.

This chapter presents new *ansa* niobium(V) metallocenes containing ancillary imido ligands.

The organoimido ligand is unique since it can contribute a total of 4 electrons through a single ligating nitrogen atom, forms strong and frequently chemically inert bonds to transition metals and, by virtue of the organo R group, its steric and electronic properties are readily modified. Thus, it seems likely that the combination of the cyclopentadienyl ligand and the organoimido ligand may lead to a rich chemistry.

Schmidt has described the *bis*cyclopentadienyl *tertiary*-butylimido derivatives [M(η-$C_5H_5)_2$(NBu^t)Cl] (M = Nb, Ta).[1] The niobium compound was prepared from [Nb(NBu^t)$(py)_2Cl_3$] (py = pyridine). A related compound, [Nb($NSiMe_3$)$(py)_2Cl_3$], has been reported by Doherty.[2] These niobium imido compounds were used as starting reagents for the chemistry presented in this chapter.

During the course of this study an alternative synthetic route to *ansa bis*cyclopentadienyl imido niobium and tantalum derivatives was reported by Herrmann and co-workers.[3]

3.2 Preparation of [Nb(η-C_5H_4-CMe_2-η-C_5H_4)($NSiMe_3$)Cl] (7)

The reaction between $NbCl_5$ and $NH(SiMe_3)_2$ in benzene gives the dimer $[Nb(NSiMe_3)(NH_2SiMe_3)Cl_3]_2$ which, when treated with pyridine, affords the niobium trimethylsilylimido derivative $[Nb(NSiMe_3)(py)_2Cl_3]$.[2] Treatment of this compound with the dipotassium salt, $[K(C_5H_4\text{-}CMe_2\text{-}C_5H_4)K]$, in THF gives yellow crystals of the diamagnetic *ansa* niobium(V) derivative [Nb(η-C_5H_4-CMe_2-η-C_5H_4)($NSiMe_3$)Cl] (**7**) according to **Figure 3.1**. Elemental analysis data obtained for a sample of these crystals were in complete agreement with the proposed empirical formula.

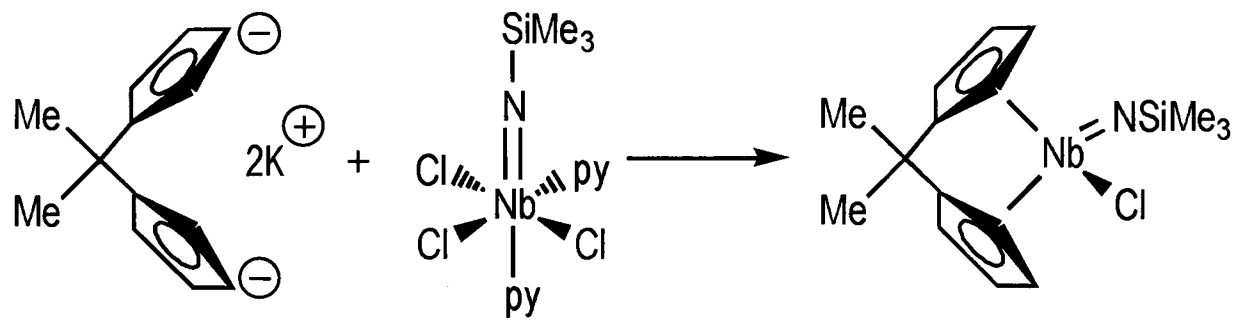

Figure 3.1 Preparation of [Nb(η-C_5H_4-CMe_2-η-C_5H_4)($NSiMe_3$)Cl] (**7**)

The ^1H NMR (C_6D_6) spectrum of **7** (**Figure 3.2**) shows the expected peaks due to the *ansa* ligand and a singlet at δ 0.06 ppm assigned to the trimethylsilyl group. The resonances due to the protons on the cyclopentadienyl rings appear, as predicted, at higher chemical shifts, typically by about 1 ppm, than those in the lower valent complexes described in **Chapter 2**.

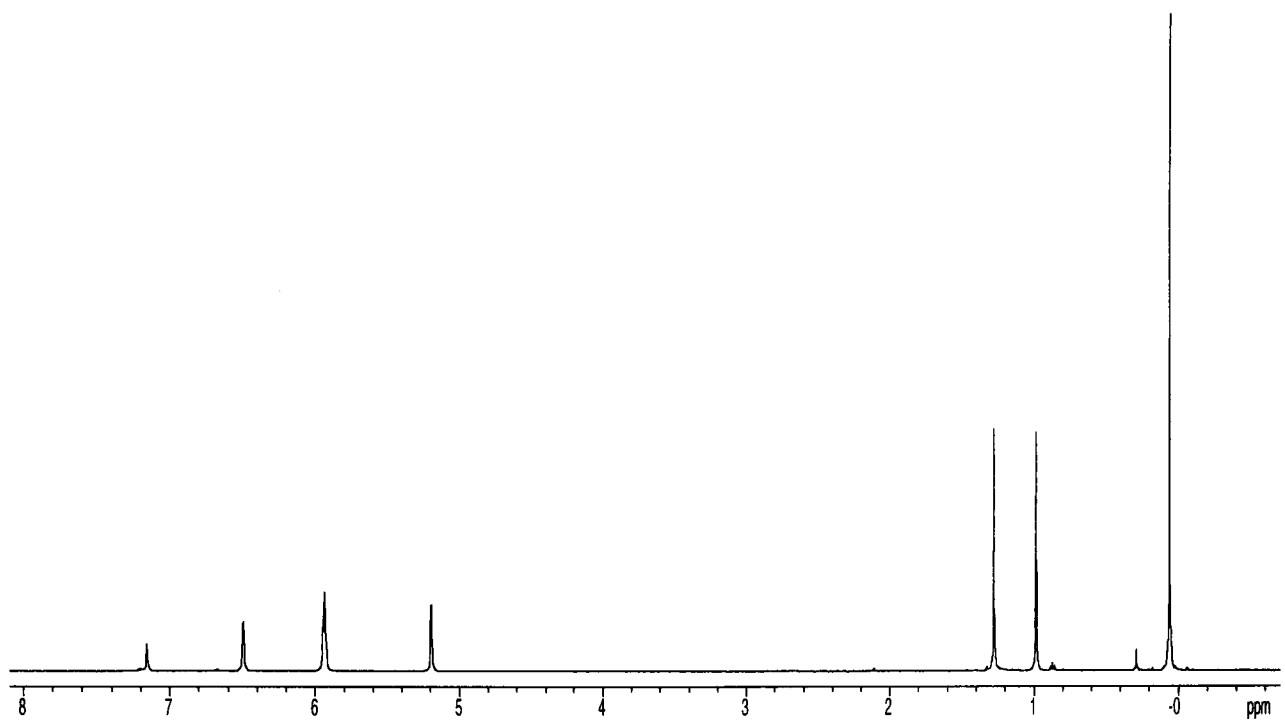

Figure 3.2 ^{1}H NMR (C_6D_6) spectrum of [Nb(η-C_5H_4-CMe_2-η-C_5H_4)($NSiMe_3$)Cl] (**7**)

In the $^{13}C\{^{1}H\}$ NMR (C_6D_6) spectrum (**Figure 3.3**) the resonance due to the *ipso* carbons on the cyclopentadienyl rings appears at higher chemical shift than the other cyclopentadienyl carbon resonances. This is in contrast with the spectra of the trivalent complexes described in **Chapter 2**, where the resonances due to the *ipso* carbons appear at lower chemical shifts than the other cyclopentadienyl ring carbon resonances. The explanation for this must lie in the differing distributions of π-electron density around the cyclopentadienyl ring, a point which has been discussed by Petersen.[4]

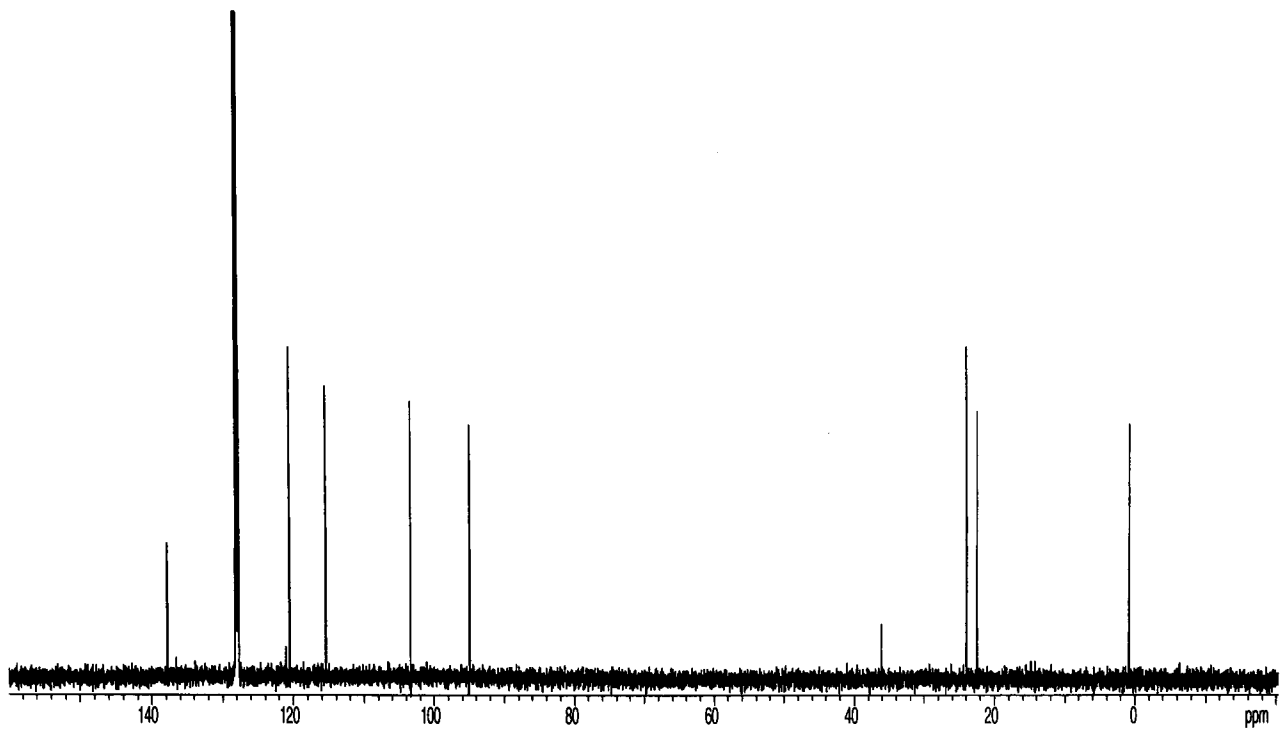

Figure 3.3 $^{13}C\{^{1}H\}$ NMR (C_6D_6) spectrum of $[Nb(\eta\text{-}C_5H_4\text{-}CMe_2\text{-}\eta\text{-}C_5H_4)(NSiMe_3)Cl]$ (**7**)

The Electron Impact ionisation mass spectrum of **7** shows peaks due to the molecular ion and fragments arising from the loss of one, two or three methyl groups, the chlorine atom or the trimethylsilylimido group. A peak corresponding to *m/z* for the parent *ansa* niobocene cation, $[Nb(\eta\text{-}C_5H_4\text{-}CMe_2\text{-}\eta\text{-}C_5H_4)^+]$, is also observed. Peaks due to fragments containing chlorine show the expected isotopic ratio.

Crystals suitable for an X-ray crystallographic structure determination were obtained by the slow evaporation of a solution of **7** in petroleum ether (b. p. 100-120 °C) under a slow stream of dinitrogen. The crystal structure of **7** has been determined and the molecular structure, with atomic numbering scheme, is shown in **Figure 3.4**. Selected interatomic distances and angles for compound **7** appear in **Table 3.1**. Full crystallographic details are presented in **Appendix D**.

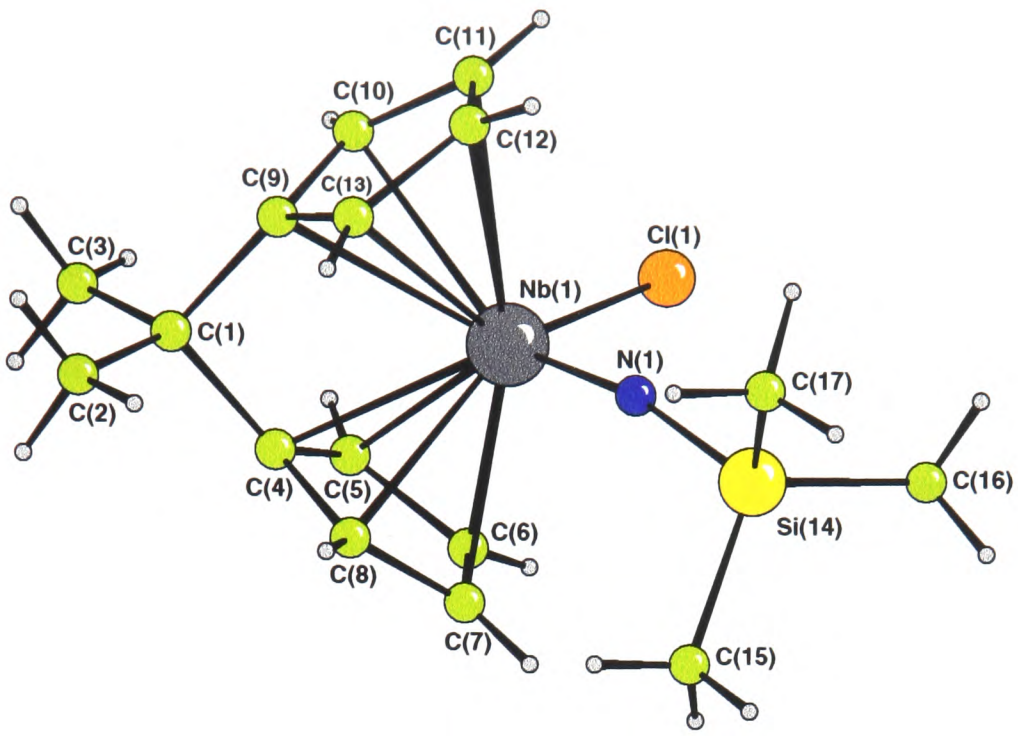

Figure 3.4 The molecular structure of [Nb(η-C_5H_4-CMe_2-η-C_5H_4)($NSiMe_3$)Cl] (**7**). Hydrogen atom labels are omitted for clarity

Bond	Length / Å	Bond	Angle / °
Nb(1)–N(1)	1.777(1)	C(2)–C(1)–C(3)	109.9(1)
Nb(1)–Cl(1)	2.4387(4)	C(4)–C(1)–C(9)	98.89(9)
Nb(1)–C(4)	2.480(1)	Cl(1)–Nb(1)–N(1)	98.21(4)
Nb(1)–C(5)	2.536(1)	Nb(1)–N(1)-Si(14)	167.71(7)
Nb(1)–C(6)	2.521(1)	Bending angle, β	112.0
Nb(1)–C(7)	2.489(1)	Cp_{cent}–Nb(1)–Cp_{cent}, γ	114.2
Nb(1)–C(8)	2.396(1)	Cp_{cent}–C(4)–C(1)	163.9
Nb(1)–C(9)	2.489(1)	Cp_{cent}–C(9)–C(1)	163.9
Nb(1)–C(10)	2.549(1)		
Nb(1)–C(11)	2.536(1)		
Nb(1)–C(12)	2.502(1)		
Nb(1)–C(13)	2.402(1)		
N(1)–Si(14)	1.737(1)		
Nb(1)–Cp_{cent}	2.17, 2.19		

Table 3.1 Selected interatomic distances and angles for [Nb(η-C_5H_4-CMe_2-η-C_5H_4)($NSiMe_3$)Cl] (**7**)

The large Nb–N–Si angle implies that the nitrogen atom is formally sp hybridised and can therefore act as a four electron donor to the metal centre. The Nb–N bond length is short and comparable with values found for other Nb=NR groups where NR is a linear four electron donor.[5] Thus it appears at first sight that **7** is a twenty electron compound.

In comparison with the structures presented in **Chapter 2**, the metal to ring centroid distances in **7** are approximately 0.2 Å longer. This is very likely to be due to a π bonding interaction between N 2p and the metal-ring antibonding $1b_1$ orbital of the bent metallocene fragment. This orbital lies above the $2a_1$ orbital and may be considered the fourth frontier orbital (**Figure 3.5**).[6] The donation of electron density from the nitrogen into this metal-ring antibonding orbital causes lengthening of the metal-carbon distances. Similar metal-carbon bond lengths are observed in all the structurally characterised imido compounds presented in this chapter. This effect is further discussed with reference to photoelectron spectra in **Section 3.8**.

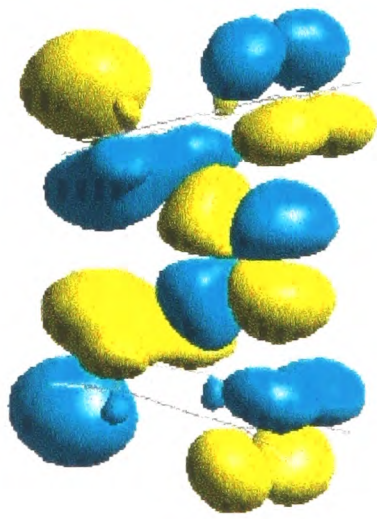

Figure 3.5 A depiction of the metal-ring antibonding $1b_1$ orbital, which may be considered as a fourth frontier orbital of the bent metallocene

Compound **7** could only be prepared in low yield (12 %). It was decided to concentrate on the niobium compound $[Nb(NBu^t)(py)_2Cl_3]$ as an alternative starting point for the synthesis of new complexes.

3.3 Preparation of $[Nb(\eta\text{-}C_5H_4\text{-}CMe_2\text{-}\eta\text{-}C_5H_4)(NBu^t)Cl]$ (8)

Treatment of $[Nb(NBu^t)(py)_2Cl_3]$[1] with $[K(C_5H_4\text{-}CMe_2\text{-}C_5H_4)K]$ in THF gives the *tertiary*-butyl imido complex, $[Nb(\eta\text{-}C_5H_4\text{-}CMe_2\text{-}\eta\text{-}C_5H_4)(NBu^t)Cl]$ (**8**), in 77 % yield (**Figure 3.6**). The yellow crystalline compound is soluble in non-polar organic solvents and is stable in air for short periods. Elemental analysis data obtained for a sample of **8** was in accordance with the proposed empirical formula.

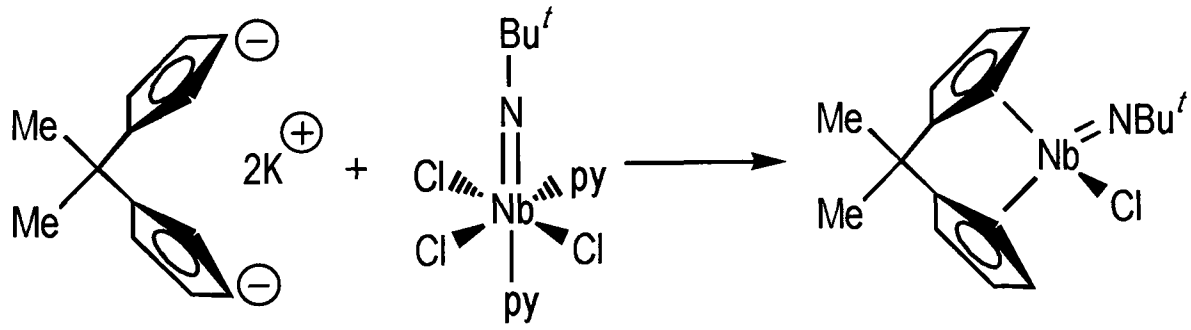

Figure 3.6 Preparation of $[Nb(\eta\text{-}C_5H_4\text{-}CMe_2\text{-}\eta\text{-}C_5H_4)(NBu^t)Cl]$ (**8**)

Assignment of the ^1H NMR (C_6D_6) spectrum (**Figure 3.7**), by analogy to that of **7**, is straightforward and is not discussed here. For comparison, the ^1H NMR (C_6D_6) spectrum of the unbridged analogue, $[Nb(\eta\text{-}C_5H_5)_2(NBu^t)Cl]$,[7] contains a singlet at δ 5.85 ppm for the cyclopentadienyl rings and a singlet at δ 0.96 ppm for the *tertiary*-butyl group.

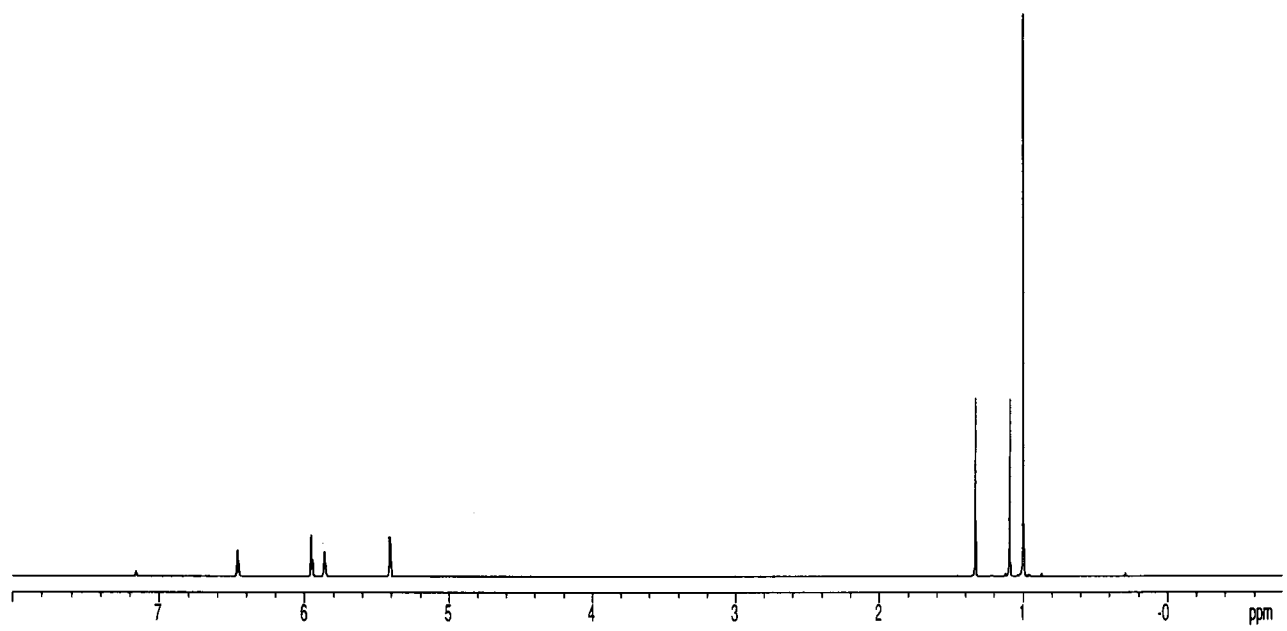

Figure 3.7 ^{1}H NMR (C_6D_6) spectrum of [Nb(η-C_5H_4-CMe_2-η-C_5H_4)(NBu^t)Cl] (**8**)

The *ansa* vanadium and tantalum analogues of **8** have been published.[8] The ^{1}H NMR resonances of [V(η-C_5H_4-CMe_2-η-C_5H_4)(NBu^t)Cl] are shifted downfield by about 1 ppm relative to those of the niobium and tantalum compounds, presumably reflecting the greater electron deficiency of vanadium(V) over its second and third row congeners.

The $^{13}C\{^{1}H\}$ NMR (C_6D_6) spectrum of **8** is shown in **Figure 3.8**. The relaxation time of the quaternary carbon of the *tertiary* butyl group is sufficiently long that approximately 20 000 scans with a long delay were required to detect its ^{13}C resonance, which appears at δ 69.0 ppm. The corresponding chemical shift in [Nb(η-C_5H_5)$_2$(NBu^t)Cl][7] is δ 69.8 ppm.

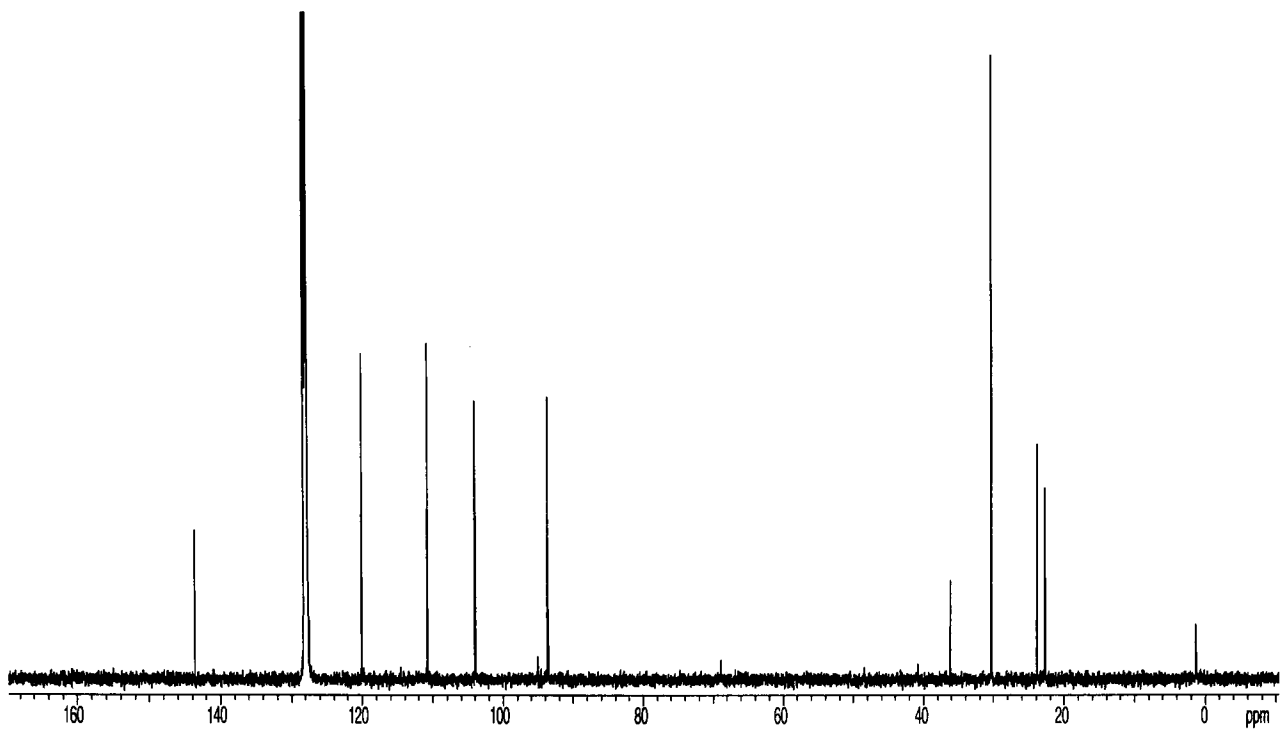

Figure 3.8 $^{13}C\{^{1}H\}$ NMR (C_6D_6) spectrum of $[Nb(\eta\text{-}C_5H_4\text{-}CMe_2\text{-}\eta\text{-}C_5H_4)(NBu^t)Cl]$ (**8**)

The Electron Impact ionisation mass spectrum of **8** shows peaks due to the molecular ion and various fragmentation products, including the parent *ansa* niobocene. Peaks due to fragments containing chlorine appear in the expected isotope ratio.

Crystals suitable for X-ray diffraction studies were obtained by cooling a solution of **8** in diethyl ether to –80 °C. The compound crystallises in the monoclinic space group $P\ 2_1/m$ and the asymmetric unit comprises half of the molecular unit. The molecular structure, along with atom labelling scheme, is shown in **Figure 3.9**. The atoms C(1), C(2), C(3), Nb(1), Cl(1), N(1), C(14) and C(16) lie on a crystallographic mirror plane. The atoms labelled with a prime are generated from their counterparts by the reflection (x, $^1/_2$–y, z). Selected interatomic distances and angles are given in **Table 3.2**. Full details of the structure determination appear in **Appendix E**.

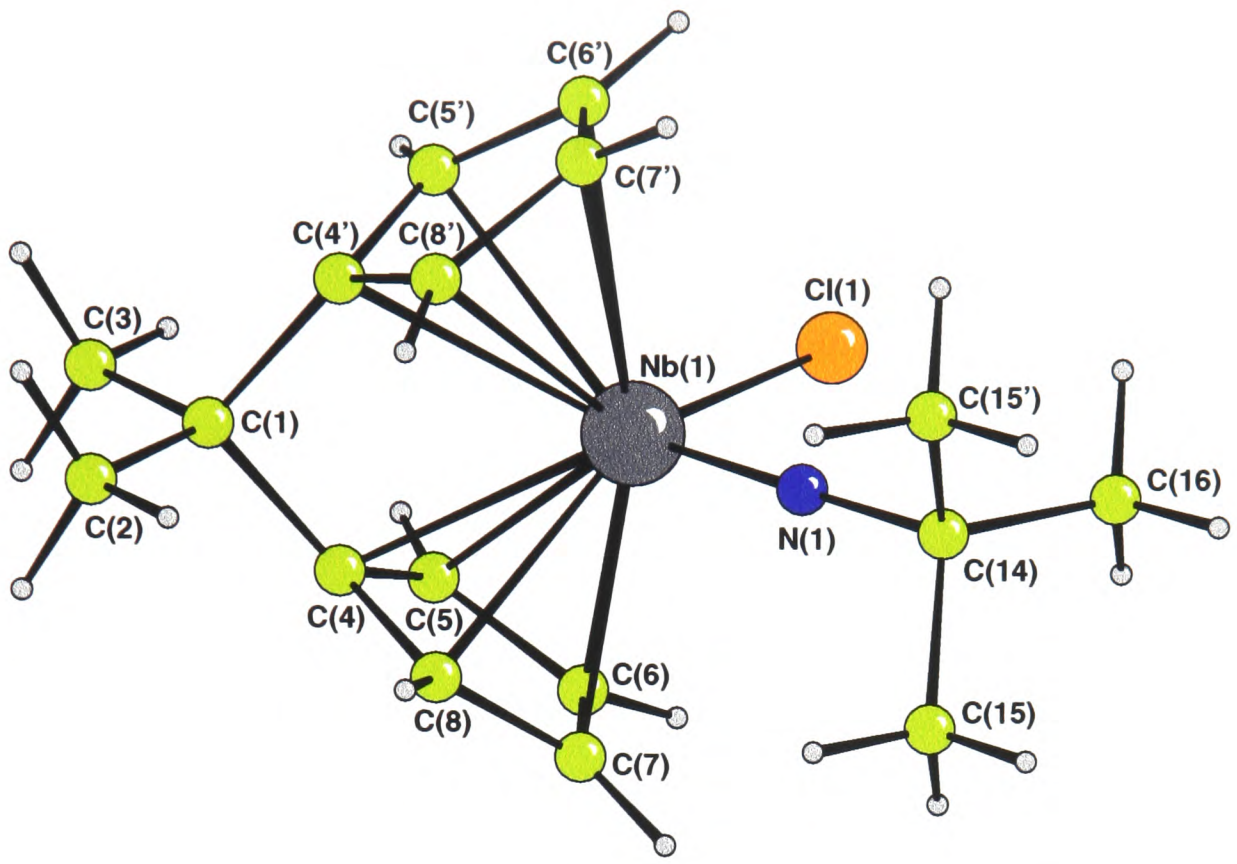

Figure 3.9 The molecular structure of [Nb(η-C_5H_4-CMe_2-η-C_5H_4)(NBu^t)Cl] (**8**). Atoms labelled with a prime are generated from their counterparts by the reflection (x, ½–y, z). Hydrogen atom labels are omitted for clarity.

Bond	Length / Å	Bond	Angle / °
Nb(1)–N(1)	1.762(3)	C(2)–C(1)–C(3)	109.6(3)
Nb(1)–Cl(1)	2.446(1)	C(4)–C(1)–C(4′)	99.3(3)
Nb(1)–C(4)	2.505(3)	Cl(1)–Nb(1)–N(1)	95.3(1)
Nb(1)–C(5)	2.557(3)	Nb(1)–N(1)–C(14)	178.4(3)
Nb(1)–C(6)	2.522(3)	Bending angle, β	112.6
Nb(1)–C(7)	2.488(3)	Cp_{cent}–Nb(1)–Cp_{cent}, γ	113.3
Nb(1)–C(8)	2.401(3)	Cp_{cent}–C(4)–C(1)	163.3
N(1)–C(14)	1.438(5)		
Nb(1)–Cp_{cent}	2.19		

Table 3.2 Selected interatomic distances and angles for [Nb(η-C_5H_4-CMe_2-η-C_5H_4)(NBu^t)Cl] (**8**)

In contrast with compound **7**, the imido group in compound **8** is almost linear (Nb–N–C = 178.4°). Selected structural parameters for the unbridged niobium analogue, $[Nb(\eta\text{-}C_5H_5)_2(NBu^t)Cl]$,[7] are given in **Table 3.3**. The values given are averaged over the two independent molecules which comprise the asymmetric unit. Disappointingly, no interesting differences are revealed between this structure and that of compound **8**, the only significant difference being that the centroid–metal–centroid angle, γ, is approximately 10° smaller in the *ansa* compound. The structural data for **8** are also comparable with those reported for the hydrazido compound, $[Nb(\eta\text{-}C_5H_4Me)_2(NNMe_2)Cl]$.[9]

Bond	Length / Å	Bond	Angle / °
Nb–N	1.763(5)	Cl–Nb–N	94.35(2)
Nb–Cl	2.458(2)	Nb–N-C	176.5(5)
Nb–C (average)	2.495(9)	Cp_{cent}–Nb–Cp_{cent}, γ	123.4
Nb–Cp_{cent}	2.21		

Table 3.3 Selected structural data for $[Nb(\eta\text{-}C_5H_5)_2(NBu^t)Cl]$

Photoelectron spectra were obtained for compound **8** and are presented in **Section 3.8**, along with the results of a Density Functional calculation.

3.4 Preparation of $[Nb(\eta\text{-}C_5H_4\text{-}CMe_2\text{-}\eta\text{-}C_5H_4)(NBu^t)Br]$ (9) and $[Nb(\eta\text{-}C_5H_4\text{-}CMe_2\text{-}\eta\text{-}C_5H_4)(NBu^t)I]$ (10)

Compound **8** readily undergoes halide exchange on treatment with trimethylsilyl bromide or iodide in light petroleum. The compounds $[Nb(\eta\text{-}C_5H_4\text{-}CMe_2\text{-}\eta\text{-}$

$C_5H_4)(NBu^t)Br]$ (**9**) and $[Nb(\eta\text{-}C_5H_4\text{-}CMe_2\text{-}\eta\text{-}C_5H_4)(NBu^t)I]$ (**10**) have been synthesised accordingly (**Figure 3.10**).

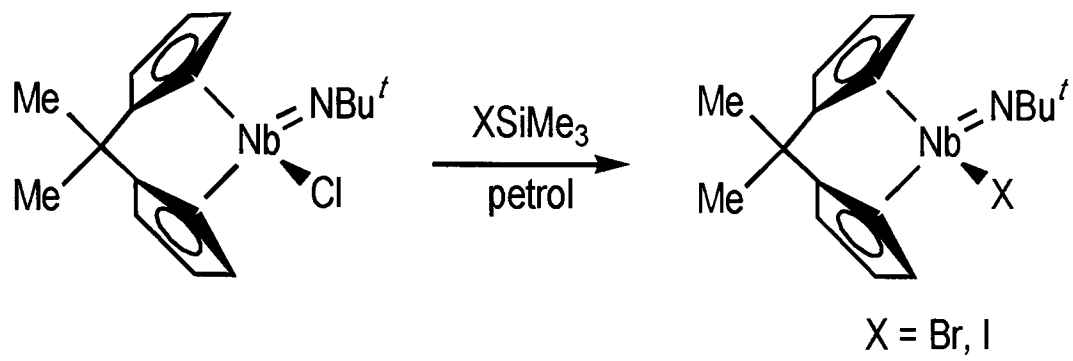

Figure 3.10 Preparation of $[Nb(\eta\text{-}C_5H_4\text{-}CMe_2\text{-}\eta\text{-}C_5H_4)(NBu^t)Br]$ (**9**) and $[Nb(\eta\text{-}C_5H_4\text{-}CMe_2\text{-}\eta\text{-}C_5H_4)(NBu^t)I]$ (**10**)

In both cases, the elemental analysis data confirm the proposed empirical formula. The ^1H and $^{13}C\{^1H\}$ NMR (C_6D_6) spectra are very similar to those of compound **8** and are assigned analogously. Mass spectra were obtained for both **9** and **10** by the Electron Impact ionisation technique. Peaks due to the molecular ion and various fragments were observed in each case. The expected isotopic ratio was observed for ^{79}Br / ^{81}Br in **9**. Spectroscopic data are available for the unbridged analogue of **9**, $[Nb(\eta\text{-}C_5H_5)_2(NBu^t)Br]$.[7] As was found for compound **8** and its analogue, the data do not differ significantly between the *ansa* and non *ansa* compounds.

Single crystals of **9** were obtained by the slow evaporation of a solution in petroleum ether (b. p. 100-120 °C). The crystal structure was solved in the monoclinic space group $P\ 2_1/m$ and the molecule is divided into two asymmetric units by a crystallographic mirror plane as in compound **8**. The molecular structure is given in **Figure 3.11** and selected interatomic distances and angles are given in **Table 3.4**. Full crystallographic details appear in **Appendix F**.

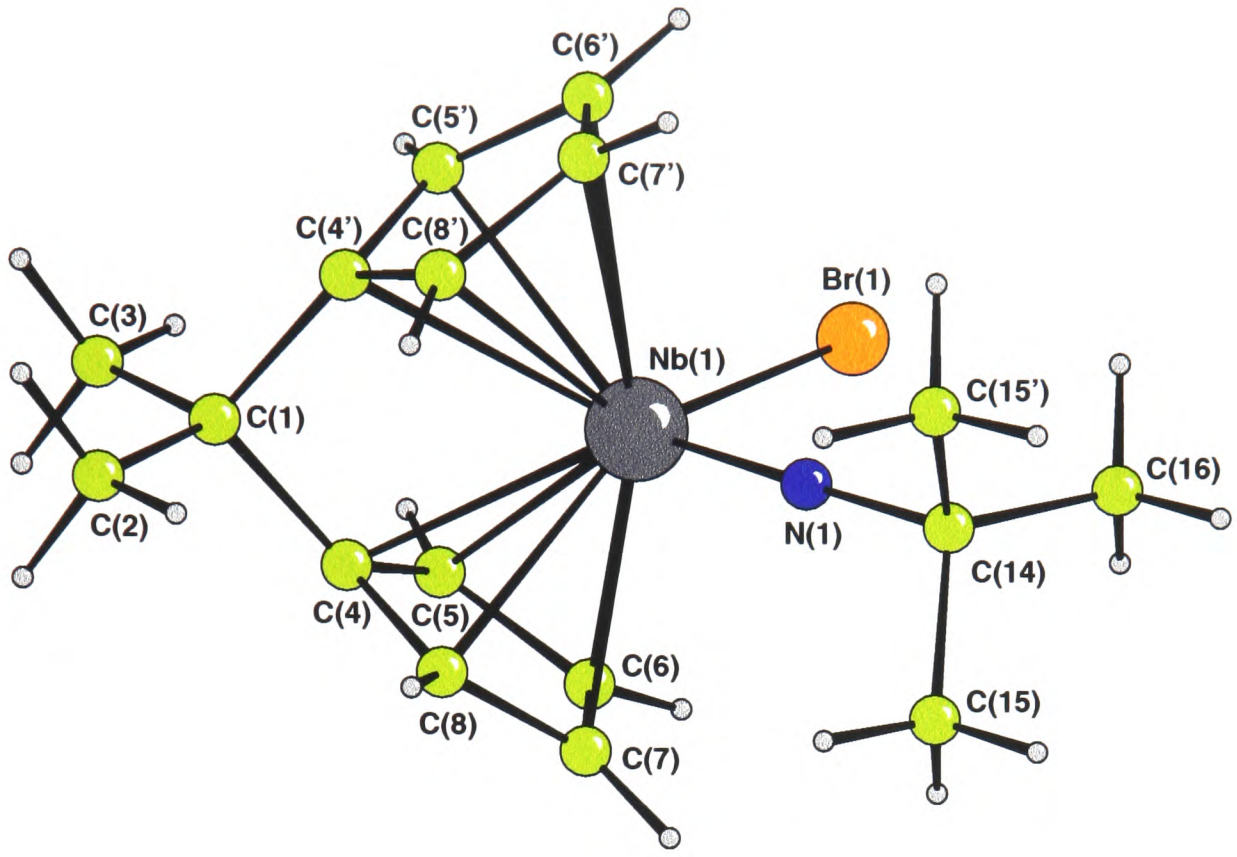

Figure 3.11 The molecular structure of [Nb(η-C_5H_4-CMe_2-η-C_5H_4)(NBu^t)Br] (**9**). Atoms labelled with a prime are generated from their counterparts by the reflection (x, ½–y, z). Hydrogen atom labels are omitted for clarity.

Bond	Length / Å	Bond	Angle / °
Nb(1)–N(1)	1.765(2)	C(2)–C(1)–C(3)	110.1(3)
Nb(1)–Br(1)	2.6022(4)	C(4)–C(1)–C(4')	99.1(2)
Nb(1)–C(4)	2.497(2)	Br(1)–Nb(1)–N(1)	93.77(8)
Nb(1)–C(5)	2.551(2)	Nb(1)–N(1)–C(14)	178.3(2)
Nb(1)–C(6)	2.523(2)	Bending angle, β	112.5
Nb(1)–C(7)	2.484(2)	Cp_{cent}–Nb(1)–Cp_{cent}, γ	113.4
Nb(1)–C(8)	2.395(2)	Cp_{cent}–C(4)–C(1)	163.5
N(1)–C(14)	1.448(3)		
Nb(1)–Cp_{cent}	2.18		

Table 3.4 Selected interatomic distances and angles for [Nb(η-C_5H_4-CMe_2-η-C_5H_4)(NBu^t)Br] (**9**)

Single crystals of **10** were obtained by slow cooling a solution in diethyl ether to –80 °C. The compound crystallises in the orthorhombic space group *P c a b*. The molecular structure is given in **Figure 3.12** and selected interatomic distances and angles are given in **Table 3.5**. Full crystallographic details appear in **Appendix G**.

The molecular structures of both **9** and **10** are similar to that of compound **8** and there are no surprising structural features. Note that bending of the imido group away from the iodide is observed in compound **10** (Nb–N–C = 171.8°).

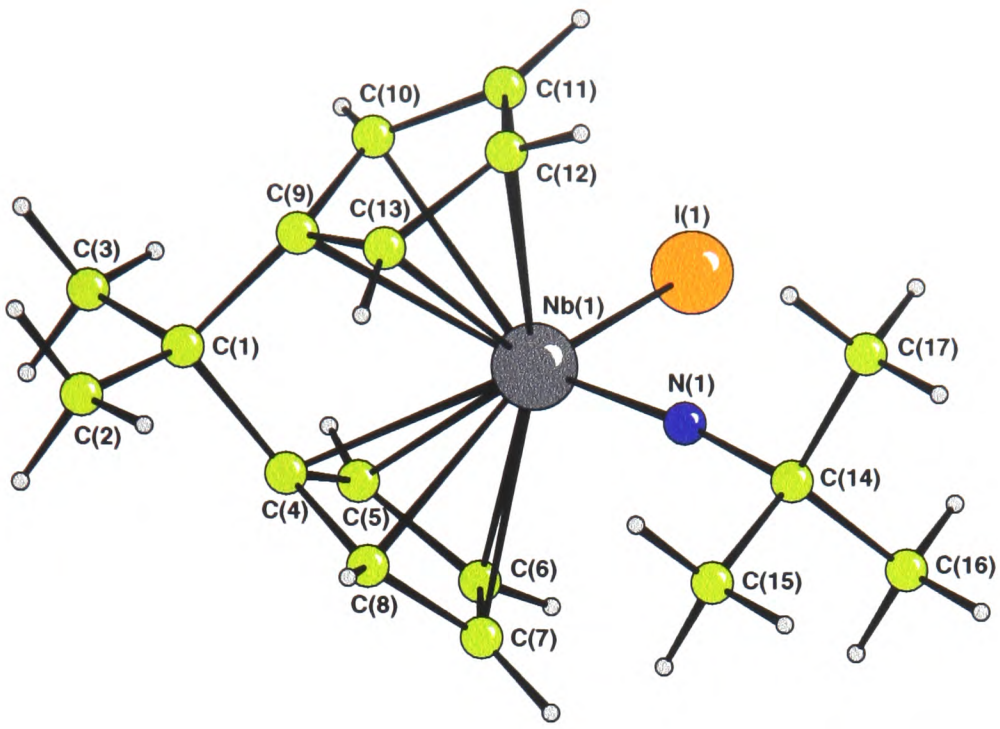

Figure 3.12 The molecular structure of [Nb(η-C_5H_4-CMe_2-η-C_5H_4)(NBu^t)I] (**10**). Hydrogen atom labels are omitted for clarity.

Bond	Length / Å	Bond	Angle / °
Nb(1)–N(1)	2.8400(3)	C(2)–C(1)–C(3)	109.4(2)
Nb(1)–I(1)	1.770(2)	C(4)–C(1)–C(9)	99.4(2)
Nb(1)–C(4)	2.486(2)	I(1)–Nb(1)–N(1)	98.91(6)
Nb(1)–C(5)	2.528(2)	Nb(1)–N(1)–C(14)	171.8(2)
Nb(1)–C(6)	2.520(3)	Bending angle, β	111.4
Nb(1)–C(7)	2.499(2)	Cp_{cent}–Nb(1)–Cp_{cent}, γ	114.2
Nb(1)–C(8)	2.397(2)	Cp_{cent}–C(4)–C(1)	163.6
Nb(1)–C(9)	2.490(2)	Cp_{cent}–C(9)–C(1)	163.4
Nb(1)–C(10)	2.551(2)		
Nb(1)–C(11)	2.533(3)		
Nb(1)–C(12)	2.490(3)		
Nb(1)–C(13)	2.386(2)		
N(1)–C(14)	1.440(3)		
Nb(1)–Cp_{cent}	2.18, 2.18		

Table 3.5 Selected interatomic distances and angles for [Nb(η-C_5H_4-CMe_2-η-C_5H_4)(NBu^t)I] (**10**)

3.5 Preparation of [Nb(η-C_5H_4-CMe_2-η-C_5H_4)(NBu^t)Me] (11)

Treatment of compound **8** with methyllithium in diethyl ether gives the corresponding methyl derivative [Nb(η-C_5H_4-CMe_2-η-C_5H_4)(NBu^t)Me] (**11**) as a yellow powder in 64 % yield (**Figure 3.13**).

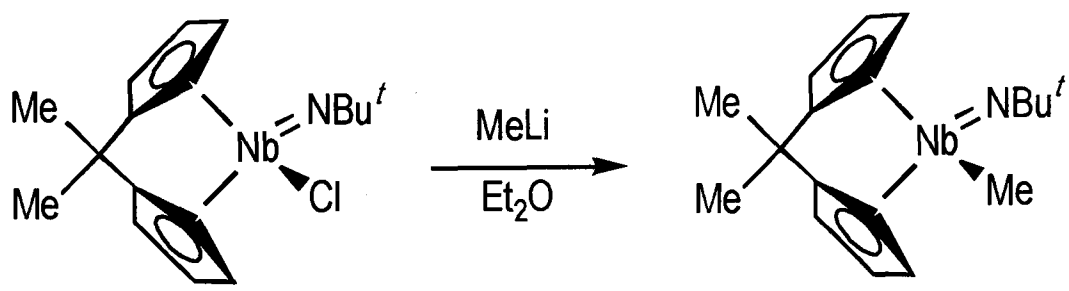

Figure 3.13 Preparation of [Nb(η-C_5H_4-CMe_2-η-C_5H_4)(NBu^t)Me] (**11**)

Elemental analysis data obtained for a sample of **11** was consistent with the proposed empirical formula. The ^{1}H NMR (CD_2Cl_2) spectrum (**Figure 3.14**) contains the usual peaks due to the *ansa bis*cyclopentadienyl and *tertiary*-butyl ligands and a singlet appearing at δ 0.76 ppm assigned to the metal bound methyl group.

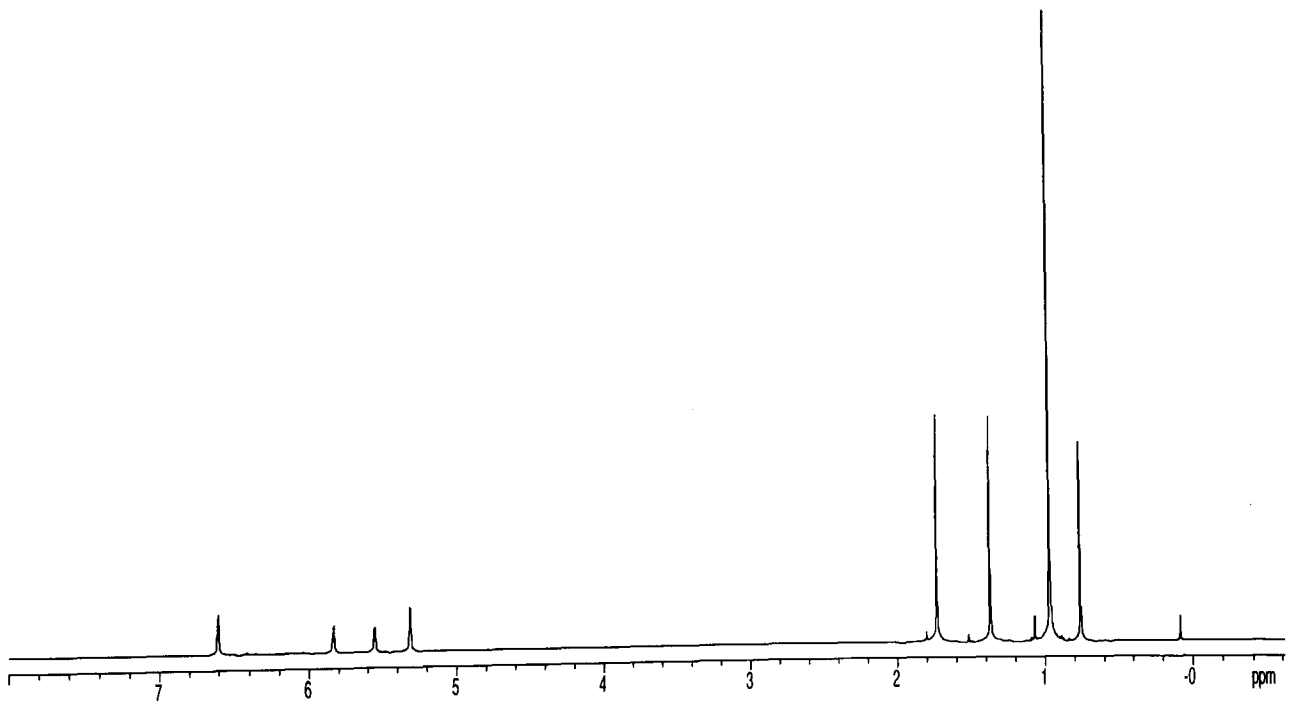

Figure 3.14 ^{1}H NMR (CD_2Cl_2) spectrum of [Nb(η-C_5H_4-CMe_2-η-C_5H_4)(NBu^t)Me] (**11**)

The $^{13}C\{^{1}H\}$ NMR (CD_2Cl_2) spectrum is shown in **Figure 3.15** and contains, in addition to *ansa* ligand and *tertiary*-butyl peaks, a broad peak centred at δ 2.3 ppm with a linewidth of approximately 55 Hz at half height which is assigned to the Nb–CH_3 resonance. This resonance was not located in the $^{13}C\{^{1}H\}$ NMR spectrum of the unbridged analogue.[7]

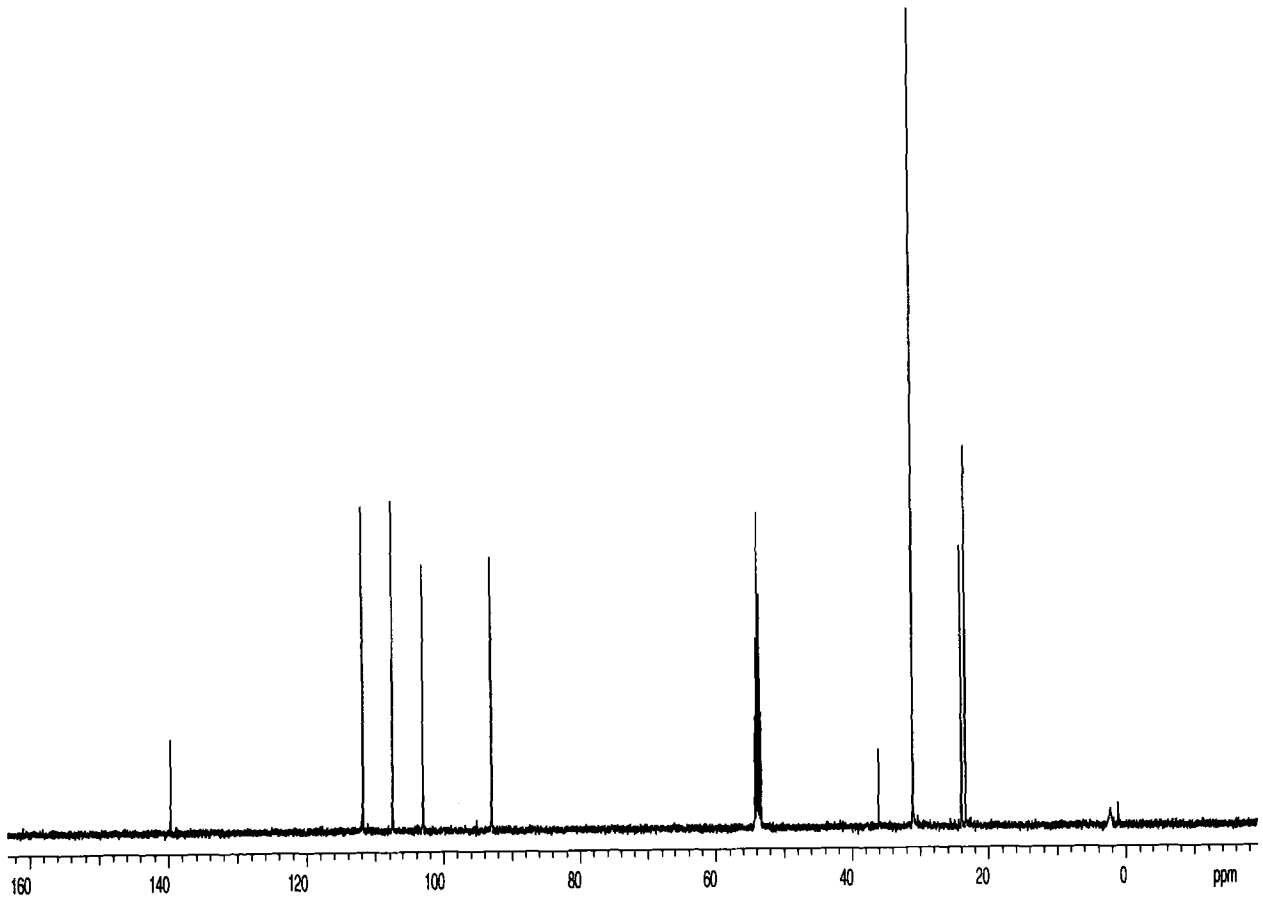

Figure 3.15 $^{13}C\{^{1}H\}$ NMR (CD_2Cl_2) spectrum of [Nb(η-C_5H_4-CMe_2-η-C_5H_4)(NBu^t)Me] (**11**)

The Electron Impact ionisation mass spectrum of **11** contains peaks due to the molecular ion and fragments resulting from the loss of one or more methyl groups or the imido ligand.

Photoelectron spectra were recorded for compound **11** and are presented in **Section 3.8**.

3.6 Preparation of [Nb(η-C_5H_4-CMe_2-η-C_5H_4)(NHBu^t)Cl][BF_4] (12)

Treatment of a yellow solution of [Nb(η-C_5H_4-CMe_2-η-C_5H_4)(NBu^t)Cl] (**8**) in diethyl ether with HBF_4 resulted in the precipitation of an orange powder. Elemental analysis of this powder was consistent with the empirical formula [Nb(η-C_5H_4-CMe_2-η-C_5H_4)(NHBu^t)Cl][BF_4] (**12**).

Attempts to obtain NMR spectroscopic data for **12** were hindered by its decomposition in chlorinated solvents, acetonitrile or DMSO and its low solubility in aromatic solvents. However, its solubility in C_6D_6 is just sufficient to allow the ^{1}H NMR spectrum to be obtained. Expected peaks for the *ansa* ligand and the *tertiary*-butyl amido ligand are found, with downfield shifts relative to the parent compound **8**. A resonance for the acidic NH was not located, possibly because it is too broad. However, the IR spectrum of **12** contains a band at 3313 cm^{-1} which is in the region expected for N–H stretching vibrations.

The closely related compound [Nb(η-$C_5H_4SiMe_3$)$_2$(NHPh)Cl][BF_4] has been prepared in an entirely analogous fashion.[10]

3.7 Unexpected isolation of [Nb(η-C_5H_4-CMe_2-η-C_5H_4)(O)Cl] (13)

A sample of [Nb(η-C_5H_4-CMe_2-η-C_5H_4)(NHBu^t)Cl][BF_4] (**12**) was dissolved in THF and a slow continuous stream of dinitrogen was passed over the solution for 12 h. Yellow single crystals were isolated which were initially presumed to be compound **12**. However, an X-ray crystallographic study revealed that this was not the case. Unfortunately, the data obtained from the selected crystal was of poor quality and six

carbon atoms remained isotropic during the final cycles of refinement. However, the connectivity is not in question and the structure determination supports the formulation of the compound as [Nb(η-C_5H_4-CMe_2-η-C_5H_4)(O)Cl] (**13**).

This assertion is corroborated by the elemental analysis and spectroscopic data, which were obtained from the same batch of crystals as the crystallographic data set. The Electrospray mass spectrum shows a peak at *m/z* corresponding to the proposed molecular ion. The ^{1}H NMR (CD_2Cl_2) data shows four peaks in the region expected for cyclopentadienyl resonances and two singlets at higher field assigned to the bridging methyl groups. There are no peaks which can be assigned to a *tertiary*-butyl imido group in the ^{1}H NMR (CD_2Cl_2) spectrum. The $^{13}C\{^1H\}$ NMR (CD_2Cl_2) spectrum is also consistent with the proposed formula.

The molecular structure of **13** is shown in **Figure 3.16** and selected interatomic distances and angles are given in **Table 3.6**. Full crystallographic details are presented in **Appendix H**.

The structure of the unbridged analogue, [Nb(η-C_5H_5)$_2$(O)Cl],[11] has been published. The molecular geometry is closely similar to that of compound **13**, except that the angle subtended by the ring centroid to niobium vectors in the unbridged compound is larger (128.2° *vs.* 115.3° in **13**). The Nb=O bond lengths in the unbridged and bridged compounds are 1.737(6) and 1.751(9) Å, respectively. However, the poor quality of the structural data for **13** does not permit comment with regard to the Nb=O bond order.

The oxo ligand is isolobal with the imido group and the metal-carbon distances in **13** are comparable to those in the imido compounds **7**- **10**, as expected.

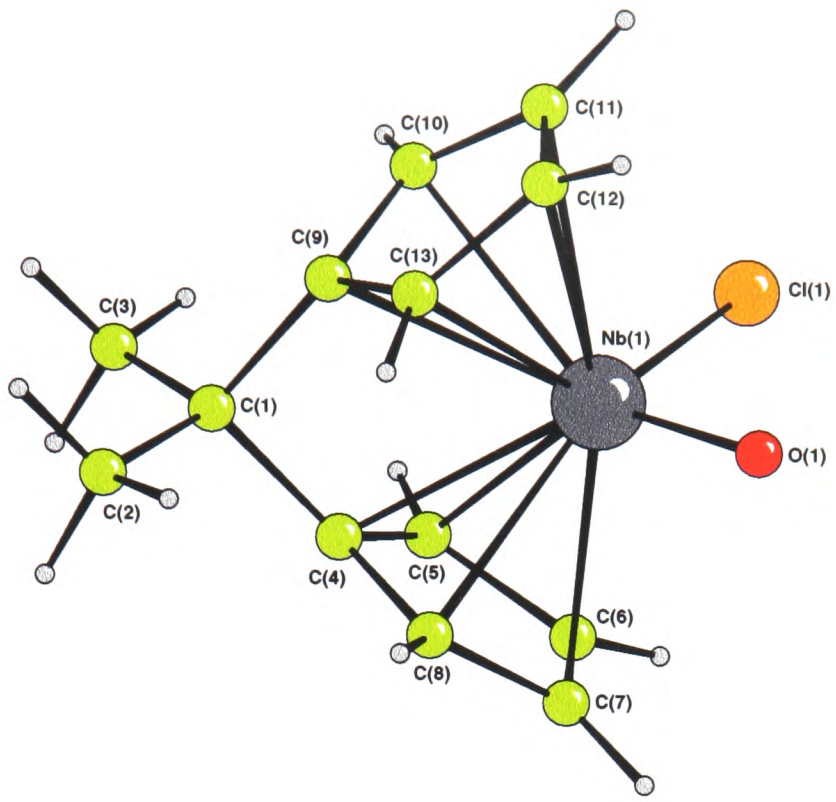

Figure 3.16 The molecular structure of [Nb(η-C_5H_4-CMe_2-η-C_5H_4)(O)Cl] (**13**). Hydrogen atom labels are omitted for clarity.

Bond	Length / Å	Bond	Angle / °
Nb(1)–O(1)	1.751(9)	C(2)–C(1)–C(3)	111.3(12)
Nb(1)–Cl(1)	2.435(4)	C(4)–C(1)–C(9)	98.5(10)
Nb(1)–C(4)	2.48(1)	O(1)–Nb(1)–Cl(1)	100.1(4)
Nb(1)–C(5)	2.50(2)	Bending angle, β	112.3
Nb(1)–C(6)	2.52(1)	Cp_{cent}–Nb(1)–Cp_{cent}, γ	115.3
Nb(1)–C(7)	2.52(1)	Cp_{cent}–C(4)–C(1)	164.1
Nb(1)–C(8)	2.42(1)	Cp_{cent}–C(9)–C(1)	163.1
Nb(1)–C(9)	2.49(1)		
Nb(1)–C(10)	2.50(1)		
Nb(1)–C(11)	2.51(1)		
Nb(1)–C(12)	2.51(1)		
Nb(1)–C(13)	2.42(1)		
Nb(1)–Cp_{cent}	2.17, 2.18		

Table 3.6 Selected interatomic distances and angles for [Nb(η-C_5H_4-CMe_2-η-C_5H_4)(O)Cl] (**13**)

The most likely reason for the unexpected formation of **13** is that trace oxygen or water from the house supply of dinitrogen was involved.

3.8 Photoelectron spectroscopy of *ansa* niobium(V) imido complexes

This section is the result of a collaboration with Tessa Dijkstra, a project student working under the supervision of Dr J. C. Green in this laboratory. The photoelectron spectra of compounds **8** and **11** were recorded and are compared with orbital energies calculated for [Nb(η-C_5H_4-CH_2-η-C_5H_4)(NMe)Cl], a simplified analogue of **8**, and with the photoelectron spectrum of [Mo(η-C_5H_5)$_2$NBu^t].[12]

3.8.1 The photoelectron spectrum of [Mo(η-C_5H_5)$_2$NBu^t]

Before discussing the photoelectron spectra of the formally twenty electron compounds **8** and **11** it is instructive to summarise the results obtained for [Mo(η-C_5H_5)$_2$NBu^t] by Green and co-workers.[12] This compound also has a twenty electron count if normal rules are followed. The short range He I photoelectron spectrum of [Mo(η-C_5H_5)$_2$NBu^t] is reproduced in **Figure 3.17** and shows two low lying ionisations. The first of these corresponds to ejection of one of the two d electrons occupying the $1a_1$ orbital. The second band is assigned, with the aid of molecular orbital calculations, to an ionisation from a b_1 orbital localised principally on the nitrogen and the cyclopentadienyl rings, as shown in **Figure 3.17**.

Similarly, Lauher and Hoffmann's extended Hückel calculations predict the existence of a completely ligand based orbital in the molecule $[Mo(\eta\text{-}C_5H_5)_2(NO)R]$. The two electrons in this orbital do not contribute to the metal centre.[13] Thus, it seems that despite the formal twenty electron count in these compounds, the eighteen electron rule is not violated.

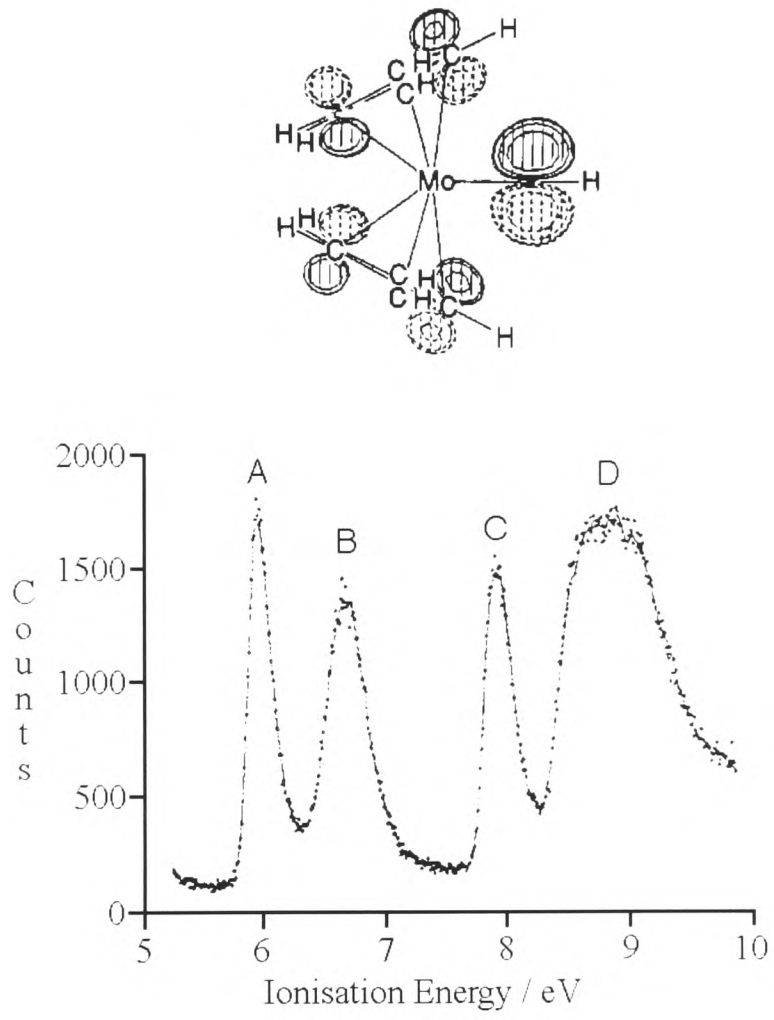

Figure 3.17 Short range He I photoelectron spectrum of $[Mo(\eta\text{-}C_5H_5)_2NBu^t]$ together with a representation of the orbital to which band B is assigned

3.8.2 Density Functional calculation on $[Nb(\eta\text{-}C_5H_4\text{-}CH_2\text{-}\eta\text{-}C_5H_4)(NMe)Cl]$

The basic strategy behind a DFT geometry optimisation is to construct a plot of the total energy of the molecule as a function of the molecular structure. To reduce computing time it is convenient to reduce the number of dimensions of this surface by

limiting the number of structural parameters where possible. Thus the backbone methyl groups in **8** were replaced with hydrogens and the *tertiary*-butyl group was replaced with a methyl group to give a model compound [Nb(η-C_5H_4-CH_2-η-C_5H_4)(NMe)Cl]. To speed up the calculation further the symmetry of the molecule was constrained to ideal, C_s. The number of steps between the input structure and the converged structure should be kept to a minimum and it is usual for the starting parameters to be derived from X-ray crystallographic data. Therefore, the bond lengths and angles from the molecular structure of **8** were used for the input structure.

Selected structural parameters for the converged geometry of [Nb(η-C_5H_4-CH_2-η-C_5H_4)(NMe)Cl] in comparison with experimental values for [Nb(η-C_5H_4-CMe_2-η-C_5H_4)(NBu^t)Cl] (**8**) are shown in **Table 3.7**. The data agree well, the average percentage deviation is of the order of only 1 % in both distances and angles.

Bond	Length / Å		Bond	Angle / °	
	DFT	X-ray		DFT	X-ray
Nb(1)–Cl(1)	2.484	2.446	Cl(1)–Nb(1)–N(1)	99.3	95.3
Nb(1)–N(1)	1.787	1.762	Nb(1)–N(1)–C(14)	177.1	178.4
N(1)–C(14)	1.415	1.438	C(4)–C(1)–C(4´)	99.3	99.3
C(1)–C(4)	1.504	1.528	Cp_{cent}–Nb(1)–Cp_{cent}	113.1	113.3
C(4)–C(5)	1.402	1.405			
C(5)–C(6)	1.435	1.424			
C(6)–C(7)	1.409	1.395			
C(7)–C(8)	1.425	1.421			
C(8)–C(4)	1.440	1.435			

Table 3.7 Selected distances and angles from the DFT geometry optimisation of [Nb(η-C_5H_4-CH_2-η-C_5H_4)(NMe)Cl] compared with X-ray crystallographic data of [Nb(η-C_5H_4-CMe_2-η-C_5H_4)(NBu^t)Cl] (**8**)

Thus, the orbital energies derived from this calculation, which are given in **Table 3.8**, can be used with some confidence to aid assignment of the photoelectron spectra. Selected orbitals are pictured in **Figure 3.18**.

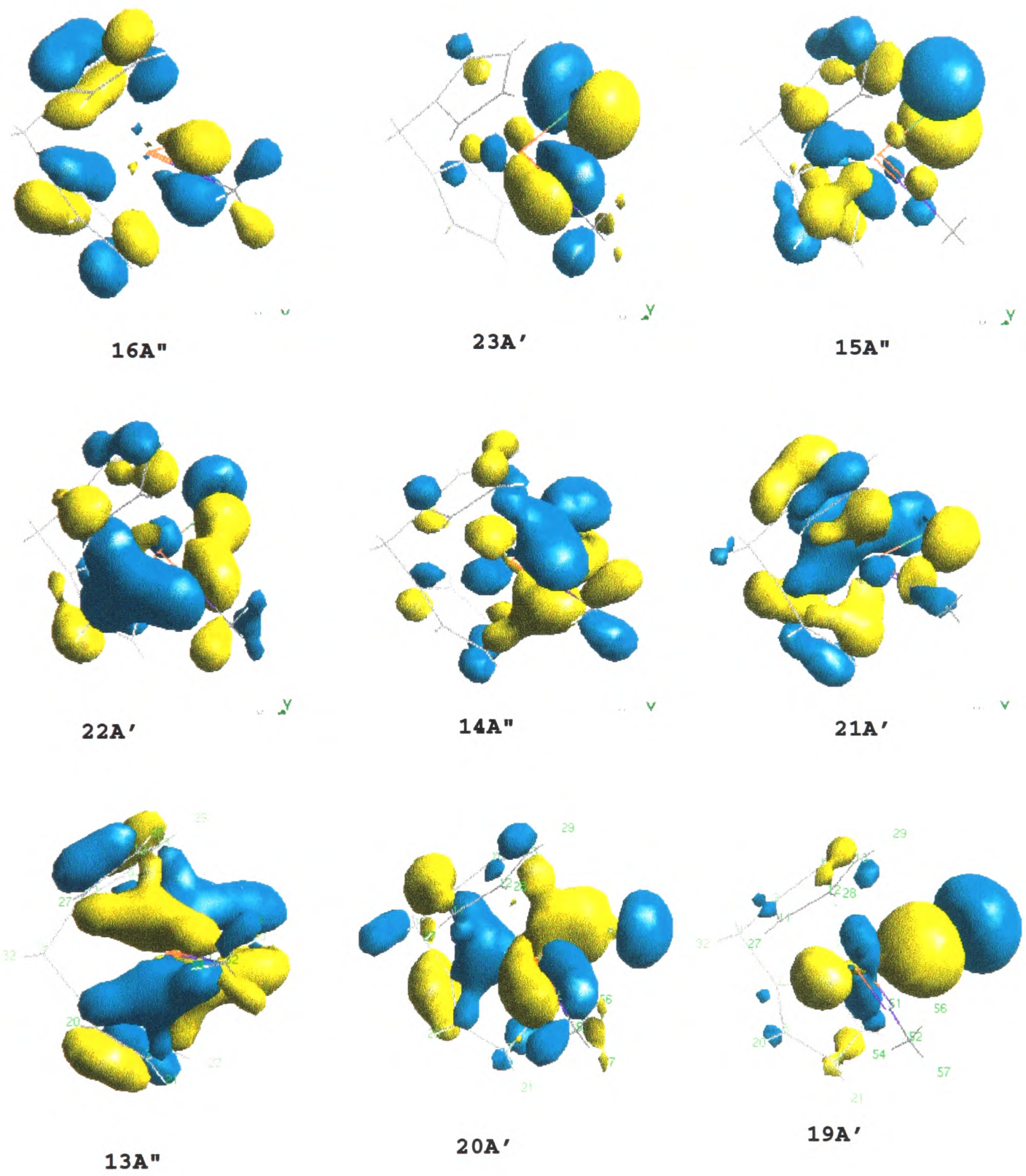

Figure 3.18 Selected molecular orbitals of [Nb(η-C_5H_4-CH_2-η-C_5H_4)(NMe)Cl]

Orbital	Energy / eV	Orbital	Energy / eV
16 A"	–5.516	21 A'	–7.356
23 A'	–6.052	13 A"	–7.870
15 A"	–6.053	20 A'	–7.886
22 A'	–7.009	19 A'	–7.990
14 A"	–7.332		

Table 3.8 Orbital energies obtained from Density Functional calculations on [Nb(η-C_5H_4-CH_2-η-C_5H_4)(NMe)Cl]

The orbitals have a lot of mixed character and it is difficult to assign specific bonding interactions to each orbital. The 16 A" orbital is antibonding between the nitrogen and cyclopentadienyl rings and has little or no metal character. The 23 A' orbital is located mainly in the *yz* plane and is M–N π-bonding with some contribution from the in-plane chlorine lone pair. The 15 A" orbital is of mixed character, this time with an appreciable contribution from the out-of-plane chlorine lone pair. The next four orbitals are principally of metal-ring bonding character. The 19 A' orbital is the M–Cl σ interaction. Owing to the mixed band structure, the assignments which follow are only tentative. However, with the aid the of calculated orbital energies and the trends observed in the He II spectra, some conclusions can be made.

3.8.3 Photoelectron spectra of [Nb(η-C_5H_4-CMe_2-η-C_5H_4)(NBu^t)Cl] (8) and [Nb(η-C_5H_4-CMe_2-η-C_5H_4)(NBu^t)Me] (11)

Good quality He I and He II photoelectron spectra were obtained for **8** and **11**. Compound **8** sublimed at 133 °C, compound **11** at 98 °C. The long range He I photoelectron spectra are shown in **Figure 3.19**. Vertical ionisation energies (IEs) and

tentative band assignments for **8** and **11** appear in **Table 3.9** and **Table 3.10**, respectively.

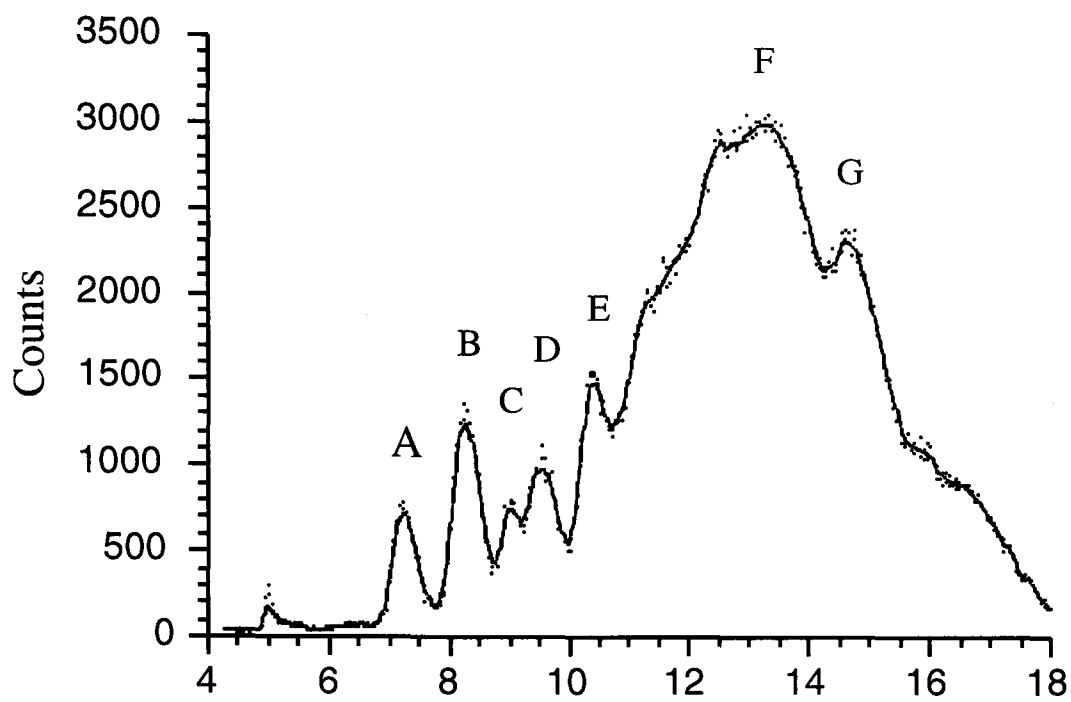

Figure 3.19 Long range He I photoelectron spectra of [Nb(η-C_5H_4-CMe_2-η-C_5H_4)(NBu^t)Cl] (**8**) (top) and [Nb(η-C_5H_4-CMe_2-η-C_5H_4)(NBu^t)Me] (**11**) (bottom).

Band	Vertical IE / eV	Assignment	Band	Vertical IE / eV	Assignment
A	7.22	16 A"	E	10.39	13 A", 20 A', 19 A'
B	8.28	23 A', 15 A"	F	13.09	Cp based
C	9.02	22 A'	G	14.62	Cp based
D	9.55	14 A", 21 A'			

Table 3.9 Vertical IEs and band assignments for $[Nb(\eta\text{-}C_5H_4\text{-}CMe_2\text{-}\eta\text{-}C_5H_4)(NBu^t)Cl]$ (**8**)

Band	Vertical IE / eV	Assignment	Band	Vertical IE / eV	Assignment
A	7.01	16 A"	B"	9.23	M-Cp, M-L
B	8.28	M-Cp, M-L	C	12.50	Cp based
B'	8.60	M-Cp, M-L	D	14.35	Cp based

Table 3.10 Vertical IEs and band assignments for $[Nb(\eta\text{-}C_5H_4\text{-}CMe_2\text{-}\eta\text{-}C_5H_4)(NBu^t)Me]$ (**11**)

The He I spectra in **Figure 3.19** can be seen to correspond roughly. The lowest energy ionisation, band A, is common to both compounds and is assigned to orbital 16 A". This molecular orbital is the result of overlap between the metal-ring antibonding $1b_1$ orbital (**Figure 3.5**) and the nitrogen p orbital of b_1 symmetry. As was mentioned in **Section 3.2**, donation of electron density from the nitrogen into this metal-ring antibonding orbital causes the metal-ring distances to be longer than in non imido compounds. Inspection of **Figure 3.18** shows that the resulting MO has virtually no metal character. A simple analogy is the case of back-bonding in metal carbonyls, where the π bonding interaction is frequently discussed in terms of donation of electron density from metal d orbitals of π symmetry into CO π^* orbitals. The

resulting MOs are found to have only a small contribution from carbon atomic orbitals.[14]

It can be seen that band A has the same origin as band B in the photoelectron spectrum of [Mo(η-C_5H_5)$_2$NBu^t]. Hence, compounds **8** and **11** add to the examples of twenty electron compounds where the two 'surplus' electrons are located in an orbital with very little metal d orbital contribution.

The calculated orbital energy of 16 A" and the observed vertical ionisation energies of band A in the spectra of **8** and **11** differ. When ionisation occurs the remaining electrons rearrange their distribution in the molecular ion. There is a reorganisation energy associated with this process and this is responsible for the difference between calculated orbital energies and the observed ionisation energies. Mixing of the orbitals after ionisation also complicates assignment of the bands. This is often a problem in low symmetry molecules such as those discussed here.

The next three low energy ionisations, bands B-D in the spectrum of **8** and bands B-B" in the spectrum of **11** are in the region expected for metal-ligand interaction orbitals. On the basis of the calculated orbital energies the bands appearing in the photoelectron spectrum of **8** are assigned as follows. Band B is assigned to 23 A' and 15 A", which lie at the same energy. Band C is assigned to 22 A' and band D is assigned to 14 A" and 21 A'. The observed intensity variation across bands B, C and D supports this assignment. In the case of the methyl compound **11**, the orbital energies derived from the geometry optimisation of [Nb(η-C_5H_4-CH_2-η-C_5H_4)(NMe)Cl] cease to be useful since inspection of **Figure 3.18** shows that there is appreciable chlorine character in all of the orbitals except 16 A". However, the

envelope containing bands B, B' and B" spans the same ionisation energy range as bands B, C and D in the photoelectron spectrum of **8**, and these bands must therefore be due to similar metal-ligand interacting orbitals as in the chloro compound.

Band E in the spectrum of **8** has no counterpart in the spectrum of **11** and is assigned to a chlorine based ionisation from 19 A'. The short range He I and He II spectra of **8** are shown in **Figure 3.20**. The intensity of band E is seen to drop considerably at the higher photon energy, an observation consistent with its assignment as arising from a halogen based ionisation. The intensity of band A is also seen to drop in the He II spectrum, again consistent with its assignment to an orbital with little metal d orbital character. The short range He I and He II spectra of **11** are shown in **Figure 3.21**. Again, the intensity of band A is decreased in the He II spectrum relative to the other bands.

The broad amorphous region above 12 eV in the spectra of both compounds is due to CH and CC ionisation bands.

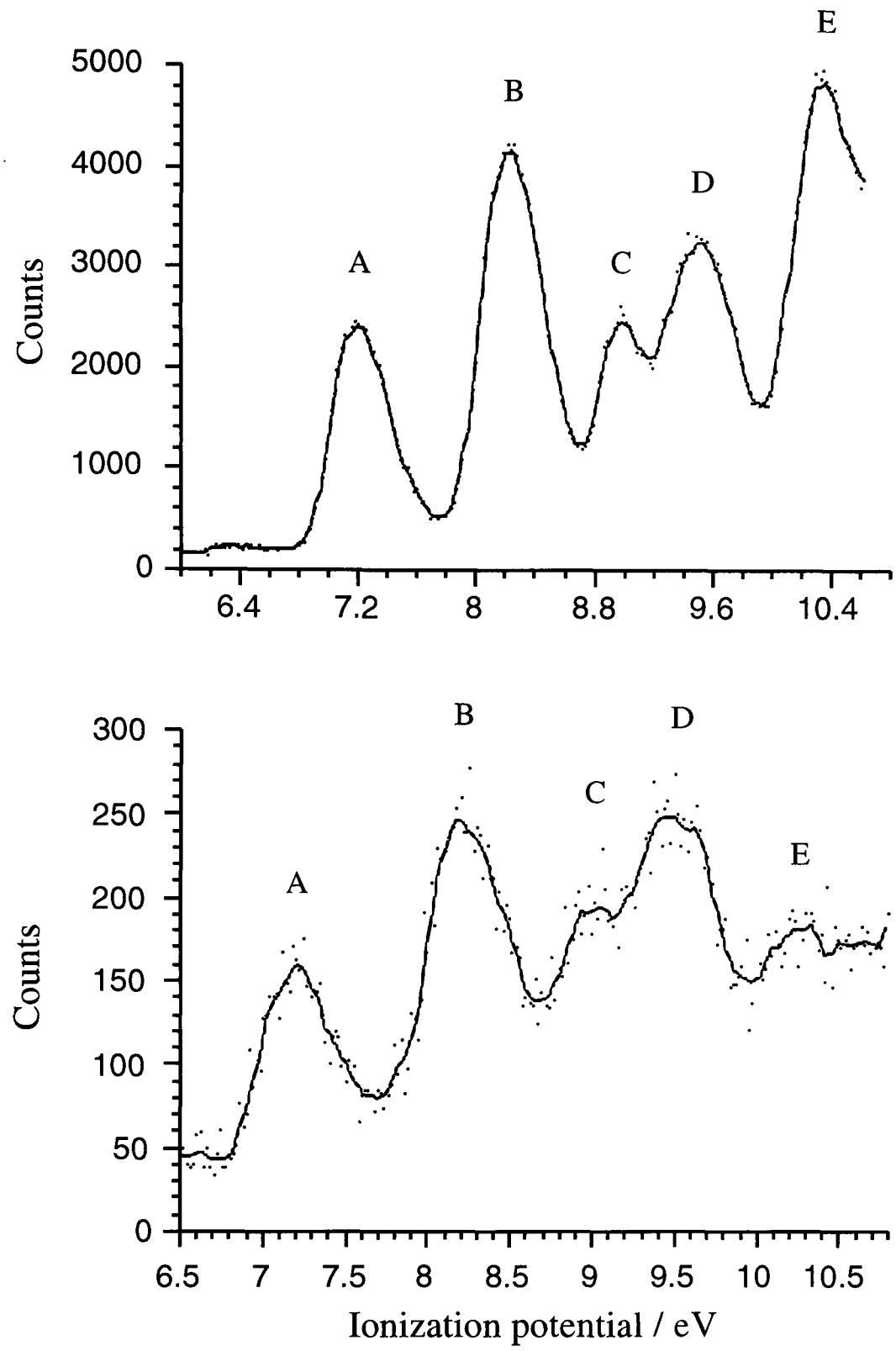

Figure 3.20 Short range He I (top) and He II (bottom) photoelectron spectra of $[Nb(\eta\text{-}C_5H_4\text{-}CMe_2\text{-}\eta\text{-}C_5H_4)(NBu^t)Cl]$ (**8**)

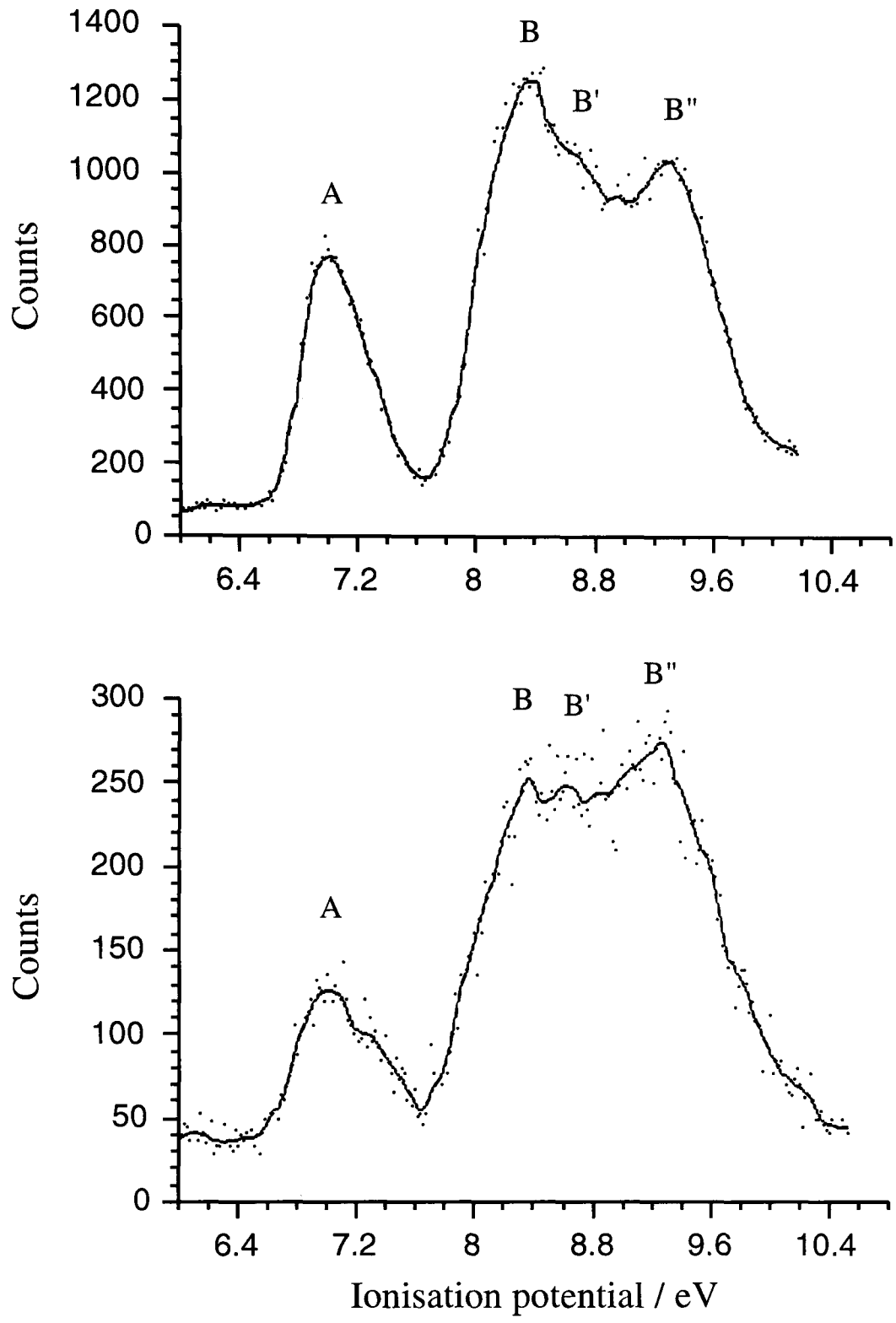

Figure 3.21 Short range He I (top) and He II (bottom) photoelectron spectra of $[Nb(\eta\text{-}C_5H_4\text{-}CMe_2\text{-}\eta\text{-}C_5H_4)(NBu^t)Me]$ (**11**)

3.8.4 Concluding remarks

Good quality He I and He II photoelectron spectra were obtained for compounds **8** and **11**. A geometry optimisation in good agreement with X-ray crystallographic data gave orbital energies consistent with the photoelectron spectra. In both compounds the HOMO is a combination of nitrogen and cyclopentadienyl orbitals which is non-bonding with respect to niobium. Thus, two electrons do not contribute to the metal and the eighteen electron rule may be considered to hold.

3.9 General comments

Use of the ancillary imido ligand has allowed entry to single carbon atom *ansa* bridged niobium chemistry in good yield *via* the compound [Nb(η-C_5H_4-CMe_2-η-C_5H_4)(NBu^t)Cl] (**8**). Compound **8** has been used to prepare other examples of *ansa* *bis*cyclopentadienyl imido niobium derivatives, as detailed in this chapter.

Many other transformations were attempted and a selection are mentioned briefly below. As was the case in **Chapter 2** the problems encountered were usually due to decomposition of the *ansa* metallocene moiety as revealed by ^1H spectroscopy of the reaction mixtures. This is presumably due to the combination of the labilising effect of the *ansa* bridge, which prevents optimal metal-ring bonding (**Section 1.4**), and competition between the imido group and the cyclopentadienyl rings (**Section 3.8**).

In attempts to prepare salts of the form [Nb(η-C_5H_4-CMe_2-η-C_5H_4)(NBu^t)L][PF_6] compound **8** was treated with $AgPF_6$ in CH_3CN or THF, with or without subsequent

addition of PMe_3. In each case a precipitate was observed, presumed to be AgCl, but no pure compound could be isolated from reaction mixture.

In further attempts to substitute the chlorine atom, compound **8** was treated with NaCCPh, $NaNH_2$, Me_3SnF, $Bu^tNHSiMe_3$, Bu^tNHLi, Bu^tOLi, Me_3SiNCO, $Me_3SiO_3SCF_3$, or Me_3SiN_3. In each of these cases the only soluble material isolated from the reaction mixture was unreacted compound **8**.

Various attempts were made to reduce compound **8**. Treatment with Na / Hg amalgam, $[NaAlH_2(OCH_2CH_2OMe)_2]$, $LiAlH_4$ or $NaBH_4$ gave mixtures of products from which no pure compound could be isolated.

Treatment of compound **8** with gaseous HCl in an attempt to cleave the imido group resulted in decomposition products.

A solution of compound **11** in toluene containing excess of CS_2 was heated at 135 °C for 48 h in a sealed ampoule. The volatiles were removed and the residue extracted into pentane. The pentane was removed under reduced pressure. IR spectroscopy showed that there had been no insertion of CS_2 into the Nb–Me bond during that time.

When compound **11** was treated with the strong Lewis acid $[B(C_6F_5)_3]$ an orange precipitate formed almost immediately. Although this reaction appears to have been successful, attempts to purify the resulting compound by crystallisation resulted in the formation of oils and this reaction was not pursued.

3.10 Summary

The new chemistry described in this chapter is summarised in **Figure 3.22**.

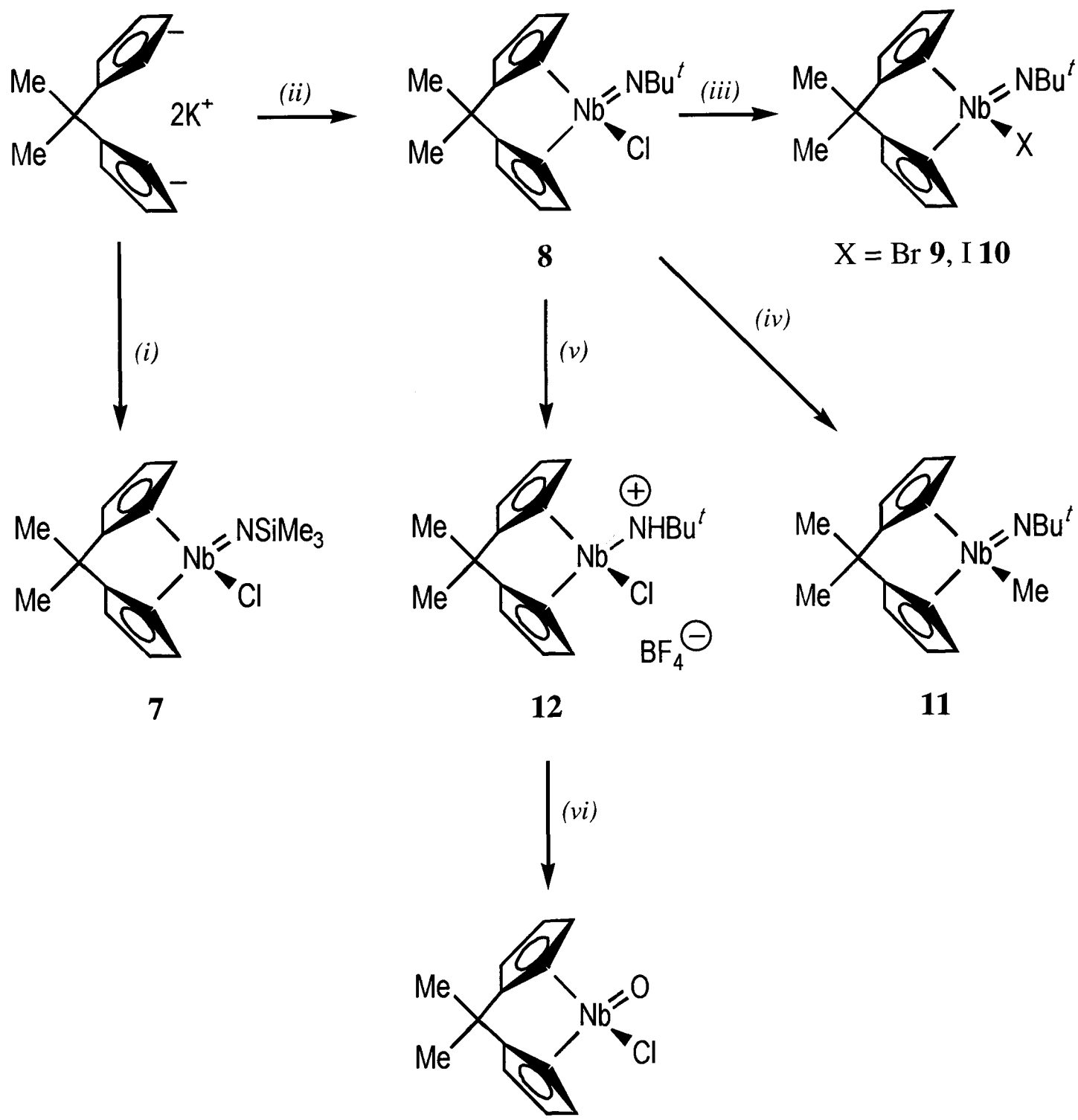

Reagents:
(i) $[Nb(NSiMe_3)(py)_2Cl_3]$ in THF
(ii) $[Nb(NBu^t)(py)_2Cl_3]$ in THF
(iii) $XSiMe_3$ (X = Br, I) in light petroleum
(iv) MeLi in Et_2O
(v) HBF_4 in Et_2O
(vi) THF, O_2 or H_2O?

Figure 3.22 Summary of reactions presented in **Chapter 3**

References for Chapter 3

1. S. Schmidt and J. Sundermeyer, *J. Organomet. Chem.*, 1994, **472**, 127.

2. C. M. Jones, M. E. Lerchen, C. J. Church, B. M. Schomber and N. M. Doherty, *Inorg. Chem.*, 1990, **29**, 1679.

3. W. A. Herrmann, W. Baratta and E. Herdtweck, *J. Organomet. Chem.*, 1997, **541**, 445.

4. C. S. Bajgur, W. R. Tikkanen and J. L. Petersen, *Inorg. Chem.*, 1985, **24**, 2539.

5. W. A. Nugent and J. M. Mayer, *Metal-Ligand Multiple Bonds,* Wiley Interscience, NY, 1988.

6. J. C. Green, *Chem. Soc. Rev.*, 1998, in press.

7. A. N. Chernega, M. L. H. Green and A. G. Suárez, *J. Chem. Soc., Dalton Trans.*, 1993, 3031.

8. N. J. Bailey, J. A. Cooper, H. Gailus, M. L. H. Green, J. T. James and M. A. Leech, *J. Chem. Soc., Dalton Trans.*, 1997, 3579.

9. M. L. H. Green, J. T. James and A. N. Chernega, *J. Chem. Soc., Dalton Trans.*, 1997, 1719.

10. Z. M. Tehrani, D. Lucas, Y. Mugnier, A. Antiñolo, A. Otero, M. Fajardo, A. Garces and C. Lopez-Mardomingo, *J. Organomet. Chem.*, 1997, **548**, 309.

11. A. L. Rheingold and J. B. Strong, *Acta Cryst.*, 1991, **47C**, 1963.

12. J. C. Green, M. L. H. Green, J. T. James, P. C. Konidaris, G. H. Maunder and P. Mountford, *J. Chem. Soc., Chem. Commun.*, 1992, 1361.

13. J. W. Lauher and R. Hoffmann, *J. Am. Chem. Soc.*, 1976, **98**, 1729.

14. J. C. Green, 1998, personal communication.

Chapter 4

Synthesis of *ansa* complexes from niobium(III) chloride

4.1 Introduction to Chapter 4

The preceding chapters describe the investigation of niobium(IV) and niobium(V) compounds as possible starting materials for the synthesis of *ansa* niobium compounds. It seemed logical to consider, also, compounds of niobium(III). The results of preliminary examinations of the usefulness of $NbCl_3$.DME as a starting material for *ansa* chemistry are presented in this chapter. This work was undertaken as the project was drawing to a close, in an effort to further systematise the approach taken towards syntheses of *ansa* niobium compounds.

Simple electron counting arguments suggest that a successful synthesis of a *bis*cyclopentadienyl compound from $NbCl_3$.DME might require the presence of an additional two electron donor ligand, since the electron count of [Nb(η-C_5H_4-CMe_2-η-C_5H_4)Cl] is only sixteen. The approach adopted, therefore, is to try to prepare [Nb(η-C_5H_4-CMe_2-η-C_5H_4)(L)Cl], where L could be either a coordinating solvent or some other ligand (**Figure 4.1**).

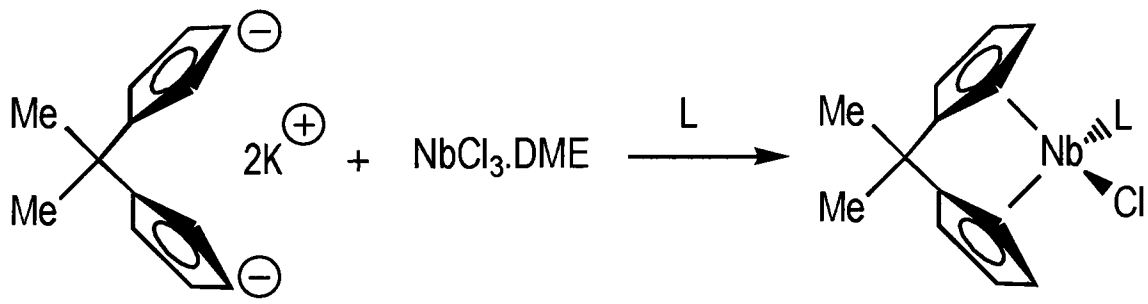

Figure 4.1 Approach to synthesis of *ansa* niobium(III) complexes

When L is a reagent other than solvent, the timing of its addition to the reaction mixture may be varied. For instance, experiments where L is added to $NbCl_3$.DME prior to addition of the *ansa* ligand dianion might produce different results to those

where L is added after reaction between $NbCl_3$.DME and the *ansa* ligand dianion has occurred.

The results of some preliminary explorations into this area of chemistry are described below.

4.2 Preparation of $NbCl_3$.DME

The compound $NbCl_3$.DME is prepared by reduction of $NbCl_5$ by two equivalents of tributyltin hydride in DME at low temperature. $NbCl_3$.DME precipitates from the reaction mixture and the tributyltin chloride by-product is washed away leaving a brick-red solid.[1] The molecular structure of $NbCl_3$.DME is still unknown. It is insoluble in THF and soluble in dichloromethane.

4.3 Reaction between $NbCl_3$.DME and $[K(C_5H_4\text{-}CMe_2\text{-}C_5H_4)K]$

No change is observed when solid $NbCl_3$.DME is added to a THF solution of $[K(C_5H_4\text{-}CMe_2\text{-}C_5H_4)K]$ at –78 °C. When the resulting suspension is allowed to warm to room temperature a deep purple solution containing a small amount of solid is obtained. If the mixture is left to stir overnight the colour of the solution changes from purple to brown. Filtration of the mixture, to remove KCl, followed by removal of the volatiles under reduced pressure gives a brown solid residue which is insoluble in light petroleum or diethyl ether, and only sparingly soluble in dichloromethane.

It is assumed that this brown solid consists of oligomers. Excess of PMe_3 was added to a dichloromethane suspension of the solid in an attempt to break up the material

into a soluble monomeric species. However, stirring for 48 h did not produce any noticeable dissolution of the material.

The reaction was repeated and watched closely as the temperature was raised. The purple colour appears swiftly at –10 °C. The temperature was then maintained below 0 °C whilst an excess of PMe_3 was added. Removal of the volatiles under reduced pressure gave a black powder which is completely insoluble in light petroleum or toluene. Since the desired compound, [Nb(η-C_5H_4-CMe_2-η-C_5H_4)(PMe_3)Cl], was expected to be soluble in non-polar solvents this method was abandoned.

4.4 Reaction between $NbCl_3$.DME and [K(C_5H_4-CMe_2-C_5H_4)K] in the presence of PMe_3

A THF solution of [K(C_5H_4-CMe_2-C_5H_4)K] was cooled to –50 °C and excess of PMe_3 was added. Addition of solid $NbCl_3$.DME to this mixture resulted in a brick-red suspension, as observed previously. On warming to –10 °C the colour again changed to purple and most of the solids dissolved although there was a small amount of residue, assumed to be KCl. The volatiles were removed from this purple solution, whilst maintaining the temperature below 0 °C, giving a purple solid residue. Extraction into light petroleum followed by filtration afforded a dark purple microcrystalline material.

The ^{1}H NMR (500 MHz, C_6D_6) spectrum of this material is entirely consistent with its formulation as [Nb(η-C_5H_4-CMe_2-η-C_5H_4)(PMe_3)Cl]. Four signals assigned to the hydrogens on the cyclopentadienyl ring appear at δ 5.64, 5.00, 4.91 and 3.81 ppm. A doublet centred at δ 0.87 ppm ($^2J_{PH}$ = 7.3 Hz) is assigned to the PMe_3 ligand and two

singlets at δ 0.60 and 0.13 ppm are assigned to the bridging methyl groups. These spectroscopic data are in close agreement with those reported for the unbridged analogue, $[Nb(\eta\text{-}C_5H_5)_2(PMe_3)Cl]$,[2] the ^1H NMR spectrum of which contains a singlet at δ 4.63 ppm and a doublet centred at δ 0.83 ppm ($^2J_{PH}$ = 8 Hz). The unbridged compound was prepared by reduction of $[Nb(\eta\text{-}C_5H_5)_2Cl_2]$ with Na / Hg amalgam in the presence of PMe_3. This route was attempted to synthesise $[Nb(\eta\text{-}C_5H_4\text{-}CMe_2\text{-}\eta\text{-}C_5H_4)(PMe_3)Cl]$ from the *ansa* niobium(IV) dichloride, $[Nb(\eta\text{-}C_5H_4\text{-}CMe_2\text{-}\eta\text{-}C_5H_4)Cl_2]$ (**1**), but it gave only decomposition products.

Unfortunately, $[Nb(\eta\text{-}C_5H_4\text{-}CMe_2\text{-}\eta\text{-}C_5H_4)(PMe_3)Cl]$ appears to be unstable in solution. Its ^{31}P NMR spectrum shows two peaks, one indicating loss of PMe_3. Attempts to recrystallise the compound failed since brown amorphous precipitates formed from freshly filtered petroleum solutions after only a few minutes. Thus, it appears that the PMe_3 ligand is labile and the ligand dissociation leads to decomposition of the compound. Attempts to recrystallise $[Nb(\eta\text{-}C_5H_4\text{-}CMe_2\text{-}\eta\text{-}C_5H_4)(PMe_3)Cl]$ from solutions in light petroleum containing a few drops of PMe_3 were also unsuccessful. This behaviour is similar to that reported in the literature for $[Nb(\eta\text{-}C_5H_5)_2(PEt_3)Cl]$, which was prepared in solution but could not be isolated as a solid.[2]

4.5 Preparation of $[Nb(\eta\text{-}C_5H_4\text{-}CMe_2\text{-}\eta\text{-}C_5H_4)\{P(OMe)_3\}Cl]$ (14)

There is little evidence to suggest that PMe_3 bonds to transition metals other than by σ-donation. However, dπ-dπ backbonding between filled metal d orbitals and vacant

phosphorus d orbitals is significant in PF_3[†] complexes, and to a certain extent in $P(OR)_3$ complexes.[3] The electronegative fluorine or oxygen substituents lower the energy of the vacant phosphorus d orbitals resulting in stronger dπ-dπ backbonding. Thus, in order to try to circumvent the problem of decomposition, trimethylphosphite was employed in the place of trimethylphosphine.

Addition of a THF solution of $[K(C_5H_4\text{-}CMe_2\text{-}C_5H_4)K]$ to a THF suspension of $NbCl_3.DME$ in the presence of an excess of $P(OMe)_3$ yields a red brown solution and a solid residue. Filtration to remove KCl followed by removal of the volatiles under reduced pressure affords a black solid. Extraction into light petroleum gives a red solution and a black residue. Attempts to derivatise the residue are described in later sections.

The petrol soluble fraction is easily crystallised by slow cooling of the red solution to –20 °C, giving red crystals of $[Nb(\eta\text{-}C_5H_4\text{-}CMe_2\text{-}\eta\text{-}C_5H_4)\{P(OMe)_3\}Cl]$ (**14**) in low yield (8 %). Elemental analysis data obtained for these crystals are in very good agreement with the proposed formula. The ^1H NMR (C_6D_6) spectrum of **14** is shown in **Figure 4.2**.

The *ansa* ligand protons of **14** have very similar chemical shifts to those of $[Nb(\eta\text{-}C_5H_4\text{-}CMe_2\text{-}\eta\text{-}C_5H_4)(PMe_3)Cl]$. A doublet centred at δ 3.46 ppm ($^3J_{PH}$ = 10 Hz) is assigned to coordinated $P(OMe)_3$. This compares to δ 3.63 ppm ($^3J_{PH}$ = 10.5 Hz) as reported for $[Nb(\eta\text{-}C_5H_5)_2\{P(OMe)_3\}Cl]$.[4] The unbridged analogue is characterised only by analytical data and ^1H NMR spectroscopy.

[†] The current opinion is that PF_3 accepts electron density *via* P–F σ* orbitals, and not into vacant d_π orbitals

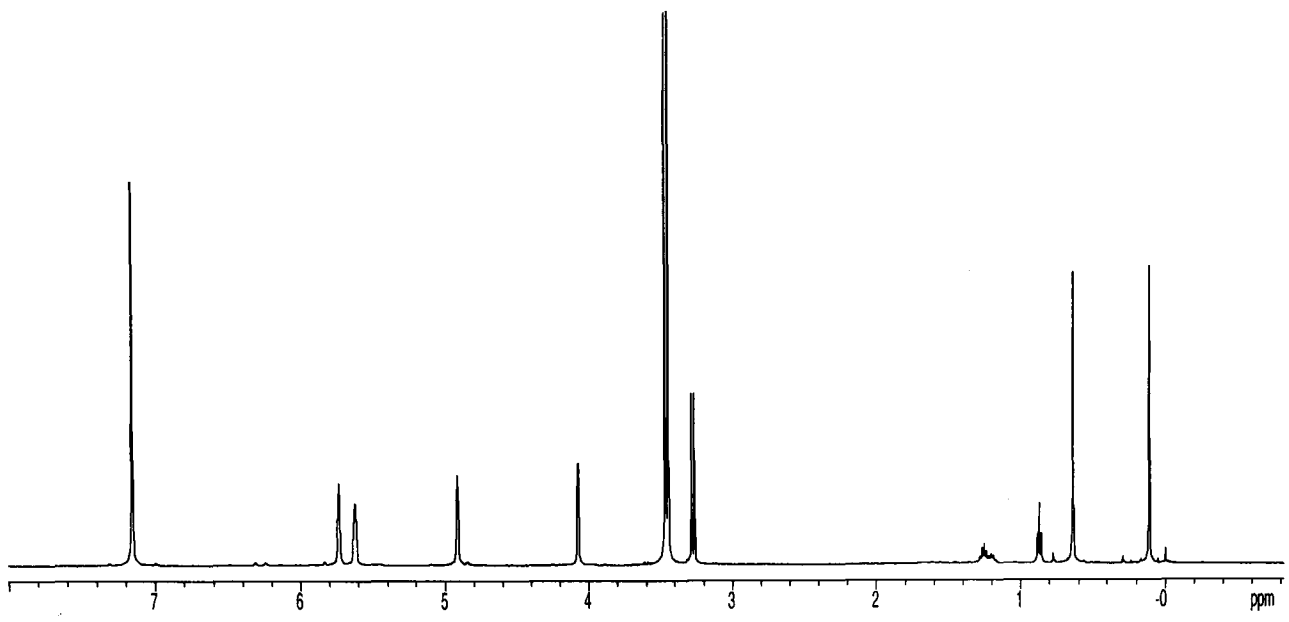

Figure 4.2 ^{1}H NMR (C_6D_6) spectrum of
$[Nb(\eta\text{-}C_5H_4\text{-}CMe_2\text{-}\eta\text{-}C_5H_4)\{P(OMe)_3\}Cl]$ (**14**)

The ^{1}H NMR spectrum of **14** suggests that there is a dissociative equilibrium in solution between bound and unbound trimethylphosphite. A doublet at δ 3.28 ($^{3}J_{PH}$ = 10.5 Hz) indicates the presence of uncoordinated $P(OMe)_3$ and close inspection of the spectrum reveals an additional set of low intensity ligand peaks which suggests the presence of a small amount of a second *ansa bis*cyclopentadienyl niobium species. This species may be $[Nb(\eta\text{-}C_5H_4\text{-}CMe_2\text{-}\eta\text{-}C_5H_4)Cl]$ or its dimer.

The $^{13}C\{^{1}H\}$ NMR (C_6D_6) spectrum of **14** shows the usual peaks arising from the carbon atoms of the *ansa bis*cyclopentadienyl ligand and a singlet at δ 52.2 ppm due to the $P(OMe)_3$ ligand. The $^{31}P\{^{1}H\}$ NMR (C_6D_6) spectrum shows a sharp peak at δ 141 ppm due to uncoordinated $P(OMe)_3$ and a broad (fwhh = 1500 Hz) resonance centred at δ 182 ppm due to the coordinated $P(OMe)_3$.

The molecular structure was determined by X-ray crystallography and is given in **Figure 4.3** with the atom labelling scheme. Selected interatomic distances and angles appear in **Table 4.1**. Full details of the structure determination appear in **Appendix I**.

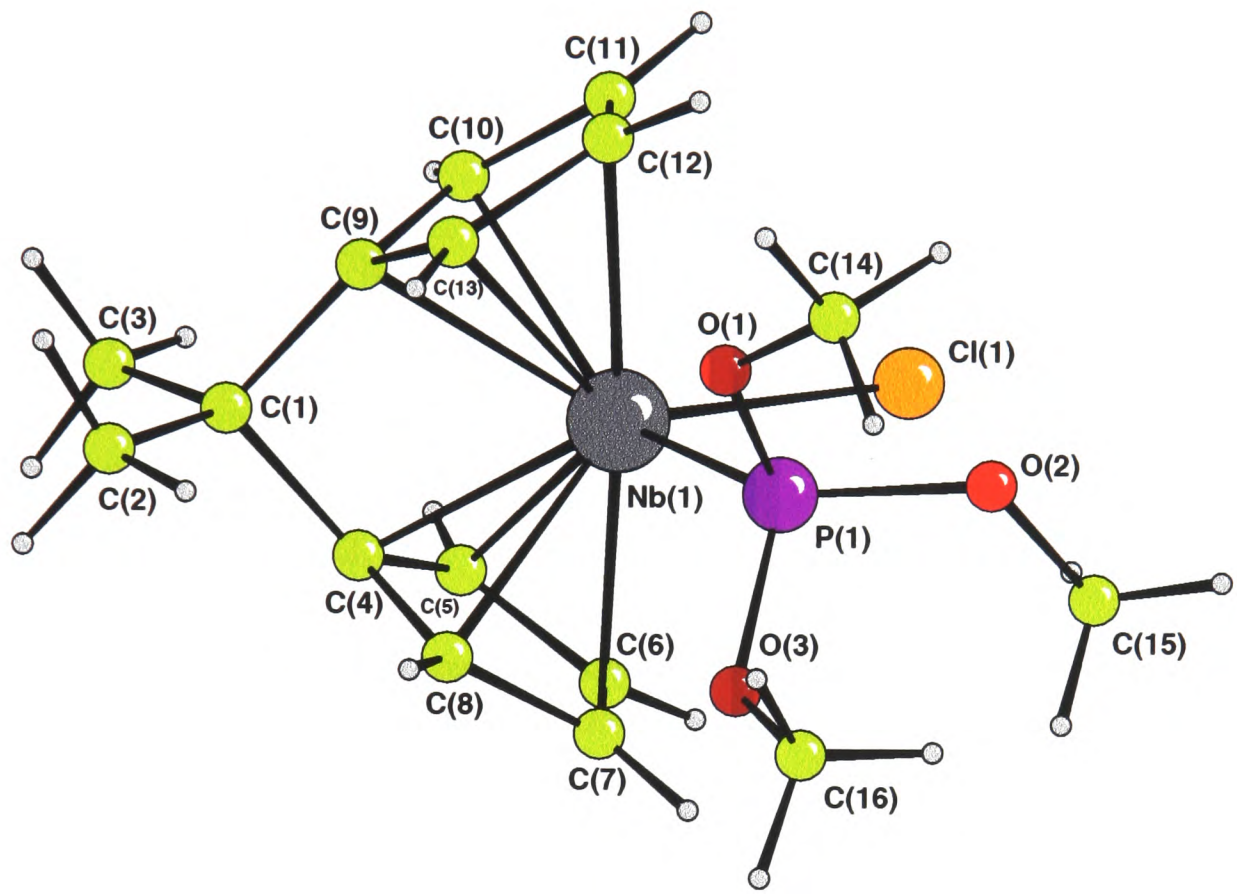

Figure 4.3 The molecular structure of [Nb(η-C_5H_4-CMe_2-η-C_5H_4){$P(OMe)_3$}Cl] (**14**). Hydrogen atom labels are omitted for clarity.

Bond	Length / Å	Bond	Angle / °
Nb(1)–P(1)	2.5304(4)	C(2)–C(1)–C(3)	109.6(1)
Nb(1)–Cl(1)	2.5301(4)	C(4)–C(1)–C(9)	96.8(1)
Nb(1)–C(4)	2.277(2)	Cl(1)–Nb(1)–P(1)	90.26(1)
Nb(1)–C(5)	2.370(2)	Bending angle, β	115.4
Nb(1)–C(6)	2.459(2)	Cp_{cent}–Nb(1)–Cp_{cent}, γ	124.3
Nb(1)–C(7)	2.388(2)	Cp_{cent}–C(4)–C(1)	163.4
Nb(1)–C(8)	2.283(2)	Cp_{cent}–C(4)–C(9)	163.4
Nb(1)–C(9)	2.278(2)		
Nb(1)–C(10)	2.378(2)		
Nb(1)–C(11)	2.465(2)		
Nb(1)–C(12)	2.385(2)		
Nb(1)–C(13)	2.285(2)		
Nb(1)–Cp_{cent}	2.02, 2.02		

Table 4.1 Selected interatomic distances and angles for [Nb(η-C_5H_4-CMe_2-η-C_5H_4){$P(OMe)_3$}Cl] (**14**)

The Nb–P bond length in **14** is slightly shorter than those reported for the half sandwich compound [Nb(η-C_5H_5)(NMe)(PMe_3)Cl_2],[5] 2.604(2) Å, and for the *ansa* η-cyclopentadienyl imido compound [Nb(η-C_5H_4-{CH_2}$_3$-N)(PMe_3)Cl_2],[6] 2.627(2) Å. This is to be expected if there is an appreciable π-bonding contribution in the Nb–P bond in **14**. A search of the Cambridge Structural Database[7] reveals only one structurally characterised niobium compound containing the $P(OMe)_3$ ligand, [Nb(η-C_5H_5)$_2${$P(OMe)_3$}(μ-PPh_2)$Cr(CO)_5$],[8] in which the Nb–$P(OMe)_3$ bond length is 2.485(1) Å. To date, there are no published structures of *bis*-η-cyclopentadienyl niobium compounds containing a Cl–Nb–P linkage.

As stated above, the yield of pure monomeric **14** obtained by this procedure is disappointingly low and we were interested in trying to utilise the residual material from the reaction which is a black solid, insoluble in light petroleum. This solid is soluble in THF or toluene and the elemental analysis data obtained (C, 43.3; H, 5.6 %) are in close, but not exact, agreement with those calculated for the formula [Nb(η-C_5H_4-CMe_2-η-C_5H_4){$P(OMe)_3$}Cl] (C, 45.5; H, 5.5 %). The pattern of peaks in the ^{1}H NMR spectrum indicates a similar symmetry environment at niobium to that in **14**. These observations are consistent with the proposal that the material is an oligomeric form of **14**. It was therefore hoped that this material could be used to pursue further chemistry.

4.6 Attempts to prepare [Nb(η-C_5H_4-CMe_2-η-C_5H_4){$P(OMe)_3$}R] (R = Me, CH_2Ph, CH_2SiMe_3)

The material assumed to be oligomeric **14** forms a dark red-brown solution in toluene. Treatment of this solution with one equivalent of MeMgBr in diethyl ether at room temperature causes a loss of the dark colour but removal of the volatiles gives an intractable brown solid.

More promising results were obtained when a suspension of oligomeric **14** in diethyl ether was treated with a solution of one equivalent of $PhCH_2MgBr$ in diethyl ether at –78 °C. After stirring for 2 days at room temperature most of the material had dissolved to give a pale brown solution. This was filtered and the volatiles removed to give a brown solid, which was then extracted with pentane. Cooling of this red pentane solution to –80 °C gave a small amount of a brown oil. The ^{1}H NMR (C_6D_6)

spectrum of this substance shows a set of cyclopentadienyl resonances at δ 5.18, 4.99, 4.25 and 4.09 ppm, a doublet centred at δ 3.18 ppm (J = 10.5 Hz) assigned to the $P(OMe)_3$ ligand, a doublet centred at δ 1.91 ppm (J = 6 Hz) due to the methylene protons of the benzyl group and two singlets at δ 0.56 and 0.48 ppm for the bridging methyl groups. As usual, the spectrum revealed the presence of a small amount of uncoordinated phosphite, presumably a result of a dissociative equilibrium. Encouraged by this NMR spectroscopic data, the preparation of $[Nb(\eta\text{-}C_5H_4\text{-}CMe_2\text{-}\eta\text{-}C_5H_4)\{P(OMe)_3\}CH_2Ph]$ was attempted again. However, the correct conditions for high yield formation remained elusive and it was not possible to isolate enough of the compound to allow purification.

Under similar conditions to the above, a suspension of oligomeric **14** was treated with a half equivalent of $[Mg(CH_2SiMe_3)_2]$. After identical work-up procedures a purple solid was obtained. The ^1H NMR spectrum revealed that this solid was not the expected alkyl niobium compound but monomeric **14**. So although this experiment was unsuccessful, it lends considerable support to the formulation of the starting material as an oligomeric form of $[Nb(\eta\text{-}C_5H_4\text{-}CMe_2\text{-}\eta\text{-}C_5H_4)\{P(OMe)_3\}Cl]$.

Similarly, Royo and co-workers were unable to prepare alkyl derivatives from $[Nb(\eta\text{-}C_5H_5)_2(PMe_3)Cl]$. They report that alkylations of $[Nb(\eta\text{-}C_5H_5)_2(PMe_3)Cl]$ using LiR (R = Me, CH_2CMe_3, CH_2Ph) give only decomposition products.[2]

4.7 Summary

This preliminary study into *ansa* niobium compounds prepared from $NbCl_3$.DME has met with some success. Treatment of $NbCl_3$.DME with [K(C_5H_4-CMe_2-C_5H_4)K] in the presence of PMe_3 or $P(OMe)_3$ leads to formation of *ansa bis*cyclopentadienyl compounds of niobium(III). In the case of $P(OMe)_3$ the compound was isolated and fully characterised. Polymeric material is also obtained from the reaction and in one example it is fortuitously converted to the monomeric form, as described.

The chemistry described in this chapter is summarised in **Figure 4.4**.

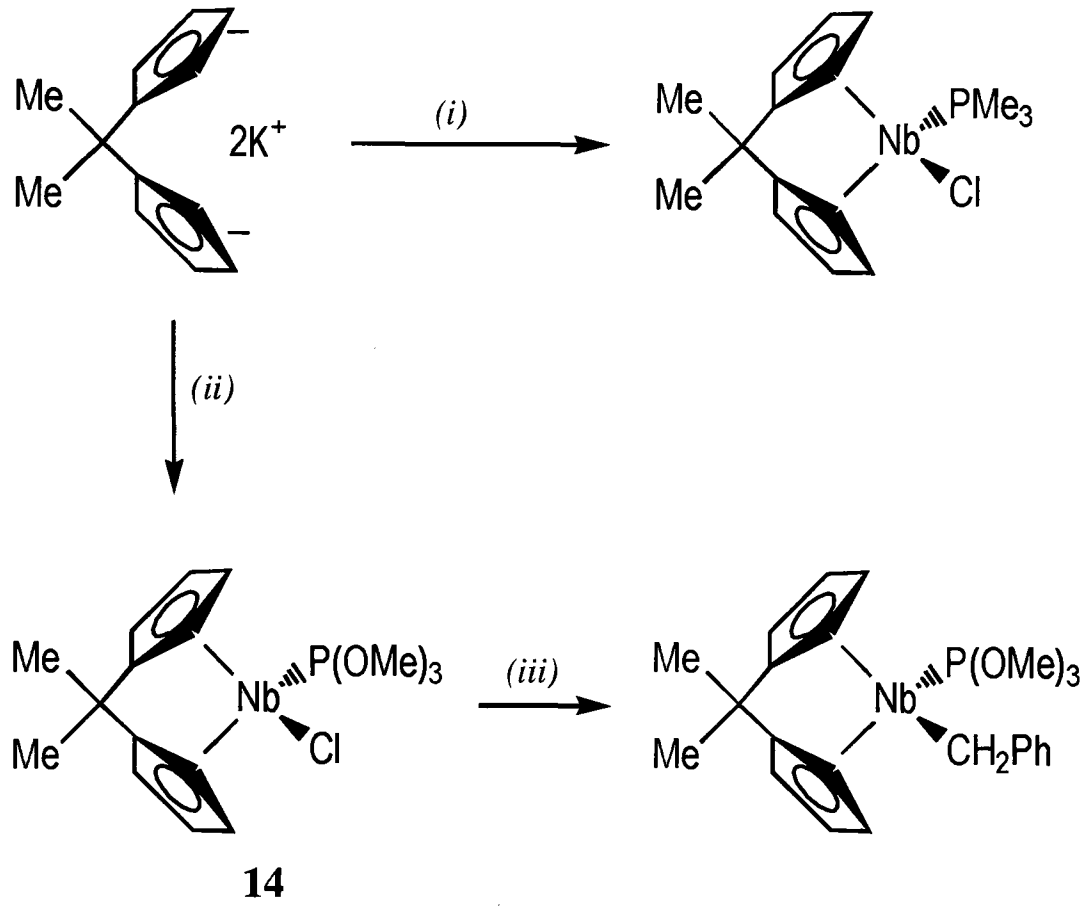

14

Reagents: *(i)* $NbCl_3$.DME / PMe_3 in THF
(ii) $NbCl_3$.DME / $P(OMe)_3$ in THF
(iii) $PhCH_2MgBr$ in Et_2O

Figure 4.4 Summary of reactions presented in **Chapter 4**

References for Chapter 4

1. S. F. Pedersen, J. B. Hartung Jr., E. J. Roskamp and P. S. Dragovich, in *Inorganic Syntheses* (R. N. Grimes, ed.), Vol. 29, p. 119, Wiley-Interscience, New York, 1992.

2. F. A. Urbanos, M. Mena, P. Royo and A. Antiñolo, *J. Organomet. Chem.*, 1984, **276**, 185.

3. J. P. Collman, L. S. Hegedus, J. R. Norton and R. G. Finke, *Principles and Applications of Organotransition Metal Chemistry,* University Science Books, Mill Valley, CA, 1987.

4. R. Serrano and P. Royo, *J. Organomet. Chem.*, 1983, **247**, 33.

5. D. N. Williams, J. P. Mitchell, A. D. Poole, U. Siemeling, W. Clegg, D. C. R. Hockless, P. A. O. Neil and V. C. Gibson, *J. Chem. Soc., Dalton Trans.*, 1992, 739.

6. D. M. Antonelli, M. L. H. Green and P. Mountford, *J. Organomet. Chem.*, 1992, **438**, C4.

7. F. H. Allen and O. Kennard, *Chemical Design Automation News*, 1993, **8**, 1 & 31.

8. P. Oudet, D. Perrey, G. Bonnet, C. Moïse and M. M. Kubicki, *Inorg. Chim. Acta*, 1995, **237**, 79.

Chapter 5

Experimental section

5.1 General details

5.1.1 Techniques

Unless otherwise stated experiments were performed under dry dinitrogen using standard Schlenk line techniques or in an inert atmosphere dry box containing dinitrogen.[1] Solvents were pre-dried over activated 4 Å molecular sieves and then distilled from Na/K alloy (light petroleum, diethyl ether, pentane and 1,2-dimethoxyethane), from sodium (petroleum ether b. p. 100-120 °C and toluene), from potassium (THF) or from phosphorus pentoxide (dichloromethane) under a slow continuous stream of dinitrogen. Light petroleum refers to the b. p. 40-60 °C fraction. Solvents were thoroughly degassed by the pump fill technique followed by re-admission of dinitrogen or by purging with dinitrogen for 15 min prior to use. Deuterated NMR solvents were dried (benzene-d_6 over sodium benzophenone ketyl, dichloromethane-d_2 over calcium hydride), distilled and degassed by the freeze-pump-thaw technique prior to use. Celite® filtration aid was purchased from Fluka Chemie and oven-dried at 100 °C prior to use.

5.1.2 Instrumentation

NMR experiments were carried out on a Varian UnityPlus 500 spectrometer (^{1}H, ^{13}C, ^{11}B, ^{31}P NMR spectra were recorded at 499.868, 125.703, 160.380 and 202.345 MHz respectively) or on a Bruker AM 300 spectrometer (^{1}H and ^{13}C NMR spectra at 300.13 and 75.5 MHz respectively). The spectra were referenced internally relative to the residual protio-solvent (^{1}H) and solvent (^{13}C) resonances relative to tetramethylsilane (^{1}H, ^{13}C; $\delta = 0$ ppm) or externally to $BF_3.Et_2O$ (^{11}B; $\delta = 0$ ppm) or

85 % H_3PO_4 (^{31}P; δ = 0 ppm). Chemical shifts (δ) are expressed in ppm, coupling constants (J) in Hz.

EPR spectra were recorded on a Varian E-line Century Series X-band spectrometer by Dr R. E. Douthwaite of this laboratory.

Electron Impact ionisation mass spectra were recorded on an AEI MS 302 Mass Spectrometer upgraded with a data handling system supplied by Mass Spectrometry Services Ltd. The calibration of this instrument was accurate to within 1%. Fast Atom Bombardment mass spectra were recorded by the EPSRC Mass Spectrometry Service at the University College of Swansea under the supervision of Dr J. A. Ballantine. The Electrospray ionisation mass spectrum was recorded by Micromass UK Limited, Floats Road, Wythenshawe, Manchester, M23 9LZ.

IR spectra were recorded on a Mattson Polaris FTIR spectrometer or a Perkin-Elmer 1710 FTIR spectrometer. Samples were prepared as pressed KBr or CsI discs. Data are quoted in cm^{-1}.

Elemental analysis data was obtained from the microanalysis department of the Inorganic Chemistry Laboratory.

5.1.3 Starting materials

The compounds $[NbCl_4.2THF]$,[2] $[Nb(NSiMe_3)(py)_2Cl_3]$,[3] $[Nb(NBu^t)(py)_2Cl_3]$,[4] $NbCl_3.DME$,[5] and $[C_5H_5\text{-}CMe_2\text{-}C_5H_5]$[6] were prepared by published procedures. The alkali metal salt $[K(C_5H_4\text{-}CMe_2\text{-}C_5H_4)K]$ was prepared from the protio ligand by treatment with potassium hydride in THF. NaSPh was prepared by Dr Grant Taylor

by the reaction between sodium sand and thiophenol in toluene. $LiBH_4$ (95 %), PMe_3 (97 %), PPh_3 (99 %), $PhCH_2MgBr$ (0.125 M in Et_2O), $BrSiMe_3$ (97 %), $ISiMe_3$ (97 %), MeLi (1.4 M in Et_2O), HBF_4 (54 wt. % in Et_2O) and $P(OMe)_3$ (99 %) were purchased from Aldrich Chemical Company and used as supplied.

5.2 Experimental details for Chapter 2

5.2.1 Preparation of [Nb(η-C_5H_4-CMe_2-η-C_5H_4)Cl_2] (1)

The compound [$NbCl_4$.2THF] (16.9 g, 44.6 mmol) was suspended in THF (100 cm^3) and stirred at RT. A suspension of [K(C_5H_4-CMe_2-C_5H_4)K] in THF (100 cm^3) was added dropwise over a period of 1 h. This brown reaction mixture was stirred for 24 h and the volatiles removed under reduced pressure to give a purple-brown solid. Soxhlet extraction of this solid with dichloromethane gave a saturated purple solution. The mother liquor of the extract was decanted off leaving the product **1** as purple crystals which were dried *in vacuo*. Further product was obtained from the mother liquor by removal of all volatiles under reduced pressure. Yield, 8.6 g (57 % based on [$NbCl_4$.2THF])

5.2.2 Preparation of [Nb(η-C_5H_4-CMe_2-η-C_5H_4)(η^2-BH_4)] (2)

A mixture of the compound [Nb(η-C_5H_4-CMe_2-η-C_5H_4)Cl_2] (**1**) (750 mg, 2.21 mmol) and $LiBH_4$ (145 mg, 6.63 mmol) was suspended in 1,2-dimethoxyethane (40 cm^3) and stirred at RT. Effervescence was observed on addition of the solvent. After 24 h the

volatiles were removed from the brown reaction mixture under reduced pressure and the resulting solid was extracted with light petroleum (2 × 50 cm^3). This dark green solution was concentrated to 30 cm^3 and cooled to –80 °C yielding the product **2** as dark green crystals. Yield, 470 mg (75 % based on compound **1**). Crystals of compound **2** suitable for X-ray diffraction were obtained by cooling a solution in petroleum ether (b. p. 100-120 °C) to –80 °C.

5.2.3 Preparation of [Nb(η-C_5H_4-CMe_2-η-C_5H_4)(PMe_3)H] (3)

The compound [Nb(η-C_5H_4-CMe_2-η-C_5H_4)(η^2-BH_4)] (**2**) (80 mg, 0.29 mmol) in benzene (30 cm^3) was treated with trimethylphosphine (0.1 cm^3, 73 mg, 1 mmol) at RT. The solution turned immediately from green to red on addition of the phosphine. This solution was stirred for 3 h and the volatiles removed *in vacuo* to give a red solid. The product was extracted into pentane (30 cm^3) to remove it from the phosphine borane adduct. Removal of the volatiles from this pentane solution under reduced pressure gave the compound **3** as a red microcrystalline solid which was purified by recrystallisation from pentane at –80 °C. Yield, 40 mg (42 % based on compound **2**). Crystals suitable for X-ray diffraction studies were obtained from a solution of compound **3** in pentane by slow cooling to –80 °C.

5.2.4 Preparation of [Nb(η-C_5H_4-CMe_2-η-C_5H_4)(PPh_3)H] (4)

A mixture of the compound [Nb(η-C_5H_4-CMe_2-η-C_5H_4)(η^2-BH_4)] (**2**) (80 mg, 0.29 mmol) and triphenylphosphine (148 mg, 0.57 mmol) was dissolved in benzene (30 cm^3) and stirred at RT for 3h. During this time the reaction mixture changed from green to deep red. The volatiles were removed under reduced pressure and the resulting red solid extracted with pentane (50 cm^3) giving a dark red solution. Removal of volatiles from this solution under reduced pressure gave the compound **4** as a red solid which was purified by recrystallisation from pentane at –80 °C. Yield, 55 mg (37 % based on compound **2**).

5.2.5 Preparation of [Nb(η-C_5H_4-CMe_2-η-C_5H_4)($SPh)_2$] (5)

A colourless solution of NaSPh (400 mg, 3.0 mmol) in THF (100 cm^3) was added dropwise at RT to a stirred suspension of the compound [Nb(η-C_5H_4-CMe_2-η-C_5H_4)Cl_2] (**1**) (500 mg, 1.5 mmol) in THF (100 cm^3) over a period of 20 min. A homogeneous red-violet solution resulted after a further 30 min stirring at RT. This solution was transferred to a Rotaflo® ampoule and heated at 80 °C under reduced pressure for 16 h. The volatiles were then removed under reduced pressure and the resulting brown solid extracted into toluene (150 cm^3) and filtered. The volatiles were removed from this violet solution under reduced pressure and the resulting purple oil extracted into diethyl ether (60 cm^3). Cooling of this diethyl ether solution to –80 °C yielded the product **5** as purple-black crystals. Yield, 108 mg (15 % based on compound **1**).

5.2.6 Preparation of [Nb(η-C_5H_4-CMe_2-η-C_5H_4)(CH_2Ph)$_2$] (6)

The compound [Nb(η-C_5H_4-CMe_2-η-C_5H_4)Cl_2] (**1**) (100 mg, 0.3 mmol) was suspended in diethyl ether (30 cm^3) and stirred at RT. Benzyl magnesium bromide (5 cm^3 of a 0.125 M solution in diethyl ether, 0.63 mmol) was added and a red colour developed after about 10 min, accompanied by dissolution of the starting material. The reaction mixture was stirred for 12 h and the volatiles were then removed under reduced pressure. The residue was extracted with light petroleum (2 × 30 cm^3) and filtered giving a red solution which on cooling to –80 °C yielded the product **6** as dark red blocks of sufficient quality for X-ray crystallographic studies. Yield, 25 mg (20 % based on compound **1**).

5.3 Experimental details for Chapter 3

5.3.1 Preparation of [Nb(η-C_5H_4-CMe_2-η-C_5H_4)($NSiMe_3$)Cl] (7)

A solution of the ligand salt [K(C_5H_4-CMe_2-C_5H_4)K] (0.60 g, 2.4 mmol) in THF (50 cm^3) was added dropwise to a solution of [Nb($NSiMe_3$)(py)$_2Cl_3$] (1.00 g, 2.3 mmol) in THF (100 cm^3) at room temperature over the course of 30 min. The reaction mixture was stirred for 1 h and the volatiles then removed under reduced pressure giving a green-black oily solid. This was extracted with pentane (2 × 30 cm^3) and filtered to give an orange solution and a black solid residue. Removal of the solvent from the filtrate under reduced pressure gave compound **7** as a spectroscopically pure pale green powder. Yield, 100 mg (12 % based on [Nb($NSiMe_3$)(py)$_2Cl_3$]). An analytically pure sample was obtained as yellow needles by recrystallisation from

pentane at –80 °C. Crystals suitable for X-ray structure determination were grown by slow evaporation of a solution in petroleum ether (b. p. 100-120 °C).

5.3.2 Preparation of [Nb(η-C_5H_4-CMe_2-η-C_5H_4)(NBu^t)Cl] (8)

In a typical preparation a solution of [Nb(NBu^t)$(py)_2Cl_3$] (1.0 g, 2.3 mmol) in THF (30 cm^3) was treated dropwise with a solution of [K(C_5H_4-CMe_2-C_5H_4)K] (0.58 g, 2.3 mmol) in THF (30 cm^3) over a period of 1 h at room temperature. The mixture was stirred for 24 h. The resulting red solution was filtered and the solvent removed under reduced pressure affording compound **8** as a brown solid in sufficient purity for subsequent studies. Yield, 0.66 g (77 % based on [Nb(NBu^t)$(py)_2Cl_3$]). An analytically pure sample was obtained as yellow needles by cooling a pentane solution to –80 °C. Crystals of sufficient quality for X-ray crystallographic studies were obtained by the slow cooling of a solution in diethyl ether to –80 °C.

5.3.3 Preparation of [Nb(η-C_5H_4-CMe_2-η-C_5H_4)(NBu^t)Br] (9) and [Nb(η-C_5H_4-CMe_2-η-C_5H_4)(NBu^t)I] (10)

To a solution of the compound [Nb(η-C_5H_4-CMe_2-η-C_5H_4)(NBu^t)Cl] (**8**) (100 mg, 0.3 mmol) in light petroleum (30 cm^3) was added $BrSiMe_3$ (0.5 cm^3, 0.6 g, 3.9 mmol) with stirring and a small amount of gelatinous orange precipitate formed. After 1 h the volatiles were removed under reduced pressure and the orange solid residue was extracted with light petroleum (2 × 30 cm^3) and filtered. The solvent was removed from the yellow filtrate under reduced pressure to give compound **9** as a yellow solid, which was recrystallised from pentane to give yellow needles. Yield, 70 mg (63 %

based on compound **8**). Crystals suitable for X-ray diffraction studies were grown by slow evaporation of a solution in petroleum ether (b. p. 100-120 °C).

In an analogous procedure a solution of compound **8** (100 mg, 0.3 mmol) was treated with $ISiMe_3$ (0.5 cm^3, 0.7 g, 3.5 mmol) yielding compound **10** as an orange microcrystalline solid. Yield, 80 mg (63 % based on compound **8**). Crystals suitable for X-ray diffraction studies were obtained by the slow cooling of a solution in diethyl ether to –80 °C.

5.3.4 Preparation of [Nb(η-C_5H_4-CMe_2-η-C_5H_4)(NBu^t)Me] (11)

A yellow solution of the compound [Nb(η-C_5H_4-CMe_2-η-C_5H_4)(NBu^t)Cl] (**8**) (0.98 g, 2.7 mmol) in diethyl ether (30 cm^3) was cooled to 0 °C and treated with MeLi (2 cm^3 of a 1.4 M solution in diethyl ether, 2.8 mmol) upon which an orange colour developed. The reaction mixture was stirred for 12 h and a white precipitate formed. The volatiles were removed under reduced pressure and the residue extracted with pentane (30 cm^3) and filtered through Celite.® The residue was washed with further portions of pentane until the washings were colourless (3 × 30 cm^3). The extracts were combined and the solvent removed under reduced pressure yielding compound **11** as a yellow microcrystalline solid which was purified by recrystallisation from pentane. Yield, 0.60 g (64 % based on compound **8**).

5.3.5 Preparation of [Nb(η-C_5H_4-CMe_2-η-C_5H_4)(NHBu^t)Cl][BF_4] (12)

A solution of the compound [Nb(η-C_5H_4-CMe_2-η-C_5H_4)(NBu^t)Cl] (**8**) (240 mg, 0.65 mmol) in diethyl ether (30 cm^3) was treated with HBF_4 (8 cm^3 of a 0.086 M solution in diethyl ether, 0.69 mmol). An orange precipitate slowly formed. The reaction mixture was stirred for 12 h and allowed to settle. The pale yellow supernatant was filtered off leaving the product (**12**) as an orange powder, which was dried *in vacuo*. Yield, 270 mg (91 % based on compound **8**).

5.3.6 Isolation of [Nb(η-C_5H_4-CMe_2-η-C_5H_4)(O)Cl] (13)

A sample of [Nb(η-C_5H_4-CMe_2-η-C_5H_4)(NHBu^t)Cl][BF_4] (**12**) was dissolved in THF and a slow continuous flow of dinitrogen from the house supply was passed over the solution for 12 h. X-ray quality yellow crystals of the compound **13** were formed.

5.4 Experimental details for Chapter 4

5.4.1 Reaction between $NbCl_3$.DME and [K(C_5H_4-CMe_2-C_5H_4)K] in the presence of PMe_3

A solution of [K(C_5H_4-CMe_2-C_5H_4)K] (430 mg, 1.73 mmol) in THF (100 cm^3) was cooled to –50 °C and approximately 1 cm^3 of PMe_3 was added. No change was observed at this stage. $NbCl_3$.DME (500 mg, 1.73 mmol) was added over the course of 15 min using a solid addition funnel. The reaction mixture was allowed to warm up slowly with stirring upon which a change from brick-red suspension to cloudy purple solution was observed. The temperature was kept below 0 °C whilst the volatiles

were removed under reduced pressure. The residue was extracted into light petroleum (2 × 50 cm^3) and filtered to remove KCl. Removal of the volatiles from this purple solution gave impure [Nb(η-C_5H_4-CMe_2-η-C_5H_4)(PMe_3)Cl] as a dark purple solid.

5.4.2 Preparation of [Nb(η-C_5H_4-CMe_2-η-C_5H_4){$P(OMe)_3$}Cl] (14)

Brick red $NbCl_3$.DME (580 mg, 2 mmol) was suspended in THF (30 cm^3) and trimethylphosphite (300 mg, 2.4 mmol) was added *via* syringe. Immediately the solid dissolved giving a dark red solution. This was cooled to –50 °C and a suspension of [K(C_5H_4-CMe_2-C_5H_4)K] (500 mg, 2 mmol) in THF (30 cm^3) was added over the course of 10 min. The reaction mixture was allowed to warm slowly to RT with stirring (3 h). The resulting dark red-brown solution was filtered and the volatiles removed under reduced pressure. The black solid residue was extracted with light petroleum (30 cm^3) and filtered giving a red solution which on cooling to –20 °C gave the product **14** as purple crystals which were of sufficient quality for X-ray crystallographic studies. Yield, 70 mg (8 % based on $NbCl_3$.DME).

5.5 Crystal structure determinations

5.5.1 General crystallographic details

Crystal data, data collection and processing parameters are given in the **Appendices**.

When an image plate diffractometer was used (**Sections 5.5.3-5.5.6**) data were corrected for Lorentz and polarisation effects and a partial absorption correction is implied by multi-frame scaling of the image plate data using equivalent reflections.

In all cases the crystallographic calculations were performed using the CRYSTALS package.[7] Neutral atom scattering factors were taken from the usual sources.[8]

Unless otherwise stated, crystallographic work was carried out in the Chemical Crystallography Laboratory, 9 Parks Road, Oxford, OX1 3PD.

5.5.2 Crystal structure determination for [Nb(η-C_5H_4-CMe_2-η-C_5H_4)(η^2-BH_4)] (2)

A crystal of compound **2** was mounted in a Lindemann glass capillary tube under N_2 and transferred to the goniometer head of an Enraf-Nonius CAD4 diffractometer. The data were collected by Mr John F. Saunders. The structure was solved by Mr Michael A. Leech using direct methods, SIR92,[9] giving non-hydrogen atom positions. Full matrix least squares refinement was performed on the structure and anisotropic thermal parameters were refined for all non-hydrogen atoms. Hydrogen atoms were located from Fourier difference maps and their positions and isotropic thermal parameters refined. A three parameter Chebyshev weighting scheme was applied.[10]

5.5.3 Crystal structure determination for [Nb(η-C_5H_4-CMe_2-η-C_5H_4)(PMe_3)H] (3)

A crystal of compound **3** was mounted in a Lindemann glass capillary tube under N_2. The data were collected by Mr John F. Saunders on a DIP2000 Image Plate diffractometer and indexed using the DENZO program.[11] A list of F_{obs} was compiled using the SCALEPACK program.[12] The structure was solved by Mr Michael A. Leech using direct methods, SIR92,[9] giving non-hydrogen atom positions. Full matrix least squares refinement was performed on the structure with anisotropic thermal parameters for all non-hydrogen atoms. The hydrogen atoms were placed geometrically and their isotropic thermal parameters refined. A three parameter Chebyshev weighting scheme was applied.[10]

5.5.4 Crystal structure determinations for [Nb(η-C_5H_4-CMe_2-η-C_5H_4)(CH_2Ph)$_2$] (6), [Nb(η-C_5H_4-CMe_2-η-C_5H_4)($NSiMe_3$)Cl] (7), [Nb(η-C_5H_4-CMe_2-η-C_5H_4)(NBu^t)Br] (9), [Nb(η-C_5H_4-CMe_2-η-C_5H_4)(NBu^t)I] (10) and [Nb(η-C_5H_4-CMe_2-η-C_5H_4){$P(OMe)_3$}Cl] (14)

Data collections and solutions were carried out by Mr Michael A. Leech. In each case a crystal was mounted on a glass fibre using a drop of highly viscous perfluoropolyether to exclude air and prevent solvent loss. It was then plunged into a cold nitrogen stream (150 K). An Oxford Cryosystems CRYOSTREAM cooling system was used. The crystal was transferred to the goniometer head of an Enraf-Nonius DIP2000 image plate diffractometer. The images were processed using the DENZO[11] and SCALEPACK[12] programs.

The structure was solved by direct methods, SIR92,[9] giving non-hydrogen atom positions. The structure was refined using full-matrix least-squares procedures with anisotropic thermal parameters for all non-hydrogen atoms. For compounds **6** and **7** the hydrogen atoms were located in difference Fourier maps and refined isotropically. For compounds **9**, **10** and **14** the hydrogen atoms were placed in calculated positions during the final cycles of refinement and their isotropic thermal parameters refined. Three parameter Chebyshev weighting schemes were applied.[10]

5.5.5 Crystal structure determination for [Nb(η-C_5H_4-CMe_2-η-C_5H_4)(NBu^t)Cl] (8)

A crystal was mounted in a similar fashion to that described in **Section 5.5.4** and transferred to the goniometer head of a FAST area-detector diffractometer driven by the software package MADNES.[13] The data were collected by Dr Simon Coles of the EPSRC X-Ray Crystallography Service at the University of Wales, Cardiff.

The structure was solved by Mr Michael A. Leech using direct methods, SIR92,[9] giving non-hydrogen atom positions and refined using full-matrix least-squares procedures with anisotropic thermal parameters for all non-hydrogen atoms. The hydrogen atoms were located in difference Fourier maps but not refined. Three parameter Chebyshev weighting schemes were applied.[10]

5.5.6 Crystal structure determination for [Nb(η-C_5H_4-CMe_2-η-C_5H_4)(O)Cl] (13)

The data was collected by Dr Linda H. Doerrer of the Inorganic Chemistry Laboratory. A crystal was mounted as described in **Section 5.5.4** and transferred to the goniometer head of an Enraf-Nonius DIP2000 image plate diffractometer. The images were processed using the DENZO[11] and SCALEPACK[12] programs. The structure was solved by direct methods, SIR92,[9] giving non-hydrogen atom positions, which were refined using full matrix least squares procedures. Hydrogen atoms were placed geometrically and not refined. During the final cycles of refinement it became apparent that the data was of insufficient quality to allow refinement of anisotropic thermal parameters for all non-hydrogen atoms. Thus six of the carbon atoms were refined with isotropic thermal parameters. As a trial, interatomic distances and angles were also generated for a solution with all carbon atoms refined isotropically. The molecular geometry was found not to differ to any significant degree from that presented.

5.6 Photoelectron spectra

Photoelectron spectra were recorded in this laboratory by Tessa Dijkstra using a PES Laboratories 0078 spectrometer consisting of a photon source, an ionisation chamber and an electron energy analyser. The photon source was a radial helium discharge produced using a cylindrical tantalum cathode and a tungsten anode. The spectra were measured at photon energies 21.22 eV (He I) and 40.81 eV (He II).

Solid samples were prepared in sealed glass capillaries which were cracked open immediately prior to being placed in the instrument. The sample probe was placed adjacent to the discharge lamp and the heat of the lamp was used to effect sublimation. The photoelectrons were separated according to their kinetic energy in an electron analyser consisting of two 127° cylindrical plates between which the potential difference was varied, and detected using a Channeltron electron multiplier. The spectra were calibrated using N_2, Xe and He.

5.7 Density functional calculations

Density functional calculations were performed by Tessa Dijkstra using the Amsterdam Density Functional program system (version 2.0.1).[14] Triple-ζ Slater-type atomic orbital basis sets were employed. The cores of the atoms were frozen, C and N up to 1s, Cl up to 2p and Nb up to 3d. A single polarisation function was included for all atoms except Nb. First order relativistic corrections were applied to the cores of all atoms using the Pauli formalism.

Energies were calculated using Vosko, Wilk and Nusair's local exchange correlation potential[15] with non-local-exchange corrections by Becke[16] and non-local-correlation corrections by Perdew.[17, 18] The non-local correction terms were utilised in calculating gradients during geometry optimisations.

References for Chapter 5

1. D. F. Shriver and M. A. Drezdzon, *The Manipulation of Air-Sensitive Compounds, 2nd Ed.,* Wiley-Interscience, NY, 1986.

2. L. E. Manzer, *Inorg. Chem.*, 1977, **16**, 525.

3. C. M. Jones, M. E. Lerchen, C. J. Church, B. M. Schomber and N. M. Doherty, *Inorg. Chem.*, 1990, **29**, 1679.

4. J. Sundermeyer, J. Putterlik, M. Foth, J. S. Field and N. Ramesar, *Chem. Ber.*, 1994, **127**, 1201.

5. S. F. Pedersen, J. B. Hartung Jr., E. J. Roskamp and P. S. Dragovich, in *Inorganic Syntheses* (R. N. Grimes, ed.), Vol. 29, p. 119, Wiley-Interscience, New York, 1992.

6. I. E. Nifant'ev, P. V. Ivchenko and M. V. Borzov, *J. Chem. Research (S)*, 1992, 162.

7. D. J. Watkin, C. K. Prout, J. R. Carruthers and P. W. Betteridge, CRYSTALS Issue 10, *Chemical Crystallography Laboratory, University of Oxford, England*, 1996.

8. *International Tables for Crystallography, 1st Ed.,* Kluwer Academic Publishers, Dordrecht, 1992.

9. A. Altomare, G. Cascarano, C. Giacovazzo, A. Guagliardi, M. C. Burla, G. Polidori and M. Camalli, *J. Appl. Cryst.*, 1994, **27**, 435.

10. J. R. Carruthers and D. J. Watkin, *Acta Cryst.*, 1979, **35A**, 698.

11. Z. Otwinowski, DENZO©, *Department of Molecular Biophysics and Biochemistry, Yale University, New Haven Connecticut, United States*, 1993.

12. Z. Otwinowski, SCALEPACK©, *Department of Molecular Biophysics and Biochemistry, Yale University, New Haven Connecticut, United States*, 1993.

13. J. W. Pflugrath and A. Messerschmitt, MADNES, Small molecule version., *Enraf-Nonius, Delft, The Netherlands*, 1991.

14. G. te Velde and E. J. Baerends, Amsterdam Density Functional (v. 2.0.1.), *Department of Theoretical Chemistry, Vrije Universiteit*, 1996.

15. S. H. Vosko, L. Wilk and M. Nusair, *Can. J. Phys.*, 1980, **58**, 1200.

16. A. D. Becke, *Phys. Rev. A*, 1988, **38**, 2398.

17. J. P. Perdew, *Phys. Rev. B*, 1986, **33**, 8822.

18. J. P. Perdew, *Phys. Rev. B*, 1986, **34**, 7046.

Chapter 6

Characterising data

6.1 Characterising data for [Nb(η-C_5H_4-CMe_2-η-C_5H_4)Cl_2] (1)

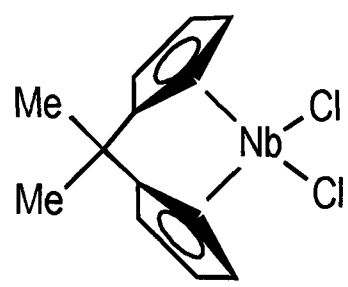

Appearance:

purple microcrystalline solid

Analytical Data: found (calculated %) for $C_{13}H_{14}Cl_2Nb$: C, 46.6 (46.7); H, 4.2 (4.2); Cl, 22.0 (21.2)

EPR: (298 K) 10 lines, g_{iso} = 1.992, $|a_{iso}|$ = 90.5 G, 9.05 mT

Mass Spectrum: (EI) machine calibration accurate to 1 %, data given for ^{35}Cl, *m/z* 336 [M^+], 305 [$M^+ - 2CH_3$], 272 [$M^+ - C_2H_2 - Cl$], 269 [$M^+ - 2CH_3 - Cl$]

IR: (KBr disc) 3106 s, 2978 m, 2963 m, 2928 s, 2903 m, 2861 w, 2731 w, 1653 w br, 1499 s, 1458 m, 1418 w, 1375 s, 1356 w, 1263 w, 1244 w, 1096 m, 1078 m, 1047 s, 936 m, 856 s, 843 s, 814 s, 737 w br, 617 m, 466 w, 417 w, 352 m and 338 m cm^{-1}

6.2 Characterising data for [Nb(η-C_5H_4-CMe_2-η-C_5H_4)(η^2-BH_4)] (2)

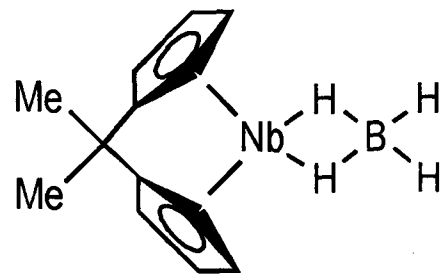

Appearance: green blocks

X-Ray Crystal Structure:

see **Appendix A**

Analytical Data: found (calculated %) for $C_{13}H_{18}BNb$: C, 55.1 (56.2); H, 6.6 (6.5)

^{1}H NMR data: (500 MHz, C_6D_6)

5.67 [4H, t, *J* 2.5 Hz, C_5H_4]

4.56 [4H, t, *J* 2.5 Hz, C_5H_4]

0.01 [6H, s, CH_3]

–3.24 [4H, br d, *J* 85 Hz, BH_4]

^{11}B NMR data: (160 MHz, C_6D_6)

23.1 [quintet, $^1J_{BH}$ 89 Hz]

^{13}C {^{1}H} NMR data: (125 MHz, C_6D_6)

106.3 [C_5H_4]

81.8 [C_5H_4, C_{ipso}]

79.6 [C_5H_4]

32.2 [CMe_2]

20.9 [CMe_2]

Mass Spectrum: (FAB) the characteristic isotope pattern was observed, data given for ^{11}B, *m/z* 280 [M^+ + 2]

IR: (KBr disc) 3104 w br, 2967 m, 2920 w, 2909 w, 2461 w, 2419 s, 2120 vw, 1709 m br, 1613 w br, 1452 m br, 1424 m br, 1385 m, 1370 m br, 1262 s, 1094 s, 1026 s, 928 w, 912 w, 864 m, 799 s and 714 m br cm^{-1}

6.3 Characterising data for [Nb(η-C_5H_4-CMe_2-η-C_5H_4)(PMe_3)H] (3)

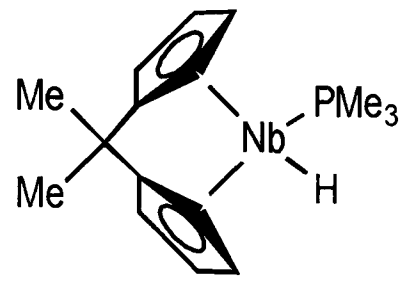

Appearance: red microcrystalline solid

X-Ray Crystal Structure:

see **Appendix B**

Analytical Data: found (calculated %) for $C_{16}H_{24}NbP$: C, 56.7 (56.4); H, 7.1 (7.1)

^{1}H NMR data: (500 MHz, C_6D_6)

5.24 [2H, m, C_5H_4]

4.49 [4H, m, C_5H_4]

4.37 [2H, m, C_5H_4]

0.82 [9H, d, $^2J_{PH}$ 7 Hz, PMe_3]

0.71 [3H, s, CH_3]

0.64 [3H, s, CH_3]

–5.03 [1H, d, $^2J_{PH}$ 39 Hz, NbH]

^{31}P {^{1}H} NMR data: (202 MHz, C_6D_6)

3.6 [s, PMe_3]

^{13}C {^{1}H} NMR data: (125 MHz, C_6D_6)

97.1 [C_5H_4]

92.2 [C_5H_4]

71.8 [C_5H_4]

69.6 [C_5H_4]

61.6 [C_5H_4, C_{ipso}]

33.2 [*C*Me_2]

23.1 [d, $^1J_{PC}$ 20 Hz, PMe_3]

22.8 [C*Me*$_2$]

22.4 [C*Me*$_2$]

IR: (KBr disc) 3051 s, 2965 vs, 2910 vs, 2872 s, 2417 m, 1747 w, 1706 m, 1646 m, 1596 m, 1536 w, 1464 w, 1446 w, 1420 m, 1377 w, 1361 m, 1294 m, 1281 w, 1260 m, 1147 m, 1115 s, 1051 m, 1023 m, 951 s, 900 s, 865 s, 807 vs, 760 s, 740 s, 715 s, 681 s, 592 m, 466 w and 425 w cm^{-1}

6.4 Characterising data for [Nb(η-C_5H_4-CMe_2-η-C_5H_4)(PPh_3)H] (4)

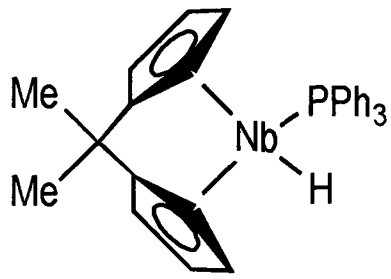

Appearance: red microcrystalline solid

Analytical Data: found (calculated %) for $C_{31}H_{30}NbP$: C, 70.0 (70.7); H, 5.7 (5.7)

^{1}H NMR data: (500 MHz, C_6D_6)

7.72-7.68 [6H, m, PPh_3]

7.01-6.93 [9H, m, PPh_3]

5.37 [2H, m, C_5H_4]

4.62 [2H, m, C_5H_4]

4.17 [2H, m, C_5H_4]

4.14 [2H, m, C_5H_4]

0.68 [6H, s, CH_3]

–4.11 [1H, d, $^2J_{PH}$ 34 Hz, NbH]

^{31}P {^{1}H} NMR data: (202 MHz, C_6D_6)

66.8 [s, PPh_3]

^{13}C {^{1}H} NMR data: (125 MHz, C_6D_6)

139.4 [d, *J* 29 Hz, PPh_3]

133.6 [d, *J* 11 Hz, PPh_3]

128.6 [m, PPh_3]

100.9 [s, C_5H_4]

94.3 [s, C_5H_4]

74.2 [s, C_5H_4]

73.0 [s, C_5H_4]

63.9 [s, C_5H_4, C_{ipso}]

33.1 [s, CMe_2]

22.7 [s, CMe_2]

22.1 [s, CMe_2]

IR: (KBr disc) 3051 s, 2963 s, 2926 s, 2380 s, 2344 m, 1963 m br, 1892 m br, 1818 m br, 1583 m, 1475 s, 1434 vs, 1380 w, 1364 w, 1325 w, 1307 w, 1262 s, 1200 w, 1180 w, 1156 w, 1119 m, 1104 m, 1088 s, 1069 m, 1026 s, 998 m, 929 w, 912 w, 899 w, 880 w, 866 w, 850 w, 803 s, 742 vs, 722 m, 694 vs, 625 w, 605 w, 542 s, 511 s, 493 s, 447 m and 424 m cm^{-1}

6.5 Characterising data for [Nb(η-C_5H_4-CMe_2-η-C_5H_4)$(SPh)_2$] (5)

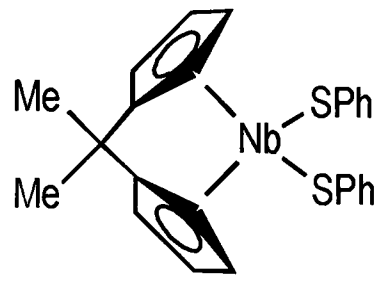

Appearance: dark red solid

Analytical Data: found (calculated %) for $C_{25}H_{24}NbS_2$: C, 62.0 (62.4); H, 5.0 (5.0); S, 13.4 (13.3)

EPR: (298 K) 10 lines, g_{iso} = 1.978, $|a_{iso}|$ = 115 G

Mass Spectrum: (EI) *m/z* 218 [$(SPh)_2^+$], 186 [SPh_2^+], 154 [Ph_2^+], 109 [SPh^+], 77 [Ph^+]

IR: (CsI disc) 3107 w, 3054 m, 2976 w, 2967 s, 2935 s, 2868 m, 1578 s, 1474 s, 1437 m, 1412 w, 1387 w, 1364 w, 1263 s, 1082 vs, 1047 s, 1024 s, 939 vs, 808 vs, 742 vs, 694 m, 600 m, 484 m and 385 w cm^{-1}

6.6 Characterising data for [Nb(η-C_5H_4-CMe_2-η-C_5H_4)(CH_2Ph)$_2$] (6)

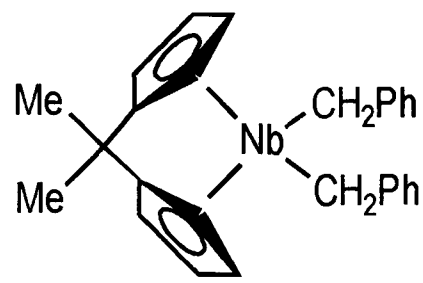

Appearance: dark red blocks

X-Ray Crystal Structure:

see **Appendix C**

Analytical Data: found (calculated %) for $C_{27}H_{28}Nb$: C, 72.7 (72.8); H, 6.5 (6.3 %)

Mass Spectrum: (FAB) the characteristic isotope pattern was observed, *m/z* 445 [M^+], 369 [M^+ – Ph], 353 [M^+ – CH_2Ph], 263 [Nb(η-C_5H_4-CMe_2-η-C_5H_4)$^+$]

IR: (KBr disc) 3068 s, 1594 s, 1483 s, 1446 m, 1411 m, 1262 s, 1202 m, 1099 s, 1027 s, 988 m, 936 w, 905 w, 849 w, 807 vs, 748 m, 740 m, 697 s and 535 w cm^{-1}

6.7 Characterising data for [Nb(η-C_5H_4-CMe_2-η-C_5H_4)($NSiMe_3$)Cl] (7)

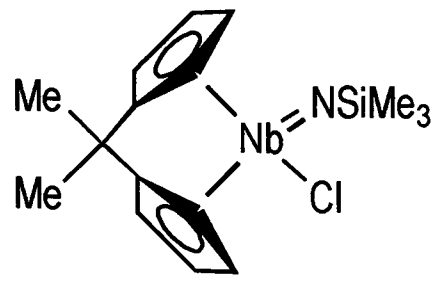

Appearance: yellow crystalline solid

X-Ray Crystal Structure:

see **Appendix D**

Analytical Data: found (calculated %) for $C_{16}H_{23}ClNNbSi$: C, 49.6 (49.8), H, 6.1 (6.0), N, 3.7 (3.6)

^{1}H NMR data: (500 MHz, C_6D_6)

6.50 [2H, m, C_5H_4]

5.94 [4H, m, C_5H_4]

5.20 [2H, m, C_5H_4]

1.28 [3H, s, CH_3]

0.99 [3H, s, CH_3]

0.06 [9H, s, $SiMe_3$]

^{13}C {^{1}H} NMR data: (125 MHz, C_6D_6)

137.9 [s, C_5H_4, C_{ipso}]

120.6 [s, C_5H_4]

115.5 [s, C_5H_4]

103.4 [s, C_5H_4]

95.0 [s, C_5H_4]

36.2 [s, CMe_2]

24.0 [s, CH_3]

22.5 [s, CH_3]

0.9 [s, $SiMe_3$]

Mass Spectrum: (EI) the correct isotope pattern was observed, data given for ^{35}Cl, *m/z* 387 [M^+], 372 [$M^+ - CH_3$], 357 [$M^+ - 2CH_3$], 352 [M^+ – Cl], 342 [$M^+ - 3CH_3$], 300 [$M^+ - NSiMe_3$], 264 [Nb(η-C_5H_4-CMe_2-η-C_5H_4)$^+$]

IR: (KBr disc) 3085 s, 2970 s, 1470 w, 1410 w, 1370 w, 1357 w, 1344 w, 1260 m, 1250 s, 1242 s, 1080 s br, 1040 s, 910 w, 840 s br, 819 s, 808 s, 792 s, 750 m, 737 s, 712 m, 635 m, 598 w, 425 m, 374 m, 350 w, 317 m cm^{-1}

6.8 Characterising data for [Nb(η-C_5H_4-CMe_2-η-C_5H_4)(NBu^t)Cl] (8)

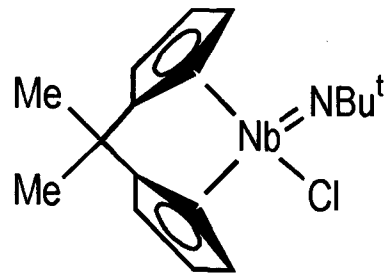

Appearance: yellow crystalline solid

X-Ray Crystal Structure:

see **Appendix E**

Analytical Data: found (calculated %) for $C_{17}H_{23}ClNNb$: C, 54.9 (55.2); H, 6.8 (6.3); N, 3.9 (3.8); Cl, 9.6 (9.6)

^{1}H NMR data: (500 MHz, C_6D_6)

6.45 [2H, m, C_5H_4]

5.93 [2H, m, C_5H_4]

5.85 [2H, m, C_5H_4]

5.40 [2H, m, C_5H_4]

1.32 [3H, s, CH_3]

1.08 [3H, s, CH_3]

0.99 [9H, s , CMe_3]

^{13}C {^{1}H} NMR data: (125 MHz, C_6D_6)

143.6 [C_5H_4, C_{ipso}]

120.1 [C_5H_4]

110.8 [C_5H_4]

104.0 [C_5H_4]

93.7 [C_5H_4]

69.0 [N*C*Me_3]

36.2 [*C*Me_2]

30.4 [C*Me*$_3$]

23.9 [C*Me*$_2$]

22.7 [C*Me*$_2$]

Mass Spectrum (EI): the characteristic isotope pattern was observed, data given for ^{35}Cl, *m/z* 369 [M^+], 354 [$M^+ - CH_3$], 334 [M^+ – Cl], 319 [$M^+ - CH_3$ – Cl], 298 [M^+ – NBu^t], 263 [Nb(η-C_5H_4-CMe_2-η-C_5H_4)$^+$], 57 [Bu^{t+}]

IR: (Nujol) 3081 m, 1605 m, 1378 m, 1368 m, 1247 s, 1218 m, 1130 w, 1070 m, 1041 m, 864 m, 846 m, 807 s, 791 m, 759 m, 737 m, 699 m, 640 w, 605 w, 550 w, 520 w, 425 w and 370 w cm^{-1}

6.9 Characterising data for [Nb(η-C_5H_4-CMe_2-η-C_5H_4)(NBu^t)Br] (9)

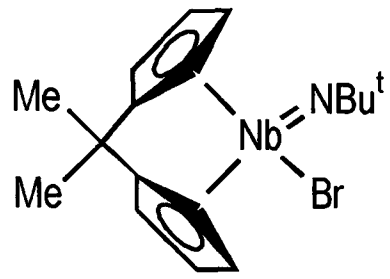

Appearance: yellow crystalline solid

X-Ray Crystal Structure:

see **Appendix F**

Analytical Data: found (calculated) for $C_{17}H_{23}BrNNb$: C, 49.6 (49.3); H, 6.0 (5.6); N, 3.5 (3.4 %)

^{1}H NMR data: (500 MHz, C_6D_6)

6.53 [2H, q, *J* 2.5 Hz, C_5H_4]

6.02 [2H, q, *J* 2.5 Hz, C_5H_4]

5.75 [2H, q, *J* 2.5 Hz, C_5H_4]

5.39 [2H, q, *J* 2.5 Hz, C_5H_4]

1.30 [3H, s, CH_3]

1.03 [3H, s, CH_3]

1.00 [9H, s, CMe_3]

^{13}C {^{1}H} NMR data: (125 MHz, C_6D_6)

143.5 [C_5H_4, C_{ipso}]

119.1 [C_5H_4]

110.7 [C_5H_4]

104.0 [C_5H_4]

93.5 [C_5H_4]

36.1 [CMe_2]

30.1 [CMe_3]

23.9 [CMe_2]

22.6 [CMe_2]

$NCMe_3$ was not located

Mass Spectrum: (EI) the characteristic isotope pattern was observed, data given for ^{81}Br, *m/z* 414 [M^+], 399 [$M^+ - CH_3$], 343 [$M^+ - NBu^t$]

IR: (KBr disc) 3079 s, 2966 s, 2940 m, 2918 m, 1470 m, 1453 m, 1441 m, 1412 m, 1398 m, 1388 w, 1369 m, 1353 s, 1246 vs br, 1216 s, 1159 w, 1141 w, 1130 w, 1099 w vbr, 1075 w, 1053 w, 1039 m, 943 w, 908 w, 880 w, 864 m, 847 m, 818 s, 808 s, 791 s, 738 s, 712 w, 605 w, 566 w, 549 w, 523 m and 429 m cm^{-1}

6.10 Characterising data for [Nb(η-C_5H_4-CMe_2-η-C_5H_4)(NBu^t)I] (10)

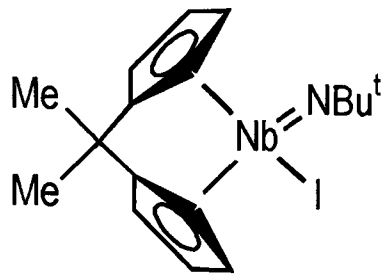

Appearance: orange crystalline solid

X-Ray Crystal Structure:

see **Appendix G**

Analytical Data: found (calculated %) for $C_{17}H_{23}INNb$: C, 43.2 (44.2); H, 5.0 (5.0); N, 3.0 (3.0)

^{1}H NMR data: (500 MHz, C_6D_6)

6.66 [2H, m, C_5H_4]

6.17 [2H, m, C_5H_4]

5.55 [2H, m, C_5H_4]

5.34 [2H, m, C_5H_4]

1.29 [3H, s, CH_3]

1.01 [9H, s, CMe_3]

0.93 [3H, s, CH_3]

^{13}C {^{1}H} NMR data: (125 MHz, C_6D_6)

142.9 [C_5H_4, C_{ipso}]

116.5 [C_5H_4]

110.1 [C_5H_4]

103.5 [C_5H_4]

93.5 [C_5H_4]

69.7 [N*C*Me_3]

35.9 [*C*Me_2]

30.0 [C*Me*$_3$]

23.8 [C*Me*$_2$]

22.3 [C*Me*$_2$]

Mass Spectrum (EI): Calibration accurate to within 1 %, *m/z* 460 [M^+], 445 [$M^+ - CH_3$], 389 [$M^+ - NBu^t$], 263 [Nb(η-C_5H_4-CMe_2-η-C_5H_4)$^+$], 127 [I^+], 71 [NBu^{t+}], 57 [Bu^{t+}]

IR: (KBr disc) 3075 s, 2967 s, 1474 m, 1451 m, 1417 m, 1398 m, 1383 m, 1371 m, 1353 m, 1262 s, 1240 vs, 1213 m, 1098 m, 1034 s, 863 m, 848 m, 800 s, 737 s, 521 m and 429 m cm^{-1}

6.11 Characterising data for [Nb(η-C_5H_4-CMe_2-η-C_5H_4)(NBu^t)Me] (11)

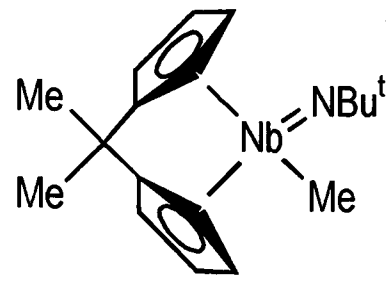

Appearance: yellow crystalline solid

Analytical Data: found (calculated %) for $C_{18}H_{26}NNb$: C, 61.5 (61.9); H, 7.5 (7.5); N, 3.8 (4.0)

^{1}H NMR data: (500 MHz, CD_2Cl_2)

6.61 [4H, q, *J* 2.5 Hz, C_5H_4]
5.84 [2H, q, *J* 3 Hz, C_5H_4]
5.56 [2H, q, *J* 2 Hz, C_5H_4]
1.73 [3H, s, CH_3]
1.37 [3H, s, CH_3]
0.97 [9H, s, CMe_3]
0.76 [3H, s, $NbCH_3$]

^{13}C {^{1}H} NMR data: (75 MHz, CD_2Cl_2)

139.7 [C_5H_4, C_{ipso}]
111.9 [C_5H_4]
107.5 [C_5H_4]
103.0 [C_5H_4]
93.0 [C_5H_4]
66.1 [$NCMe_3$]
36.1 [CMe_2]
31.1 [CMe_3]
24.0 [CMe_2]
23.3 [CMe_2]
2.3 [br, fwhh = 55 Hz, $NbCH_3$]

Mass Spectrum: (EI) the characteristic isotope pattern was observed, *m/z* 349 [M^+], 334 [$M^+ - CH_3$], 319 [$M^+ - 2CH_3$], 278 [$M^+ - NBu^t$], 263 [Nb(η-C_5H_4-CMe_2-η-C_5H_4)$^+$]

IR: (KBr disc) 3089 m, 2985 w, 2970 sh, 2964 s, 2950 w, 2920 w, 2900 w, 2860 sh, 2820 sh, 1469 m, 1445 sh, 1439 m, 1413 m, 1400 sh, 1385 w, 1368 w, 1350 m, 1300 w, 1250 s, 1211 m, 1129 m, 1100 w br, 1057 w, 1050 w, 1034 m, 1010 sh, 943 w, 910 w, 879 w, 849 m, 839 m, 802 s, 782 sh, 738 s, 712 w, 682 w, 605 w, 563 w, 544 w, 520 m, 470 m, 420 m, 365 w, 345 w and 310 sh cm^{-1}

6.12 Characterising data for [Nb(η-C_5H_4-CMe_2-η-C_5H_4)(NHBu^t)Cl][BF_4] (12)

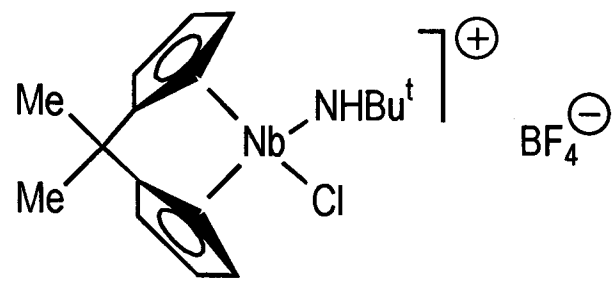

Appearance: orange powder

Analytical Data: found (calculated %) for $C_{17}H_{24}BClF_4NNb$: C, 44.4 (44.6); H, 5.5 (5.3); N, 2.8 (3.1)

^{1}H NMR data: (500 MHz, C_6D_6)

6.70 [2H, m, C_5H_4]

6.21 [2H, m, C_5H_4]

5.90 [2H, m, C_5H_4]

4.39 [2H, m, C_5H_4]

1.08 [9H, s, CMe_3]

0.92 [3H, s, CH_3]

0.52 [3H, s, CH_3]

IR: (Nujol) 3313 m, 3191 m, 3102 m, 2725 w, 1737 m br, 1621 w br, 1513 m, 1503 m, 1414 m, 1300 m, 1290 m, 1271 m, 1220 m, 1196 m, 1062 s, 1044 s, 951 w, 901 m, 877 w, 864 m, 850 m, 833 m, 762 m, 734 m, 591 w, 523 w, 450 w, 407 w cm^{-1}

6.13 Characterising data for [Nb(η-C_5H_4-CMe_2-η-C_5H_4)(O)Cl] (13)

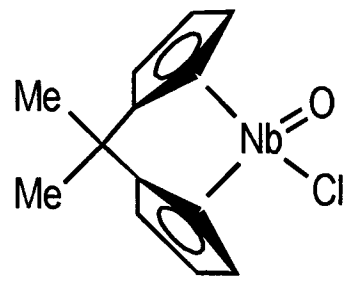

Appearance: yellow blocks

X-Ray Crystal Structure:

see **Appendix H**

Analytical Data: found (calculated %) for $C_{13}H_{14}ClNbO$: C, 49.5 (49.6); H, 4.4 (4.5)

^{1}H NMR data: (500 MHz, CD_2Cl_2)

6.75 [2H, m, C_5H_4]

6.62 [2H, m, C_5H_4]

6.32 [2H, m, C_5H_4]

5.34 [2H, m, C_5H_4]

1.95 [3H, s, CH_3]

1.49 [3H, s, CH_3]

^{13}C {^{1}H} NMR data: (125 MHz, CD_2Cl_2)

131.8 [s, C_5H_4, C_{ipso}]

123.0 [s, C_5H_4]

120.9 [s, C_5H_4]

104.7 [s, C_5H_4]

99.4 [s, C_5H_4]

37.5 [s, CMe_2]

24.9 [s, CMe_2]

22.7 [s, CMe_2]

Mass: (Electrospray) the characteristic isotope pattern was observed, data given for ^{35}Cl, *m/z* 314.9 [M^+, base peak]

IR: (KBr disc) 3109 s, 3098 s, 3080 s, 3063 s, 2984 s, 1471 m, 1450 m, 1415 m, 1390 m, 1374 m, 1346 m, 1263 m, 1219 w, 1143 w, 1105 w, 1087 m, 1075 m, 1064 m, 1031 m, 958 w, 947 w, 909 w, 875 s, 861 s, 847 s, 834 s, 825 s, 812 s, 741 s, 711 m, 594 w, 541 w and 440 w cm^{-1}

6.14 Characterising data for [Nb(η-C_5H_4-CMe_2-η-C_5H_4){$P(OMe)_3$}Cl] (14)

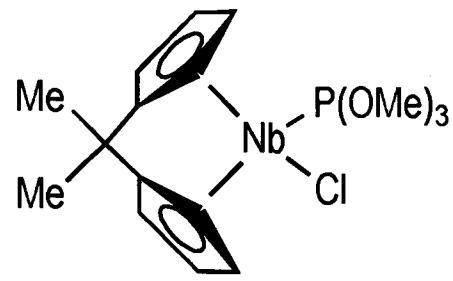

Appearance: purple blocks

X-Ray Crystal Structure:

see **Appendix I**

Analytical Data: found (calculated %) for $C_{16}H_{23}ClNbO_3P$: C, 45.0 (45.5); H, 5.7 (5.5)

^{1}H NMR data: (500 MHz, C_6D_6)

5.74 [2H, m, C_5H_4]

5.63 [2H, m, C_5H_4]

4.92 [2H, m, C_5H_4]

4.08 [2H, m, C_5H_4]

3.46 [9H, d, $^3J_{PH}$ 10 Hz, $P(OMe)_3$]

0.64 [3H, s, CH_3]

0.11 [3H, s, CH_3]

^{31}P {^{1}H} NMR data: (202 MHz, C_6D_6)

182 [br s, fwhh ~1500 Hz, $P(OMe)_3$]

^{13}C {^{1}H} NMR data: (125 MHz, C_6D_6)

118.2 [s, C_5H_4]

98.7 [s, C_5H_4]

81.0 [s, C_5H_4]

74.1 [s, C_5H_4, C_{ipso}]

72.8 [s, C_5H_4]

52.2 [s, $P(OMe)_3$]

31.4 [s, CMe_2]

22.6 [s, CMe_2]

20.9 [s, CMe_2]

IR: (CsI disc) 3066 s, 2951 s, 1455 m, 1417 m, 1390 m, 1376 m, 1267 s, 1184 m, 1050 s, 1025 s, 934 w, 868 m, 826 m, 792 m, 766 m, 749 m, 718 m, 603 w, 554 m, 523 m, 465 w, 458 w, 428 w and 405 w cm^{-1}

Appendix A

The crystal structure of

[Nb(η-C_5H_4-CMe_2-η-C_5H_4)(η^2-BH_4)] (2)

A.1 Crystal data, data collection and processing parameters for [Nb(η-C$_5$H$_4$-CMe$_2$-η-C$_5$H$_4$)(η^2-BH$_4$)] (2)

Molecular formula	$C_{13}H_{18}BNb$
Formula weight / AMU	278.00
Crystal system	Monoclinic
Space group	*C* 2/*c*
a / Å	10.565(6)
b / Å	12.648(7)
c / Å	9.802(6)
β / °	107.03(4)
Unit-cell volume / Å^3	1252.3
Formula units per cell, *Z*	4
ρ_{calc} / g cm^{-3}	1.48
μ / mm^{-1}	0.89
Crystal size / mm	0.1 x 0.15 x 0.3
θ_{max} / °	24
Radiation	Mo-K_α
	λ = 0.71069 Å
Scan type	2θ/ω
No. of reflections:	
total	2755
unique	985
in refinement [$I > 3\sigma(I)$]	800
R_{merge}	0.043
No. of variables	97
Residual electron density: min, max / e Å^{-3}	–0.61, 1.11
R	0.034
R_w	0.039
Temperature / K	293

A.2 Interatomic distances (Å) for [Nb(η-C$_5$H$_4$-CMe$_2$-η-C$_5$H$_4$)(η^2-BH$_4$)] (2)

Atoms marked with a prime are generated from their counterparts by the symmetry operation (– x, y, ½ – z).

B(1)–H(11)	1.25(7)	C(5)–H(51)	0.94(5)
B(1)–H(12)	1.07(6)	C(6)–H(61)	0.98(6)
C(1)–C(2)	1.518(7)	C(7)–H(71)	0.85(7)
C(1)–C(4)	1.514(6)	C(8)–H(81)	0.88(5)
C(4)–C(5)	1.440(6)	Nb(1)–B(1)	2.36(1)
C(5)–C(6)	1.402(8)	Nb(1)–C(4)	2.262(4)
C(6)–C(7)	1.387(8)	Nb(1)–C(5)	2.308(5)
C(7)–C(8)	1.401(8)	Nb(1)–C(6)	2.419(5)
C(8)–C(4)	1.431(6)	Nb(1)–C(7)	2.418(5)
C(2)–H(21)	0.88(6)	Nb(1)–C(8)	2.302(5)
C(2)–H(22)	0.99(6)	Nb(1)–H(11)	1.94(7)
C(2)–H(23)	0.94(5)		

A.3 Bond angles (°) for [Nb(η-C$_5$H$_4$-CMe$_2$-η-C$_5$H$_4$)(η^2-BH$_4$)] (2)

Atoms marked with a prime are generated from their counterparts by the symmetry operation (– x, y, ½ – z).

B(1)–Nb(1)–H(11′)	32.0(21)	C(4)–Nb(1)–C(7)	58.6(2)
C(1)–C(2)–H(21)	109.5(39)	C(4)–Nb(1)–C(8)	36.5(2)
C(1)–C(2)–H(22)	112.8(34)	C(4)–Nb(1)–C(8′)	83.5(2)
C(1)–C(2)–H(23)	114.1(31)	C(4)–Nb(1)–H(11)	136.9(20)
C(1)–C(4)–C(8)	125.4(4)	C(4)–Nb(1)–H(11′)	137.6(20)
C(2)–C(1)–C(2′)	108.5(6)	C(5)–C(4)–C(1)	124.5(3)
C(4)–C(1)–C(2′)	112.6(3)	C(5)–C(4)–C(8)	106.4(4)
C(4)–C(1)–C(2)	113.0(3)	C(5)–C(6)–C(7)	109.2(5)
C(4)–C(1)–C(4′)	96.9(5)	C(5)–C(6)–H(61)	120.9(35)
C(4)–C(5)–H(51)	122.8(31)	C(5)–Nb(1)–B(1)	122.1(1)
C(4)–C(8)–C(7)	108.1(4)	C(5)–Nb(1)–C(5′)	115.8(2)
C(4)–C(8)–H(81)	129.3(35)	C(5)–Nb(1)–C(7′)	119.1(2)
C(4)–Nb(1)–B(1)	149.9(1)	C(5)–Nb(1)–C(7)	57.5(2)
C(4)–Nb(1)–C(4′)	60.1(2)	C(5)–Nb(1)–C(8)	59.8(2)
C(4)–Nb(1)–C(5)	36.7(2)	C(5)–Nb(1)–C(8′)	86.5(2)
C(4)–Nb(1)–C(5′)	83.2(2)	C(5)–Nb(1)–H(11′)	101.0(20)
C(4)–Nb(1)–C(7′)	116.0(2)	C(5)–Nb(1)–H(11)	135.3(19)

C(6)–C(5)–C(4)	107.5(4)	C(8)–Nb(1)–H(11)	100.4(20)
C(6)–C(5)–H(51)	129.6(31)	C(8)–Nb(1)–H(11´)	135.8(19)
C(6)–C(7)–C(8)	108.7(4)	H(11)–B(1)–H(11´)	110.4(67)
C(6)–C(7)–H(71)	123.3(44)	H(11)–Nb(1)–H(11´)	64.0(42)
C(6´)–Nb(1)–B(1)	92.9(1)	H(12)–B(1)–H(11´)	100.6(42)
C(6)–Nb(1)–B(1)	92.9(1)	H(12)–B(1)–H(11)	116.1(42)
C(6)–Nb(1)–C(4´)	115.7(2)	H(12)–B(1)–H(12´)	113.6(66)
C(6)–Nb(1)–C(4)	58.5(2)	H(21)–C(2)–H(22)	115.3(52)
C(6)–Nb(1)–C(5´)	140.4(2)	H(21)–C(2)–H(23)	98.2(47)
C(6)–Nb(1)–C(5)	34.4(2)	H(23)–C(2)–H(22)	106.2(43)
C(6)–Nb(1)–C(6´)	174.2(3)	Nb(1)–B(1)–H(11)	55.2(33)
C(6)–Nb(1)–C(7´)	146.2(2)	Nb(1)–B(1)–H(12)	123.2(33)
C(6)–Nb(1)–C(7)	33.3(2)	Nb(1)–C(4)–C(1)	101.5(3)
C(6)–Nb(1)–C(8´)	119.1(2)	Nb(1)–C(4)–C(5)	73.4(3)
C(6)–Nb(1)–C(8)	57.3(2)	Nb(1)–C(4)–C(8)	73.3(3)
C(6)–Nb(1)–H(11)	100.9(19)	Nb(1)–C(5)–C(4)	69.9(2)
C(6)–Nb(1)–H(11´)	84.1(19)	Nb(1)–C(5)–C(6)	77.1(3)
C(7)–C(6)–H(61)	128.7(36)	Nb(1)–C(5)–H(51)	121.4(30)
C(7)–C(8)–H(81)	122.3(35)	Nb(1)–C(6)–C(5)	68.5(3)
C(7)–Nb(1)–B(1)	92.7(1)	Nb(1)–C(6)–C(7)	73.3(3)
C(7)–Nb(1)–C(7´)	174.5(3)	Nb(1)–C(6)–H(61)	114.5(34)
C(7)–Nb(1)–C(8´)	140.7(2)	Nb(1)–C(7)–C(6)	73.4(3)
C(7)–Nb(1)–C(8)	34.4(2)	Nb(1)–C(7)–C(8)	68.2(3)
C(7)–Nb(1)–H(11´)	101.4(19)	Nb(1)–C(7)–H(71)	117.7(43)
C(7)–Nb(1)–H(11)	83.3(19)	Nb(1)–C(8)–C(4)	70.2(2)
C(8)–C(7)–H(71)	127.4(43)	Nb(1)–C(8)–C(7)	77.3(3)
C(8)–Nb(1)–B(1)	122.0(1)	Nb(1)–C(8)–H(81)	122.7(32)
C(8)–Nb(1)–C(8´)	116.0(2)	Nb(1)–H(11)–B(1)	92.8(38)

A.4 Fractional atomic coordinates and isotropic thermal parameters for [Nb(η-C$_5$H$_4$-CMe$_2$-η-C$_5$H$_4$)(η^2-BH$_4$)] (2)

Atom	x/*a*	y/*b*	z/*c*	U(iso)	Occ	
Nb(1)	0.0000	0.22147(5)	0.2500	0.0383	1.0000	U_{ani}
B(1)	0.0000	0.0347(8)	0.2500	0.0814	1.0000	U_{ani}
C(1)	0.0000	0.4556(5)	0.2500	0.0461	1.0000	U_{ani}
C(2)	0.1200(6)	0.5258(5)	0.3103(7)	0.0619	1.0000	U_{ani}
C(4)	–0.0206(4)	0.3763(3)	0.3571(5)	0.0412	1.0000	U_{ani}
C(5)	0.0842(5)	0.3185(4)	0.4561(5)	0.0465	1.0000	U_{ani}
C(6)	0.0268(5)	0.2312(4)	0.5034(5)	0.0518	1.0000	U_{ani}
C(7)	–0.1082(5)	0.2306(4)	0.4356(5)	0.0527	1.0000	U_{ani}
C(8)	–0.1396(5)	0.3179(4)	0.3437(5)	0.0470	1.0000	U_{ani}
H(11)	–0.100(7)	0.091(6)	0.201(7)	0.0974	1.0000	U_{iso}
H(12)	0.031(6)	–0.012(5)	0.174(6)	0.0819	1.0000	U_{iso}
H(21)	0.111(6)	0.561(5)	0.385(6)	0.0731	1.0000	U_{iso}

H(22)	0.141(6)	0.570(5)	0.236(6)	0.0721	1.0000	U_{iso}
H(23)	0.198(5)	0.489(4)	0.356(5)	0.0487	1.0000	U_{iso}
H(51)	0.173(5)	0.342(4)	0.485(5)	0.0517	1.0000	U_{iso}
H(61)	0.082(6)	0.175(5)	0.560(6)	0.0699	1.0000	U_{iso}
H(71)	–0.159(6)	0.180(5)	0.442(6)	0.0747	1.0000	U_{iso}
H(81)	–0.221(5)	0.333(4)	0.295(5)	0.0483	1.0000	U_{iso}

A.5 Anisotropic thermal parameters for [Nb(η-C$_5$H$_4$-CMe$_2$-η-C$_5$H$_4$)(η^2-BH$_4$)] (2)

Atom	U(11)	U(22)	U(33)	U(23)	U(13)	U(12)
Nb(1)	0.0368(3)	0.0391(3)	0.0391(3)	0.0000	0.0113(2)	0.0000
B(1)	0.14(1)	0.042(5)	0.101(8)	0.0000	0.049(8)	0.0000
C(1)	0.052(4)	0.042(3)	0.048(3)	0.0000	0.018(3)	0.0000
C(2)	0.076(4)	0.056(3)	0.069(3)	–0.013(3)	0.031(3)	–0.021(3)
C(4)	0.039(2)	0.044(2)	0.044(2)	–0.004(2)	0.016(2)	–0.001(2)
C(5)	0.043(2)	0.057(3)	0.041(2)	0.000(2)	0.012(2)	–0.002(2)
C(6)	0.063(3)	0.059(3)	0.039(2)	0.005(2)	0.017(2)	0.006(3)
C(7)	0.060(3)	0.058(3)	0.055(3)	–0.001(3)	0.030(2)	–0.013(2)
C(8)	0.039(2)	0.057(3)	0.048(2)	–0.002(2)	0.014(2)	0.000(2)

A.6 Additional structural information for [Nb(η-C$_5$H$_4$-CMe$_2$-η-C$_5$H$_4$)(η^2-BH$_4$)] (2)

Nb–Cp_{cent} / Å	2.01
Bending angle, β /°	114.1
Cp_{cent}–Nb–Cp_{cent}, γ /°	125.0
Cp_{cent}–C_{ipso}–C_{bridge} /°	163.9

Appendix B

The crystal structure of

[Nb(η-C_5H_4-CMe_2-η-C_5H_4)(PMe_3)H] (3)

B.1 Crystal data, data collection and processing parameters for [Nb(η-C$_5$H$_4$-CMe$_2$-η-C$_5$H$_4$)(PMe$_3$)H] (3)

Molecular formula	$C_{16}H_{24}NbP$
Formula weight / AMU	340.25
Crystal system	Orthorhombic
Space group	*P b c a*
a / Å	12.205(2)
b / Å	15.330(3)
c / Å	17.175(2)
Unit-cell volume / Å^3	3213.5
Formula units per cell, *Z*	8
ρ_{calc} / g cm^{-3}	1.42
μ / mm^{-1}	0.80
Crystal size / mm	0.2 x 0.2 x 0.3
θ_{max} / °	26
Radiation	Mo-K_α
	λ = 0.71069 Å
Scan type	ω
No. of reflections:	
total	18079
unique	3958
in refinement [$I > 3\sigma(I)$]	1538
R_{merge}	0.083
No. of variables	163
Residual electron density: min, max / e Å^{-3}	–0.56, 0.45
R	0.056
R_w	0.032
Temperature / K	298

B.2 Interatomic distances (Å) for [Nb(η-C$_5$H$_4$-CMe$_2$-η-C$_5$H$_4$)(PMe$_3$)H] (3)

Nb(1)–P(1)	2.553(2)	C(1)–C(2)	1.54(1)
Nb(1)–C(4)	2.273(7)	C(1)–C(3)	1.53(1)
Nb(1)–C(5)	2.294(6)	C(1)–C(4)	1.54(1)
Nb(1)–C(6)	2.382(7)	C(1)–C(9)	1.54(1)
Nb(1)–C(7)	2.437(8)	C(4)–C(5)	1.44(1)
Nb(1)–C(8)	2.347(6)	C(5)–C(6)	1.43(1)
Nb(1)–C(9)	2.272(9)	C(6)–C(7)	1.40(1)
Nb(1)–C(10)	2.295(8)	C(7)–C(8)	1.39(1)
Nb(1)–C(11)	2.388(8)	C(8)–C(4)	1.41(1)
Nb(1)–C(12)	2.434(7)	C(9)–C(10)	1.45(1)
Nb(1)–C(13)	2.366(9)	C(10)–C(11)	1.43(1)
P(1)–C(14)	1.828(8)	C(11)–C(12)	1.38(1)
P(1)–C(15)	1.82(1)	C(12)–C(13)	1.43(1)
P(1)–C(16)	1.82(1)	C(13)–C(9)	1.44(1)

B.3 Bond angles (°) for [Nb(η-C$_5$H$_4$-CMe$_2$-η-C$_5$H$_4$)(PMe$_3$)H] (3)

C(1)–C(4)–C(5)	122.9(7)	C(7)–Nb(1)–C(13)	115.5(4)
C(1)–C(9)–C(10)	124.2(6)	C(8)–C(4)–C(1)	125.5(7)
C(1)–C(9)–C(13)	123.2(7)	C(8)–C(4)–C(5)	107.3(8)
C(3)–C(1)–C(2)	109.4(8)	C(8)–C(7)–C(6)	108.5(9)
C(3)–C(1)–C(9)	113.4(6)	C(8)–Nb(1)–C(4)	35.4(3)
C(4)–C(1)–C(2)	112.6(7)	C(8)–Nb(1)–C(5)	59.3(3)
C(4)–C(1)–C(3)	111.2(7)	C(8)–Nb(1)–C(6)	57.2(3)
C(4)–C(1)–C(9)	98.5(6)	C(8)–Nb(1)–C(7)	33.7(3)
C(4)–C(5)–C(6)	106.3(7)	C(8)–Nb(1)–C(9)	83.4(3)
C(4)–C(8)–C(7)	109.4(8)	C(8)–Nb(1)–C(10)	116.8(3)
C(4)–Nb(1)–C(5)	36.8(3)	C(8)–Nb(1)–C(11)	140.3(3)
C(4)–Nb(1)–C(6)	59.2(3)	C(8)–Nb(1)–C(12)	116.6(3)
C(4)–Nb(1)–C(7)	57.9(3)	C(8)–Nb(1)–C(13)	84.5(3)
C(4)–Nb(1)–C(9)	61.8(3)	C(9)–C(1)–C(2)	111.5(7)
C(4)–Nb(1)–C(10)	86.1(3)	C(9)–Nb(1)–C(5)	85.4(3)
C(4)–Nb(1)–C(11)	119.1(3)	C(9)–Nb(1)–C(13)	36.2(3)
C(4)–Nb(1)–C(13)	82.8(3)	C(10)–C(9)–C(13)	108.4(7)
C(6)–Nb(1)–C(5)	35.6(3)	C(10)–Nb(1)–C(13)	60.4(3)
C(6)–Nb(1)–C(7)	33.8(3)	C(10)–Nb(1)–C(5)	89.7(3)
C(6)–Nb(1)–C(9)	118.8(3)	C(10)–Nb(1)–C(9)	37.0(3)
C(6)–Nb(1)–C(10)	123.5(3)	C(11)–C(10)–C(9)	106.0(7)
C(6)–Nb(1)–C(13)	139.7(3)	C(11)–C(12)–C(13)	109.7(7)
C(7)–C(6)–C(5)	108.5(8)	C(11)–Nb(1)–C(5)	123.8(3)
C(7)–Nb(1)–C(5)	58.1(3)	C(11)–Nb(1)–C(6)	151.5(3)
C(7)–Nb(1)–C(9)	116.1(3)	C(11)–Nb(1)–C(7)	173.4(4)
C(7)–Nb(1)–C(10)	143.4(3)	C(11)–Nb(1)–C(9)	59.2(3)

C(11)–Nb(1)–C(10)	35.6(3)	Nb(1)–C(8)–C(7)	76.7(5)
C(11)–Nb(1)–C(13)	57.8(3)	Nb(1)–C(9)–C(1)	99.7(5)
C(12)–C(11)–C(10)	109.6(7)	Nb(1)–C(9)–C(10)	72.3(5)
C(12)–C(13)–C(9)	106.4(8)	Nb(1)–C(9)–C(13)	75.5(5)
C(12)–Nb(1)–C(4)	116.2(3)	Nb(1)–C(10)–C(9)	70.6(5)
C(12)–Nb(1)–C(5)	143.2(3)	Nb(1)–C(10)–C(11)	75.8(5)
C(12)–Nb(1)–C(6)	173.9(3)	Nb(1)–C(11)–C(10)	68.6(4)
C(12)–Nb(1)–C(7)	141.0(3)	Nb(1)–C(11)–C(12)	75.2(5)
C(12)–Nb(1)–C(9)	58.4(3)	Nb(1)–C(12)–C(11)	71.5(5)
C(12)–Nb(1)–C(10)	58.2(3)	Nb(1)–C(12)–C(13)	70.1(4)
C(12)–Nb(1)–C(11)	33.3(3)	Nb(1)–C(13)–C(9)	68.4(5)
C(12)–Nb(1)–C(13)	34.6(3)	Nb(1)–C(13)–C(12)	75.3(5)
C(13)–Nb(1)–C(5)	116.1(3)	Nb(1)–P(1)–C(14)	114.1(4)
C(14)–P(1)–C(15)	101.2(5)	Nb(1)–P(1)–C(15)	123.5(4)
C(14)–P(1)–C(16)	101.7(5)	Nb(1)–P(1)–C(16)	113.2(3)
C(16)–P(1)–C(15)	100.1(5)	P(1)–Nb(1)–C(4)	139.8(2)
Nb(1)–C(4)–C(1)	99.8(4)	P(1)–Nb(1)–C(5)	130.8(3)
Nb(1)–C(4)–C(5)	72.4(4)	P(1)–Nb(1)–C(6)	95.4(2)
Nb(1)–C(4)–C(8)	75.1(4)	P(1)–Nb(1)–C(7)	83.5(2)
Nb(1)–C(5)–C(4)	70.8(4)	P(1)–Nb(1)–C(8)	105.5(2)
Nb(1)–C(5)–C(6)	75.5(4)	P(1)–Nb(1)–C(9)	142.6(2)
Nb(1)–C(6)–C(5)	68.9(4)	P(1)–Nb(1)–C(10)	133.2(2)
Nb(1)–C(6)–C(7)	75.3(5)	P(1)–Nb(1)–C(11)	98.1(2)
Nb(1)–C(7)–C(6)	70.9(5)	P(1)–Nb(1)–C(12)	86.0(2)
Nb(1)–C(7)–C(8)	69.6(5)	P(1)–Nb(1)–C(13)	107.4(2)
Nb(1)–C(8)–C(4)	69.4(4)		

B.4 Fractional atomic coordinates and isotropic thermal parameters for [Nb(η-C$_5$H$_4$-CMe$_2$-η-C$_5$H$_4$)(PMe$_3$)H] (3)

Atom	x/*a*	y/*b*	z/*c*	U(iso)	Occ	
Nb(1)	0.35475(5)	–0.13626(3)	–0.22842(4)	0.0436	1.0000	U_{ani}
P(1)	0.3336(2)	–0.2297(1)	–0.1063(1)	0.0532	1.0000	U_{ani}
C(1)	0.2821(7)	–0.0397(5)	–0.3681(6)	0.0574	1.0000	U_{ani}
C(2)	0.3617(8)	0.0132(5)	–0.4193(5)	0.0666	1.0000	U_{ani}
C(3)	0.1661(7)	–0.0318(5)	–0.4008(5)	0.0646	1.0000	U_{ani}
C(4)	0.2861(6)	–0.0121(4)	–0.2819(6)	0.0503	1.0000	U_{ani}
C(5)	0.3866(7)	0.0104(4)	–0.2424(6)	0.0567	1.0000	U_{ani}
C(6)	0.3661(8)	–0.0008(4)	–0.1610(5)	0.0565	1.0000	U_{ani}
C(7)	0.2573(9)	–0.0277(5)	–0.1513(6)	0.0635	1.0000	U_{ani}
C(8)	0.2096(6)	–0.0360(4)	–0.2244(6)	0.0527	1.0000	U_{ani}
C(9)	0.3207(6)	–0.1350(4)	–0.3585(5)	0.0522	1.0000	U_{ani}
C(10)	0.4340(7)	–0.1607(5)	–0.3476(5)	0.0571	1.0000	U_{ani}
C(11)	0.4308(8)	–0.2452(5)	–0.3119(6)	0.0619	1.0000	U_{ani}
C(12)	0.3231(8)	–0.2704(5)	–0.3009(5)	0.0595	1.0000	U_{ani}
C(13)	0.2514(8)	–0.2034(4)	–0.3284(6)	0.0609	1.0000	U_{ani}
C(14)	0.4120(8)	–0.3312(5)	–0.1083(7)	0.0759	1.0000	U_{ani}
C(15)	0.2016(9)	–0.2680(6)	–0.0699(8)	0.0996	1.0000	U_{ani}
C(16)	0.3870(9)	–0.1774(5)	–0.0188(6)	0.0802	1.0000	U_{ani}
H(21)	0.4384	0.0045	–0.4001	0.0725	1.0000	U_{iso}
H(22)	0.3562	–0.0072	–0.4744	0.0725	1.0000	U_{iso}
H(23)	0.3424	0.0764	–0.4163	0.0725	1.0000	U_{iso}
H(31)	0.1155	–0.0702	–0.3705	0.0674	1.0000	U_{iso}
H(32)	0.1410	0.0301	–0.3968	0.0674	1.0000	U_{iso}
H(33)	0.1658	–0.0502	–0.4567	0.0674	1.0000	U_{iso}
H(51)	0.4568	0.0301	–0.2670	0.0569	1.0000	U_{iso}
H(61)	0.4202	0.0087	–0.1180	0.0582	1.0000	U_{iso}
H(71)	0.2200	–0.0392	–0.1004	0.0671	1.0000	U_{iso}
H(81)	0.1329	–0.0559	–0.2349	0.0550	1.0000	U_{iso}
H(101)	0.5009	–0.1264	–0.3619	0.0583	1.0000	U_{iso}
H(111)	0.4964	–0.2806	–0.2970	0.0655	1.0000	U_{iso}
H(121)	0.2989	–0.3269	–0.2772	0.0600	1.0000	U_{iso}
H(131)	0.1694	–0.2039	–0.3271	0.0614	1.0000	U_{iso}
H(141)	0.3994	–0.3640	–0.0587	0.0772	1.0000	U_{iso}
H(142)	0.4916	–0.3176	–0.1138	0.0772	1.0000	U_{iso}
H(143)	0.3874	–0.3676	–0.1533	0.0772	1.0000	U_{iso}
H(151)	0.2134	–0.3032	–0.0217	0.1027	1.0000	U_{iso}
H(152)	0.1541	–0.2168	–0.0579	0.1027	1.0000	U_{iso}
H(153)	0.1658	–0.3049	–0.1105	0.1027	1.0000	U_{iso}
H(161)	0.3765	–0.2171	0.0268	0.0807	1.0000	U_{iso}
H(162)	0.3472	–0.1215	–0.0096	0.0807	1.0000	U_{iso}
H(163)	0.4670	–0.1653	–0.0259	0.0807	1.0000	U_{iso}

B.5 Anisotropic thermal parameters for [Nb(η-C$_5$H$_4$-CMe$_2$-η-C$_5$H$_4$)(PMe$_3$)H] (3)

Atom	U(11)	U(22)	U(33)	U(23)	U(13)	U(12)
Nb(1)	0.0432(4)	0.0436(3)	0.0446(4)	–0.0033(3)	0.0003(4)	0.0035(3)
P(1)	0.055(1)	0.052(1)	0.054(1)	0.0028(9)	–0.005(1)	0.0069(9)
C(1)	0.059(6)	0.058(4)	0.060(7)	0.012(4)	0.004(5)	–0.007(3)
C(2)	0.081(7)	0.088(5)	0.053(6)	0.017(4)	0.016(6)	–0.021(5)
C(3)	0.063(6)	0.085(5)	0.057(6)	0.018(4)	–0.012(5)	–0.010(4)
C(4)	0.048(5)	0.039(3)	0.070(7)	0.009(4)	0.001(4)	0.001(3)
C(5)	0.059(5)	0.046(3)	0.068(7)	0.002(4)	–0.001(4)	–0.005(3)
C(6)	0.074(7)	0.052(4)	0.052(6)	–0.014(3)	–0.010(5)	0.005(4)
C(7)	0.083(7)	0.058(5)	0.063(8)	–0.008(4)	0.017(6)	0.018(5)
C(8)	0.054(5)	0.050(4)	0.061(6)	0.006(4)	0.015(5)	0.011(3)
C(9)	0.055(5)	0.052(4)	0.054(5)	–0.011(4)	0.009(4)	–0.007(4)
C(10)	0.061(6)	0.071(5)	0.046(6)	–0.010(4)	0.010(4)	–0.001(4)
C(11)	0.074(7)	0.065(5)	0.059(7)	–0.011(4)	0.006(5)	0.023(4)
C(12)	0.077(7)	0.058(4)	0.049(6)	–0.008(4)	0.004(5)	–0.008(4)
C(13)	0.076(6)	0.052(4)	0.058(7)	–0.003(4)	–0.006(5)	–0.009(4)
C(14)	0.091(7)	0.060(4)	0.084(9)	0.009(4)	–0.005(6)	0.013(4)
C(15)	0.076(8)	0.111(8)	0.13(1)	0.038(8)	0.000(7)	–0.008(5)
C(16)	0.103(9)	0.088(6)	0.059(8)	0.010(5)	–0.011(6)	0.004(5)

B.6 Additional structural information for [Nb(η-C$_5$H$_4$-CMe$_2$-η-C$_5$H$_4$)(PMe$_3$)H] (3)

Nb–Cp$_{cent}$ / Å	2.01, 2.01
Bending angle, β /°	117.3
Cp$_{cent}$–Nb–Cp$_{cent}$, γ /°	126.1
Cp$_{cent}$–C$_{ipso}$–C$_{bridge}$ /°	162.0, 161.8
C(1)–Nb(1)–P(1) /°	156

Appendix C

The crystal structure of

[Nb(η-C_5H_4-CMe_2-η-C_5H_4)(CH_2Ph)$_2$] (6)

C.1 Crystal data, data collection and processing parameters for [Nb(η-C$_5$H$_4$-CMe$_2$-η-C$_5$H$_4$)(CH$_2$Ph)$_2$] (6)

Molecular formula	$C_{27}H_{28}Nb$
M	445.43
Crystal system	Triclinic
Space group	P –1
a / Å	8.785(1)
b / Å	11.721(1)
c / Å	12.081(1)
α / °	63.295(2)
β / °	70.592(2)
γ / °	72.161(2)
Unit-cell volume / Å^3	1029.77
Z	2
ρ_{calc} / g cm^{-3}	1.44
F(000)	457.59
h, k, l ranges	–10 to 11, –12 to 15, 0-15
Temperature / K	150
μ / mm^{-1}	0.57
Crystal size / mm	0.50 × 0.40 × 0.25
θ_{max} / °	26
Radiation type	Mo-K_α
Wavelength / Å	0.71069
Scan type	ω
No. of reflections:	
total	7954
unique	4023
in refinement [$I > 5\sigma(I)$]	2952
R_{merge}	0.015
Number of variables	366
$\Delta\rho_{min, max}$ / e Å^{-3}	–0.40, 0.22
R	0.016
R_w	0.017

C.2 Interatomic distances (Å) for [Nb(η-C5H4-CMe2-η-C5H4)(CH2Ph)2] (6)

C(1)–C(2)	1.526(2)	Nb(1)–C(10)	2.368(1)
C(1)–C(3)	1.528(2)	Nb(1)–C(11)	2.457(1)
C(1)–C(4)	1.532(2)	Nb(1)–C(12)	2.443(1)
C(1)–C(9)	1.528(2)	Nb(1)–C(13)	2.354(1)
C(4)–C(5)	1.430(2)	Nb(1)–C(14)	2.277(1)
C(4)–C(8)	1.426(2)	Nb(1)–C(21)	2.284(1)
C(5)–C(6)	1.416(2)	C(2)–H(21)	0.92(2)
C(6)–C(7)	1.399(2)	C(2)–H(22)	0.95(2)
C(7)–C(8)	1.417(2)	C(2)–H(23)	0.99(2)
C(9)–C(10)	1.431(2)	C(3)–H(31)	0.94(2)
C(9)–C(13)	1.430(2)	C(3)–H(32)	0.95(2)
C(10)–C(11)	1.415(2)	C(3)–H(33)	0.95(2)
C(11)–C(12)	1.404(2)	C(5)–H(51)	0.93(2)
C(12)–C(13)	1.406(2)	C(6)–H(61)	0.95(2)
C(14)–C(15)	1.489(2)	C(7)–H(71)	0.94(2)
C(15)–C(16)	1.397(2)	C(8)–H(81)	0.95(2)
C(15)–C(20)	1.399(2)	C(10)–H(101)	0.95(2)
C(16)–C(17)	1.386(2)	C(11)–H(111)	0.97(2)
C(17)–C(18)	1.378(3)	C(12)–H(121)	0.93(2)
C(18)–C(19)	1.385(3)	C(13)–H(131)	0.97(2)
C(19)–C(20)	1.387(2)	C(14)–H(141)	0.99(2)
C(21)–C(22)	1.484(2)	C(14)–H(142)	0.90(2)
C(22)–C(23)	1.402(2)	C(16)–H(161)	0.93(2)
C(22)–C(27)	1.405(2)	C(17)–H(171)	1.02(2)
C(23)–C(24)	1.377(2)	C(18)–H(181)	0.95(3)
C(24)–C(25)	1.387(3)	C(19)–H(191)	1.00(2)
C(25)–C(26)	1.382(3)	C(20)–H(201)	0.98(2)
C(26)–C(27)	1.386(2)	C(21)–H(211)	0.95(2)
Nb(1)–C(4)	2.325(1)	C(21)–H(212)	0.93(2)
Nb(1)–C(5)	2.361(2)	C(23)–H(231)	0.94(2)
Nb(1)–C(6)	2.451(1)	C(24)–H(241)	1.00(2)
Nb(1)–C(7)	2.461(1)	C(25)–H(251)	0.90(3)
Nb(1)–C(8)	2.367(1)	C(26)–H(261)	0.95(2)
Nb(1)–C(9)	2.322(1)	C(27)–H(271)	0.99(2)

C.3 Bond angles (°) for [Nb(η-C$_5$H$_4$-CMe$_2$-η-C$_5$H$_4$)(CH$_2$Ph)$_2$] (6)

C(1)–C(4)–C(5)	125.0(1)	C(7)–Nb(1)–C(10)	139.41(5)
C(1)–C(4)–C(8)	124.2(1)	C(7)–Nb(1)–C(11)	172.03(5)
C(1)–C(9)–C(10)	124.7(1)	C(7)–Nb(1)–C(12)	144.49(6)
C(1)–C(9)–C(13)	124.9(1)	C(7)–Nb(1)–C(13)	117.40(5)
C(2)–C(1)–C(3)	109.5(1)	C(7)–Nb(1)–C(14)	83.09(5)
C(2)–C(1)–C(4)	111.3(1)	C(7)–Nb(1)–C(21)	103.70(5)
C(2)–C(1)–C(9)	112.9(1)	C(7)–Nb(1)–C(8)	34.06(5)
C(3)–C(1)–C(4)	112.3(1)	C(7)–Nb(1)–C(9)	114.38(5)
C(3)–C(1)–C(9)	111.8(1)	C(8)–Nb(1)–C(10)	113.63(5)
C(4)–C(1)–C(9)	98.8(1)	C(8)–Nb(1)–C(11)	138.34(5)
C(4)–C(5)–C(6)	108.0(1)	C(8)–Nb(1)–C(12)	117.48(5)
C(4)–C(8)–C(7)	108.1(1)	C(8)–Nb(1)–C(13)	85.22(5)
C(4)–Nb(1)–C(10)	82.78(5)	C(8)–Nb(1)–C(14)	96.30(5)
C(4)–Nb(1)–C(11)	115.04(5)	C(8)–Nb(1)–C(21)	136.54(5)
C(4)–Nb(1)–C(12)	114.73(5)	C(8)–Nb(1)–C(9)	81.90(5)
C(4)–Nb(1)–C(13)	82.34(5)	C(9)–C(10)–C(11)	108.3(1)
C(4)–Nb(1)–C(14)	131.63(5)	C(9)–C(13)–C(12)	108.3(1)
C(4)–Nb(1)–C(21)	129.37(5)	C(9)–Nb(1)–C(10)	35.53(5)
C(4)–Nb(1)–C(5)	35.53(5)	C(9)–Nb(1)–C(11)	57.65(5)
C(4)–Nb(1)–C(6)	57.59(5)	C(9)–Nb(1)–C(12)	57.64(5)
C(4)–Nb(1)–C(7)	57.40(5)	C(9)–Nb(1)–C(13)	35.60(5)
C(4)–Nb(1)–C(8)	35.37(5)	C(9)–Nb(1)–C(14)	129.93(5)
C(4)–Nb(1)–C(9)	60.02(5)	C(9)–Nb(1)–C(21)	130.75(5)
C(5)–C(4)–C(8)	106.9(1)	C(10)–C(11)–C(12)	108.1(1)
C(5)–C(6)–C(7)	108.4(1)	C(10)–C(9)–C(13)	106.6(1)
C(5)–Nb(1)–C(10)	87.11(5)	C(10)–Nb(1)–C(11)	34.05(5)
C(5)–Nb(1)–C(11)	119.50(5)	C(10)–Nb(1)–C(12)	56.59(5)
C(5)–Nb(1)–C(12)	139.71(5)	C(10)–Nb(1)–C(13)	58.13(5)
C(5)–Nb(1)–C(13)	114.10(5)	C(10)–Nb(1)–C(14)	135.24(5)
C(5)–Nb(1)–C(14)	137.64(5)	C(10)–Nb(1)–C(21)	95.36(5)
C(5)–Nb(1)–C(21)	93.91(6)	C(11)–C(12)–C(13)	108.7(1)
C(5)–Nb(1)–C(6)	34.17(5)	C(11)–Nb(1)–C(12)	33.29(5)
C(5)–Nb(1)–C(7)	56.49(5)	C(11)–Nb(1)–C(13)	56.63(5)
C(5)–Nb(1)–C(8)	58.08(5)	C(11)–Nb(1)–C(14)	102.13(5)
C(5)–Nb(1)–C(9)	82.90(5)	C(11)–Nb(1)–C(21)	83.07(5)
C(6)–C(7)–C(8)	108.4(1)	C(12)–Nb(1)–C(13)	34.03(6)
C(6)–Nb(1)–C(10)	119.74(5)	C(12)–Nb(1)–C(14)	80.59(5)
C(6)–Nb(1)–C(11)	147.28(6)	C(12)–Nb(1)–C(21)	105.34(5)
C(6)–Nb(1)–C(12)	172.31(5)	C(13)–Nb(1)–C(14)	94.34(5)
C(6)–Nb(1)–C(13)	138.59(5)	C(13)–Nb(1)–C(21)	138.24(5)
C(6)–Nb(1)–C(14)	104.30(5)	C(14)–C(15)–C(16)	120.9(1)
C(6)–Nb(1)–C(21)	81.34(6)	C(14)–C(15)–C(20)	122.6(1)
C(6)–Nb(1)–C(7)	33.09(6)	C(14)–Nb(1)–C(21)	83.04(5)
C(6)–Nb(1)–C(8)	56.57(5)	C(15)–C(16)–C(17)	121.7(2)
C(6)–Nb(1)–C(9)	115.15(5)	C(15)–C(20)–C(19)	122.0(2)

C(16)–C(15)–C(20)	116.5(1)	C(7)–C(6)–H(61)	126.1(11)
C(16)–C(17)–C(18)	120.7(2)	C(7)–C(8)–H(81)	125.6(12)
C(17)–C(18)–C(19)	119.1(2)	C(8)–C(7)–H(71)	126.1(13)
C(18)–C(19)–C(20)	120.1(2)	C(9)–C(10)–H(101)	126.1(11)
C(21)–C(22)–C(23)	121.7(1)	C(9)–C(13)–H(131)	125.7(11)
C(21)–C(22)–C(27)	121.8(1)	C(10)–C(11)–H(111)	125.7(11)
C(22)–C(23)–C(24)	122.0(1)	C(11)–C(10)–H(101)	125.5(11)
C(22)–C(27)–C(26)	121.5(1)	C(11)–C(12)–H(121)	124.4(12)
C(23)–C(22)–C(27)	116.4(1)	C(12)–C(11)–H(111)	126.2(11)
C(23)–C(24)–C(25)	120.5(2)	C(12)–C(13)–H(131)	125.9(11)
C(24)–C(25)–C(26)	119.0(2)	C(13)–C(12)–H(121)	126.8(12)
C(25)–C(26)–C(27)	120.6(2)	C(15)–C(14)–H(141)	109.5(11)
Nb(1)–C(4)–C(1)	100.45(9)	C(15)–C(14)–H(142)	108.9(12)
Nb(1)–C(4)–C(5)	73.62(9)	C(15)–C(16)–H(161)	116.7(12)
Nb(1)–C(4)–C(8)	73.90(8)	C(15)–C(20)–H(201)	120.1(12)
Nb(1)–C(5)–C(4)	70.86(8)	C(16)–C(17)–H(171)	117.4(13)
Nb(1)–C(5)–C(6)	76.40(9)	C(17)–C(16)–H(161)	121.6(12)
Nb(1)–C(6)–C(5)	69.43(8)	C(17)–C(18)–H(181)	118.6(15)
Nb(1)–C(6)–C(7)	73.85(9)	C(18)–C(17)–H(171)	121.9(13)
Nb(1)–C(7)–C(6)	73.06(9)	C(18)–C(19)–H(191)	119.6(13)
Nb(1)–C(7)–C(8)	69.30(8)	C(19)–C(18)–H(181)	122.3(15)
Nb(1)–C(8)–C(4)	70.72(8)	C(19)–C(20)–H(201)	117.8(12)
Nb(1)–C(8)–C(7)	76.64(9)	C(20)–C(19)–H(191)	120.4(13)
Nb(1)–C(9)–C(1)	100.69(9)	C(22)–C(21)–H(211)	111.1(11)
Nb(1)–C(9)–C(10)	73.98(8)	C(22)–C(21)–H(212)	112.6(11)
Nb(1)–C(9)–C(13)	73.42(8)	C(22)–C(23)–H(231)	119.4(12)
Nb(1)–C(10)–C(11)	76.45(8)	C(22)–C(27)–H(271)	119.7(11)
Nb(1)–C(10)–C(9)	70.49(8)	C(23)–C(24)–H(241)	119.2(13)
Nb(1)–C(11)–C(10)	69.51(8)	C(24)–C(23)–H(231)	118.6(12)
Nb(1)–C(11)–C(12)	72.81(8)	C(24)–C(25)–H(251)	119.0(14)
Nb(1)–C(12)–C(11)	73.90(8)	C(25)–C(24)–H(241)	120.1(13)
Nb(1)–C(12)–C(13)	69.50(8)	C(25)–C(26)–H(261)	118.4(14)
Nb(1)–C(13)–C(12)	76.47(8)	C(26)–C(25)–H(251)	122.0(14)
Nb(1)–C(13)–C(9)	70.98(8)	C(26)–C(27)–H(271)	118.8(11)
Nb(1)–C(14)–C(15)	119.3(1)	C(27)–C(26)–H(261)	121.0(14)
Nb(1)–C(21)–C(22)	116.2(1)	H(21)–C(2)–H(22)	109.5(19)
C(1)–C(2)–H(21)	108.2(13)	H(21)–C(2)–H(23)	107.9(19)
C(1)–C(2)–H(22)	111.0(14)	H(22)–C(2)–H(23)	108.6(19)
C(1)–C(2)–H(23)	111.6(12)	H(31)–C(3)–H(32)	108.1(19)
C(1)–C(3)–H(31)	109.7(14)	H(31)–C(3)–H(33)	107.0(19)
C(1)–C(3)–H(32)	110.1(14)	H(32)–C(3)–H(33)	108.8(19)
C(1)–C(3)–H(33)	113.0(13)	H(141)–C(14)–H(142)	106.6(16)
C(4)–C(5)–H(51)	127.1(12)	H(211)–C(21)–H(212)	106.3(16)
C(4)–C(8)–H(81)	126.2(12)	Nb(1)–C(5)–H(51)	117.3(12)
C(5)–C(6)–H(61)	125.4(11)	Nb(1)–C(6)–H(61)	122.2(12)
C(6)–C(5)–H(51)	124.8(12)	Nb(1)–C(7)–H(71)	122.8(13)
C(6)–C(7)–H(71)	125.5(13)	Nb(1)–C(8)–H(81)	117.2(12)

Nb(1)–C(10)–H(101)	116.8(10)	Nb(1)–C(14)–H(141)	105.2(11)
Nb(1)–C(11)–H(111)	122.7(10)	Nb(1)–C(14)–H(142)	106.7(11)
Nb(1)–C(12)–H(121)	121.0(11)	Nb(1)–C(21)–H(211)	107.6(12)
Nb(1)–C(13)–H(131)	117.8(11)	Nb(1)–C(21)–H(212)	102.4(11)

C.4 Fractional atomic coordinates and isotropic thermal parameters for [Nb(η-C$_5$H$_4$-CMe$_2$-η-C$_5$H$_4$)(CH$_2$Ph)$_2$] (6)

Atom	x/*a*	y/*b*	z/*c*	U(iso)	Occ	
Nb(1)	0.25399(2)	0.24214(1)	0.35284(1)	0.0161	1.0000	U_{ani}
C(1)	0.2223(2)	0.5106(1)	0.1473(1)	0.0245	1.0000	U_{ani}
C(2)	0.1711(2)	0.5470(2)	0.0249(2)	0.0311	1.0000	U_{ani}
C(3)	0.2564(2)	0.6307(2)	0.1477(2)	0.0301	1.0000	U_{ani}
C(4)	0.3694(2)	0.3978(1)	0.1644(1)	0.0218	1.0000	U_{ani}
C(5)	0.3907(2)	0.2862(2)	0.1374(1)	0.0239	1.0000	U_{ani}
C(6)	0.5041(2)	0.1857(2)	0.2052(2)	0.0251	1.0000	U_{ani}
C(7)	0.5527(2)	0.2324(2)	0.2739(2)	0.0245	1.0000	U_{ani}
C(8)	0.4692(2)	0.3624(2)	0.2511(1)	0.0226	1.0000	U_{ani}
C(9)	0.0976(2)	0.4463(1)	0.2672(1)	0.0215	1.0000	U_{ani}
C(10)	0.0092(2)	0.3549(1)	0.2805(2)	0.0220	1.0000	U_{ani}
C(11)	–0.0478(2)	0.2840(1)	0.4119(2)	0.0227	1.0000	U_{ani}
C(12)	0.0057(2)	0.3286(2)	0.4802(2)	0.0236	1.0000	U_{ani}
C(13)	0.0952(2)	0.4274(1)	0.3932(1)	0.0229	1.0000	U_{ani}
C(14)	0.3195(2)	0.1371(1)	0.5464(1)	0.0213	1.0000	U_{ani}
C(15)	0.3349(2)	0.2144(1)	0.6106(1)	0.0212	1.0000	U_{ani}
C(16)	0.2218(2)	0.2199(2)	0.7220(2)	0.0282	1.0000	U_{ani}
C(17)	0.2369(2)	0.2887(2)	0.7847(2)	0.0364	1.0000	U_{ani}
C(18)	0.3649(2)	0.3546(2)	0.7383(2)	0.0350	1.0000	U_{ani}
C(19)	0.4790(2)	0.3512(2)	0.6280(2)	0.0318	1.0000	U_{ani}
C(20)	0.4637(2)	0.2821(2)	0.5657(2)	0.0265	1.0000	U_{ani}
C(21)	0.2212(2)	0.0409(1)	0.3906(1)	0.0203	1.0000	U_{ani}
C(22)	0.1942(2)	0.0264(1)	0.2831(1)	0.0209	1.0000	U_{ani}
C(23)	0.3210(2)	–0.0321(2)	0.2073(2)	0.0262	1.0000	U_{ani}
C(24)	0.2984(2)	–0.0412(2)	0.1043(2)	0.0316	1.0000	U_{ani}
C(25)	0.1474(2)	0.0082(2)	0.0717(2)	0.0314	1.0000	U_{ani}
C(26)	0.0189(2)	0.0645(2)	0.1457(2)	0.0292	1.0000	U_{ani}
C(27)	0.0412(2)	0.0730(1)	0.2499(2)	0.0242	1.0000	U_{ani}
H(21)	0.256(3)	0.577(2)	–0.043(2)	0.039(5)	1.0000	U_{iso}
H(22)	0.075(3)	0.613(2)	0.018(2)	0.046(6)	1.0000	U_{iso}
H(23)	0.150(3)	0.471(2)	0.021(2)	0.034(5)	1.0000	U_{iso}
H(31)	0.343(3)	0.662(2)	0.078(2)	0.044(6)	1.0000	U_{iso}
H(32)	0.161(3)	0.698(2)	0.140(2)	0.043(6)	1.0000	U_{iso}
H(33)	0.289(3)	0.613(2)	0.222(2)	0.037(5)	1.0000	U_{iso}
H(51)	0.338(2)	0.278(2)	0.086(2)	0.030(5)	1.0000	U_{iso}
H(61)	0.540(2)	0.101(2)	0.204(2)	0.027(4)	1.0000	U_{iso}

H(71)	0.627(3)	0.185(2)	0.327(2)	0.038(5)	1.0000	U_{iso}
H(81)	0.476(2)	0.415(2)	0.289(2)	0.031(5)	1.0000	U_{iso}
H(101)	–0.005(2)	0.341(2)	0.213(2)	0.021(4)	1.0000	U_{iso}
H(111)	–0.111(2)	0.216(2)	0.448(2)	0.025(4)	1.0000	U_{iso}
H(121)	–0.013(2)	0.295(2)	0.569(2)	0.023(4)	1.0000	U_{iso}
H(131)	0.148(2)	0.474(2)	0.415(2)	0.026(4)	1.0000	U_{iso}
H(141)	0.425(2)	0.077(2)	0.533(2)	0.029(5)	1.0000	U_{iso}
H(142)	0.243(2)	0.087(2)	0.598(2)	0.023(4)	1.0000	U_{iso}
H(161)	0.137(2)	0.175(2)	0.752(2)	0.029(5)	1.0000	U_{iso}
H(171)	0.152(3)	0.287(2)	0.867(2)	0.039(5)	1.0000	U_{iso}
H(181)	0.372(3)	0.401(2)	0.784(2)	0.053(6)	1.0000	U_{iso}
H(191)	0.574(3)	0.397(2)	0.595(2)	0.046(6)	1.0000	U_{iso}
H(201)	0.550(3)	0.278(2)	0.490(2)	0.035(5)	1.0000	U_{iso}
H(211)	0.314(2)	–0.020(2)	0.420(2)	0.029(5)	1.0000	U_{iso}
H(212)	0.133(2)	0.027(2)	0.461(2)	0.022(4)	1.0000	U_{iso}
H(231)	0.425(3)	–0.066(2)	0.227(2)	0.031(5)	1.0000	U_{iso}
H(241)	0.395(3)	–0.078(2)	0.049(2)	0.044(6)	1.0000	U_{iso}
H(251)	0.136(3)	0.003(2)	0.003(2)	0.043(6)	1.0000	U_{iso}
H(261)	–0.085(3)	0.095(2)	0.124(2)	0.044(6)	1.0000	U_{iso}
H(271)	–0.054(2)	0.112(2)	0.302(2)	0.027(4)	1.0000	U_{iso}

C.5 Anisotropic thermal parameters for [Nb(η-C$_5$H$_4$-CMe$_2$-η-C$_5$H$_4$)(CH$_2$Ph)$_2$] (6)

Atom	U(11)	U(22)	U(33)	U(23)	U(13)	U(12)
Nb(1)	0.01402(6)	0.01714(7)	0.01717(7)	–0.00677(5)	–0.00254(4)	–0.00363(4)
C(1)	0.0236(7)	0.0232(7)	0.0245(7)	–0.0066(6)	–0.0051(6)	–0.0054(6)
C(2)	0.0309(8)	0.0330(9)	0.0244(8)	–0.0030(7)	–0.0072(7)	–0.0051(8)
C(3)	0.0309(8)	0.0224(8)	0.038(1)	–0.0069(7)	–0.0035(8)	–0.0101(7)
C(4)	0.0203(6)	0.0234(7)	0.0205(7)	–0.0059(6)	0.0002(6)	–0.0083(6)
C(5)	0.0226(7)	0.0302(8)	0.0199(7)	–0.0101(6)	0.0014(6)	–0.0085(6)
C(6)	0.0210(7)	0.0266(8)	0.0267(8)	–0.0115(7)	0.0040(6)	–0.0047(6)
C(7)	0.0162(6)	0.0290(8)	0.0264(8)	–0.0069(7)	–0.0011(6)	–0.0056(6)
C(8)	0.0186(6)	0.0269(7)	0.0251(8)	–0.0082(7)	–0.0011(6)	–0.0103(6)
C(9)	0.0203(6)	0.0185(6)	0.0240(7)	–0.0069(6)	–0.0060(6)	–0.0008(6)
C(10)	0.0173(6)	0.0226(7)	0.0262(7)	–0.0076(6)	–0.0070(6)	–0.0026(6)
C(11)	0.0154(6)	0.0222(7)	0.0294(8)	–0.0084(6)	–0.0025(6)	–0.0027(6)
C(12)	0.0199(7)	0.0258(7)	0.0235(8)	–0.0109(7)	–0.0016(6)	0.0009(6)
C(13)	0.0219(7)	0.0219(7)	0.0266(8)	–0.0127(6)	–0.0038(6)	–0.0010(6)
C(14)	0.0213(7)	0.0209(7)	0.0221(7)	–0.0065(6)	–0.0061(6)	–0.0057(6)
C(15)	0.0227(7)	0.0192(7)	0.0235(7)	–0.0057(6)	–0.0109(6)	–0.0015(6)
C(16)	0.0260(7)	0.0320(8)	0.0315(9)	–0.0155(7)	–0.0046(7)	–0.0079(7)
C(17)	0.0391(9)	0.043(1)	0.039(1)	–0.0250(9)	–0.0082(8)	–0.0049(8)
C(18)	0.051(1)	0.0335(9)	0.043(1)	–0.0206(8)	–0.0178(9)	–0.0090(8)
C(19)	0.0428(9)	0.0289(8)	0.038(1)	–0.0065(7)	–0.0189(8)	–0.0147(8)
C(20)	0.0287(7)	0.0283(8)	0.0255(8)	–0.0061(7)	–0.0105(7)	–0.0086(7)
C(21)	0.0201(7)	0.0200(7)	0.0211(7)	–0.0066(6)	–0.0061(6)	–0.0043(6)
C(22)	0.0247(7)	0.0178(6)	0.0232(7)	–0.0053(6)	–0.0067(6)	–0.0079(6)
C(23)	0.0261(7)	0.0271(7)	0.0301(8)	–0.0133(7)	–0.0083(7)	–0.0046(6)
C(24)	0.0344(8)	0.0388(9)	0.0314(9)	–0.0194(8)	–0.0038(7)	–0.0108(8)
C(25)	0.0436(9)	0.044(1)	0.0270(8)	–0.0152(8)	–0.0111(7)	–0.0172(8)
C(26)	0.0316(8)	0.0333(8)	0.0339(9)	–0.0100(7)	–0.0142(7)	–0.0113(7)
C(27)	0.0234(7)	0.0242(7)	0.0302(8)	–0.0097(7)	–0.0085(6)	–0.0071(6)

C.6 Additional structural information for [Nb(η-C$_5$H$_4$-CMe$_2$-η-C$_5$H$_4$)(CH$_2$Ph)$_2$] (6)

Nb–Cp$_{cent}$ / Å	2.07, 2.06
Bending angle, β /°	114.5
Cp$_{cent}$–Nb–Cp$_{cent}$, γ /°	123.1
Cp$_{cent}$–C$_{ipso}$–C$_{bridge}$ /°	163.0, 163.1

Appendix D

The crystal structure of

[Nb(η-C_5H_4-CMe_2-η-C_5H_4)($NSiMe_3$)Cl] (7)

D.1 Crystal data, data collection and processing parameters for [Nb(η-C$_5$H$_4$-CMe$_2$-η-C$_5$H$_4$)(NSiMe$_3$)Cl] (7)

Molecular formula	$C_{16}H_{23}ClNNbSi$
M	385.81
Crystal system	Monoclinic
Space group	$P\,2_1/n$
a / Å	6.904(1)
b / Å	25.236(1)
c / Å	9.820(1)
β / °	91.512(2)
Unit-cell volume / Å^3	1710.34
Z	4
ρ_{calc} / g cm^{-3}	1.50
F(000)	783.93
h, k, l ranges	–7 to 8, 0-31, 0-12
Temperature / K	150
μ / mm^{-1}	0.89
Crystal size / mm	0.3 × 0.3 × 0.5
θ_{max} / °	26.5
Radiation type	Mo-K_α
Wavelength / Å	0.71069
Scan type	ω
No. of reflections:	
total	9686
unique	3299
in refinement [$I > 5\sigma(I)$]	3094
R_{merge}	0.016
Number of variables	285
$\Delta\rho_{min,\,max}$ / e Å^{-3}	–0.77, 0.81
R	0.020
R_w	0.022

D.2 Interatomic distances (Å) for [Nb(η-C_5H_4-CMe_2-η-C_5H_4)(NSiMe_3)Cl] (7)

C(1)–C(2)	1.521(2)	Si(14)–C(15)	1.864(1)
C(1)–C(3)	1.531(2)	Si(14)–C(16)	1.868(2)
C(1)–C(4)	1.533(2)	Si(14)–C(17)	1.859(2)
C(4)–C(5)	1.395(2)	C(2)–H(21)	0.92(2)
C(4)–C(8)	1.439(2)	C(2)–H(22)	0.98(2)
C(5)–C(6)	1.428(2)	C(2)–H(23)	0.93(2)
C(6)–C(7)	1.393(2)	C(3)–H(31)	0.91(2)
C(7)–C(8)	1.423(2)	C(3)–H(32)	0.95(2)
C(9)–C(1)	1.530(2)	C(3)–H(33)	0.98(2)
C(9)–C(10)	1.401(2)	C(5)–H(51)	0.96(2)
C(10)–C(11)	1.432(2)	C(6)–H(61)	0.87(2)
C(11)–C(12)	1.388(2)	C(7)–H(71)	0.91(2)
C(13)–C(12)	1.417(2)	C(8)–H(81)	0.90(2)
C(13)–C(9)	1.435(2)	C(10)–H(101)	0.94(2)
N(1)–Si(14)	1.737(1)	C(11)–H(111)	0.92(2)
Nb(1)–C(4)	2.480(1)	C(12)–H(121)	0.94(2)
Nb(1)–C(5)	2.536(1)	C(13)–H(131)	0.98(2)
Nb(1)–C(6)	2.521(1)	C(15)–H(151)	0.96(2)
Nb(1)–C(7)	2.489(1)	C(15)–H(152)	0.95(2)
Nb(1)–C(8)	2.396(1)	C(15)–H(153)	1.01(3)
Nb(1)–C(9)	2.489(1)	C(16)–H(161)	0.95(3)
Nb(1)–C(10)	2.549(1)	C(16)–H(162)	0.92(4)
Nb(1)–C(11)	2.536(1)	C(16)–H(163)	0.98(4)
Nb(1)–C(12)	2.502(1)	C(17)–H(171)	0.98(3)
Nb(1)–C(13)	2.402(1)	C(17)–H(172)	0.93(3)
Nb(1)–Cl(1)	2.4387(4)	C(17)–H(173)	1.00(3)
Nb(1)–N(1)	1.777(1)		

D.3 Bond angles (°) for [Nb(η-C_5H_4-CMe_2-η-C_5H_4)(NSiMe_3)Cl] (7)

C(1)–C(4)–C(5)	125.4(1)	C(5)–C(4)–C(8)	107.3(1)
C(1)–C(4)–C(8)	123.6(1)	C(5)–C(6)–C(7)	108.4(1)
C(2)–C(1)–C(3)	109.9(1)	C(5)–Nb(1)–C(6)	32.81(4)
C(4)–C(1)–C(2)	112.1(1)	C(5)–Nb(1)–C(7)	54.20(4)
C(4)–C(1)–C(3)	111.6(1)	C(5)–Nb(1)–C(8)	55.06(5)
C(4)–C(5)–C(6)	108.5(1)	C(6)–C(7)–C(8)	107.8(1)
C(4)–C(8)–C(7)	107.7(1)	C(6)–Nb(1)–C(7)	32.28(5)
C(4)–Nb(1)–C(5)	32.27(5)	C(6)–Nb(1)–C(8)	55.08(5)
C(4)–Nb(1)–C(6)	54.52(4)	C(7)–Nb(1)–C(8)	33.81(5)
C(4)–Nb(1)–C(7)	55.45(4)	C(9)–C(1)–C(2)	112.0(1)
C(4)–Nb(1)–C(8)	34.27(4)	C(9)–C(1)–C(3)	111.9(1)

C(9)–C(1)–C(4)	98.89(9)	Cl(1)–Nb(1)–C(5)	87.99(3)
C(9)–C(10)–C(11)	108.1(1)	Cl(1)–Nb(1)–C(6)	80.05(4)
C(9)–C(13)–C(12)	108.0(1)	Cl(1)–Nb(1)–C(7)	105.71(4)
C(9)–Nb(1)–C(4)	55.84(4)	Cl(1)–Nb(1)–C(8)	135.13(3)
C(9)–Nb(1)–C(5)	75.57(4)	Cl(1)–Nb(1)–C(9)	119.60(3)
C(9)–Nb(1)–C(6)	107.17(4)	Cl(1)–Nb(1)–C(10)	88.08(3)
C(9)–Nb(1)–C(7)	109.51(4)	Cl(1)–Nb(1)–C(11)	80.53(4)
C(9)–Nb(1)–C(8)	78.47(4)	Cl(1)–Nb(1)–C(12)	106.09(4)
C(9)–Nb(1)–C(10)	32.26(4)	Cl(1)–Nb(1)–C(13)	135.16(3)
C(9)–Nb(1)–C(11)	54.30(4)	N(1)–Nb(1)–C(4)	130.59(5)
C(9)–Nb(1)–C(12)	55.08(4)	N(1)–Nb(1)–C(5)	139.62(4)
C(10)–C(11)–C(12)	108.5(1)	N(1)–Nb(1)–C(6)	108.89(5)
C(10)–C(9)–C(1)	125.6(1)	N(1)–Nb(1)–C(7)	85.95(5)
C(10)–Nb(1)–C(4)	75.67(4)	N(1)–Nb(1)–C(8)	96.49(5)
C(10)–Nb(1)–C(5)	79.24(4)	N(1)–Nb(1)–C(9)	131.21(5)
C(10)–Nb(1)–C(6)	110.64(4)	N(1)–Nb(1)–C(10)	140.47(4)
C(10)–Nb(1)–C(7)	129.94(4)	N(1)–Nb(1)–C(11)	109.74(5)
C(10)–Nb(1)–C(8)	106.28(4)	N(1)–Nb(1)–C(12)	87.13(4)
C(10)–Nb(1)–C(11)	32.72(4)	N(1)–Nb(1)–C(13)	97.37(5)
C(10)–Nb(1)–C(12)	53.88(4)	N(1)–Nb(1)–Cl(1)	98.21(4)
C(11)–Nb(1)–C(4)	107.07(4)	N(1)–Si(14)–C(15)	108.93(6)
C(11)–Nb(1)–C(5)	110.64(4)	N(1)–Si(14)–C(16)	106.70(7)
C(11)–Nb(1)–C(6)	138.69(5)	N(1)–Si(14)–C(17)	111.46(7)
C(11)–Nb(1)–C(7)	162.42(5)	Nb(1)–C(4)–C(1)	102.66(7)
C(11)–Nb(1)–C(8)	132.45(4)	Nb(1)–C(4)–C(5)	76.05(7)
C(11)–Nb(1)–C(12)	31.98(5)	Nb(1)–C(4)–C(8)	69.64(7)
C(12)–Nb(1)–C(4)	109.11(4)	Nb(1)–C(5)–C(4)	71.69(7)
C(12)–Nb(1)–C(5)	129.51(4)	Nb(1)–C(5)–C(6)	73.03(7)
C(12)–Nb(1)–C(6)	162.13(4)	Nb(1)–C(6)–C(5)	74.16(7)
C(12)–Nb(1)–C(7)	148.10(5)	Nb(1)–C(6)–C(7)	72.58(7)
C(12)–Nb(1)–C(8)	116.80(5)	Nb(1)–C(7)–C(6)	75.14(7)
C(13)–C(12)–C(11)	108.0(1)	Nb(1)–C(7)–C(8)	69.52(7)
C(13)–C(9)–C(1)	123.5(1)	Nb(1)–C(8)–C(4)	76.09(7)
C(13)–C(9)–C(10)	107.2(1)	Nb(1)–C(8)–C(7)	76.67(8)
C(13)–Nb(1)–C(10)	54.79(4)	Nb(1)–C(9)–C(1)	102.38(7)
C(13)–Nb(1)–C(11)	54.63(5)	Nb(1)–C(9)–C(10)	76.23(7)
C(13)–Nb(1)–C(12)	33.50(4)	Nb(1)–C(9)–C(13)	69.66(6)
C(13)–Nb(1)–C(4)	78.32(4)	Nb(1)–C(10)–C(11)	73.14(7)
C(13)–Nb(1)–C(5)	106.03(4)	Nb(1)–C(10)–C(9)	71.51(7)
C(13)–Nb(1)–C(6)	132.59(4)	Nb(1)–C(11)–C(10)	74.15(7)
C(13)–Nb(1)–C(7)	117.14(5)	Nb(1)–C(11)–C(12)	72.67(7)
C(13)–Nb(1)–C(8)	83.94(4)	Nb(1)–C(12)–C(11)	75.36(8)
C(13)–Nb(1)–C(9)	34.06(4)	Nb(1)–C(12)–C(13)	69.39(7)
C(15)–Si(14)–C(16)	111.00(8)	Nb(1)–C(13)–C(12)	77.11(8)
C(17)–Si(14)–C(15)	108.25(8)	Nb(1)–C(13)–C(9)	76.28(7)
C(17)–Si(14)–C(16)	110.52(8)	Nb(1)–N(1)–Si(14)	167.71(7)
Cl(1)–Nb(1)–C(4)	119.56(3)	C(1)–C(2)–H(21)	107.9(14)

C(1)–C(2)–H(22)	112.3(12)	H(151)–C(15)–H(153)	106.1(19)
C(1)–C(2)–H(23)	110.8(15)	H(152)–C(15)–H(151)	112.4(21)
C(1)–C(3)–H(31)	113.7(12)	H(152)–C(15)–H(153)	108.1(19)
C(1)–C(3)–H(32)	108.5(12)	H(161)–C(16)–H(162)	102.0(27)
C(1)–C(3)–H(33)	109.4(13)	H(161)–C(16)–H(163)	107.9(26)
C(4)–C(5)–H(51)	125.4(11)	H(162)–C(16)–H(163)	102.0(28)
C(4)–C(8)–H(81)	126.0(10)	H(172)–C(17)–H(171)	104.6(21)
C(5)–C(6)–H(61)	124.6(12)	H(172)–C(17)–H(173)	110.2(22)
C(6)–C(5)–H(51)	125.9(11)	H(173)–C(17)–H(171)	105.9(21)
C(6)–C(7)–H(71)	123.9(12)	Nb(1)–C(5)–H(51)	116.9(10)
C(7)–C(6)–H(61)	127.0(12)	Nb(1)–C(6)–H(61)	120.5(11)
C(7)–C(8)–H(81)	126.2(10)	Nb(1)–C(7)–H(71)	118.4(11)
C(8)–C(7)–H(71)	128.2(12)	Nb(1)–C(8)–H(81)	115.3(10)
C(9)–C(10)–H(101)	124.3(11)	Nb(1)–C(10)–H(101)	117.4(10)
C(9)–C(13)–H(131)	126.6(9)	Nb(1)–C(11)–H(111)	119.4(11)
C(10)–C(11)–H(111)	125.3(11)	Nb(1)–C(12)–H(121)	118.5(11)
C(11)–C(10)–H(101)	127.5(11)	Nb(1)–C(13)–H(131)	115.1(9)
C(11)–C(12)–H(121)	129.0(12)	Si(14)–C(15)–H(151)	109.8(13)
C(12)–C(11)–H(111)	126.2(11)	Si(14)–C(15)–H(152)	110.5(13)
C(12)–C(13)–H(131)	125.3(9)	Si(14)–C(15)–H(153)	109.8(14)
C(13)–C(12)–H(121)	122.9(12)	Si(14)–C(16)–H(161)	112.3(18)
H(22)–C(2)–H(21)	111.0(17)	Si(14)–C(16)–H(162)	116.4(22)
H(22)–C(2)–H(23)	106.3(17)	Si(14)–C(16)–H(163)	114.9(20)
H(23)–C(2)–H(21)	108.5(19)	Si(14)–C(17)–H(171)	115.3(16)
H(31)–C(3)–H(32)	109.9(17)	Si(14)–C(17)–H(172)	109.5(17)
H(31)–C(3)–H(33)	107.3(18)	Si(14)–C(17)–H(173)	111.2(15)
H(32)–C(3)–H(33)	108.0(18)		

D.4 Fractional atomic coordinates and isotropic thermal parameters for [Nb(η-C5H4-CMe2-η-C5H4)(NSiMe3)Cl] (7)

Atom	x/*a*	y/*b*	z/*c*	U(iso)	Occ	
Nb(1)	0.21612(2)	–0.123309(4)	0.259088(9)	0.0130	1.0000	U_{ani}
N(1)	0.3101(2)	–0.18869(4)	0.2738(1)	0.0182	1.0000	U_{ani}
Si(14)	0.40770(5)	–0.24918(1)	0.32492(3)	0.0179	1.0000	U_{ani}
Cl(1)	–0.12793(5)	–0.14528(1)	0.25713(3)	0.0255	1.0000	U_{ani}
C(1)	0.3909(2)	–0.00662(5)	0.2416(1)	0.0195	1.0000	U_{ani}
C(2)	0.6079(2)	0.00372(6)	0.2435(1)	0.0253	1.0000	U_{ani}
C(3)	0.2807(3)	0.04594(6)	0.2311(1)	0.0273	1.0000	U_{ani}
C(4)	0.3291(2)	–0.03916(4)	0.3648(1)	0.0174	1.0000	U_{ani}
C(5)	0.1395(2)	–0.04455(5)	0.4087(1)	0.0209	1.0000	U_{ani}
C(6)	0.1296(2)	–0.09072(5)	0.4924(1)	0.0226	1.0000	U_{ani}
C(7)	0.3139(2)	–0.11302(6)	0.5034(1)	0.0209	1.0000	U_{ani}
C(8)	0.4386(2)	–0.08315(5)	0.4195(1)	0.0188	1.0000	U_{ani}
C(9)	0.3289(2)	–0.04518(4)	0.1284(1)	0.0173	1.0000	U_{ani}

C(10)	0.1388(2)	–0.05306(5)	0.0792(1)	0.0200	1.0000	U_{ani}
C(11)	0.1305(2)	–0.10333(5)	0.0117(1)	0.0219	1.0000	U_{ani}
C(12)	0.3147(2)	–0.12542(5)	0.0158(1)	0.0203	1.0000	U_{ani}
C(13)	0.4380(2)	–0.09141(5)	0.0934(1)	0.0182	1.0000	U_{ani}
C(15)	0.5584(2)	–0.23908(6)	0.4831(1)	0.0279	1.0000	U_{ani}
C(16)	0.1989(3)	–0.29414(6)	0.3571(2)	0.0303	1.0000	U_{ani}
C(17)	0.5647(3)	–0.27762(7)	0.1924(2)	0.0316	1.0000	U_{ani}
H(21)	0.636(3)	0.0229(8)	0.167(2)	0.035(5)	1.0000	U_{iso}
H(22)	0.684(3)	–0.0291(8)	0.248(2)	0.030(5)	1.0000	U_{iso}
H(23)	0.645(4)	0.0233(9)	0.320(2)	0.047(6)	1.0000	U_{iso}
H(31)	0.149(3)	0.0422(7)	0.232(2)	0.028(5)	1.0000	U_{iso}
H(32)	0.317(3)	0.0633(8)	0.150(2)	0.035(5)	1.0000	U_{iso}
H(33)	0.318(3)	0.0685(9)	0.308(2)	0.041(5)	1.0000	U_{iso}
H(51)	0.032(3)	–0.0227(7)	0.380(2)	0.028(4)	1.0000	U_{iso}
H(61)	0.025(3)	–0.1019(7)	0.531(2)	0.026(4)	1.0000	U_{iso}
H(71)	0.342(3)	–0.1428(7)	0.553(2)	0.027(4)	1.0000	U_{iso}
H(81)	0.564(3)	–0.0898(6)	0.406(2)	0.017(4)	1.0000	U_{iso}
H(101)	0.036(3)	–0.0300(7)	0.095(2)	0.027(4)	1.0000	U_{iso}
H(111)	0.022(3)	–0.1181(7)	–0.028(2)	0.023(4)	1.0000	U_{iso}
H(121)	0.357(3)	–0.1576(8)	–0.021(2)	0.029(4)	1.0000	U_{iso}
H(131)	0.575(3)	–0.0980(6)	0.115(2)	0.022(4)	1.0000	U_{iso}
H(151)	0.619(4)	–0.2716(9)	0.509(2)	0.049(6)	1.0000	U_{iso}
H(152)	0.649(4)	–0.2114(9)	0.471(2)	0.046(6)	1.0000	U_{iso}
H(153)	0.473(4)	–0.2289(9)	0.561(2)	0.054(6)	1.0000	U_{iso}
H(161)	0.160(4)	–0.313(1)	0.278(3)	0.069(8)	1.0000	U_{iso}
H(162)	0.220(5)	–0.321(1)	0.420(3)	0.10(1)	1.0000	U_{iso}
H(163)	0.084(6)	–0.277(1)	0.393(3)	0.09(1)	1.0000	U_{iso}
H(171)	0.502(4)	–0.2827(9)	0.103(3)	0.055(6)	1.0000	U_{iso}
H(172)	0.605(4)	–0.312(1)	0.219(3)	0.062(7)	1.0000	U_{iso}
H(173)	0.679(4)	–0.255(1)	0.177(3)	0.060(7)	1.0000	U_{iso}

D.5 Anisotropic thermal parameters for [Nb(η-C$_5$H$_4$-CMe$_2$-η-C$_5$H$_4$)(NSiMe$_3$)Cl] (7)

Atom	U(11)	U(22)	U(33)	U(23)	U(13)	U(12)
Nb(1)	0.0132(1)	0.01170(8)	0.01439(8)	0.00049(3)	0.00040(4)	0.00125(3)
N(1)	0.0195(6)	0.0166(5)	0.0186(4)	0.0003(4)	–0.0007(4)	0.0001(4)
Si(14)	0.0206(2)	0.0144(2)	0.0205(2)	0.0022(1)	0.0012(1)	0.0036(1)
Cl(1)	0.0156(2)	0.0302(2)	0.0358(2)	0.0014(1)	0.0015(1)	–0.0022(1)
C(1)	0.0278(8)	0.0156(5)	0.0173(5)	0.0009(4)	0.0015(5)	–0.0019(5)
C(2)	0.0318(9)	0.0273(7)	0.0218(6)	–0.0014(5)	0.0017(5)	–0.0108(6)
C(3)	0.047(1)	0.0156(6)	0.0286(7)	0.0020(5)	0.0020(7)	0.0032(5)
C(4)	0.0248(7)	0.0147(5)	0.0151(5)	–0.0026(4)	0.0005(4)	–0.0013(5)
C(5)	0.0258(8)	0.0197(6)	0.0207(6)	–0.0055(4)	0.0037(5)	0.0032(5)
C(6)	0.0312(9)	0.0247(6)	0.0186(6)	–0.0041(5)	0.0095(5)	–0.0043(5)
C(7)	0.0335(9)	0.0194(5)	0.0141(6)	–0.0001(5)	–0.0005(5)	–0.0011(5)
C(8)	0.0203(8)	0.0202(6)	0.0167(5)	–0.0025(4)	–0.0020(4)	0.0010(5)
C(9)	0.0224(7)	0.0162(5)	0.0153(5)	0.0038(4)	0.0004(4)	–0.0011(4)
C(10)	0.0233(8)	0.0194(6)	0.0193(5)	0.0043(4)	–0.0017(5)	0.0033(5)
C(11)	0.0260(8)	0.0256(7)	0.0168(5)	0.0018(5)	–0.0048(5)	–0.0027(5)
C(12)	0.0292(8)	0.0193(6)	0.0154(6)	–0.0014(4)	0.0031(5)	–0.0010(5)
C(13)	0.0191(7)	0.0198(5)	0.0167(5)	0.0015(4)	0.0034(4)	0.0005(5)
C(15)	0.0313(9)	0.0278(7)	0.0291(7)	0.0053(5)	–0.0067(6)	0.0061(6)
C(16)	0.0341(9)	0.0248(6)	0.0364(8)	0.0059(6)	–0.0001(6)	–0.0070(6)
C(17)	0.037(1)	0.0318(8)	0.0346(8)	–0.0038(6)	0.0086(7)	0.0125(6)

D.6 Additional structural information for [Nb(η-C$_5$H$_4$-CMe$_2$-η-C$_5$H$_4$)(NSiMe$_3$)Cl] (7)

Nb–Cp$_{cent}$ / Å	2.17, 2.19
Bending angle, β /°	112.0
Cp$_{cent}$–Nb–Cp$_{cent}$, γ /°	114.2
Cp$_{cent}$–C$_{ipso}$–C$_{bridge}$ /°	163.9, 163.9

Appendix E

The crystal structure of

[Nb(η-C_5H_4-CMe_2-η-C_5H_4)(NBu^t)Cl] (8)

E.1 Crystal data, data collection and processing parameters for [Nb(η-C$_5$H$_4$-CMe$_2$-η-C$_5$H$_4$)(NBu^t)Cl] (8)

Molecular formula	$C_{17}H_{23}ClNNb$
M	369.73
Crystal system	Monoclinic
Space group	*P* $2_1/m$
a / Å	6.862(1)
b / Å	10.402(1)
c / Å	11.744(1)
β / °	98.73(1)
Unit-cell volume / Å^3	828.56
Z	2
ρ_{calc} / g cm^{-3}	1.48
F(000)	375.83
h, k, l ranges	–7 to 7, 0-11, 0-12
Temperature / K	150
μ / mm^{-1}	0.85
Crystal size / mm	0.07 × 0.11 × 0.28
θ_{max} / °	26
Radiation type	Mo-K_α
Wavelength / Å	0.71069
Scan type	ω
No. of reflections:	
total	3648
unique	1349
in refinement [$I > 3\sigma(I)$]	1104
R_{merge}	0.073
Number of variables	104
$\Delta\rho_{min, max}$ / e Å^{-3}	–0.41, 0.55
R	0.028
R_w	0.030

E.2 Interatomic distances (Å) for [Nb(η-C$_5$H$_4$-CMe$_2$-η-C$_5$H$_4$)(NBu^t)Cl] (8)

Atoms marked with a prime are generated from their counterparts by the symmetry operation (x, ½ – y, z).

C(1)–C(2)	1.529(6)	Nb(1)–Cl(1)	2.446(1)
C(1)–C(3)	1.524(6)	Nb(1)–N(1)	1.762(3)
C(1)–C(4)	1.528(4)	C(2)–H(21)	0.998(4)
C(4)–C(5)	1.405(4)	C(2)–H(22)	1.013(2)
C(5)–C(6)	1.424(4)	C(3)–H(31)	1.006(5)
C(6)–C(7)	1.395(4)	C(3)–H(32)	1.012(2)
C(7)–C(8)	1.421(4)	C(5)–H(51)	1.011(3)
C(8)–C(4)	1.435(4)	C(6)–H(61)	1.020(3)
C(14)–C(15)	1.528(4)	C(7)–H(71)	1.007(3)
C(14)–C(16)	1.531(6)	C(8)–H(81)	1.009(3)
N(1)–C(14)	1.438(5)	C(15)–H(151)	1.006(4)
Nb(1)–C(4)	2.505(3)	C(15)–H(152)	1.010(4)
Nb(1)–C(5)	2.557(3)	C(15)–H(153)	0.993(3)
Nb(1)–C(6)	2.522(3)	C(16)–H(161)	0.999(4)
Nb(1)–C(7)	2.488(3)	C(16)–H(162)	1.006(3)
Nb(1)–C(8)	2.401(3)		

E.3 Bond angles (°) for [Nb(η-C$_5$H$_4$-CMe$_2$-η-C$_5$H$_4$)(NBu^t)Cl] (8)

Atoms marked with a prime are generated from their counterparts by the symmetry operation (x, ½ – y, z).

C(1)–C(4)–C(5)	125.0(3)	Cl(1)–Nb(1)–C(6)	80.57(7)
C(1)–C(4)–C(8)	123.8(2)	Cl(1)–Nb(1)–C(7)	106.29(6)
C(2)–C(1)–C(4)	111.6(2)	Cl(1)–Nb(1)–C(8)	135.41(6)
C(3)–C(1)–C(2)	109.6(3)	Cl(1)–Nb(1)–N(1)	95.3(1)
C(3)–C(1)–C(4)	112.2(2)	N(1)–C(14)–C(15)	109.2(2)
C(4)–C(1)–C(4′)	99.3(3)	N(1)–C(14)–C(16)	107.0(3)
C(4)–C(5)–C(6)	108.0(2)	N(1)–Nb(1)–C(4)	133.25(9)
C(4)–C(8)–C(7)	108.2(2)	N(1)–Nb(1)–C(5)	140.42(6)
C(4)–Nb(1)–C(4′)	55.4(1)	N(1)–Nb(1)–C(6)	109.23(7)
C(4)–Nb(1)–C(5)	32.21(9)	N(1)–Nb(1)–C(7)	87.43(7)
C(4)–Nb(1)–C(5′)	75.24(9)	N(1)–Nb(1)–C(8)	99.40(9)
C(4)–Nb(1)–C(6′)	106.49(9)	Nb(1)–C(4)–C(1)	102.5(2)
C(4)–Nb(1)–C(6)	54.18(9)	Nb(1)–C(4)–C(5)	75.9(1)
C(4)–Nb(1)–C(7′)	108.75(9)	Nb(1)–C(4)–C(8)	69.1(1)
C(4)–Nb(1)–C(7)	55.18(9)	Nb(1)–C(5)–C(4)	71.9(1)
C(4)–Nb(1)–C(8)	33.92(9)	Nb(1)–C(5)–C(6)	72.4(2)
C(4)–Nb(1)–C(8′)	77.69(9)	Nb(1)–C(6)–C(5)	75.1(2)
C(5)–C(4)–C(8)	107.2(2)	Nb(1)–C(6)–C(7)	72.5(2)
C(5)–C(6)–C(7)	108.9(2)	Nb(1)–C(7)–C(6)	75.2(2)
C(5)–Nb(1)–C(5′)	79.0(1)	Nb(1)–C(7)–C(8)	69.8(1)
C(5)–Nb(1)–C(6′)	110.23(9)	Nb(1)–C(8)–C(4)	77.0(1)
C(5)–Nb(1)–C(6)	32.55(9)	Nb(1)–C(8)–C(7)	76.5(2)
C(5)–Nb(1)–C(7′)	129.33(9)	Nb(1)–N(1)–C(14)	178.4(3)
C(5)–Nb(1)–C(7)	54.08(9)	C(1)–C(2)–H(31)	109.9(3)
C(5)–Nb(1)–C(8′)	105.47(9)	C(1)–C(2)–H(32)	109.6(3)
C(5)–Nb(1)–C(8)	54.79(9)	C(1)–C(3)–H(21)	109.6(4)
C(6)–C(7)–C(8)	107.5(2)	C(1)–C(3)–H(22)	110.1(3)
C(6)–Nb(1)–C(6′)	138.3(1)	C(4)–C(5)–H(51)	125.7(3)
C(6)–Nb(1)–C(7′)	161.60(9)	C(4)–C(8)–H(81)	125.5(2)
C(6)–Nb(1)–C(7)	32.3(1)	C(5)–C(6)–H(61)	125.7(3)
C(6)–Nb(1)–C(8′)	131.58(9)	C(6)–C(5)–H(51)	126.3(3)
C(6)–Nb(1)–C(8)	54.84(9)	C(6)–C(7)–H(71)	126.4(3)
C(7)–Nb(1)–C(7′)	147.3(1)	C(7)–C(6)–H(61)	125.3(3)
C(7)–Nb(1)–C(8′)	116.16(9)	C(7)–C(8)–H(81)	126.3(3)
C(7)–Nb(1)–C(8)	33.72(9)	C(8)–C(7)–H(71)	126.1(3)
C(8)–Nb(1)–C(8′)	83.1(1)	C(14)–C(15)–H(151)	109.9(3)
C(15)–C(14)–C(15′)	110.8(4)	C(14)–C(15)–H(152)	109.8(3)
C(16)–C(14)–C(15)	110.2(2)	C(14)–C(15)–H(153)	110.7(3)
Cl(1)–Nb(1)–C(4)	119.63(6)	C(14)–C(16)–H(161)	110.5(4)
Cl(1)–Nb(1)–C(5)	88.16(7)	C(14)–C(16)–H(162)	110.1(3)

H(21)–C(3)–H(22)	104.3(3)	H(161)–C(16)–H(162)	108.8(3)
H(22)–C(3)–H(22´)	117.9(4)	H(162)–C(16)–H(162´)	108.5(4)
H(31)–C(2)–H(32)	104.8(3)	Nb(1)–C(5)–H(51)	121.3(2)
H(32)–C(2)–H(32´)	117.8(4)	Nb(1)–C(6)–H(61)	118.5(2)
H(151)–C(15)–H(152)	108.2(3)	Nb(1)–C(7)–H(71)	120.6(2)
H(151)–C(15)–H(153)	109.3(3)	Nb(1)–C(8)–H(81)	112.5(2)
H(152)–C(15)–H(153)	108.9(3)		

E.4 Fractional atomic coordinates and isotropic thermal parameters for [Nb(η-C$_5$H$_4$-CMe$_2$-η-C$_5$H$_4$)(NBu^t)Cl] (8)

Atom	x/*a*	y/*b*	z/*c*	U(iso)	Occ	
Nb(1)	0.65711(5)	0.2500	0.24439(3)	0.0147	1.0000	U_{ani}
N(1)	0.6975(4)	0.2500	0.0998(3)	0.0173	1.0000	U_{ani}
Cl(1)	0.2972(1)	0.2500	0.19937(9)	0.0277	1.0000	U_{ani}
C(1)	0.9039(6)	0.2500	0.4990(3)	0.0209	1.0000	U_{ani}
C(2)	1.1293(6)	0.2500	0.5207(4)	0.0272	1.0000	U_{ani}
C(3)	0.8258(7)	0.2500	0.6139(4)	0.0309	1.0000	U_{ani}
C(4)	0.8223(4)	0.1380(3)	0.4220(2)	0.0193	1.0000	U_{ani}
C(5)	0.6267(4)	0.0937(3)	0.4088(2)	0.0231	1.0000	U_{ani}
C(6)	0.5889(4)	0.0234(3)	0.3037(2)	0.0240	1.0000	U_{ani}
C(7)	0.7602(4)	0.0205(3)	0.2533(2)	0.0212	1.0000	U_{ani}
C(8)	0.9036(4)	0.0969(2)	0.3225(2)	0.0191	1.0000	U_{ani}
C(14)	0.7246(6)	0.2500	–0.0193(3)	0.0211	1.0000	U_{ani}
C(15)	0.8375(5)	0.1291(4)	–0.0441(3)	0.0364	1.0000	U_{ani}
C(16)	0.5190(7)	0.2500	–0.0913(4)	0.0326	1.0000	U_{ani}
H(21)	0.6775	0.2500	0.5997	0.0500	1.0000	U_{iso}
H(22)	0.8618	0.1667	0.6564	0.0500	1.0000	U_{iso}
H(31)	1.1809	0.2500	0.4457	0.0500	1.0000	U_{iso}
H(32)	1.1787	0.1667	0.5593	0.0500	1.0000	U_{iso}
H(51)	0.5302	0.1096	0.4643	0.0500	1.0000	U_{iso}
H(61)	0.4578	–0.0179	0.2703	0.0500	1.0000	U_{iso}
H(71)	0.7792	–0.0271	0.1811	0.0500	1.0000	U_{iso}
H(81)	1.0389	0.1196	0.3049	0.0500	1.0000	U_{iso}
H(151)	0.7617	0.0504	–0.0272	0.0500	1.0000	U_{iso}
H(152)	0.9699	0.1272	0.0070	0.0500	1.0000	U_{iso}
H(153)	0.8587	0.1273	–0.1259	0.0500	1.0000	U_{iso}
H(161)	0.5291	0.2500	–0.1752	0.0500	1.0000	U_{iso}
H(162)	0.4437	0.1715	–0.0732	0.0500	1.0000	U_{iso}

E.5 Anisotropic thermal parameters for [Nb(η-C$_5$H$_4$-CMe$_2$-η-C$_5$H$_4$)(NBu^t)Cl] (8)

Atom	U(11)	U(22)	U(33)	U(23)	U(13)	U(12)
Nb(1)	0.0149(2)	0.0141(2)	0.0158(2)	0.0000	0.0035(1)	0.0000
Cl(1)	0.0154(5)	0.0393(6)	0.0360(6)	0.0000	0.0054(4)	0.0000
N(1)	0.013(1)	0.018(2)	0.022(2)	0.0000	0.002(1)	0.0000
C(1)	0.027(2)	0.019(2)	0.017(2)	0.0000	0.003(2)	0.0000
C(2)	0.027(2)	0.026(2)	0.029(2)	0.0000	–0.006(2)	0.0000
C(3)	0.055(3)	0.029(2)	0.019(2)	0.0000	0.010(2)	0.0000
C(4)	0.024(1)	0.017(1)	0.020(1)	0.006(1)	0.002(1)	–0.000(1)
C(5)	0.030(2)	0.020(1)	0.025(1)	0.006(1)	0.008(1)	–0.003(1)
C(6)	0.028(2)	0.017(1)	0.030(2)	0.004(1)	0.001(1)	–0.005(1)
C(7)	0.031(2)	0.013(1)	0.023(1)	–0.001(1)	0.001(1)	0.002(1)
C(8)	0.024(1)	0.013(1)	0.023(1)	0.002(1)	0.004(1)	0.002(1)
C(14)	0.029(2)	0.021(2)	0.016(2)	0.0000	0.005(2)	0.0000
C(15)	0.062(2)	0.045(2)	0.026(2)	–0.002(2)	0.017(1)	0.022(2)
C(16)	0.036(3)	0.040(3)	0.024(2)	0.0000	–0.007(2)	0.0000

E.6 Additional structural information for [Nb(η-C$_5$H$_4$-CMe$_2$-η-C$_5$H$_4$)(NBu^t)Cl] (8)

Nb–Cp$_{cent}$ / Å	2.19
Bending angle, β /°	112.6
Cp$_{cent}$–Nb–Cp$_{cent}$, γ /°	113.3
Cp$_{cent}$–C$_{ipso}$–C$_{bridge}$ /°	163.3

Appendix F

The crystal structure of

[Nb(η-C_5H_4-CMe_2-η-C_5H_4)(NBu^t)Br] (9)

F.1 Crystal data, data collection and processing parameters for [Nb(η-C$_5$H$_4$-CMe$_2$-η-C$_5$H$_4$)(NBu^t)Br] (9)

Molecular formula	$C_{17}H_{23}BrNNb$
M	414.19
Crystal system	Monoclinic
Space group	$P2_1/m$
a / Å	7.117(1)
b / Å	10.239(1)
c / Å	11.746(1)
β / °	98.267(3)
Unit-cell volume / Å^3	847.05
Z	2
ρ_{calc} / g cm^{-3}	1.62
F(000)	410.85
h, k, l ranges	–8 to 8, 0-12, 0-14
Temperature / K	150
μ / mm^{-1}	3.01
Crystal size / mm	0.15 × 0.25 × 0.25
θ_{max} / °	26
Radiation type	Mo-K_α
Wavelength / Å	0.71069
Scan type	ω
No. of reflections:	
total	3623
unique	1751
in refinement [$I > 3\sigma(I)$]	1583
R_{merge}	0.028
Number of variables	153
$\Delta\rho_{min, max}$ / e Å^{-3}	–0.87, 0.46
R	0.027
R_w	0.032

F.2 Interatomic distances (Å) for [Nb(η-C$_5$H$_4$-CMe$_2$-η-C$_5$H$_4$)(NBu^t)Br] (9)

Atoms marked with a prime are generated from their counterparts by the symmetry operation (x, ½ – y, z).

Nb(1)–Br(1)	2.6022(4)	C(1)–C(3)	1.535(4)
Nb(1)–N(1)	1.765(2)	C(1)–C(4)	1.527(3)
Nb(1)–C(4)	2.497(2)	C(4)–C(5)	1.386(3)
Nb(1)–C(5)	2.551(2)	C(5)–C(6)	1.427(3)
Nb(1)–C(6)	2.523(2)	C(6)–C(7)	1.397(3)
Nb(1)–C(7)	2.484(2)	C(7)–C(8)	1.415(3)
Nb(1)–C(8)	2.395(2)	C(8)–C(4)	1.440(3)
N(1)–C(14)	1.448(3)	C(14)–C(15)	1.517(3)
C(1)–C(2)	1.530(5)	C(14)–C(16)	1.521(5)

F.3 Bond angles (°) for [Nb(η-C$_5$H$_4$-CMe$_2$-η-C$_5$H$_4$)(NBu^t)Br] (9)

Atoms marked with a prime are generated from their counterparts by the symmetry operation (x, ½ – y, z).

Br(1)–Nb(1)–C(4)	120.19(5)	C(7)–Nb(1)–C(7′)	147.8(1)
Br(1)–Nb(1)–C(5)	89.00(5)	C(7)–Nb(1)–C(8′)	116.60(7)
Br(1)–Nb(1)–C(6)	80.55(6)	C(7′)–Nb(1)–C(8′)	33.65(7)
Br(1)–Nb(1)–C(7)	106.04(5)	C(7)–Nb(1)–C(8)	33.65(7)
Br(1)–Nb(1)–C(8)	135.50(5)	C(8)–C(4)–C(5)	107.1(2)
Br(1)–Nb(1)–N(1)	93.77(8)	C(8)–C(7)–C(6)	107.8(2)
C(1)–C(4)–C(5)	125.7(2)	C(8)–Nb(1)–C(5′)	105.46(7)
C(1)–C(4)–C(8)	123.3(2)	C(8)–Nb(1)–C(5)	54.63(7)
C(2)–C(1)–C(3)	110.1(3)	C(8)–Nb(1)–C(6′)	131.99(7)
C(4)–C(1)–C(2)	112.1(2)	C(8)–Nb(1)–C(6)	54.95(7)
C(4)–C(1)–C(3)	111.5(2)	C(8)–Nb(1)–C(8′)	83.5(1)
C(4)–C(1)–C(4′)	99.1(2)	C(15)–C(14)–C(15′)	110.2(3)
C(4)–C(5)–C(6)	108.9(2)	C(15)–C(14)–C(16)	111.1(2)
C(4)–Nb(1)–C(4′)	55.46(9)	N(1)–C(14)–C(15)	108.9(2)
C(4)–Nb(1)–C(5)	31.86(7)	N(1)–C(14)–C(16)	106.6(3)
C(4)–Nb(1)–C(5′)	75.00(7)	N(1)–Nb(1)–C(4)	133.92(8)
C(4)–Nb(1)–C(6′)	106.50(7)	N(1)–Nb(1)–C(5)	140.55(5)
C(4)–Nb(1)–C(6)	54.23(7)	N(1)–Nb(1)–C(6)	109.25(5)
C(4)–Nb(1)–C(8)	34.15(7)	N(1)–Nb(1)–C(7)	87.73(5)
C(4)–Nb(1)–C(8′)	78.02(7)	N(1)–Nb(1)–C(8)	99.83(8)
C(5)–Nb(1)–C(5′)	78.8(1)	Nb(1)–C(4)–C(1)	102.6(1)
C(5)–Nb(1)–C(6)	32.65(7)	Nb(1)–C(4)–C(5)	76.2(1)
C(6)–Nb(1)–C(5′)	110.02(7)	Nb(1)–C(4)–C(8)	69.0(1)
C(6)–Nb(1)–C(6′)	137.9(1)	Nb(1)–C(5)–C(4)	71.9(1)
C(7)–C(6)–C(5)	108.1(2)	Nb(1)–C(5)–C(6)	72.6(1)
C(7)–C(8)–C(4)	107.9(2)	Nb(1)–C(6)–C(5)	74.7(1)
C(7)–Nb(1)–C(4′)	108.89(7)	Nb(1)–C(6)–C(7)	72.3(1)
C(7)–Nb(1)–C(4)	55.22(6)	Nb(1)–C(7)–C(6)	75.4(1)
C(7)–Nb(1)–C(5′)	129.13(7)	Nb(1)–C(7)–C(8)	69.7(1)
C(7)–Nb(1)–C(5)	53.96(7)	Nb(1)–C(8)–C(4)	76.8(1)
C(7)–Nb(1)–C(6′)	161.60(7)	Nb(1)–C(8)–C(7)	76.6(1)
C(7)–Nb(1)–C(6)	32.38(7)	Nb(1)–N(1)–C(14)	178.3(2)

F.4 Fractional atomic coordinates and isotropic thermal parameters for [Nb(η-C$_5$H$_4$-CMe$_2$-η-C$_5$H$_4$)(NBu^t)Br] (9)

Atom	x/*a*	y/*b*	z/*c*	U(iso)	Occ	
Nb(1)	0.16293(3)	0.2500	0.24445(2)	0.0155	1.0000	U_{ani}
Br(1)	–0.20516(4)	0.2500	0.19329(3)	0.0317	1.0000	U_{ani}
N(1)	0.2009(4)	0.2500	0.0992(2)	0.0188	1.0000	U_{ani}
C(1)	0.3984(5)	0.2500	0.4978(2)	0.0253	1.0000	U_{ani}
C(2)	0.6156(5)	0.2500	0.5184(3)	0.0329	1.0000	U_{ani}
C(3)	0.3209(7)	0.2500	0.6132(3)	0.0410	1.0000	U_{ani}
C(4)	0.3183(3)	0.1365(2)	0.4215(2)	0.0217	1.0000	U_{ani}
C(5)	0.1325(3)	0.0919(2)	0.4087(2)	0.0257	1.0000	U_{ani}
C(6)	0.0945(3)	0.0200(2)	0.3038(2)	0.0269	1.0000	U_{ani}
C(7)	0.2607(3)	0.0169(2)	0.2535(2)	0.0244	1.0000	U_{ani}
C(8)	0.3981(3)	0.0942(2)	0.3218(2)	0.0206	1.0000	U_{ani}
C(14)	0.2260(5)	0.2500	–0.0209(2)	0.0232	1.0000	U_{ani}
C(15)	0.3355(4)	0.1285(3)	–0.0454(2)	0.0427	1.0000	U_{ani}
C(16)	0.0281(6)	0.2500	–0.0900(3)	0.0369	1.0000	U_{ani}
H(21)	0.6641	0.2500	0.4428	0.0306	1.0000	U_{iso}
H(22)	0.6614	0.1703	0.5629	0.0306	1.0000	U_{iso}
H(31)	0.1791	0.2500	0.5988	0.0361	1.0000	U_{iso}
H(32)	0.3668	0.1703	0.6579	0.0361	1.0000	U_{iso}
H(51)	0.0406	0.1074	0.4639	0.0259	1.0000	U_{iso}
H(61)	–0.0297	–0.0207	0.2720	0.0248	1.0000	U_{iso}
H(71)	0.2791	–0.0313	0.1819	0.0229	1.0000	U_{iso}
H(81)	0.5278	0.1156	0.3039	0.0195	1.0000	U_{iso}
H(151)	0.3470	0.1249	–0.1292	0.0418	1.0000	U_{iso}
H(152)	0.2655	0.0492	–0.0242	0.0418	1.0000	U_{iso}
H(153)	0.4645	0.1305	0.0008	0.0418	1.0000	U_{iso}
H(161)	0.0382	0.2500	–0.1740	0.0353	1.0000	U_{iso}
H(162)	–0.0433	0.1716	–0.0689	0.0353	1.0000	U_{iso}

F.5 Anisotropic thermal parameters for [Nb(η-C_5H_4-CMe_2-η-C_5H_4)(NBu^t)Br] (9)

Atom	U(11)	U(22)	U(33)	U(23)	U(13)	U(12)
Nb(1)	0.0171(2)	0.0122(2)	0.0175(2)	0.0000	0.00362(9)	0.0000
Br(1)	0.0174(2)	0.0345(2)	0.0434(2)	0.0000	0.0056(1)	0.0000
N(1)	0.020(1)	0.018(1)	0.019(1)	0.0000	0.0028(9)	0.0000
C(1)	0.038(2)	0.019(1)	0.018(1)	0.0000	0.001(1)	0.0000
C(2)	0.040(2)	0.022(2)	0.032(2)	0.0000	–0.010(1)	0.0000
C(3)	0.070(3)	0.034(2)	0.020(1)	0.0000	0.008(2)	0.0000
C(4)	0.032(1)	0.013(1)	0.0201(9)	0.0029(7)	0.0045(7)	0.0006(8)
C(5)	0.032(1)	0.020(1)	0.027(1)	0.0039(8)	0.0101(8)	–0.0040(8)
C(6)	0.033(1)	0.014(1)	0.034(1)	0.0038(8)	0.0031(9)	–0.0074(8)
C(7)	0.033(1)	0.014(1)	0.025(1)	–0.0004(8)	0.0032(8)	0.0020(8)
C(8)	0.026(1)	0.0120(9)	0.0232(9)	0.0007(7)	0.0032(7)	0.0023(8)
C(14)	0.033(2)	0.019(1)	0.018(1)	0.0000	0.004(1)	0.0000
C(15)	0.059(2)	0.042(2)	0.030(1)	–0.003(1)	0.013(1)	0.019(1)
C(16)	0.039(2)	0.042(2)	0.026(2)	0.0000	–0.006(1)	0.0000

F.6 Additional structural information for [Nb(η-C_5H_4-CMe_2-η-C_5H_4)(NBu^t)Br] (9)

Nb–Cp_{cent} / Å	2.18
Bending angle, β /°	112.5
Cp_{cent}–Nb–Cp_{cent}, γ /°	113.4
Cp_{cent}–C_{ipso}–C_{bridge} /°	163.5

Appendix G

The crystal structure of

[Nb(η-C_5H_4-CMe_2-η-C_5H_4)(NBu^t)I] (10)

G.1 Crystal data, data collection and processing parameters for [Nb(η-C$_5$H$_4$-CMe$_2$-η-C$_5$H$_4$)(NBu^t)I] (10)

Molecular formula	$C_{17}H_{23}INNb$
M	461.19
Crystal system	Orthorhombic
Space group	*P c a b*
a / Å	13.062(1)
b / Å	15.744(1)
c / Å	16.813(1)
Unit-cell volume / Å^3	3457.56
Z	8
ρ_{calc} / g cm^{-3}	1.77
F(000)	1784.44
h, k, l ranges	0-26, 0-19, 0-45
Temperature / K	150
μ / mm^{-1}	2.43
Crystal size / mm	0.4 × 0.4 × 0.4
θ_{max} / °	26
Radiation type	Mo-K_α
Wavelength / Å	0.71069
Scan type	ω
No. of reflections:	
total	8066
unique	3479
in refinement [$I > 5\sigma(I)$]	2889
R_{merge}	0.029
Number of variables	182
$\Delta\rho_{min, max}$ / e Å^{-3}	–0.83, 1.01
R	0.025
R_w	0.036

G.2 Interatomic distances (Å) for [Nb(η-C$_5$H$_4$-CMe$_2$-η-C$_5$H$_4$)(NBu^t)I] (10)

Nb(1)–I(1)	2.8400(3)	C(1)–C(4)	1.524(3)
Nb(1)–N(1)	1.770(2)	C(1)–C(9)	1.524(3)
Nb(1)–C(4)	2.486(2)	C(4)–C(5)	1.397(3)
Nb(1)–C(5)	2.528(2)	C(4)–C(8)	1.439(3)
Nb(1)–C(6)	2.520(3)	C(5)–C(6)	1.424(4)
Nb(1)–C(7)	2.499(2)	C(6)–C(7)	1.390(4)
Nb(1)–C(8)	2.397(2)	C(7)–C(8)	1.419(4)
Nb(1)–C(9)	2.490(2)	C(9)–C(10)	1.392(3)
Nb(1)–C(10)	2.551(2)	C(9)–C(13)	1.445(3)
Nb(1)–C(11)	2.533(3)	C(10)–C(11)	1.443(4)
Nb(1)–C(12)	2.490(3)	C(11)–C(12)	1.392(4)
Nb(1)–C(13)	2.386(2)	C(12)–C(13)	1.413(4)
N(1)–C(14)	1.440(3)	C(14)–C(15)	1.537(4)
C(1)–C(2)	1.533(3)	C(14)–C(16)	1.538(4)
C(1)–C(3)	1.526(4)	C(14)–C(17)	1.524(4)

G.3 Bond angles (°) for [Nb(η-C_5H_4-CMe_2-η-C_5H_4)(NBu^t)I] (10)

C(1)–C(4)–C(5)	124.9(2)	C(8)–Nb(1)–C(9)	77.14(8)
C(1)–C(4)–C(8)	124.2(2)	C(8)–Nb(1)–C(10)	105.94(8)
C(1)–C(9)–C(10)	125.2(2)	C(8)–Nb(1)–C(11)	130.58(9)
C(1)–C(9)–C(13)	123.6(2)	C(8)–Nb(1)–C(12)	112.93(9)
C(2)–C(1)–C(3)	109.4(2)	C(8)–Nb(1)–C(13)	80.30(9)
C(2)–C(1)–C(4)	111.3(2)	C(9)–C(10)–C(11)	108.2(2)
C(2)–C(1)–C(9)	112.2(2)	C(9)–C(13)–C(12)	108.1(2)
C(3)–C(1)–C(4)	111.7(2)	C(9)–Nb(1)–C(10)	32.03(8)
C(3)–C(1)–C(9)	112.5(2)	C(9)–Nb(1)–C(11)	54.42(8)
C(4)–C(1)–C(9)	99.4(2)	C(9)–Nb(1)–C(12)	55.34(8)
C(4)–C(5)–C(6)	108.5(2)	C(9)–Nb(1)–C(13)	34.39(8)
C(4)–C(8)–C(7)	107.9(2)	C(10)–C(11)–C(12)	108.2(2)
C(4)–Nb(1)–C(5)	32.35(7)	C(10)–C(9)–C(13)	107.2(2)
C(4)–Nb(1)–C(6)	54.46(8)	C(10)–Nb(1)–C(11)	32.97(8)
C(4)–Nb(1)–C(7)	55.25(8)	C(10)–Nb(1)–C(12)	54.17(8)
C(4)–Nb(1)–C(8)	34.23(8)	C(10)–Nb(1)–C(13)	54.97(8)
C(4)–Nb(1)–C(9)	55.72(7)	C(11)–C(12)–C(13)	108.1(2)
C(4)–Nb(1)–C(10)	76.63(7)	C(11)–Nb(1)–C(12)	32.16(9)
C(4)–Nb(1)–C(11)	107.90(8)	C(11)–Nb(1)–C(13)	54.88(9)
C(4)–Nb(1)–C(12)	108.45(8)	C(12)–Nb(1)–C(13)	33.60(9)
C(4)–Nb(1)–C(13)	77.05(8)	C(15)–C(14)–C(16)	110.3(2)
C(5)–C(4)–C(8)	106.9(2)	C(15)–C(14)–C(17)	109.6(2)
C(5)–C(6)–C(7)	108.5(2)	C(16)–C(14)–C(17)	110.2(2)
C(5)–Nb(1)–C(6)	32.78(8)	I(1)–Nb(1)–C(4)	115.72(5)
C(5)–Nb(1)–C(7)	54.07(8)	I(1)–Nb(1)–C(5)	84.86(5)
C(5)–Nb(1)–C(8)	55.05(8)	I(1)–Nb(1)–C(6)	80.54(6)
C(5)–Nb(1)–C(9)	76.70(8)	I(1)–Nb(1)–C(7)	108.14(7)
C(5)–Nb(1)–C(10)	82.40(8)	I(1)–Nb(1)–C(8)	135.03(6)
C(5)–Nb(1)–C(11)	114.41(8)	I(1)–Nb(1)–C(9)	115.90(6)
C(5)–Nb(1)–C(12)	131.63(8)	I(1)–Nb(1)–C(10)	85.45(6)
C(5)–Nb(1)–C(13)	106.11(8)	I(1)–Nb(1)–C(11)	81.25(7)
C(6)–C(7)–C(8)	107.8(2)	I(1)–Nb(1)–C(12)	108.88(6)
C(6)–Nb(1)–C(7)	32.16(9)	I(1)–Nb(1)–C(13)	135.68(6)
C(6)–Nb(1)–C(8)	54.91(9)	I(1)–Nb(1)–N(1)	98.91(6)
C(6)–Nb(1)–C(9)	107.81(8)	N(1)–C(14)–C(15)	108.4(2)
C(6)–Nb(1)–C(10)	114.26(9)	N(1)–C(14)–C(16)	108.3(2)
C(6)–Nb(1)–C(11)	143.72(9)	N(1)–C(14)–C(17)	110.0(2)
C(6)–Nb(1)–C(12)	162.82(8)	N(1)–Nb(1)–C(4)	133.30(8)
C(6)–Nb(1)–C(13)	130.57(9)	N(1)–Nb(1)–C(5)	137.98(9)
C(7)–Nb(1)–C(8)	33.60(9)	N(1)–Nb(1)–C(6)	106.15(9)
C(7)–Nb(1)–C(9)	108.49(8)	N(1)–Nb(1)–C(7)	85.65(9)
C(7)–Nb(1)–C(10)	131.43(8)	N(1)–Nb(1)–C(8)	99.08(9)
C(7)–Nb(1)–C(11)	162.83(9)	N(1)–Nb(1)–C(9)	134.38(9)
C(7)–Nb(1)–C(12)	142.93(9)	N(1)–Nb(1)–C(10)	139.49(9)
C(7)–Nb(1)–C(13)	112.95(9)	N(1)–Nb(1)–C(11)	107.50(9)

N(1)–Nb(1)–C(12)	86.94(9)	Nb(1)–C(9)–C(1)	102.3(1)
N(1)–Nb(1)–C(13)	100.00(9)	Nb(1)–C(9)–C(10)	76.4(1)
Nb(1)–C(4)–C(1)	102.5(1)	Nb(1)–C(9)–C(13)	68.9(1)
Nb(1)–C(4)–C(5)	75.5(1)	Nb(1)–C(10)–C(11)	72.8(1)
Nb(1)–C(4)–C(8)	69.5(1)	Nb(1)–C(10)–C(9)	71.6(1)
Nb(1)–C(5)–C(4)	72.2(1)	Nb(1)–C(11)–C(10)	74.2(1)
Nb(1)–C(5)–C(6)	73.3(1)	Nb(1)–C(11)–C(12)	72.2(1)
Nb(1)–C(6)–C(5)	73.9(1)	Nb(1)–C(12)–C(11)	75.6(2)
Nb(1)–C(6)–C(7)	73.1(1)	Nb(1)–C(12)–C(13)	69.2(1)
Nb(1)–C(7)–C(6)	74.8(2)	Nb(1)–C(13)–C(9)	76.8(1)
Nb(1)–C(7)–C(8)	69.3(1)	Nb(1)–C(13)–C(12)	77.2(2)
Nb(1)–C(8)–C(4)	76.3(1)	Nb(1)–N(1)–C(14)	171.8(2)
Nb(1)–C(8)–C(7)	77.1(1)		

G.4 Fractional atomic coordinates and isotropic thermal parameters for [Nb(η-C$_5$H$_4$-CMe$_2$-η-C$_5$H$_4$)(NBu^t)I] (10)

Atom	x/*a*	y/*b*	z/*c*	U(iso)	Occ	
Nb(1)	0.41059(2)	0.35217(1)	0.28856(1)	0.0194	1.0000	U_{ani}
I(1)	0.40174(2)	0.17808(1)	0.33225(1)	0.0330	1.0000	U_{ani}
N(1)	0.4578(2)	0.3405(1)	0.1905(1)	0.0239	1.0000	U_{ani}
C(1)	0.3452(2)	0.4930(1)	0.4147(1)	0.0241	1.0000	U_{ani}
C(2)	0.3473(2)	0.5892(2)	0.4008(2)	0.0309	1.0000	U_{ani}
C(3)	0.3091(2)	0.4749(2)	0.4994(2)	0.0306	1.0000	U_{ani}
C(4)	0.4494(2)	0.4532(1)	0.3981(1)	0.0209	1.0000	U_{ani}
C(5)	0.4817(2)	0.3743(2)	0.4268(1)	0.0239	1.0000	U_{ani}
C(6)	0.5645(2)	0.3453(2)	0.3787(2)	0.0276	1.0000	U_{ani}
C(7)	0.5852(2)	0.4067(2)	0.3215(2)	0.0268	1.0000	U_{ani}
C(8)	0.5110(2)	0.4720(2)	0.3294(1)	0.0247	1.0000	U_{ani}
C(9)	0.2816(2)	0.4466(2)	0.3524(1)	0.0242	1.0000	U_{ani}
C(10)	0.2401(2)	0.3657(2)	0.3614(2)	0.0257	1.0000	U_{ani}
C(11)	0.2183(2)	0.3321(2)	0.2834(2)	0.0297	1.0000	U_{ani}
C(12)	0.2443(2)	0.3935(2)	0.2274(1)	0.0278	1.0000	U_{ani}
C(13)	0.2887(2)	0.4629(2)	0.2680(1)	0.0272	1.0000	U_{ani}
C(14)	0.5001(2)	0.3436(2)	0.1115(1)	0.0239	1.0000	U_{ani}
C(15)	0.5423(2)	0.4334(2)	0.0970(2)	0.0338	1.0000	U_{ani}
C(16)	0.5867(2)	0.2777(2)	0.1060(2)	0.0323	1.0000	U_{ani}
C(17)	0.4172(2)	0.3238(2)	0.0504(2)	0.0318	1.0000	U_{ani}
H(21)	0.3662	0.6008	0.3440	0.0324	1.0000	U_{iso}
H(22)	0.3991	0.6158	0.4367	0.0324	1.0000	U_{iso}
H(23)	0.2782	0.6135	0.4119	0.0324	1.0000	U_{iso}
H(31)	0.2408	0.5018	0.5081	0.0312	1.0000	U_{iso}
H(32)	0.3597	0.4983	0.5381	0.0312	1.0000	U_{iso}
H(33)	0.3033	0.4119	0.5070	0.0312	1.0000	U_{iso}
H(51)	0.4518	0.3436	0.4734	0.0236	1.0000	U_{iso}

H(61)	0.6015	0.2901	0.3852	0.0285	1.0000	U_{iso}
H(71)	0.6414	0.4049	0.2814	0.0267	1.0000	U_{iso}
H(81)	0.5030	0.5221	0.2933	0.0248	1.0000	U_{iso}
H(101)	0.2281	0.3358	0.4132	0.0257	1.0000	U_{iso}
H(111)	0.1891	0.2749	0.2716	0.0308	1.0000	U_{iso}
H(121)	0.2339	0.3894	0.1688	0.0280	1.0000	U_{iso}
H(131)	0.3194	0.5143	0.2429	0.0267	1.0000	U_{iso}
H(151)	0.5971	0.4462	0.1372	0.0354	1.0000	U_{iso}
H(152)	0.4862	0.4760	0.1023	0.0354	1.0000	U_{iso}
H(153)	0.5725	0.4369	0.0424	0.0354	1.0000	U_{iso}
H(161)	0.6179	0.2792	0.0520	0.0331	1.0000	U_{iso}
H(162)	0.6409	0.2916	0.1468	0.0331	1.0000	U_{iso}
H(163)	0.5587	0.2200	0.1172	0.0331	1.0000	U_{iso}
H(171)	0.3894	0.2657	0.0610	0.0322	1.0000	U_{iso}
H(172)	0.3606	0.3665	0.0556	0.0322	1.0000	U_{iso}
H(173)	0.4467	0.3264	–0.0040	0.0322	1.0000	U_{iso}

G.5 Anisotropic thermal parameters for [Nb(η-C$_5$H$_4$-CMe$_2$-η-C$_5$H$_4$)(NBu^t)I] (10)

Atom	U(11)	U(22)	U(33)	U(23)	U(13)	U(12)
Nb(1)	0.0235(1)	0.0193(1)	0.0164(1)	–0.00002(7)	–0.00019(7)	–0.00260(7)
I(1)	0.0591(2)	0.0197(1)	0.0322(1)	0.00074(6)	–0.00627(8)	–0.00531(6)
N(1)	0.030(1)	0.0206(9)	0.0222(9)	–0.0008(8)	0.0001(8)	–0.0016(8)
C(1)	0.026(1)	0.022(1)	0.025(1)	–0.0040(9)	–0.0020(9)	–0.0002(9)
C(2)	0.034(1)	0.022(1)	0.042(1)	–0.004(1)	–0.007(1)	0.004(1)
C(3)	0.031(1)	0.035(1)	0.029(1)	–0.007(1)	0.003(1)	–0.004(1)
C(4)	0.023(1)	0.020(1)	0.022(1)	–0.0027(8)	–0.0026(9)	–0.0056(9)
C(5)	0.026(1)	0.024(1)	0.022(1)	–0.0002(9)	–0.0035(9)	–0.0010(9)
C(6)	0.029(1)	0.029(1)	0.027(1)	–0.004(1)	–0.006(1)	0.006(1)
C(7)	0.023(1)	0.036(1)	0.026(1)	–0.007(1)	0.0017(9)	–0.0034(9)
C(8)	0.027(1)	0.024(1)	0.025(1)	0.0007(9)	–0.0009(9)	–0.0062(9)
C(9)	0.019(1)	0.028(1)	0.027(1)	–0.0026(9)	–0.0003(9)	–0.0000(9)
C(10)	0.024(1)	0.031(1)	0.025(1)	–0.004(1)	0.0020(9)	–0.0080(9)
C(11)	0.028(1)	0.036(1)	0.030(1)	–0.006(1)	–0.002(1)	–0.010(1)
C(12)	0.026(1)	0.037(1)	0.024(1)	–0.003(1)	–0.0047(9)	–0.001(1)
C(13)	0.024(1)	0.027(1)	0.032(1)	0.003(1)	–0.0028(9)	0.0026(9)
C(14)	0.029(1)	0.025(1)	0.019(1)	–0.0004(9)	0.0009(9)	0.0006(9)
C(15)	0.045(1)	0.028(1)	0.035(1)	0.005(1)	0.009(1)	–0.004(1)
C(16)	0.032(1)	0.035(1)	0.030(1)	–0.002(1)	–0.0000(9)	0.004(1)
C(17)	0.035(1)	0.040(2)	0.023(1)	0.000(1)	–0.003(1)	0.004(1)

G.6 Additional structural information for [Nb(η-C$_5$H$_4$-CMe$_2$-η-C$_5$H$_4$)(NBu^t)I] (10)

Nb–Cp$_{cent}$ / Å	2.18, 2.18
Bending angle, β /°	111.4
Cp$_{cent}$–Nb–Cp$_{cent}$, γ /°	114.2
Cp$_{cent}$–C$_{ipso}$–C$_{bridge}$ /°	163.6, 163.4

Appendix H

The crystal structure of

[Nb(η-C_5H_4-CMe_2-η-C_5H_4)(O)Cl] (13)

H.1 Crystal data, data collection and processing parameters for [Nb(η-C$_5$H$_4$-CMe$_2$-η-C$_5$H$_4$)(O)Cl] (13)

Molecular formula	$C_{13}H_{14}ClNbO$
M	314.61
Crystal system	Monoclinic
Space group	*P* $2_1/n$
a / Å	8.028(1)
b / Å	14.565(1)
c / Å	10.436(1)
β / °	98.90(1)
Unit-cell volume / Å^3	1205.57
Z	4
ρ_{calc} / g cm^{-3}	1.73
F(000)	623.68
h, k, l ranges	0-9, 0-18, –12 to 12
Temperature / K	150
μ / mm^{-1}	1.15
Crystal size / mm	0.5 × 0.5 × 0.5
θ_{max} / °	27
Radiation type	Mo-K_α
Wavelength / Å	0.71609 Å
Scan type	ω
No. of reflections:	
total	1374
unique	1319
in refinement [$I > 2\sigma(I)$]	1022
R_{merge}	0.079
Number of variables	145
$\Delta\rho_{min,\ max}$ / e Å^{-3}	–0.76, 0.96
R	0.071
R_w	0.075

H.2 Interatomic distances (Å) for [Nb(η-C$_5$H$_4$-CMe$_2$-η-C$_5$H$_4$)(O)Cl] (13)

Nb(1)–Cl(1)	2.435(4)	C(2)–C(1)	1.56(2)
Nb(1)–O1)	1.751(9)	C(3)–C(1)	1.49(2)
Nb(1)–C(4)	2.48(1)	C(4)–C(1)	1.54(2)
Nb(1)–C(5)	2.50(2)	C(4)–C(8)	1.45(2)
Nb(1)–C(6)	2.52(1)	C(5)–C(4)	1.42(2)
Nb(1)–C(7)	2.52(1)	C(5)–C(6)	1.48(2)
Nb(1)–C(8)	2.42(1)	C(7)–C(6)	1.39(2)
Nb(1)–C(9)	2.49(1)	C(7)–C(8)	1.45(2)
Nb(1)–C(10)	2.50(1)	C(10)–C(11)	1.40(2)
Nb(1)–C(11)	2.51(1)	C(10)–C(9)	1.41(2)
Nb(1)–C(12)	2.51(1)	C(11)–C(12)	1.42(2)
Nb(1)–C(13)	2.42(1)	C(13)–C(12)	1.41(2)
C(1)–C(9)	1.55(2)	C(13)–C(9)	1.45(2)

H.3 Bond angles (°) for [Nb(η-C$_5$H$_4$-CMe$_2$-η-C$_5$H$_4$)(O)Cl] (13)

C(2)–C(1)–C(3)	111.3(12)	C(6)–Nb(1)–C(12)	164.9(5)
C(2)–C(1)–C(9)	109.4(12)	C(7)–C(6)–C(5)	106.9(11)
C(3)–C(1)–C(9)	112.9(12)	C(7)–C(8)–C(4)	108.1(11)
C(4)–C(1)–C(2)	110.4(11)	C(7)–Nb(1)–C(4)	55.9(4)
C(4)–C(1)–C(3)	113.6(11)	C(7)–Nb(1)–C(5)	54.6(5)
C(4)–C(1)–C(9)	98.5(10)	C(7)–Nb(1)–C(6)	32.0(5)
C(4)–C(5)–C(6)	109.2(12)	C(7)–Nb(1)–C(8)	34.1(4)
C(4)–Nb(1)–C(6)	56.3(4)	C(7)–Nb(1)–C(9)	109.3(4)
C(4)–Nb(1)–C(8)	34.3(4)	C(7)–Nb(1)–C(10)	133.5(5)
C(4)–Nb(1)–C(9)	56.1(4)	C(7)–Nb(1)–C(11)	163.6(5)
C(4)–Nb(1)–C(10)	78.0(5)	C(7)–Nb(1)–C(12)	141.2(5)
C(4)–Nb(1)–C(11)	108.4(5)	C(7)–Nb(1)–C(13)	112.8(5)
C(4)–Nb(1)–C(12)	108.7(4)	C(8)–C(4)–C(1)	125.0(12)
C(4)–Nb(1)–C(13)	77.1(5)	C(8)–Nb(1)–C(9)	77.2(4)
C(5)–C(4)–C(1)	124.5(12)	C(8)–Nb(1)–C(12)	111.6(5)
C(5)–C(4)–C(8)	106.6(11)	C(9)–C(13)–C(12)	109.6(13)
C(5)–Nb(1)–C(4)	33.0(5)	C(9)–Nb(1)–C(12)	55.8(5)
C(5)–Nb(1)–C(6)	34.2(4)	C(10)–C(9)–C(1)	125.0(12)
C(5)–Nb(1)–C(8)	55.6(5)	C(10)–C(9)–C(13)	106.0(12)
C(5)–Nb(1)–C(9)	77.9(4)	C(10)–C(11)–C(12)	110.1(14)
C(5)–Nb(1)–C(10)	84.3(5)	C(10)–Nb(1)–C(6)	117.4(5)
C(5)–Nb(1)–C(11)	115.9(5)	C(10)–Nb(1)–C(8)	107.0(5)
C(5)–Nb(1)–C(12)	133.5(4)	C(10)–Nb(1)–C(9)	32.7(5)
C(5)–Nb(1)–C(13)	107.1(5)	C(10)–Nb(1)–C(11)	32.4(5)
C(6)–C(7)–C(8)	109.0(11)	C(10)–Nb(1)–C(12)	55.0(5)
C(6)–Nb(1)–C(8)	55.8(5)	C(10)–Nb(1)–C(13)	55.2(5)
C(6)–Nb(1)–C(9)	110.3(4)	C(11)–C(10)–C(9)	108.6(13)

C(11)–C(12)–C(13)	105.5(14)	Nb(1)–C(6)–C(7)	74.0(8)
C(11)–Nb(1)–C(12)	32.9(5)	Nb(1)–C(7)–C(6)	74.0(9)
C(11)–Nb(1)–C(13)	54.4(5)	Nb(1)–C(7)–C(8)	69.0(8)
C(11)–Nb(1)–C(6)	146.5(5)	Nb(1)–C(8)–C(4)	75.2(8)
C(11)–Nb(1)–C(8)	130.2(5)	Nb(1)–C(8)–C(7)	76.9(8)
C(11)–Nb(1)–C(9)	54.2(5)	Nb(1)–C(9)–C(1)	102.4(8)
C(13)–C(9)–C(1)	124.7(12)	Nb(1)–C(9)–C(10)	74.0(7)
C(13)–Nb(1)–C(12)	33.2(5)	Nb(1)–C(9)–C(13)	70.1(7)
C(13)–Nb(1)–C(6)	132.0(5)	Nb(1)–C(10)–C(9)	73.2(7)
C(13)–Nb(1)–C(8)	79.9(5)	Nb(1)–C(10)–C(11)	74.1(7)
C(13)–Nb(1)–C(9)	34.3(4)	Nb(1)–C(11)–C(10)	73.5(8)
Cl(1)–Nb(1)–C(4)	115.8(3)	Nb(1)–C(11)–C(12)	73.5(8)
Cl(1)–Nb(1)–C(5)	84.5(4)	Nb(1)–C(12)–C(11)	73.6(8)
Cl(1)–Nb(1)–C(6)	80.7(3)	Nb(1)–C(12)–C(13)	69.9(8)
Cl(1)–Nb(1)–C(7)	108.9(4)	Nb(1)–C(13)–C(9)	75.6(7)
Cl(1)–Nb(1)–C(8)	135.8(3)	Nb(1)–C(13)–C(12)	76.9(8)
Cl(1)–Nb(1)–C(9)	115.5(3)	O(1)–Nb(1)–C(4)	133.0(5)
Cl(1)–Nb(1)–C(10)	84.5(4)	O(1)–Nb(1)–C(5)	138.1(4)
Cl(1)–Nb(1)–C(11)	81.5(4)	O(1)–Nb(1)–C(6)	105.0(4)
Cl(1)–Nb(1)–C(12)	109.8(3)	O(1)–Nb(1)–C(7)	85.2(4)
Cl(1)–Nb(1)–C(13)	135.4(4)	O(1)–Nb(1)–C(8)	98.7(5)
Nb(1)–C(4)–C(1)	102.9(9)	O(1)–Nb(1)–C(9)	132.8(4)
Nb(1)–C(4)–C(5)	74.3(8)	O(1)–Nb(1)–C(10)	137.5(5)
Nb(1)–C(4)–C(8)	70.5(8)	O(1)–Nb(1)–C(11)	105.9(5)
Nb(1)–C(5)–C(4)	72.6(8)	O(1)–Nb(1)–C(12)	84.4(5)
Nb(1)–C(5)–C(6)	73.6(8)	O(1)–Nb(1)–C(13)	98.5(5)
Nb(1)–C(6)–C(5)	72.2(8)	O(1)–Nb(1)–Cl(1)	100.1(4)

H.4 Fractional atomic coordinates and isotropic thermal parameters for [Nb(η-C$_5$H$_4$-CMe$_2$-η-C$_5$H$_4$)(O)Cl] (13)

Atom	x/*a*	y/*b*	z/*c*	U(iso)	Occ	
Nb(1)	0.2293(1)	0.49605(9)	0.8200(1)	0.0131	1.0000	U_{ani}
Cl(1)	–0.0515(4)	0.4436(3)	0.7270(3)	0.0272	1.0000	U_{ani}
O(1)	0.262(1)	0.4307(7)	0.9625(9)	0.0221	1.0000	U_{ani}
C(1)	0.410(2)	0.646(1)	0.664(1)	0.017(3)	1.0000	U_{iso}
C(2)	0.591(2)	0.684(1)	0.711(2)	0.0321	1.0000	U_{ani}
C(3)	0.335(2)	0.686(1)	0.536(1)	0.026(3)	1.0000	U_{iso}
C(4)	0.298(2)	0.6570(9)	0.770(1)	0.0155	1.0000	U_{ani}
C(5)	0.120(2)	0.652(1)	0.749(1)	0.0250	1.0000	U_{ani}
C(6)	0.060(2)	0.633(1)	0.873(1)	0.022(3)	1.0000	U_{iso}
C(7)	0.202(2)	0.630(1)	0.968(1)	0.0224	1.0000	U_{ani}
C(8)	0.352(2)	0.639(1)	0.907(1)	0.017(3)	1.0000	U_{iso}
C(9)	0.417(2)	0.540(1)	0.660(1)	0.015(3)	1.0000	U_{iso}
C(10)	0.291(2)	0.483(1)	0.593(1)	0.0259	1.0000	U_{ani}

C(11)	0.310(2)	0.394(1)	0.645(1)	0.0265	1.0000	U_{ani}
C(12)	0.447(2)	0.392(1)	0.749(1)	0.021(3)	1.0000	U_{iso}
C(13)	0.509(2)	0.483(1)	0.762(1)	0.0244	1.0000	U_{ani}
H(21)	0.6442	0.6499	0.7900	0.0275	1.0000	U_{iso}
H(22)	0.5840	0.7513	0.7344	0.0275	1.0000	U_{iso}
H(23)	0.6608	0.6777	0.6409	0.0275	1.0000	U_{iso}
H(31)	0.2254	0.6564	0.5037	0.0238	1.0000	U_{iso}
H(32)	0.3137	0.7549	0.5475	0.0238	1.0000	U_{iso}
H(33)	0.4142	0.6794	0.4725	0.0238	1.0000	U_{iso}
H(51)	0.0465	0.6561	0.6599	0.0264	1.0000	U_{iso}
H(61)	–0.0610	0.6248	0.8861	0.0200	1.0000	U_{iso}
H(71)	0.2003	0.6234	1.0645	0.0206	1.0000	U_{iso}
H(81)	0.4743	0.6349	0.9503	0.0193	1.0000	U_{iso}
H(101)	0.2034	0.5042	0.5190	0.0255	1.0000	U_{iso}
H(111)	0.2360	0.3380	0.6129	0.0275	1.0000	U_{iso}
H(121)	0.4932	0.3383	0.8035	0.0189	1.0000	U_{iso}
H(131)	0.6043	0.5056	0.8303	0.0210	1.0000	U_{iso}

H.5 Anisotropic thermal parameters for [Nb(η-C$_5$H$_4$-CMe$_2$-η-C$_5$H$_4$)(O)Cl] (13)

Atom	U(11)	U(22)	U(33)	U(23)	U(13)	U(12)
Nb(1)	0.0169(6)	0.0115(6)	0.0117(5)	0.0013(6)	0.0052(4)	0.0005(6)
Cl(1)	0.023(2)	0.036(2)	0.023(2)	0.004(2)	0.003(1)	–0.010(2)
O(1)	0.034(5)	0.012(5)	0.022(5)	0.007(5)	0.009(4)	0.004(4)
C(2)	0.039(9)	0.028(8)	0.035(8)	–0.002(8)	0.023(7)	–0.021(7)
C(4)	0.023(7)	0.003(6)	0.023(7)	–0.004(5)	0.010(5)	–0.002(5)
C(5)	0.019(7)	0.030(9)	0.028(7)	0.004(7)	0.010(6)	0.019(7)
C(7)	0.042(8)	0.015(7)	0.013(6)	0.004(6)	0.013(6)	0.007(6)
C(10)	0.041(8)	0.020(8)	0.019(6)	0.004(7)	0.011(6)	0.004(7)
C(11)	0.037(9)	0.020(8)	0.026(7)	–0.008(7)	0.018(6)	0.004(7)
C(13)	0.029(7)	0.026(8)	0.020(6)	0.000(6)	0.010(5)	0.018(6)

H.6 Additional structural information for [Nb(η-C$_5$H$_4$-CMe$_2$-η-C$_5$H$_4$)(O)Cl] (13)

Nb–Cp$_{cent}$ / Å	2.17, 2.18
Bending angle, β /°	112.3
Cp$_{cent}$–Nb–Cp$_{cent}$, γ /°	115.3
Cp$_{cent}$–C$_{ipso}$–C$_{bridge}$ /°	164.1, 163.1

Appendix I

The crystal structure of

[Nb(η-C_5H_4-CMe_2-η-C_5H_4){$P(OMe)_3$}Cl] (14)

I.1 Crystal data, data collection and processing parameters for [Nb(η-C$_5$H$_4$-CMe$_2$-η-C$_5$H$_4$){P(OMe)$_3$}Cl] (14)

Molecular formula	$C_{16}H_{23}NbClO_3P$
M	422.69
Crystal system	Triclinic
Space group	*P*–1
a / Å	7.4350(2)
b / Å	10.3300(5)
c / Å	12.2990(7)
α / °	108.050(2)
β / °	99.797(3)
γ / °	103.024(3)
Unit-cell volume / Å^3	845.14
Z	2
ρ_{calc} / g cm^{-3}	1.66
F(000)	428.05
h, k, l ranges	–9 to 8, –13 to 12, 0-15
Temperature / K	100
μ / mm^{-1}	0.94
Crystal size / mm	0.15 × 0.30 × 0.30
θ_{max} / °	26.7
Radiation type	Mo-K_α
Wavelength / Å	0.71609
Scan type	ω
No. of reflections:	
total	3190
unique	3190
in refinement [$I > 2\sigma(I)$]	3105
R_{merge}	0.015
Number of variables	200
$\Delta\rho_{min, max}$ / e Å^{-3}	–0.64, 0.55
R	0.026
R_w	0.031

I.2 Interatomic distances (Å) for [Nb(η-C_5H_4-CMe_2-η-C_5H_4){P(OMe)$_3$}Cl] (14)

Nb(1)–Cl(1)	2.5301(4)	P(1)–O(2)	1.616(1)
Nb(1)–P(1)	2.5304(4)	P(1)–O(3)	1.611(1)
Nb(1)–C(4)	2.277(2)	C(1)–C(3)	1.530(2)
Nb(1)–C(5)	2.370(2)	C(1)–C(4)	1.531(3)
Nb(1)–C(6)	2.459(2)	C(1)–C(9)	1.527(2)
Nb(1)–C(7)	2.388(2)	C(2)–C(1)	1.528(3)
Nb(1)–C(8)	2.283(2)	C(4)–C(5)	1.447(3)
Nb(1)–C(9)	2.278(2)	C(4)–C(8)	1.441(2)
Nb(1)–C(10)	2.378(2)	C(5)–C(6)	1.409(3)
Nb(1)–C(11)	2.465(2)	C(6)–C(7)	1.412(3)
Nb(1)–C(12)	2.385(2)	C(7)–C(8)	1.434(3)
Nb(1)–C(13)	2.285(2)	C(9)–C(10)	1.450(2)
O(1)–C(14)	1.435(2)	C(9)–C(13)	1.441(2)
O(2)–C(15)	1.443(3)	C(10)–C(11)	1.407(3)
O(3)–C(16)	1.442(2)	C(11)–C(12)	1.404(3)
P(1)–O(1)	1.597(1)	C(12)–C(13)	1.444(3)

I.3 Bond angles (°) for [Nb(η-C_5H_4-CMe_2-η-C_5H_4){P(OMe)$_3$}Cl] (14)

C(1)–C(4)–C(5)	124.3(2)	C(7)–Nb(1)–C(8)	35.67(7)
C(1)–C(4)–C(8)	124.1(2)	C(9)–C(1)–C(3)	112.6(1)
C(1)–C(9)–C(10)	123.5(2)	C(9)–C(1)–C(4)	96.8(1)
C(1)–C(9)–C(13)	125.1(2)	C(9)–C(10)–C(11)	107.6(2)
C(2)–C(1)–C(3)	109.6(1)	C(9)–C(13)–C(12)	106.5(2)
C(2)–C(1)–C(4)	112.0(1)	C(9)–Nb(1)–C(4)	60.26(6)
C(2)–C(1)–C(9)	112.5(1)	C(9)–Nb(1)–C(5)	81.32(6)
C(4)–C(1)–C(3)	112.9(2)	C(9)–Nb(1)–C(6)	114.10(6)
C(4)–C(5)–C(6)	107.7(2)	C(9)–Nb(1)–C(7)	117.73(6)
C(4)–C(8)–C(7)	106.6(2)	C(9)–Nb(1)–C(8)	84.86(6)
C(4)–Nb(1)–C(5)	36.22(6)	C(9)–Nb(1)–C(10)	36.21(6)
C(4)–Nb(1)–C(6)	58.13(6)	C(9)–Nb(1)–C(11)	58.02(6)
C(4)–Nb(1)–C(7)	59.16(6)	C(9)–Nb(1)–C(12)	59.36(6)
C(4)–Nb(1)–C(8)	36.84(6)	C(9)–Nb(1)–C(13)	36.80(6)
C(5)–C(4)–C(8)	107.8(2)	C(10)–C(9)–C(13)	107.8(1)
C(5)–C(6)–C(7)	108.8(2)	C(10)–C(11)–C(12)	109.3(2)
C(5)–Nb(1)–C(6)	33.86(6)	C(10)–Nb(1)–C(4)	80.93(6)
C(5)–Nb(1)–C(7)	57.64(6)	C(10)–Nb(1)–C(5)	81.08(6)
C(5)–Nb(1)–C(8)	60.17(6)	C(10)–Nb(1)–C(6)	112.35(6)
C(6)–C(7)–C(8)	109.0(2)	C(10)–Nb(1)–C(7)	137.02(6)
C(6)–Nb(1)–C(7)	33.83(6)	C(10)–Nb(1)–C(8)	115.01(6)
C(6)–Nb(1)–C(8)	58.37(7)	C(10)–Nb(1)–C(11)	33.73(6)

C(10)–Nb(1)–C(12)	57.56(6)	Nb(1)–C(10)–C(11)	76.5(1)
C(10)–Nb(1)–C(13)	60.06(7)	Nb(1)–C(11)–C(10)	69.7(1)
C(11)–C(12)–C(13)	108.8(2)	Nb(1)–C(11)–C(12)	70.1(1)
C(11)–Nb(1)–C(4)	113.68(6)	Nb(1)–C(12)–C(11)	76.3(1)
C(11)–Nb(1)–C(5)	112.09(6)	Nb(1)–C(12)–C(13)	68.3(1)
C(11)–Nb(1)–C(6)	136.93(7)	Nb(1)–C(13)–C(9)	71.3(1)
C(11)–Nb(1)–C(7)	169.68(7)	Nb(1)–C(13)–C(12)	75.8(1)
C(11)–Nb(1)–C(8)	142.73(7)	Nb(1)–P(1)–O(1)	112.47(5)
C(11)–Nb(1)–C(12)	33.61(7)	Nb(1)–P(1)–O(2)	124.67(5)
C(11)–Nb(1)–C(13)	58.20(7)	Nb(1)–P(1)–O(3)	111.62(5)
C(12)–Nb(1)–C(4)	118.18(7)	O(1)–P(1)–O(2)	98.64(7)
C(12)–Nb(1)–C(5)	137.23(6)	O(3)–P(1)–O(1)	104.74(8)
C(12)–Nb(1)–C(6)	169.78(6)	O(3)–P(1)–O(2)	102.38(7)
C(12)–Nb(1)–C(7)	154.86(7)	P(1)–Nb(1)–C(4)	119.95(4)
C(12)–Nb(1)–C(8)	125.50(7)	P(1)–Nb(1)–C(5)	138.05(4)
C(12)–Nb(1)–C(13)	35.93(6)	P(1)–Nb(1)–C(6)	109.49(4)
C(13)–Nb(1)–C(4)	85.27(6)	P(1)–Nb(1)–C(7)	80.56(4)
C(13)–Nb(1)–C(5)	115.53(6)	P(1)–Nb(1)–C(8)	84.42(4)
C(13)–Nb(1)–C(6)	143.21(6)	P(1)–Nb(1)–C(9)	119.66(5)
C(13)–Nb(1)–C(7)	125.14(7)	P(1)–Nb(1)–C(10)	138.04(5)
C(13)–Nb(1)–C(8)	90.74(7)	P(1)–Nb(1)–C(11)	109.75(5)
Cl(1)–Nb(1)–C(4)	134.78(5)	P(1)–Nb(1)–C(12)	80.69(5)
Cl(1)–Nb(1)–C(5)	98.71(5)	P(1)–Nb(1)–C(13)	84.26(5)
Cl(1)–Nb(1)–C(6)	81.35(5)	P(1)–O(1)–C(14)	126.7(1)
Cl(1)–Nb(1)–C(7)	98.63(5)	P(1)–O(2)–C(15)	116.7(1)
Cl(1)–Nb(1)–C(8)	134.26(5)	P(1)–O(3)–C(16)	121.2(1)
Cl(1)–Nb(1)–C(9)	134.97(4)		
Cl(1)–Nb(1)–C(10)	98.93(5)		
Cl(1)–Nb(1)–C(11)	81.42(5)		
Cl(1)–Nb(1)–C(12)	98.04(5)		
Cl(1)–Nb(1)–C(13)	133.95(5)		
Cl(1)–Nb(1)–P(1)	90.26(1)		
Nb(1)–C(4)–C(1)	101.3(1)		
Nb(1)–C(4)–C(5)	75.4(1)		
Nb(1)–C(4)–C(8)	71.81(9)		
Nb(1)–C(5)–C(4)	68.37(9)		
Nb(1)–C(5)–C(6)	76.5(1)		
Nb(1)–C(6)–C(5)	69.6(1)		
Nb(1)–C(6)–C(7)	70.3(1)		
Nb(1)–C(7)–C(6)	75.8(1)		
Nb(1)–C(7)–C(8)	68.17(9)		
Nb(1)–C(8)–C(4)	71.35(9)		
Nb(1)–C(8)–C(7)	76.2(1)		
Nb(1)–C(9)–C(1)	101.3(1)		
Nb(1)–C(9)–C(10)	75.6(1)		
Nb(1)–C(9)–C(13)	71.9(1)		
Nb(1)–C(10)–C(9)	68.16(9)		

I.4 Fractional atomic coordinates and isotropic thermal parameters for [Nb(η-C_5H_4-CMe_2-η-C_5H_4){$P(OMe)_3$}Cl] (14)

Atom	x/*a*	y/*b*	z/*c*	U(iso)	Occ	
Nb(1)	0.09602(2)	0.36326(1)	0.17966(1)	0.0078	1.0000	U_{ani}
P(1)	0.00160(7)	0.17367(4)	0.26655(4)	0.0101	1.0000	U_{ani}
Cl(1)	–0.18827(7)	0.22875(5)	0.00183(4)	0.0176	1.0000	U_{ani}
O(1)	0.1699(2)	0.1072(1)	0.2953(1)	0.0182	1.0000	U_{ani}
O(2)	–0.1712(2)	0.0271(1)	0.2000(1)	0.0146	1.0000	U_{ani}
O(3)	–0.0466(2)	0.2380(1)	0.3916(1)	0.0166	1.0000	U_{ani}
C(1)	0.4380(3)	0.6189(2)	0.2983(2)	0.0123	1.0000	U_{ani}
C(2)	0.5673(3)	0.6439(2)	0.4182(2)	0.0168	1.0000	U_{ani}
C(3)	0.5137(3)	0.7408(2)	0.2569(2)	0.0169	1.0000	U_{ani}
C(4)	0.2284(3)	0.5959(2)	0.3011(1)	0.0113	1.0000	U_{ani}
C(5)	0.0800(3)	0.5979(2)	0.2092(2)	0.0129	1.0000	U_{ani}
C(6)	–0.0973(3)	0.5282(2)	0.2213(2)	0.0142	1.0000	U_{ani}
C(7)	–0.0643(3)	0.4782(2)	0.3153(2)	0.0141	1.0000	U_{ani}
C(8)	0.1376(3)	0.5190(2)	0.3666(2)	0.0129	1.0000	U_{ani}
C(9)	0.4113(3)	0.4726(2)	0.2064(2)	0.0115	1.0000	U_{ani}
C(10)	0.3277(3)	0.4328(2)	0.0809(2)	0.0148	1.0000	U_{ani}
C(11)	0.2690(3)	0.2830(2)	0.0299(2)	0.0178	1.0000	U_{ani}
C(12)	0.3050(3)	0.2268(2)	0.1189(2)	0.0163	1.0000	U_{ani}
C(13)	0.3960(3)	0.3433(2)	0.2306(2)	0.0135	1.0000	U_{ani}
C(14)	0.1494(3)	–0.0351(2)	0.2932(2)	0.0202	1.0000	U_{ani}
C(15)	–0.3605(3)	0.0406(2)	0.1693(2)	0.0205	1.0000	U_{ani}
C(16)	–0.0877(3)	0.1520(2)	0.4620(2)	0.0186	1.0000	U_{ani}
H(21)	0.5804	0.7406	0.4754	0.0151	1.0000	U_{iso}
H(22)	0.6960	0.6367	0.4090	0.0151	1.0000	U_{iso}
H(23)	0.5094	0.5698	0.4495	0.0151	1.0000	U_{iso}
H(31)	0.4293	0.7249	0.1786	0.0163	1.0000	U_{iso}
H(32)	0.5152	0.8334	0.3163	0.0163	1.0000	U_{iso}
H(33)	0.6466	0.7455	0.2495	0.0163	1.0000	U_{iso}
H(51)	0.1003	0.6416	0.1484	0.0132	1.0000	U_{iso}
H(61)	–0.2253	0.5164	0.1712	0.0153	1.0000	U_{iso}
H(71)	–0.1662	0.4227	0.3412	0.0149	1.0000	U_{iso}
H(81)	0.2036	0.4979	0.4347	0.0117	1.0000	U_{iso}
H(101)	0.3148	0.5001	0.0384	0.0132	1.0000	U_{iso}
H(111)	0.2110	0.2255	–0.0565	0.0173	1.0000	U_{iso}
H(121)	0.2728	0.1227	0.1071	0.0156	1.0000	U_{iso}
H(131)	0.4405	0.3358	0.3096	0.0126	1.0000	U_{iso}
H(141)	0.2792	–0.0477	0.3149	0.0211	1.0000	U_{iso}
H(142)	0.0790	–0.1056	0.2119	0.0211	1.0000	U_{iso}
H(143)	0.0772	–0.0529	0.3513	0.0211	1.0000	U_{iso}
H(151)	–0.4548	–0.0564	0.1290	0.0191	1.0000	U_{iso}
H(152)	–0.3935	0.0921	0.2433	0.0191	1.0000	U_{iso}
H(153)	–0.3645	0.0956	0.1155	0.0191	1.0000	U_{iso}

H(161)	0.0249	0.1181	0.4834	0.0192	1.0000	U_{iso}
H(162)	–0.2020	0.0676	0.4158	0.0192	1.0000	U_{iso}
H(163)	–0.1137	0.2099	0.5361	0.0192	1.0000	U_{iso}

I.5 Anisotropic thermal parameters for [Nb(η-C₅H₄-CMe₂-η-C₅H₄){P(OMe)₃}Cl] (14)

Atom	U(11)	U(22)	U(33)	U(23)	U(13)	U(12)
Nb(1)	0.0077(1)	0.0090(1)	0.0070(1)	0.00344(7)	0.00254(7)	0.00205(7
P(1)	0.0114(2)	0.0090(2)	0.0094(2)	0.0036(2)	0.0022(2)	0.0020(2)
Cl(1)	0.0143(2)	0.0229(2)	0.0108(2)	0.0075(2)	–0.0007(2)	–0.0025(2)
O(1)	0.0155(7)	0.0152(6)	0.0250(7)	0.0104(5)	0.0018(6)	0.0047(5)
O(2)	0.0129(7)	0.0113(6)	0.0162(6)	0.0050(5)	0.0007(5)	–0.0003(5)
O(3)	0.0282(8)	0.0118(6)	0.0126(6)	0.0069(5)	0.0090(6)	0.0047(5)
C(1)	0.0119(9)	0.0118(8)	0.0116(7)	0.0040(6)	0.0026(7)	0.0016(6)
C(2)	0.016(1)	0.0162(8)	0.0141(8)	0.0043(7)	–0.0004(7)	0.0013(7)
C(3)	0.014(1)	0.0150(8)	0.0217(9)	0.0092(7)	0.0043(7)	0.0005(7)
C(4)	0.0152(9)	0.0078(7)	0.0112(8)	0.0029(6)	0.0045(7)	0.0036(6)
C(5)	0.014(1)	0.0123(8)	0.0162(8)	0.0072(6)	0.0056(7)	0.0061(6)
C(6)	0.014(1)	0.0149(8)	0.0168(8)	0.0068(7)	0.0058(7)	0.0071(7)
C(7)	0.017(1)	0.0147(8)	0.0161(8)	0.0072(7)	0.0095(7)	0.0083(7)
C(8)	0.018(1)	0.0108(7)	0.0108(7)	0.0030(6)	0.0069(7)	0.0048(6)
C(9)	0.0071(9)	0.0152(8)	0.0121(8)	0.0050(6)	0.0037(7)	0.0022(6)
C(10)	0.0123(9)	0.0200(9)	0.0122(8)	0.0053(7)	0.0069(7)	0.0026(7)
C(11)	0.015(1)	0.0218(9)	0.0145(8)	0.0023(7)	0.0096(7)	0.0037(7)
C(12)	0.013(1)	0.0157(8)	0.0207(9)	0.0040(7)	0.0080(8)	0.0061(7)
C(13)	0.0104(9)	0.0139(8)	0.0171(8)	0.0050(7)	0.0051(7)	0.0055(6)
C(14)	0.027(1)	0.0167(9)	0.0234(9)	0.0112(7)	0.0077(8)	0.0120(8)
C(15)	0.013(1)	0.024(1)	0.024(1)	0.0143(8)	0.0016(8)	0.0012(7)
C(16)	0.029(1)	0.0145(8)	0.0154(8)	0.0090(7)	0.0100(8)	0.0045(7)

I.6 Additional structural information for [Nb(η-C₅H₄-CMe₂-η-C₅H₄){P(OMe)₃}Cl] (14)

Nb–Cp_{cent} / Å	2.02, 2.02
Bending angle, β /°	115.4
Cp_{cent}–Nb–Cp_{cent}, γ /°	124.3
Cp_{cent}–C_{ipso}–C_{bridge} /°	163.4, 163.4